NASA CR-73397
(Available to the Public)
TRW ER-7256-24

AIRCREW OXYGEN SYSTEM DEVELOPMENT CARBON DIOXIDE CONCENTRATOR SUBSYSTEM REPORT

by

R. G. Huebscher and A. D. Babinsky

PREPARED UNDER CONTRACT NO. NAS 2-4444

BY

TRW INC.
CLEVELAND OHIO

FOR
AMES RESEARCH CENTER
NATIONAL AERONAUTICS AND
SPACE ADMINISTRATION

July 1970

TRW
MECHANICAL PRODUCTS DIVISION

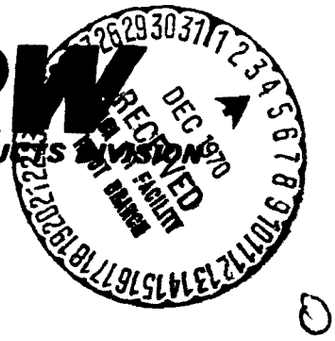

05

NASA CR-73397
(Available to the Public)

AIRCREW OXYGEN SYSTEM DEVELOPMENT
CARBON DIOXIDE CONCENTRATOR SUBSYSTEM REPORT

by

R. G. Huebscher and A. D. Babinsky

July 1970

Prepared under Contract No. NAS2-4444

by

TRW Inc.
Cleveland, Ohio

for

AMES RESEARCH CENTER
NATIONAL AERONAUTICS AND SPACE ADMINISTRATION

FOREWORD

The development work described herein, which was conducted by the Mechanical Products Division of TRW Inc. was performed under NASA Contract NAS2-4444. Initial development was conducted by C. F. Williams. Inputs were made by R. J. Kiraly in the thermal design and water balance studies. Electrolyte studies (yielding the electrolyte change to Cs_2CO_3) and the Design II developemnt were conducted by R. G. Huebscher. The carbon dioxide concentrator development task was part of the aircrew oxygen system development program under the overall direction of A. D. Babinsky. The contract technical monitor was P. D. Quattrone, Bictechnology Division, NASA Ames Research Center, Moffett Field, California.

TABLE OF CONTENTS

	PAGE
LIST OF FIGURES	iii
LIST OF TABLES	vi
SUMMARY	viii
INTRODUCTION	1
CARBON DIOXIDE CONCENTRATOR THEORY OF OPERATION	3
SINGLE CELL PROGRAM	6
Cell Design	6
Test Rig Description	6
Test Rig Modifications	13
Parametric Tests	19
Test Results	19
CARBON DIOXIDE CONCENTRATOR MODULE - DESIGN I	29
Design Objectives	29
Module Design	29
Design Modifications	35
CONCENTRATOR MODULE TEST RIG	45
Ten-Cell Module Configuration	45
Fifteen-Cell Module Configuration	49
PARAMETRIC TEST - DESIGN I MODULE	55
Design Condition Operation	55
Temperature Variation	58
Oxygen Circulation Rate	58
Hydrogen Flowrate Variation	58
Carbon Dioxide Transfer Rate Variation	58
Design Current Density Variation	66
CARBON DIOXIDE CONCENTRATOR DESIGN II MODULE	67
Heat and Moisture Removal Evaluation	67
Fin-Cooled Module	67
Static Water Feed Module	67
Circulating Electrolyte	68
Selected Approach	68
Electrolyte Study	68
Criteria for Electrolyte Selection	69
Survey of Alkali Metal Carbonates	72
Test Data	74

continued-

TABLE OF CONTENTS - continued

	PAGE
Water Tolerance of Cesium Carbonation Solutions	85
Module Design	86
Performance Analysis, CDCM I	86
Design, CDCM II	89
Module Fabrication	91
Verification Testing	101
Single Cells	101
Four-Cell Module Assembly	103
PARAMETRIC TESTS - DESIGN II MODULE	109
Fifteen-Cell Module Assembly	109
Performance as a Function of Ratio: CO_2 Transfer Rate to Current	112
Effect of Stack Temperature	119
Effect of pO_2 at Cathode (N_2 diluent)	123
Effect of Hydrogen Feed Rate	123
Effect of Oxygen Recycle Rate	128
Pressure Drop Data	128
Performance Summary Comparison	128
LIFE TESTING	133
Design I Module	133
Cyclic Testing	133
Endurance Testing	133
Long-Term Operation	133
Module Moisture Balance Tests	133
Design II Module	138
Single Cells	138
Nickel Encplates	138
Polysulfone Endplates	142
Titanium Endplates	142
Design II Cells	142
CONCLUSIONS	153
RECOMMENDATIONS	154
APPENDIX A - CARBON DIOXIDE CONCENTRATOR - THERMAL ANALYSIS	A-1
APPENDIX B - POST-TEST INSPECTION OF CARBON DIOXIDE CONCENTRATOR SINGLE CELLS	B-1

LIST OF FIGURES

FIGURES		PAGE
1	Schematic Representation of Carbon Dioxide Concentrator Cell. .	4
2	CO_2 Concentrator Single Cell Hardware	7
3	CO_2 Concentrator Cell with Exmet Gas Cavity Filler	9
4	CO_2 Concentrator Cell Assembly	10
5	CO_2 Concentrator Cell in Insulation Jacket	11
6	Plumbing Schematic, Single Station, Single Cell CDC Test Stand.	12
7	CO_2 Concentrator Test Rigs, Front View	14
8	CO_2 Concentrator Test Rigs, Rear View	15
9	Electrical Schematic, Single Station, Single Cell CDC Test Stand	16
10	Load Control - CO_2 Concentrator Single Cell	18
11	Polysulfone Cell - Post-Test Condition	20
12	CO_2 Concentrator Cell Polarization Curve	21
13	CO_2 Concentrator Single Cell Parametric Test - Variation of Reactant Pressures	23
14	CO_2 Concentrator Single Cell Parametric Test - Variation of CO_2% at O_2 Inlet (O_2 Flow Rate and CO_2 Flow Rate Variable) . .	24
15	CO_2 Concentrator Single Cell Parametric Test - Variation of Hydrogen Flow Rate	25
16	CO_2 Concentrator Single Cell Parametric Test - Variation of Cell Temperature	27
17	CO_2 Concentrator Single Cell Parametric Test - Variation of Current Density	28
18	CO_2 Concentrator Module Cell Construction Schematic	31
19	CO_2 Concentrator Module Cell Components	32
20	CO_2 Concentrator Module O_2 Side - Pressure Drop Characteristics	33
21	CO_2 Concentrator Module H_2 Side - Pressure Drop Characteristics	34
22	CO_2 Concentrator - 10 Cell Module	40
23	Hydrogen Manifold - Original Design	41
24	Hydrogen Manifold - Series Hydrogen Flow	42
25	Hydrogen Manifold - Series Flow with Humidity Exchange Cells .	43
26	CO_2 Concentrator Module Test System Schematic	46
27	CO_2 Concentrator Module Test System Control Schematic	47
28	CO_2 Concentrator Gas Analysis Wiring Schematic	48

continued-

LIST OF FIGURES - continued

FIGURES		PAGE
29	CO_2 Concentrator Module Test System	50
30	Plumbing Schematic, CDCM Test Stand	52
31	Electrical Schematic, CDCM Test Stand	53
32	CO_2 Concentrator Fifteen-Cell Module Test Rig	54
33	CO_2 Concentrator Module Parametric Test - Operation near Design Point	57
34	Performance of CDCM I - Effect of Stack Temperature	60
35	Performance of CDCM I - Effect of Oxygen Recycle Rate	62
36	Performance of CDCM I - Effect of Hydrogen Feed Rate	64
37	Performance of CDCM I - Specific Transfer Rate	65
38	Water Vapor Pressure of Aqueous Solutions of K_2CO_3	70
39	Specific Volume of Aqueous Solutions of K_2CO_3	71
40	Solubility of K_2CO_3 in Aqueous Solutions of $KHCO_3$ and Vice Versa at Several Temperatures	77
41	Apparatus Used to Determine Dew Point of Aqueous Electrolyte Solutions	78
42	Vapor Pressure Depression for Aqueous Solutions of Cs_2CO_3 at Two Temperatures	80
43	Water Vapor Pressure of Aqueous Solutions of Cs_2CO_3	81
44	Specific Volume of Aqueous Cs_2CO_3 Solutions	83
45	Phase Diagram Cs_2CO_3 - H_2O	84
46	Temperature Profile - Transverse Section	88
47	Water Vapor Pressure of Aqueous Solutions of Cs_2CO_3 - Module Operating Conditions Superimposed	92
48	Temperature Profile from Cell to Cell and Cell Edge to Cell Center (over working area). Maximum and Minimum Electrolyte Concentrations	93
49	CO_2 Concentrator Assembly (15 Cell) NAOS	96
50	CO_2 Concentrator Module Section through O_2 Manifold	97
5	Carbon Dioxide Concentrator Module Components	
52	Plastic Cell Housing Components for Redesigned CO_2 Concentrator	100
53	Fin Plate Assembly for Redesigned CO_2 Concentrator	102
54	Four-Cell Redesigned CO_2 Concentrator Module	104

continued-

LIST OF FIGURES - continue

FIGURES		PAGE
55	Design Verification Run - 4-Cell Concentrator Module	106
56	Design Verification Run - 4-Cell Carbonation Module	107
57	15-Cell Module with Shroud and Blowers	110
58	Module Installed in Test System	111
59	Performance as a Function of the Ratio, CO_2 Transfer to Current	116
60	Performance as a Function of the Ratio, CO_2 Transfer to Current	117
61	Performance of CDCM II, Specific Transfer Rate	118
62	Performance of CDCM II, CO_2 Transfer Rate, pCO_2 at Cathode, Stack Current and Voltage	120
63	Performance of CDCM II - Effect of Stack Temperature	122
64	Performance of CDCM II - Effect of pO_2 at Cathode	125
65	Performance of CDCM II - Effect of Hydrogen Feed Rate	127
66	Performance of CDCM II - Effect of Oxygen Recycle Rate	130
67	H_2 & O_2 Side Pressure Drop, 15-Cell Stack	131
68	CO_2 Concentrator Module No. SN-01 - Test Summary	136
69	Performance of CDCM II on Life Test	139
70	CO_2 Concentrator Single Cell (1 Ni) Life Test with K_2CO_3 Electrolyte	140
71	CO_2 Concentrator Single Cell (2Ni) Life Test Performance	141
72	CO_2 Concentrator Single Cell (1 Ni) Life Test with Cs_2CO_3 Electrolyte	143
73	CO_2 Concentrator Single Cell (2 Ni) Life Test with Cs_2CO_3 Electrolyte	144
74	CO_2 Concentrator Single Cell (2P) Life Test	147
75	CO_2 Concentrator Single Cell (1Ti) Life Test	149
76	CO_2 Concentrator Single Cell (1M) Life Test with Cs_2CO_3 Electrolyte	151
77	CO_2 Concentrator Single Cell (2M) Life Test with Cs_2CO_3 Electrolyte	152

LIST OF TABLES

TABLE		PAGE
I	CO_2 Concentrator Single Cell Physical Characteristics	8
II	CO_2 Concentrator Module Design Requirements	30
III	CO_2 Concentrator Module Thermal Characteristics	36
IV	CO_2 Concentrator Module Stress Analysis Summary	37
V	CO_2 Module Design Summary	38
VI	MAOS CO_2 Concentrator Module Parts List	39
VII	CO_2 Concentrator Module Operation Near Design Point Conditions	56
VIII	CO_2 Concentrator Module Operation Temperature Variation Data	59
IX	CO_2 Concentrator Module Operation O_2 Circulation Rate Data	61
X	Effect of Hydrogen Feed Rate	63
XI	Solution Volume Change, K_2CO_3	72
XII	Room Temperature Solubility & Saturation Temperature Depression for Five Alkali Metal Carbonates	73
XIII	Dew Point Depression of Aqueous Cs_2CO_3 Solutions	79
XIV	Density of Aqueous Cs_2CO_3 Solutions at Room Temperature	82
XV	Solution Volume Change, Cs_2CO_3	86
XVI	CDCM Design Summary	90
XVII	Concentration Excursions & Volume Changes in CDCM	94
XVIII	Materials Selections, CDCM II	98
XIX	Operating Conditions for Design Verification Test Run	105
XX	CDCM Test Sequence	113
XXI	Performance as a Function of the Ratio, CO_2 Transfer to Current	114
XXII	Effect of Stack Temperature	121
XXIII	Effect of Oxygen Partial Pressure	124
XXIV	Effect of Hydrogen Feed Rate	126
XXV	Effect of Oxygen Recycle Rate	129
XXVI	Performance Summary Comparison to Design Objectives	132
XXVII	CO_2 Concentrator Cyclic Testing Start-Up/Shut-Down Procedure.	134

continued

LIST OF TABLES - continued

TABLE		PAGE
XXVIII	NAOS CO_2 Concentrator Cyclic Test Sequence	135
XXIX	CO_2 Concentrator Single Cell (1Ni) Life Test Shutdown Summary	145
XXX	CO_2 Concentrator Single Cell (2Ni) Life Test Shutdown Summary	146
XXXI	CO_2 Concentrator Single Cell (2P) Life Test Shutdown Summary	148
XXXII	CO_2 Concentrator Single Cell (1Ti) Life Test Shutdown Summary	150

AIRCREW OXYGEN SYSTEM DEVELOPMENT
CARBON DIOXIDE CONCENTRATOR SUBSYSTEM REPORT

by

R. G. Huebscher and A. D. Babinsky

SUMMARY

Liquid oxygen systems (LOX) currently used in military aircraft present a significant logistics problem. To replace these LOX systems, a program was initiated under Contract NAS2-[illegible]4 to develop a closed loop aircrew oxygen system which generates oxygen on board the aircraft as required. A water electrolysis module is used as the oxygen generator and the amount of oxygen required is decreased significantly through the use of a closed loop rebreather system. The rebreather loop functions to condition the exhaled gas such that it can be reused in the breathing cycle. The rebreather must remove exhaled carbon dioxide, nitrogen, water vapor and heat.

Removal of carbon dioxide is accomplished by a TRW-developed electrochemical Carbon Dioxide Concentrating Module (CDCM). The module consists of cells in which two porous electrodes are separated by an asbestos capillary matrix containing an aqueous solution of an alkali metal carbonate. Cell plates adjacent to the electrodes provide passageways for distributing the gaseous reactants over the surface of the electrodes.

The simplified chemical and electrochemical reactions are:

Cathode

$$1/2\ O_2 + H_2O + 2e^- \longrightarrow 2OH^-$$

Catholyte

$$CO_2 + 2OH^- \longrightarrow CO_3^= + H_2O$$

Anode

$$H_2 + 2OH^- \longrightarrow 2H_2O + 2e^-$$

Anolyte

$$CO_3^= + H_2O \longrightarrow CO_2 + 2OH^-$$

Overall Reaction

$$1/2\ O_2 + H_{2\,(anode)} + CO_{2\,(cathode)} \longrightarrow H_2O + CO_{2\,(anode)} + \text{elec. energy} + \text{heat}$$

The reaction of oxygen and water forms hydroxyl ions (OH^-), a well-known "getter" of carbon dioxide (for example, LiOH). Any carbon dioxide which passes over

the electrolyte, now rich in hydroxyl ions, reacts to form carbonate ions ($CO_3^{=}$). At the opposite electrode (anode) the reaction of hydrogen and hydroxyl ions to form water causes the electrolyte to be deficient in hydroxyl ions. Thus, carbon dioxide is given off, completing the transfer of carbon dioxide from the oxygen atmosphere to the hydrogen atmosphere. Hydrogen is available to the module as a waste product from the water electrolysis module, thereby permitting the concentrator to be operated in the hydrogen depolarized mode. In this mode of operation the unit generates power much as a fuel cell and has the capability of supplying electrical power to other portions of the NAOS system if desired.

This system is completely static, the only moving parts being in the subsystems which service the concentrator cells. The system readily lends itself to zero gravity operation since mass transfer occurs only in the gaseous state. There are no free liquids or components dependent upon gravity operation.

At the start of the program, available data covered narrow operating ranges for small single cells. Thus, parametric testing of single cells was conducted to provide the necessary data to design a specific full-scale carbon dioxide concentrator.

Four small cells utilizing differing materials of construction, and internal cell geometry were fabricated. A parametric test rig and a three-cell, life test rig were designed and fabricated for the single cell effort. The parametric test rig was used to determine the performance of the cells over a wide range of conditions. The instrumentation utilized in the parametric test stand was more accurate and complete than that used on the life stands in which all three cells were run at the same conditions of gas flow, pressure and dew point. Separate current loading systems were provided for the cells, thus allowing each unit to be run at a different current density.

Parametric tests were conducted to characterize cell performance as a function of reactant pressure, oxygen, carbon dioxide and hydrogen flow rate, cell temperature, and current density.

Two cells utilizing nickel endplates were run on life test. One of these units was run for 13,071 hours and the other for 11,684 hours. Additional cells tested on the life test rig comprised two units with polysulfone endplates, one unit with titanium endplates and two units of module configuration. The purpose of these tests was to obtain data on the compatibility of cell materials when exposed to normal carbon dioxide concentrator cell operating environments. After completion of these tests, the units were torn down and examined for evidence of corrosion. Very little change in appearance of cell components prior to and after the test was noted as summarized in Appendix B.

The Carbon Dioxide Concentrator Module (CDCM) was designed as a laboratory test module utilizing air-cooled fins for heat removal and the matrix type of construction referenced above that permits operation of the module in any attitude. The physical characteristics of the first unit, referred to as CDCM I, are summarized as follows:

Electrode Area:	35 in^2 (per cell)
Electrode Type:	AB-6
Electrolyte Matrix:	Asbestos
Electrolyte:	Potassium Carbonate
Cell Material:	Machined polysulfone
Gas Cavity Spacer:	Expanded silver
Heat Removal Plates (current collectors):	Silver
Seals:	Ethylene propylene O-rings
Cell Size (overall):	7.5 x 13.8 x 0.17
Current Density (max.):	40 ASF
No. of Cells per Module:	10
Module Size (overall):	7.5 x 13.8 x 3.2
CO_2 Transfer Rate:	0.117 lb/hr
CO_2 Partial Pressure:	3.8mm Hg

The individual cell structural components were machined from extruded polysulfone sheet. Endplates were machined of 5/16" thick stainless steel plate. Current collectors were fabricated by stack milling silver sheet stock. Gas cavity spacer material was fabricated from expanded silver sheet. Electrodes and asbestos matrices and frames were hand-cut to size. Module assembly was accomplished by stacking the individual components for ten cells on an assembly fixture. Insulated drawbolts, torqued in a pre-determined pattern completed the assembly.

A test stand was designed and assembled to provide all the services, controls and instrumentation required for operation of the carbon dioxide concentrator module in accordance with the test plan. This plan included parametric, cyclic and extended life tests. The test system is equipped with an oxygen recycle and oxygen/carbon dioxide feed system to typify the operation of the module when part of the Rebreather System. With this test system, the operator has the capability of controlling and monitoring the module current, average cell temperature, dew point temperature of both oxygen and hydrogen entering the module, carbon dioxide flow rate into the recycle loop, the oxygen recycle rate through the loop, the hydrogen flow rate into the module, the total gas pressures on the oxygen and hydrogen sides, and the partial pressure of the oxygen on the recycle side. For the various ranges of the above-mentioned independent parameters, the operator can observe the following dependent parameters: individual cell voltages, module voltage, carbon dioxide concentration in the

effluent oxygen and hydrogen streams, and the oxygen consumption of the module. Test points were provided to check the performance of the gas analyzers within the test system as well as to obtain a more complete survey of the carbon dioxide concentrations and other gas components with a Beckman GC-2 Gas Chromatograph. Internal cell iR drop and cell iR-free voltages can be determined with the aid of an interrupter circuit built into the test stand.

The parametric test series was designed to provide operating data for the carbon dioxide concentrator module as a function of the following: cell temperature, oxygen circulation rate, hydrogen flow rate, current density, and carbon dioxide transfer rate.

During the course of the parametric test series it became apparent that a uniform distribution of hydrogen to the ten cells was not being achieved. Consequently, the internal manifolding of the hydrogen stream was changed from a parallel to a series flow configuration. In the modified flow system, the first cell in the series configuration receives pure hydrogen and the last cell in the stack receives approximately 70 percent hydrogen and 30 percent carbon dioxide. Stable performance was obtained using this flow pattern with the ten cell module tested.

Subsequent parametric tests disclosed that the unit could transfer carbon dioxide at the design rate of 0.45 slpm at a current of 10 amperes while maintaining the carbon dioxide level at the oxygen exit end of the stack below 0.3 percent. This determination was made with a hydrogen flow rate of 1.7 slpm, an oxygen recycle rate of 2.7 SCFM and a stack temperature in the range of 117-130°F. The electrolyte used in these tests was 30 w/w% K_2CO_3 solution.

After completion of the parametric test series, life tests were conducted with the module. Moisture balance difficulties in long term operation led to the design and fabrication of CDCM II. Prior to initiation of the redesign, an analysis was made of alternate means of removing heat and moisture from the unit. The analysis included the original fin-cooled unit as well as a unit employing static water feed to provide both increased water tolerance, gas humidity conditioning and evaporative cooling, and a unit utilizing a circulating electrolyte. Consideration of the advantages, disadvantages and requirements of the above concepts for CDCM II led to the conclusion that a redesigned, fin-cooled concentrator module using an alternate electrolyte would best meet all the objectives.

The design objectives for the second unit were: increased carbon dioxide transfer capability (100% overcapacity); elimination of any possibility of corrosion; elimination of excessive internal temperature gradients; utilization of a superior electrolyte to provide increased performance and water tolerance; improved sealing; decreased pressure drops; utilization of methods of construction amenable to mass production; and utilization of materials that would permit operation in the carbonation (non-depolarized) mode.

During the initial phases of the NAOS development program, potassium carbonate electrolyte was utilized in both single cell and module tests. During the carefully controlled tests, possible with the NAOS-developed equipment, it was disclosed that bicarbonate formation and precipitation was occurring. The

precipitate accumulated within the anode and masked this electrode from the gas phase, seriously reducing performance. In addition, gas ports on the hydrogen side of the cell were blocked.

A survey of all of the alkali metal carbonates and bicarbonates with respect to solubility limits and vapor pressure depression was initiated. A study was made to determine the criteria for electrolyte selection from which candidate alkali metal carbonates could be selected. Some of the required property data for this selection was available in the literature and some was determined by test during the program. From this analysis cesium carbonate emerged as the preferred electrolyte although rubidium carbonate very likely could also be utilized. Virtually no property data was available on the latter.

From a review of the materials examined in the Carbonation Cell Materials Compatibility study, NASA CR-1481, titanium was selected as the most desirable metallic material and ethylene propylene rubber was selected for the sealing material. Knowing the thermal conductance of all cell components as well as property data for aqueous solutions of cesium carbonate (such as solution volume and vapor pressure data) the water tolerance of the unit was maximized. The physical characteristics of the redesigned concentrator, CDCM II, are summarized in the following:

Electrode Area:	35 in^2 (per cell)
Electrode Type:	AB-6
Electrolyte Matrix:	Asbestos
Electrolyte:	Cs_2CO_3
Cell Material:	Injection molded polysulfone
Gas Cavity Spacer:	Expanded titanium
Heat Removal Plates (current collectors):	Titanium clad copper
Seals.	Flat, ethylene-propylene gaskets
Cell Size (overall):	7.7 x 13.7 x 0.15
Current Density (max.):	40 ASF
No. of Cells per Module:	15
Module Size (overall):	7.7 x 13.7 x 4.5
CO_2 Transfer Rate:	0.234 lb/hr
CO_2 Partial Pressure:	3.8mm Hg

Polysulfone plastic was utilized for the cell housing parts. These were injection molded in an aluminum mold using an eight ounce molding machine. Endplates were machined from 5/16" thick stainless steel plate. Current collectors were fabricated by die cutting copper sheet stock. Titanium clads were die cut and adhesively bonded to both sides of the copper sheet. The titanium sheets were welded to each other in the region of through manifold holes. Gas cavity spacer material was fabricated from expanded titanium sheet The flat gaskets were die cut from EPR. Electrodes and asbestos matrices were hand-cut to size. Module assembly was accomplished by stacking the individual components for fifteen cells on an assembly fixture. Insulated drawbolts, equipped with spring washers, were torqued in a pre-determined pattern to complete the assembly.

The test stand was modified to provide a fifteen-cell capability. In addition, the oxygen dehumidifier was replaced by a device that would permit both humidification and dehumidification. The oxygen recycle loop was equipped with a flowmeter and was trace-heated. The flow capability of the stand was increased in accordance with the 100% overcapacity requirement for CDCM II.

A four-cell module was assembled to conduct a design verification test. This unit was run for 76 hours in the hydrogen depolarized mode at which time the hydrogen source was valved off. The unit was then run in the powered mode for 62 hours. The module was then disassembled and tear-down observations made.

Parametric tests were subsequently conducted upon a 15-cell module for the purpose of obtaining performance as a function of the ratio of carbon dioxide transfer rate to current to determine the effect of stack temperature on performance, effect of pCO_2 at the cathode (with N_2 as diluent), and the effect of hydrogen feed rate, and oxygen recycle rate on stack performance. The parametric tests disclosed that the unit could transfer carbon dioxide at the design rate of 0.45 slpm at a current of 5 amperes while maintaining the carbon dioxide level at the oxygen exit end of the stack below 0.3%. At the 100% overload condition (at a stack current of 10 amperes) the carbon dioxide level at the oxygen exit end of the stack was approximately 0.2%. These data were taken with a hydrogen flow rate of 1.7 slpm, an oxygen recycle rate of approximately 3.6 SCFM and a stack temperature of 110°F. The electrolyte used in these tests was 55 w/w% Cs_2CO_3 solution.

An increase in stack temperature markedly increased stack voltage, however, the carbon dioxide level in the rebreather loop increased slightly. Stack voltage decreased slightly at a pO_2 of 3 psia, however, the unit functioned stably at a pO_2 of 1.1 psia. When hydrogen feed rate was reduced to a value near stoichiometric, the carbon dioxide level in the hydrogen leaving the unit was in the order of 90%. The voltage of the last cell in the stack was still acceptable. The test data showed that increased oxygen recycle rate decreased the carbon dioxide level in the rebreather loop with all other conditions constant. After completion of the parametric test series, a life test was conducted upon the 15-cell module. A total of 1,845 continuous load hours were logged on the second module with 509 hours of this as parametric test time. A total of 169 hours were logged on the predecessor module that was damaged during a test rig malfunction. No electrolyte recharges were necessary to sustain the operation of either unit during the test effort. The life test on the second unit was terminated by completion of contract requirement.

The major conclusions relative to the carbon dioxide concentrator module assembly based on information derived from the NAOS development program are:

1. Silver is not a suitable material for long-term module operation over the complete range of operation from full load to open circuit conditions.

2. Potassium carbonate solution is not a suitable electrolyte for stable operation.

3. Long-term operation of carbon dioxide concentrator cells and modules is feasible using cesium carbonate electrolyte.

4. The titanium clad copper assembly is suitable for use as a bipolar plate in the carbon dioxide concentrator.

5. The carbon dioxide concentrator module meets the system design requirements for carbon dioxide removal, using the series hydrogen flow pattern.

6. The carbon dioxide concentrator module is capable of maintaining carbon dioxide partial pressures below 1mm Hg in the closed loop system.

7. The ability of the concentrator module to maintain design performance capability for extended periods of continuous operation was successfully demonstrated.

8. Operation of the module in an ON-OFF cycle characteristic of short-term aircraft operation is entirely satisfactory.

9. Full operation after long storage periods is possible.

Based on NAOS program experience, it is recommended that a carbon dioxide module development program should be continued, incorporating the following:

1. Perform investigation necessary to provide additional data on methods which can be used to increase the specific transfer rate of carbon dioxide at low carbon dioxide partial pressures.

2. Module development should be continued with the objective of developing an efficient carbon dioxide concentrator for use in either aircraft or spacecraft life support systems.

Several appendices are included in this report to provide additional details in the following two areas: 1) thermal analysis to determine most effective means of heat removal for a concentrator subsystem designed for use in the F-111 aircraft; and 2) detailed results of the photographic and visual study of component parts of the small cells by post-test disassembly and inspection.

INTRODUCTION

TRW, under NASA Contract NAS2-4444, developed an aircrew oxygen system using electrochemical oxygen generation and carbon dioxide removal. The objective of the program was to develop a feasibility demonstration model of a safe, reliable, compact system which could replace the presently used LOX systems.

Aircraft oxygen systems are currently limited to the use of stored supplies of oxygen in the form of liquid oxygen or high pressure gaseous oxygen. Use of oxygen from these sources limits the duration of a mission to the amount of stored gases and creates somewhat of a problem in logistics and service to provide the needed oxygen.

A means of avoiding these problems is the provision of a method of continuously generating oxygen on board the aircraft as oxygen is required. This can be accomplished electrochemically by electrolysis of water or concentration of oxygen from ambient air. The size and power requirements of these electrochemical oxygen generators would be large when coupled to an open loop aircraft oxygen system. If, however, a rebreather loop is provided such that the oxygen used corresponds to the pilot's metabolic consumption, the size of the oxygen generator and rebreather loop becomes competitive with a present-day LOX converter system.

Generation of oxygen by water electrolysis was selected to make the system independent of air source (high altitude or space application). The water is replenished by refill of a water tank between missions.

The rebreather loop functions to recondition the exhaled gas such that it can be reused in the breathing cycle. The rebreather thus removes exhaled carbon dioxide, nitrogen, water vapor and heat.

Removal of carbon dioxide is accomplished by an electrochemical carbon dioxide concentrator module. Carbon dioxide is removed by the module from the circulating rebreather loop gases and transferred across the cells in the module into a flowing stream of hydrogen and then vented overboard.

This report describes the development and test of this carbon dioxide concentrator.

The design philosophy was to develop a Carbon Dioxide Concentrator Module (CDCM) of laboratory type (non-optimized with respect to weight, volume or performance) design, with the capability for operation independent of gravitational orientation. The development of the Carbon Dioxide Concentrator Subsystem consisted of the following subtasks:

- Design, fabricate and perform parametric tests - small single cells.
- Design, fabricate and perform parametric tests - ten-cell module (Design I).
- Conduct a series of cold startup, short-term cyclic tests to determine applicability of CDCM design to aircraft type use profiles.

- Long-term life tests on single cells and modules to demonstrate long-term performance stability and materials suitability for extended use when exposed to electrolyte-temperature-pressure-voltage-gas operating environment.
- Perform a thermal balance study on CDCM to determine most suitable cooling mode for application to a system installed in an F-111 aircraft - reported in Appendix A.
- Perform post-test inspection of single cells following completion of life test to determine the condition of materials selected and used in single cell design, fabrication and test.
- Develop Design II module with improved operating characteristics and increased capacity. Perform parametric and life tests.

Design I modules were also used in the Laboratory Breadboard System tests and in the Flight Breadboard System Test Program. A Design II module is now installed in the Laboratory Breadboard System.

Performance of the Design I CDCM was satisfactory in short-term tests but not in long-term tests. With the design changes incorporated into Design II, the CDCM performance was satisfactory in all respects meeting, and in many instances, exceeding design specifications.

CARBON DIOXIDE CONCENTRATOR THEORY OF OPERATION

Man produces carbon dioxide at a rate of approximately 0.1 lb/hr. In a closed environment, such as an aircraft rebreather loop, this amount must be removed while limiting the concentration to approximately 7.6mm Hg.

The carbon dioxide concentrator developed by TRW accomplishes this in an electrochemical cell shown schematically in Figure 1. The cell consists of two porous electrodes separated by an asbestos capillary matrix which contains aqueous cesium carbonate (Cs_2CO_3). Cell plates adjacent to the electrodes provide passageways for distributing the gaseous reactants over the surface of the electrodes. The simplified reactions are shown in Figure 1.

The reaction of oxygen and water forms hydroxyl (OH^-) ions, a well-known "getter" of carbon dioxide (for example, LiOH). Any carbon dioxide which passes over the electrolyte, now rich in hydroxyl ions (OH^-), reacts to form carbonate ions ($CO_3^=$). At the opposite electrode (anode) the reaction of hydrogen and hydroxyl ions (OH^-) to form water causes the electrolyte to be deficient in hydroxyl ions (OH^-). Thus, carbon dioxide is given off, completing the transfer of carbon dioxide from the oxygen atmosphere to the hydrogen atmosphere.

The asbestos capillary matrix holds the electrolyte in proper contact with the electrodes regardless of the orientation of the cell, produces a uniform separation of the electrodes, and when filled with electrolyte, isolates the reactant gases. The matrix is compressed between the electrodes, the current collectors, and cell plates; thus, a compact cell is formed that is highly resistant to shock and vibration.

This is a completely static system, the only moving parts being in the subsystems which service the concentrator cells. The system readily lends itself to zero gravity operation since mass transfer occurs only in the gaseous state. There are no free liquids or components dependent upon gravity.

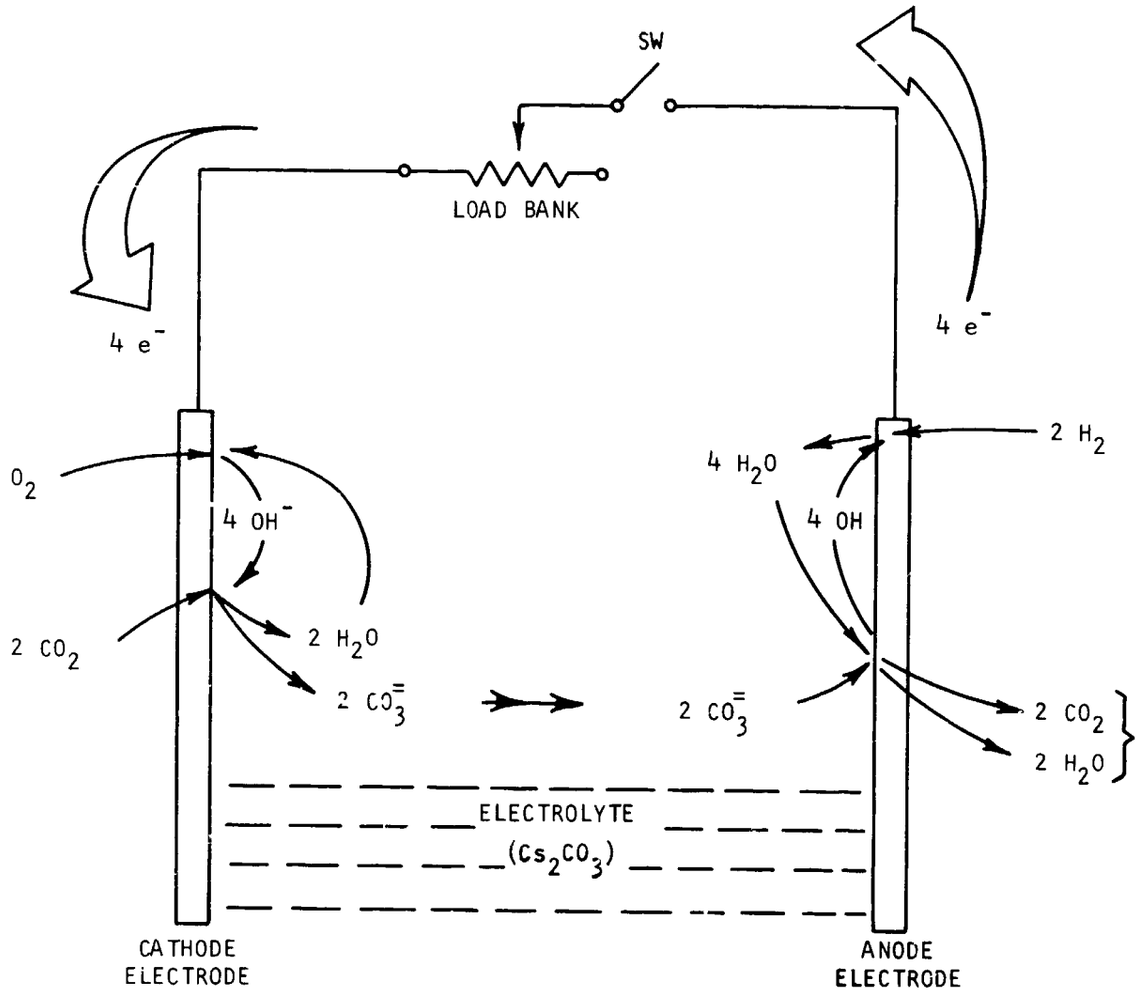

$O_2 + 2\ H_2O + 4\ e^- \longrightarrow 4\ OH^-$ (ELECTRODE)

$2\ CO_2 + 4\ OH^- \longrightarrow 2\ CO_3^= + 2\ H_2O$

(CATHOLYTE)

$H_2 + 4\ OH^- \longrightarrow 4\ H_2O + 4\ e^-$ (ELECTRODE)

$2\ CO_3^= + 2\ H_2O \longrightarrow 2\ CO_2 + 4\ OH^-$

(ANOLYTE)

OVERALL REACTION:

$$O_2 + 2\ CO_2 + 2\ H_2 \longrightarrow 2\ CO_2 + 2\ H_2O + \text{ELECTRICAL ENERGY} + \text{HEAT}$$

FIGURE 1 SCHEMATIC REPRESENTATION OF CARBON DIOXIDE CONCENTRATOR CELL

SINGLE CELL PROGRAM

The carbon dioxide concentrator is a new concept conceived and developed at TRW. At the program start, data available covered narrow operating ranges for small single cells. Thus, parametric testing of single cells was conducted to provide the necessary data to design a specific full scale carbon dioxide concentrator. In the following paragraphs the single cell construction and test data are presented.

Cell Design

The components of a single cell used in parametric testing are shown in Figure 2. A 30-mil asbestos matrix is sandwiched between two electrodes. End plates of both polysulfone and nickel 200 were machined to form gas cavities. A flat gasket of ethylene propylene seals the cell and a polysulfone spacer insures that the cell end plates and electrodes are a fixed distance apart (27 mils). The basic cell is completed by copper cold plates as shown in the figure. The physical characteristics of these cells is summarized in Table I. The two cells, which used polysulfone end plates, were redesigned when a cell failure indicated that the heat transfer characteristics of the cell was inadequate. This allowed the testing of a configuration similar to that which was used in the module. Figures 3 and 4 show the cell components and an assembled cell. Figure 5 is a photograph of a cell after it has been thermally insulated.

Test Rig Description

The single cell carbon dioxide concentrator test rigs, i.e., the parametric test rig and the life test rig, are similar in design; therefore they will be discussed as one unit except where significant differences exist. The basic difference in the two units is the testing conducted with each unit. The parametric rig was used to check the performance over a wide range of conditions. Therefore, the instrumentation is more accurate and complete, including 150mm rotameters for precise flow measurement and gauges to measure pressure drop across the cells. The life stand was used for long-term operation, hence less instrumentation and provisions for the installation of three cells. These cells were run at the same conditions of gas flow pressure and dew point, however, separate load controls allow cell loading to be changed as required. The stand is of modular design consisting of an electrical system and a mechanical system.

The mechanical system consists of the humidifier, coolant system, and control panel. The humidifier consists of a tank within a tank (see Figure 6, the inner tank humidifies hydrogen while the outer tank humidifies the oxygen. A sparger is used in the oxygen side for gas dispersion. Float-type level switches are used in both tanks to signal low water level. The construction of the saturator is such that operating pressures up to 40 psia can be tolerated. The tanks are insulated and temperature is maintained by using two 500w cylindrical heaters.

The coolant system consists of a 12-liter stainless steel beaker connected to a 6 gpm circulating pump. The beaker is insulated and its temperature is controlled with a 600w cylindrical heater.

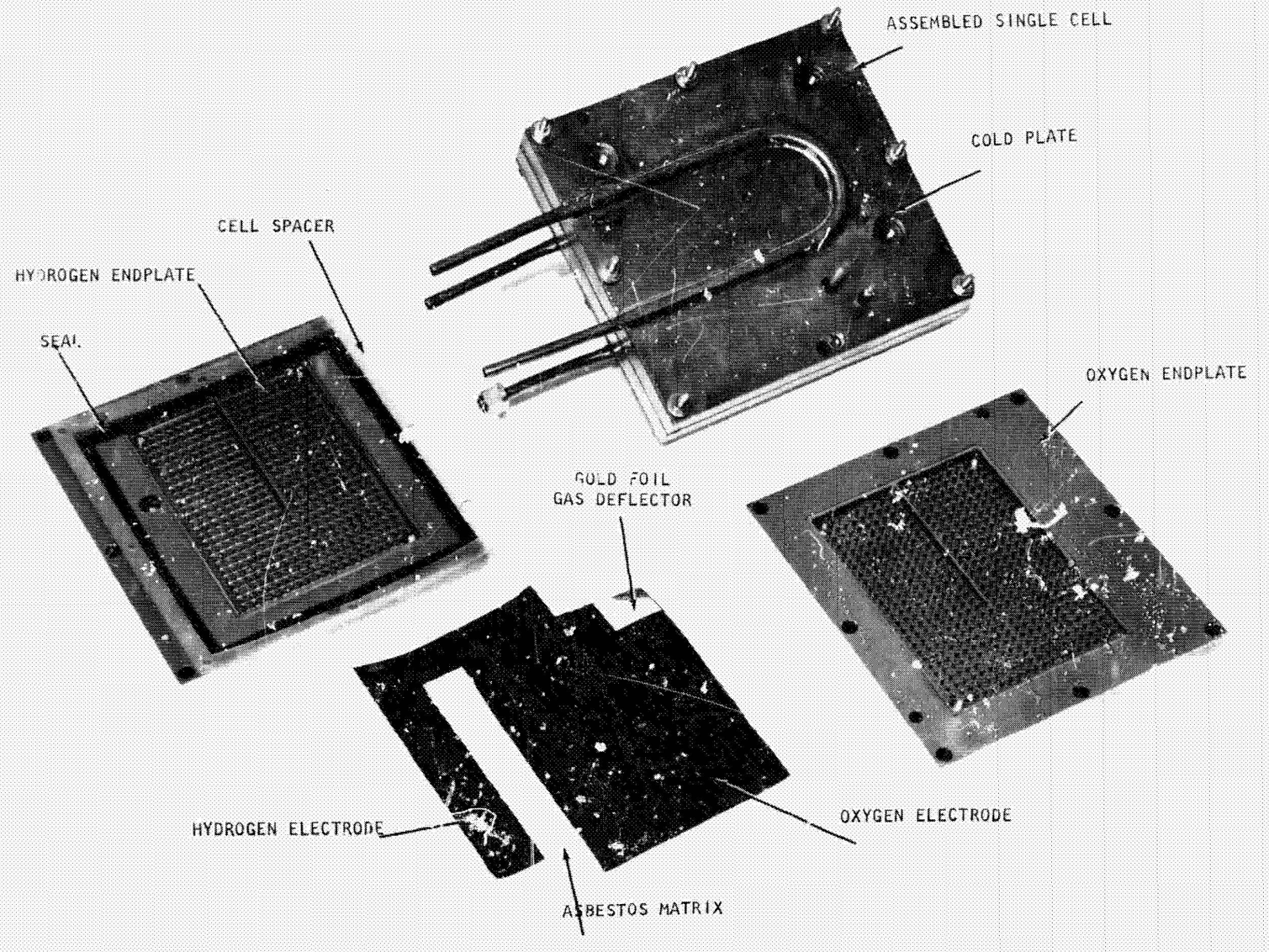

FIGURE 2 CO_2 CONCENTRATOR SINGLE CELL HARDWARE

TABLE I

CO_2 CONCENTRATOR SINGLE CELL
PHYSICAL CHARACTERISTICS

Cell #	1 NI - 1	2 NI - 2	1 P - 2	2 P - 1
Endplate Material	Nickel	Nickel	Polysulfone	Polysulfone
Heat Dissipation	-	-	Nickel	Silver
Cavity Material	-	-	Titanium Expanded Metal	Titanium Expanded Metal
Electrodes	0.15 sq. ft.	0.15 sq. ft.	0.15 sq. ft.	0.15 sq. ft.
Anode	AB-6	AB-6	AB-6	AB-6
Cathode	AB-6	BB-6	BB-6	AB-6
Matrix Thickness	30 mil	30 mil	30 mil	30 mil

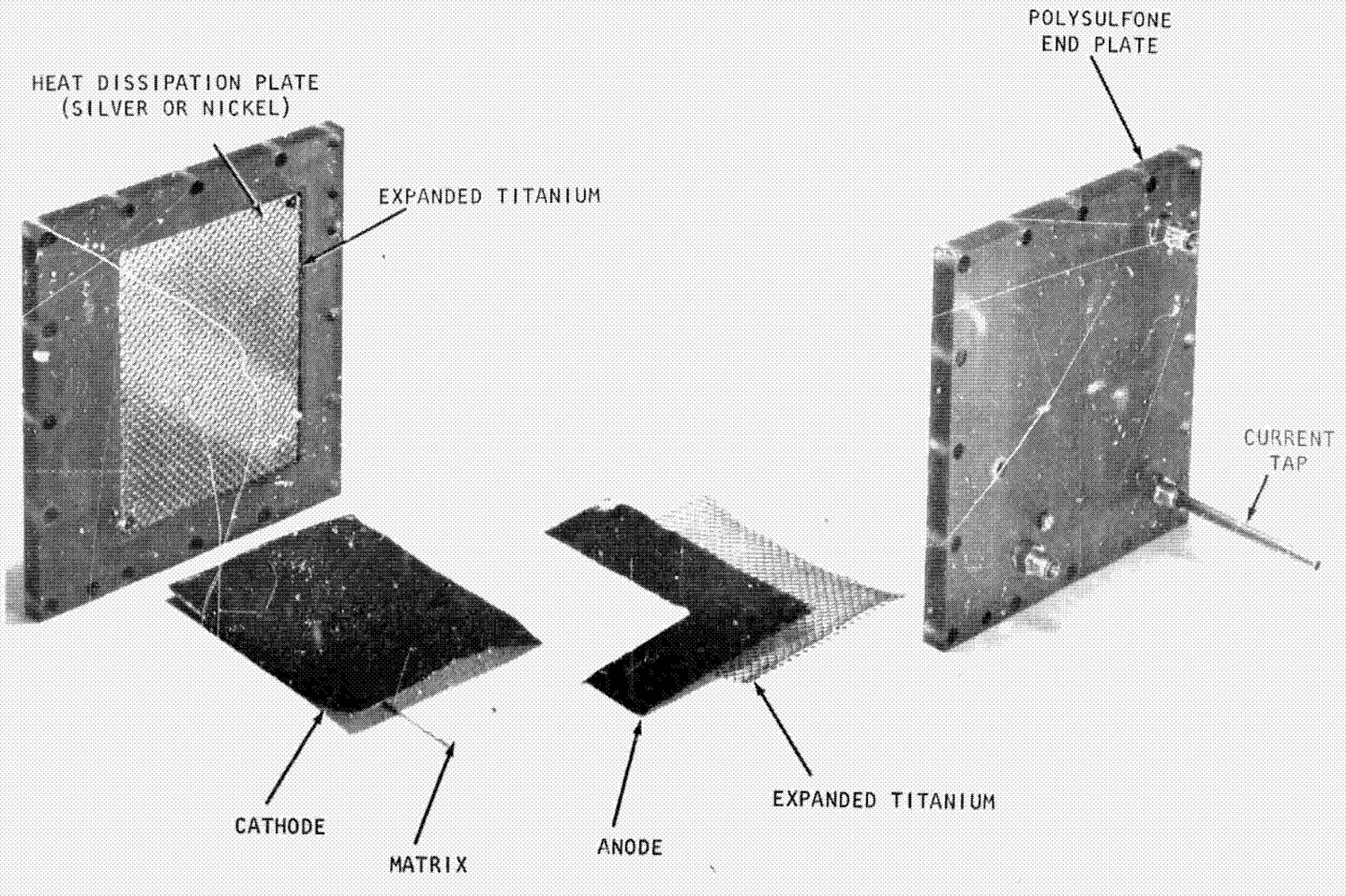

FIGURE 3 CO_2 CONCENTRATOR CELL WITH EXMET GAS CAVITY FILLER

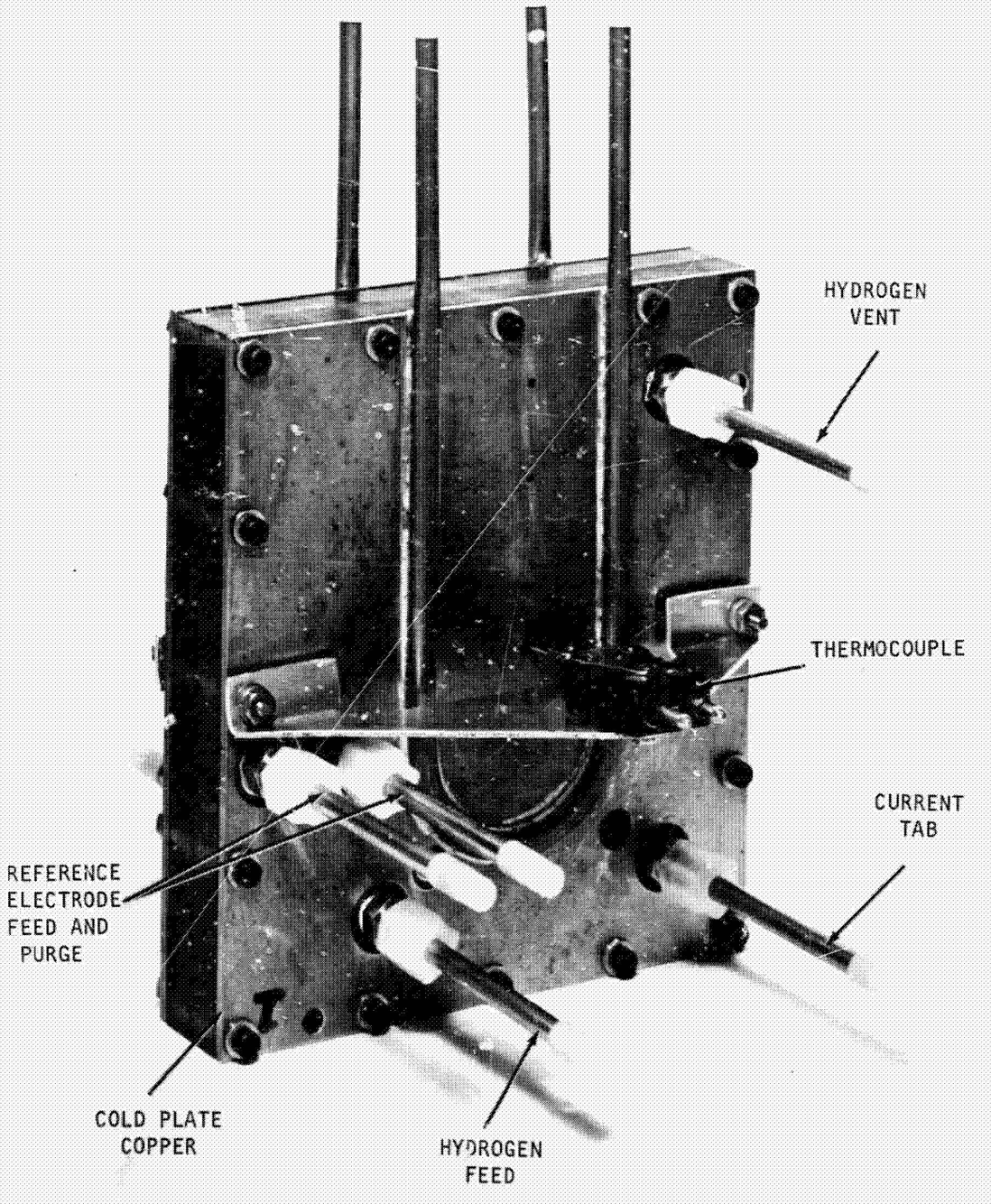

FIGURE 4 CO_2 CONCENTRATOR CELL ASSEMBLY

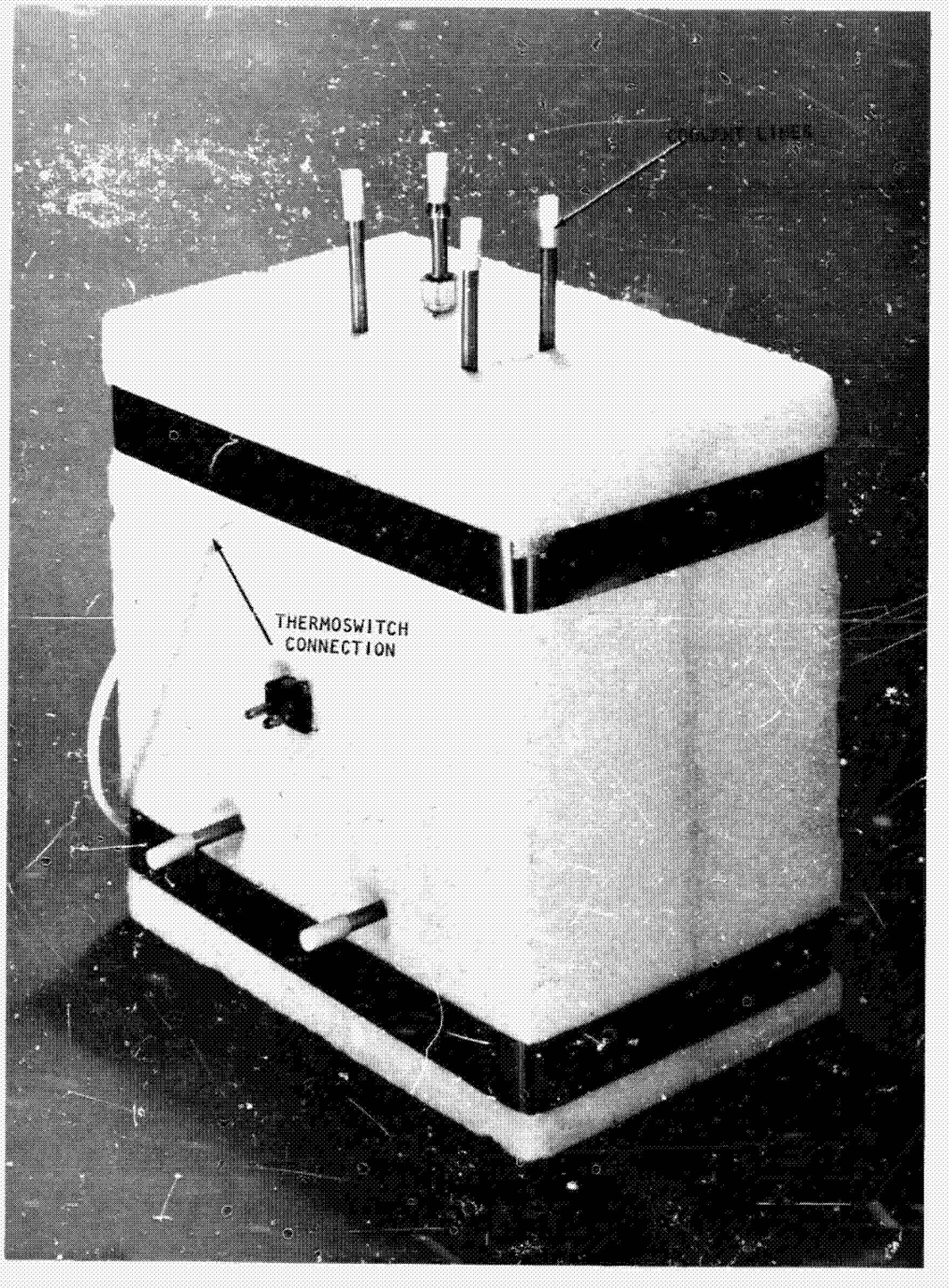

FIGURE 5 CO_2 CONCENTRATOR CELL IN INSULATION JACKET

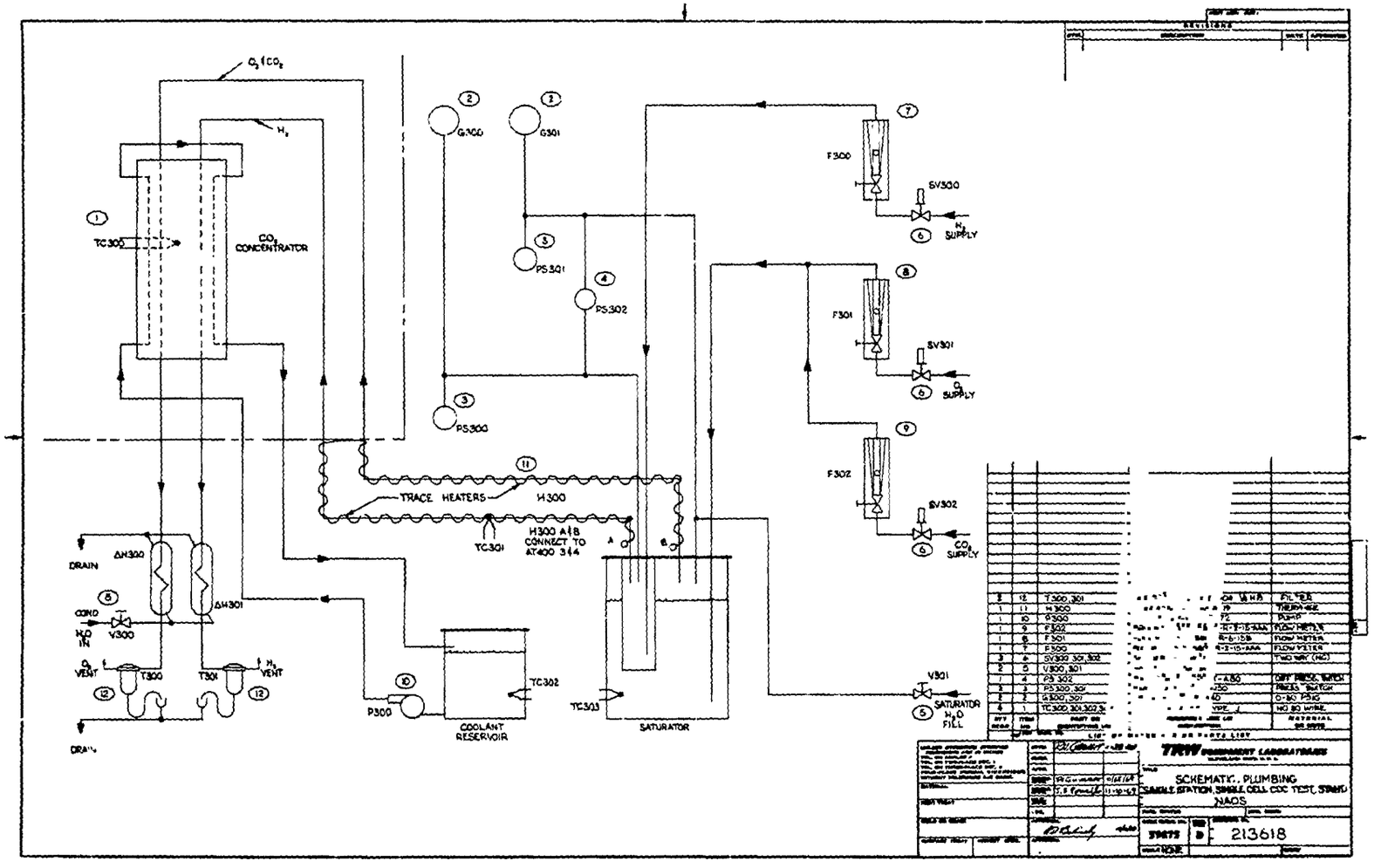

FIGURE 6 PLUMBING SCHEMATIC, SINGLE STATION, SINGLE CELL CDC TEST STAND

The control panels contain all gauges and valves necessary for control of gas pressure and flow (see Figure 7). All lines to the control panel are trace-heated and insulated to prevent condensation. The cells are mounted on a shelf directly in the rear of the control panel (see Figure 8).

The electrical system shown schematically in Figure 9 provides temperature and power control for the test stands. Circuits are included which will automatically shut the system down should any of the following malfunctions occur: oxygen-carbon dioxide, or hydrogen pressure over 25 psig, differential pressure over 15 psid between the gas cavities, and cell temperature over 200°F. If any of these malfunctions take place, the gas supplies are shut off by solenoid valves provided for this purpose. In case of a power failure, a set of holding contacts prevent a restart when power is restored. Override switches are provided for all shut-down modes. These may be employed for startup and any other situation where it is necessary to exceed an established shutdown limit.

On the parametric rig, temperatures are read out on two pyrometers whereas on the life rig one pyrometer and a thermocouple switch are used. Humidifier and coolant temperature control is provided by two ON-OFF controllers which maintain a temperature differential between the saturator tank and the coolant tank. This differential is adjustable from 0 to 15°F. On the life test stand the cell and humidifier temperatures are independently adjustable.

Cell load control on both systems was accomplished on the early test rigs by adjusting wirewound rheostates until the desired load is obtained. The load time meters are started whenever the load switch is actuated. Voltmeter bypass and shorting switches are provided to complete the cell control functions. The life stand includes three sets of load controls, i.e., voltmeter, ammeter, rheostat, elapsed time meter, and appropriate switches.

Test Rig Modifications. - Modifications were made to the carbon dioxide concentrator single cell parametric test rig and life test rig to decrease or eliminate service time and improve test rig performance. During life tests, the daily service requirement prior to modification was to empty the condensate traps located in the gas discharge lines from the cells. To eliminate this service requirement, U-tube overflow devices were installed on each of the condensate traps. To insure positive removal of moisture from the exit gases and eliminate backpressure buildup due to condensate accumulation downstream of the traps, water condensers were installed upstream of each of the four condensate traps. These water condensers are of simple concentric tube construction. Another highly desirable improvement for life testing of the single cells was to change the method of load control.

Initially, the loads for the single cell concentrators in the test rigs were variable power resistors. The cell currents varied as cell voltage varied. To eliminate these current fluctuations, constant current load circuits were designed for the test rigs.

The active control element in the constant current loads is a power transistor which must have at least two volts and preferably four or five volts across it to perform properly. A low voltage DC power supply is required in series with the transistor load control to provide this minimum voltage for the transistor as shown below.

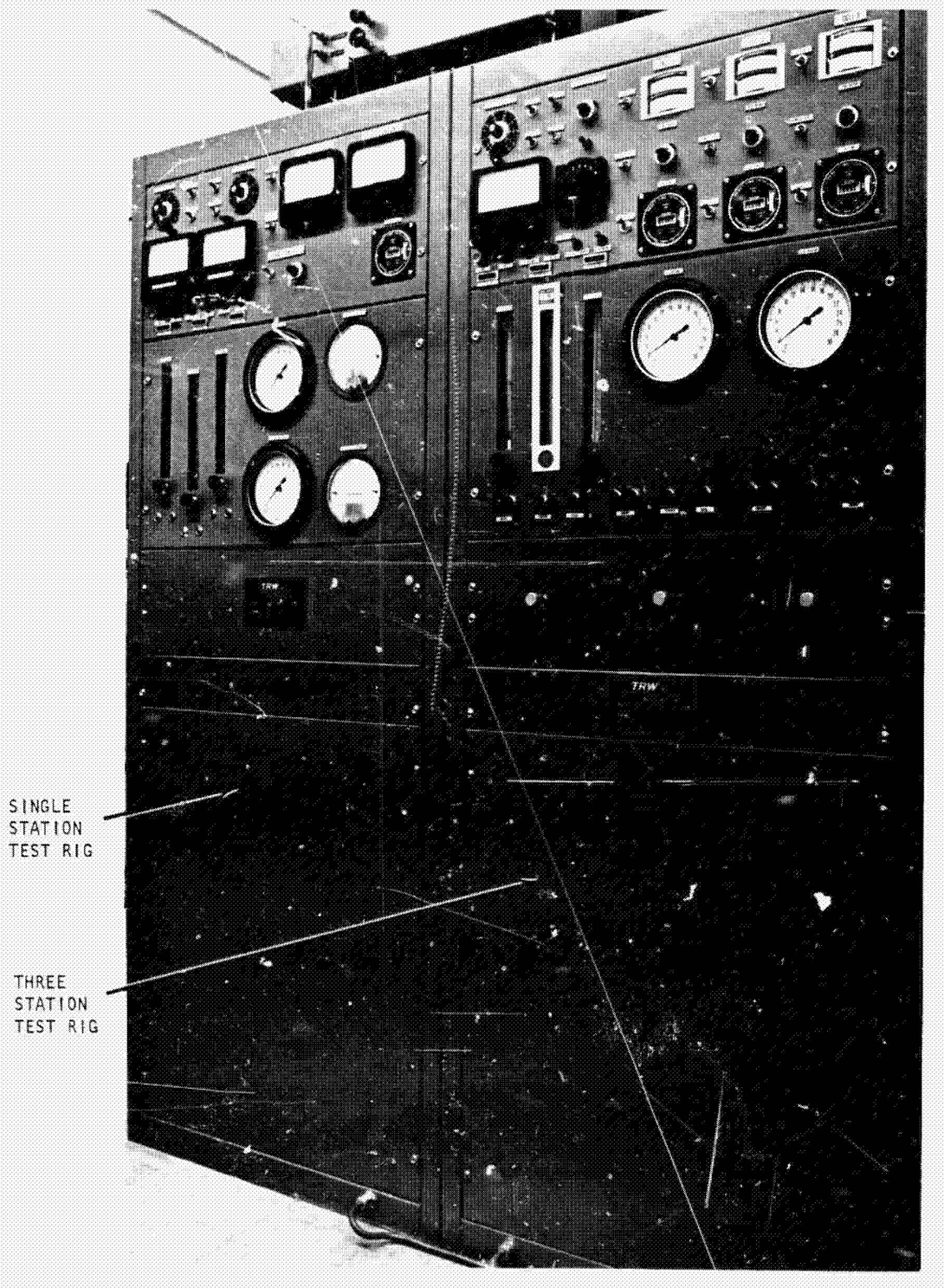

FIGURE 7 CO_2 CONCENTRATOR TEST RIGS, FRONT VIEW

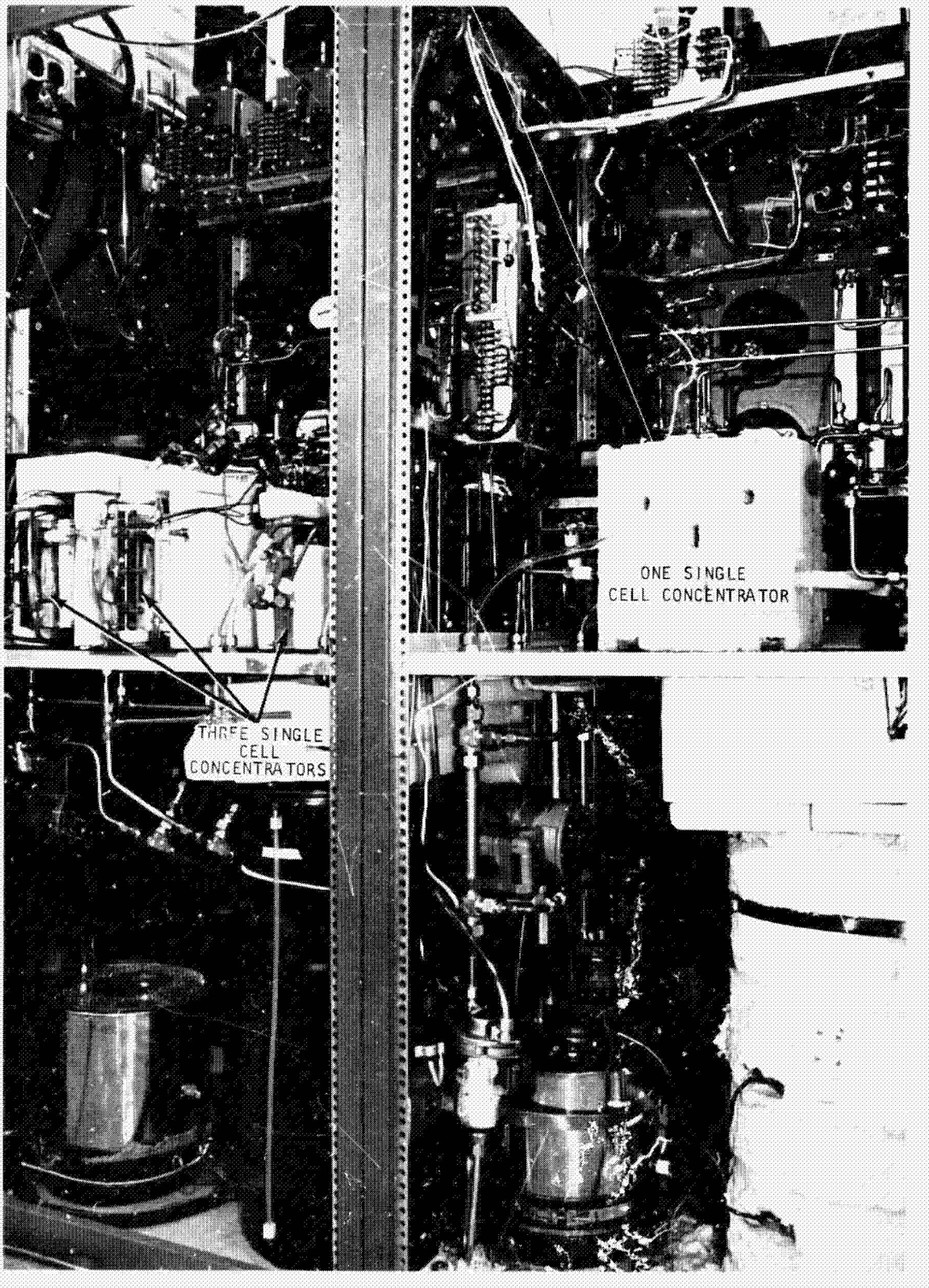

FIGURE 8 CO_2 CONCENTRATOR TEST RIGS, REAR VIEW

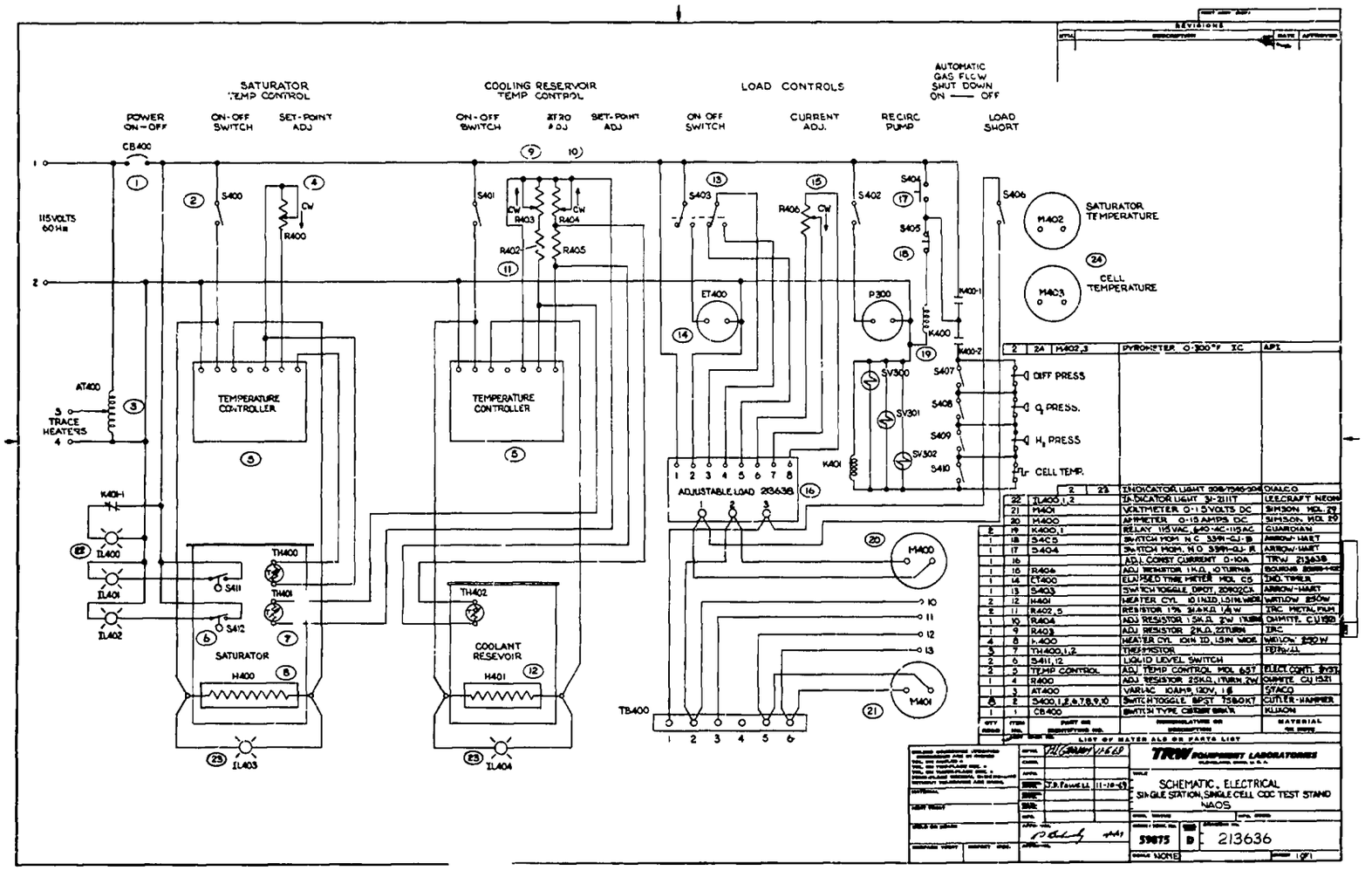

FIGURE 9 ELECTRICAL SCHEMATIC, SINGLE STATION, SINGLE CELL CDC TEST STAND

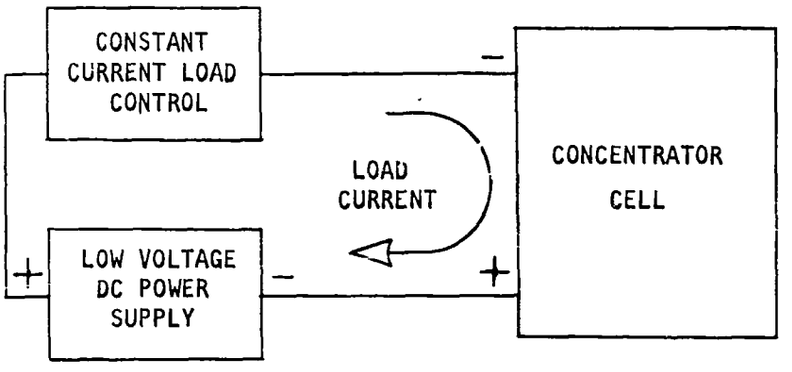

With this configuration, the concentrator cell voltage can vary down to zero with no change in cell current. The ratings of the new constant current loads are listed below.

1. Current: 0 to 10 amps
2. Voltage: -1 to +5 volts
3. Current regulation for oad voltage variation from 0 to 5 volts: 0.1%

One of the constant current loads was built and its performance verified. Figure 10 is a photograph of the first load control unit. Three additional units were built in order to have individual controls for each of the four single cell test stations.

Difficulty was also encountered in operating more than one single cell on the three-cell capacity life test stand. This was mainly due to maldistribution in the hydrogen flows. Originally this flow was designed to be of a parallel nature. Improper distribution resulted and series flow was attempted. This again caused undesirable conditions for downstream cells with respect to moisture balance and carbon dioxide content. The following modification eliminated the problem.

Parallel flow was accomplished by using fine metering valves with vernier handles to regulate the required hydrogen flows to the cells. To reduce the influence of downstream pressure fluctuations on individual flow rates, the pressure level upstream of these fine metering valves was maintained at 2-3 psi above cell pressure.

To improve general accuracy in gas flows in the life test stand, more accurate flow meters were used in place of the initial flow meters for the hydrogen, oxygen and carbon dioxide gases. During the modifications of both the para metric and life test stands, improvements, resulting from rerouting coolant or gas lines to improve fluid temperature controls were incorporated.

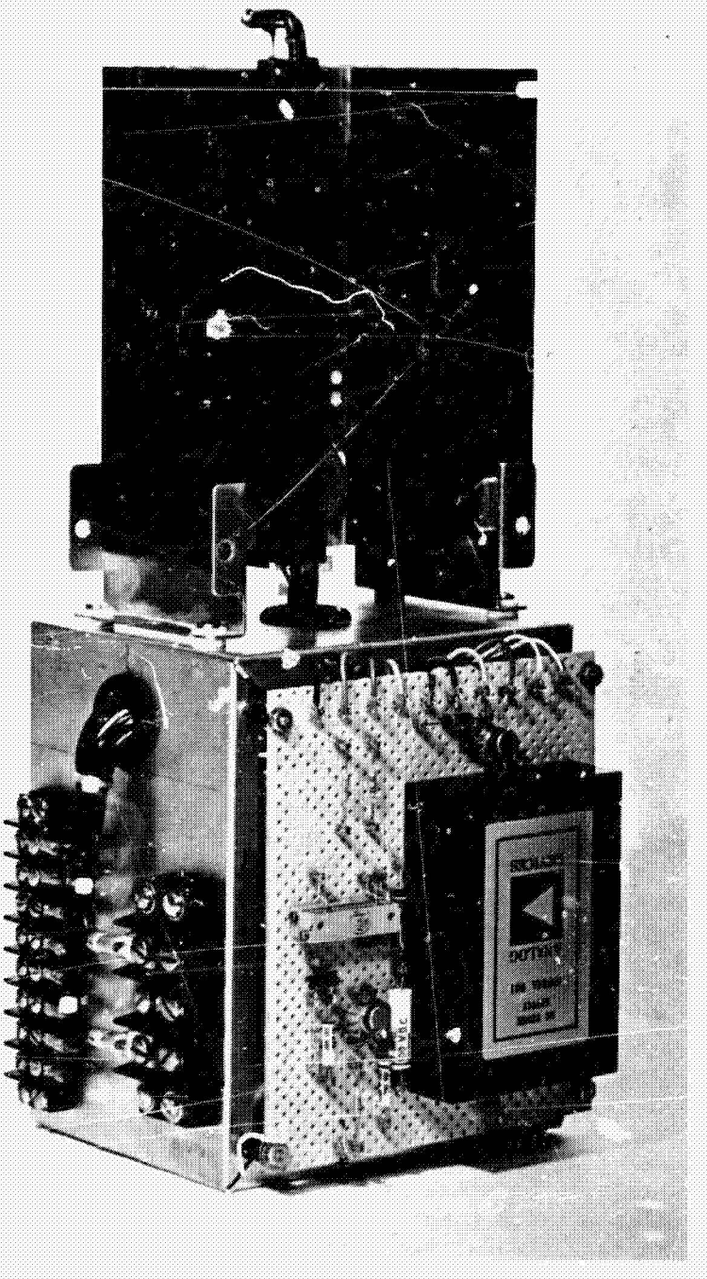

FIGURE 10 LOAD CONTROL - CO_2 CONCENTRATOR SINGLE CELL

Parametric Tests

Parametric tests of carbon dioxide concentrator single cells were conducted to provide information on system performance as a function of the parameters: pressure, temperature, flowrate (of oxygen, carbon dioxide and hydrogen) and current density. The two parameters of chief concern were: the carbon dioxide transfer rate and the maximum current density at which the cell could transfer carbon dioxide.

Two cells were assembled. The first used polysulfone end plates. This cell was used during the initial checkout of the test stand. During warm-up the cell failed due to a crossover. This was believed to be due to improper operation of the cell and humidifier temperature control. The cell temperature controller was subsequently altered to a differential temperature control. Figure 11 is a photograph showing the area in which the failure occurred. The darkened condition of the polysulfone pins indicates that the local temperature exceeded 700°F. The maximum temperature recorded was 105°F by a thermocouple approximately one inch from the darkened area. In an improved cell construction, a metal plate was included to allow better heat dissipation.

The failure of the polysulfone cell and subsequent disassembly suggested a cell design change which improved the cell. The redesigned cells closely duplicated the subsequent module design concept.

The second cell was constructed using nickel end plates. Electrical performance of this cell is illustrated in Figure 12. The curve from 0 to 30 amps per square foot is typical of the performance expected for NAOS. Carbon dioxide was supplied to the oxygen inlet stream at a rate equivalent to the transfer rate at 25 amps per square foot (ASF). Above 30 ASF the hydrogen flow rate was increased as noted in the figure, however, the carbon dioxide flow rate remained constant.

A Kordesh-Marko bridge was used to determine the potential drop attributed to internal resistance. The results show an internal resistance varying from 0.013 ohms to 0.018 ohms over a five-day period.

Test Results. - Initial testing included stand de-bugging, integration of monitoring equipment and operator familiarization. Parametric testing was then carried out followed by an extended period of nearly unattended operation. An overview of this period of testing leads to the following conclusions:

- Maintenance of proper cell water balance is critical and has the greatest effect on cell operation.
- The cell is rugged and easily recovers from such out-of-tolerance conditions as high pressure differential, low hydrogen feed, etc.
- Flushing the cell with fresh electrolyte restores original performance.

Changes in cell operating conditions generally result in slow performance changes. Much of the data scatter is attributable to not reaching a steady-state operating point.

FIGURE 11 POLYSULFONE CELL - POST-TEST CONDITION

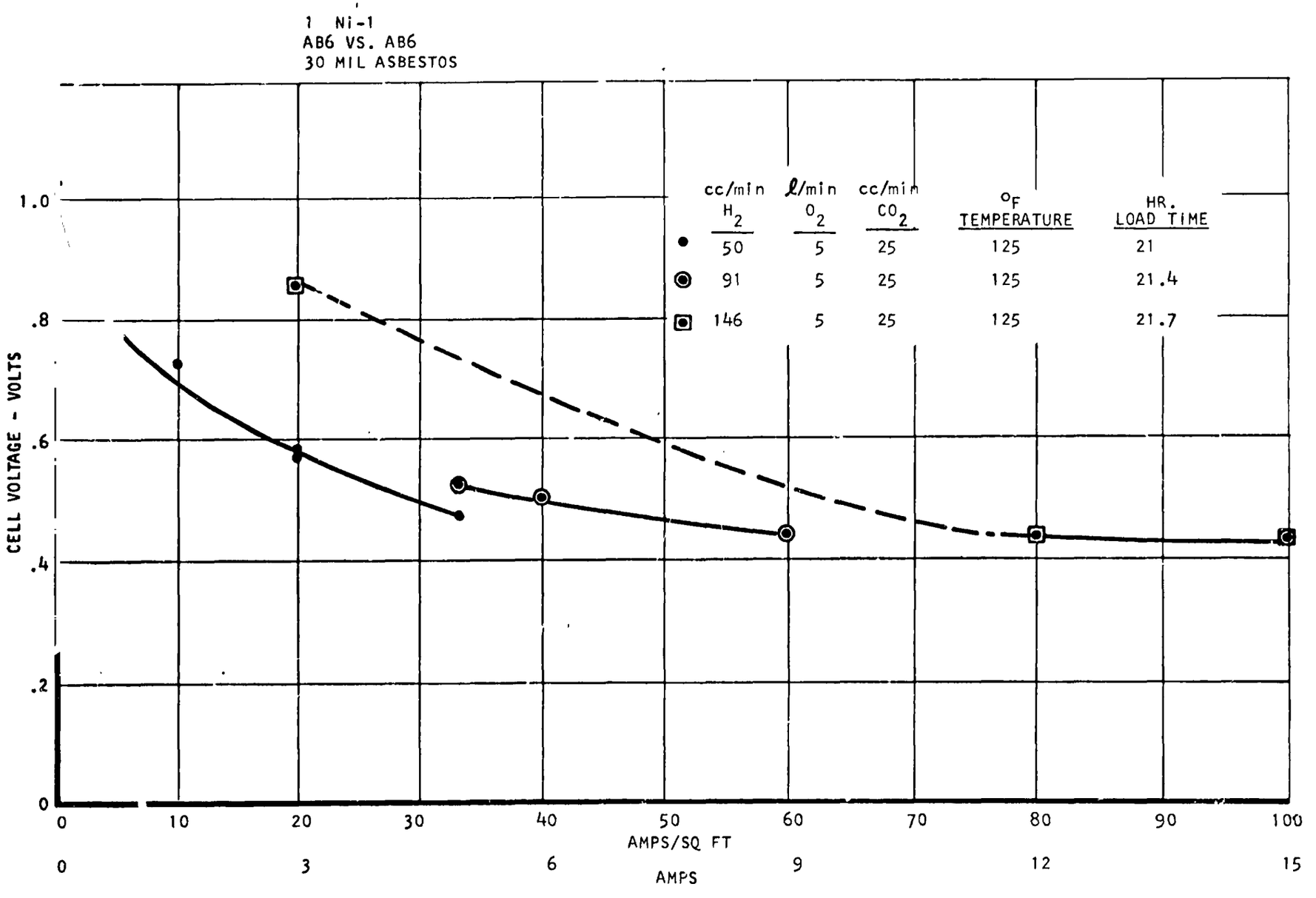

FIGURE 12 CO_2 CONCENTRATOR CELL POLARIZATION CURVE

The conclusions drawn from the parametric tests were tentative based on the small amount of data taken to cover a wide variation of many parameters. Parametric test results follow.

1. Pressure Variation. Reactant pressures were increased from 1 atm. to a maximum of 10 psig. This was an operating limitation imposed both by the stand and the reactant supply system. Cell voltage at constant current increased as expected. The carbon dioxide transfer rate data may be in error due to the speed with which the data was taken. The rig was not able to maintain a constant pressure for extended periods without constant adjustment. The results are summarized in Figure 13. In this figure and those following, the bars representing data shows the extent of the data spread; no bars represent single measurements. It was difficult to maintain steady pressure conditions at pressures above 5 psig and therefore, these data points are not considered to be accurate.

2. Flowrate Variation.
   A. Oxygen flowrate was varied over the range 2 standard liters/min. to 8.6 standard liters/min. while operating at constant current density, carbon dioxide feed rate, and hydrogen feed rate. This corresponds to operation at lower and lower carbon dioxide volume percentage in the oxygen (a volume percentage of 0.25% carbon dioxide was reached). The results, presented in Figure 14, indicate that the carbon dioxide level could be held at or below 0.25% if such an operating mode is desired. Oxygen flowrate above did not appear to significantly affect cell performance.

   B. Carbon dioxide flowrate was varied over the range of 21.6 standard cc/min to 57 standard cc/min, this also represents a change in the percent of carbon dioxide present in the oxygen entering the concentrator. The results shown in Figure 14, which shows an increasing carbon dioxide transfer rate with increasing carbon dioxide concentration, suggested a possible modification to the NAOS system. The pilot, who exhales air containing 3% carbon dioxide could cause circulation of this air through the concentrator by his normal breathing. The air, after passing through the concentrator, would be low in carbon dioxide concentration and could be recycled to the pilot. The circulating blower would be eliminated, increasing system reliability and lowering system weight, volume and power. Tests were performed in this mode on the laboratory breadboard system.

   C. Hydrogen flow was varied over the range 25 standard cc/min to 135 standard cc/min, while operating at constant current, pressure, carbon dioxide and oxygen flowrates. The results are summarized in Figure 15. The trend observable in the transfer rate curve was not expected. Further data was obtained from the module testing to supply more information to define the effect of hydrogen flow.

3. Temperature Variation. Cell temperature was varied over the range of 105°F to 125°F while operating at constant current, pressure, and gas flowrate. Cell voltage increases with increasing temperature as expected. The data point at 150°F occurred after the 105°F point and was not maintained for a sufficient

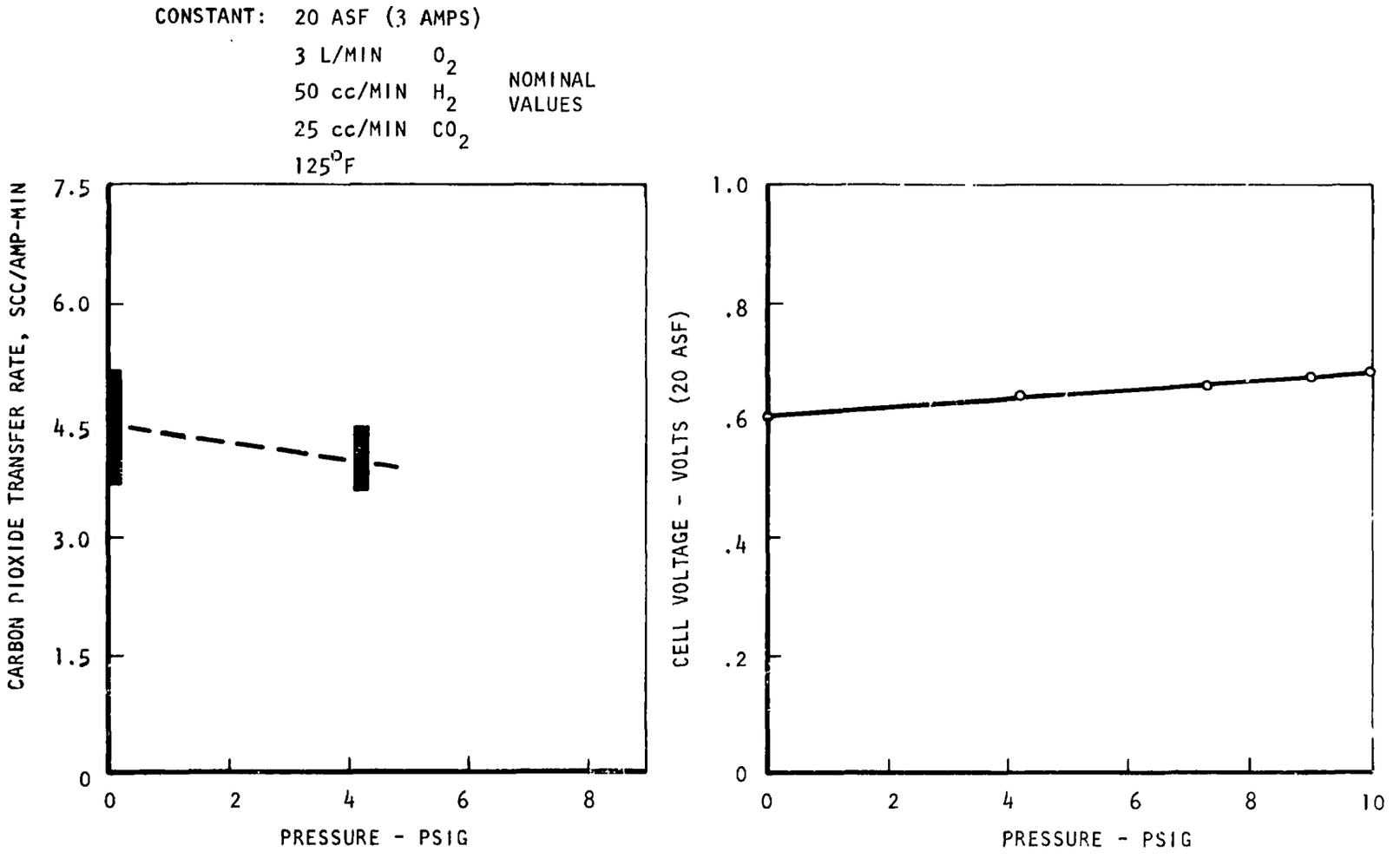

FIGURE 13 CO_2 CONCENTRATOR
SINGLE CELL PARAMETRIC TEST-VARIATION OF REACTANT PRESSURES

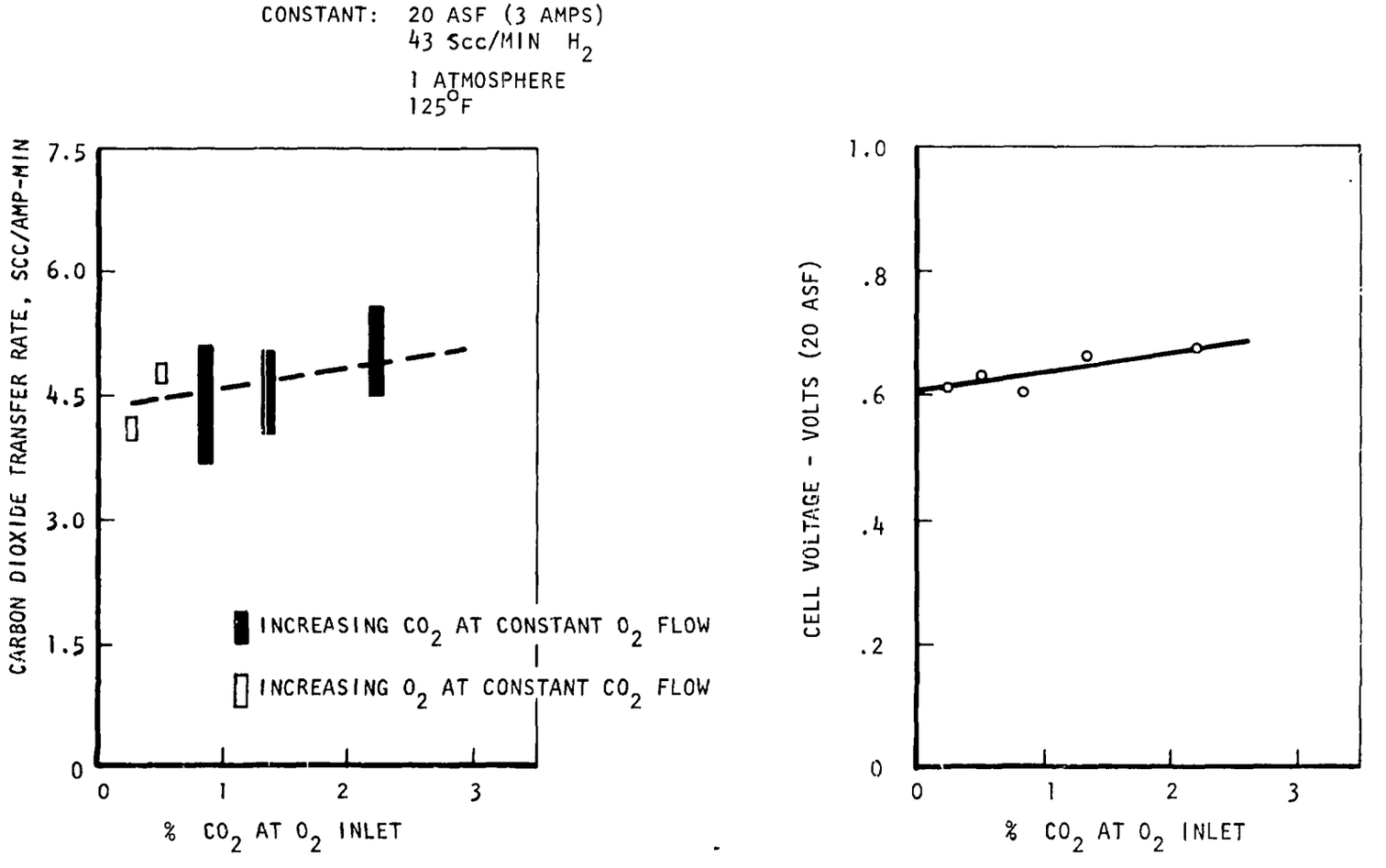

FIGURE 14 CO_2 CONCENTRATOR
SINGLE CELL PARAMETRIC TEST-VARIATION OF CO_2 % AT O_2 INLET (O_2 FLOW RATE AND CO_2 FLOW RATE VARIABLE)

CONSTANT: 20 ASF (3 AMPS)
2.6 SL/MIN O_2
21.6 Scc/MIN CO_2
1 ATMOSPHERE
125°F

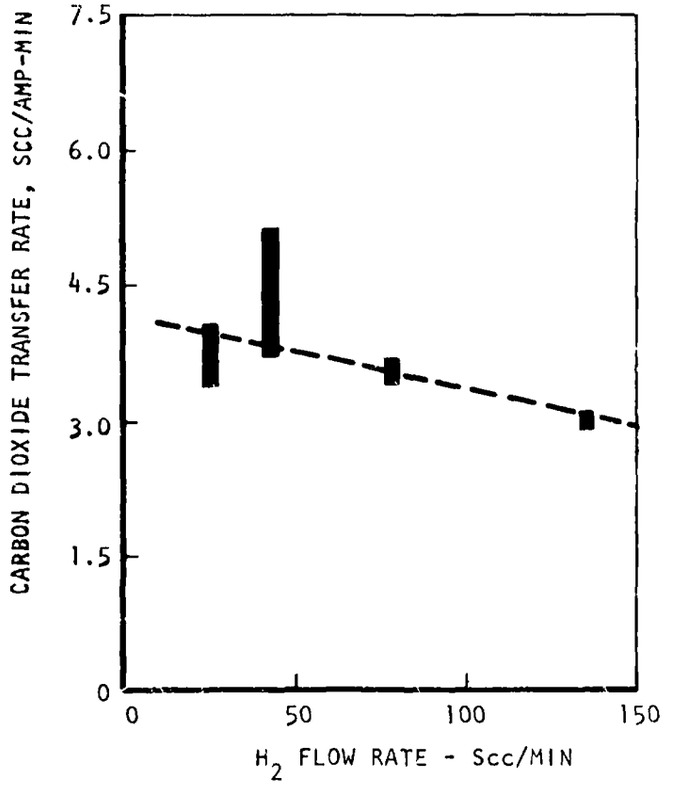

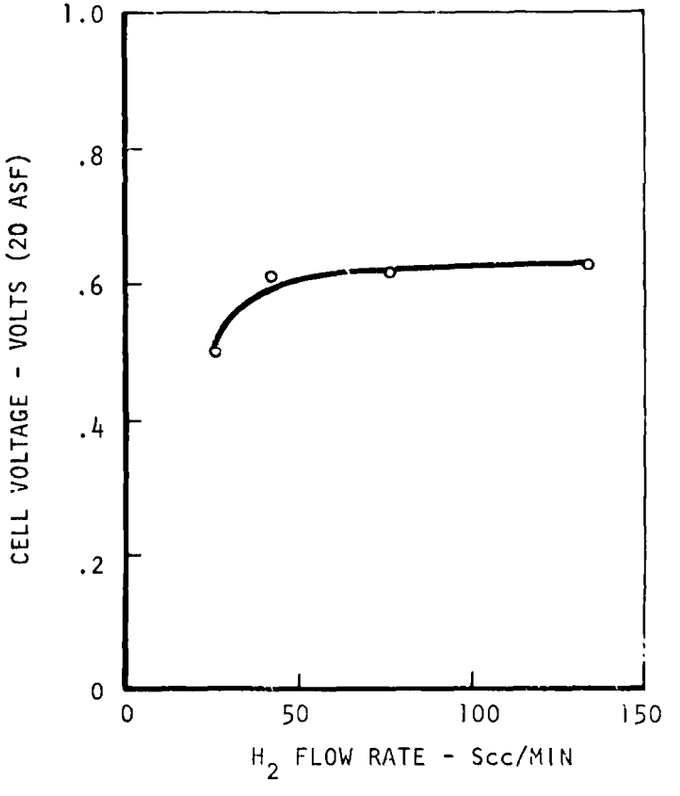

FIGURE 15 CO_2 CONCENTRATOR
SINGLE CELL PARAMETRIC TEST-VARIATION OF HYDROGEN FLOW RATE

length of time to obtain a chromatograph reading. It is also suspected that the voltage had not reached its equilibrium point. A trend was evident in the carbon dioxide transfer rate, decreasing with increasing temperature. The results are presented in Figure 16.

4. Current Density Variation. Current density was varied over the range 20 amperes per square foot (ASF) to 100 ASF while attempting to maintain the flowrate of hydrogen, oxygen and carbon dioxide in a constant relationship. Due to a test rig limitation on carbon dioxide flowrate, this was not possible at current densities higher than 70 ASF. This is indicated in Figure 17 by the solid line which breaks at 70 ASF. Since sufficient carbon dioxide could not be supplied to the cell it is possible that this was the reason the transfer rate is low.

Another explanation is that the variation of transfer rate is primarily due to the hydrogen flow which occurred as the current decreased giving the effect shown in Figure 14.

5. Special Tests. The redesigned polysulfone cell shown in Figure 3 was tested in the parametric test rig. This testing verified that the flow passages created by the expanded metal did not create a noticeable pressure differential at the flowrates expected in the ten-cell module. The differential pressure observed at 3 sl/min of oxygen averaged 1.5 inches of water. At 50 scc/min of hydrogen no pressure drop was observed, using a gauge having a maximum pressure measurement of 2 inches of water. Both results were identical to those obtained with the pin structure cells.

It should be noted that all single cell parametric testing was accomplished using the K_2CO_3 electrolyte prior to the switch to cesium carbonate electrolyte.

CONSTANT: 20 ASF (3 AMPS)
2.6 L/MIN O_2
43.0 Scc/MIN H_2
21.6 Scc/MIN CO_2
1 ATMOSPHERE

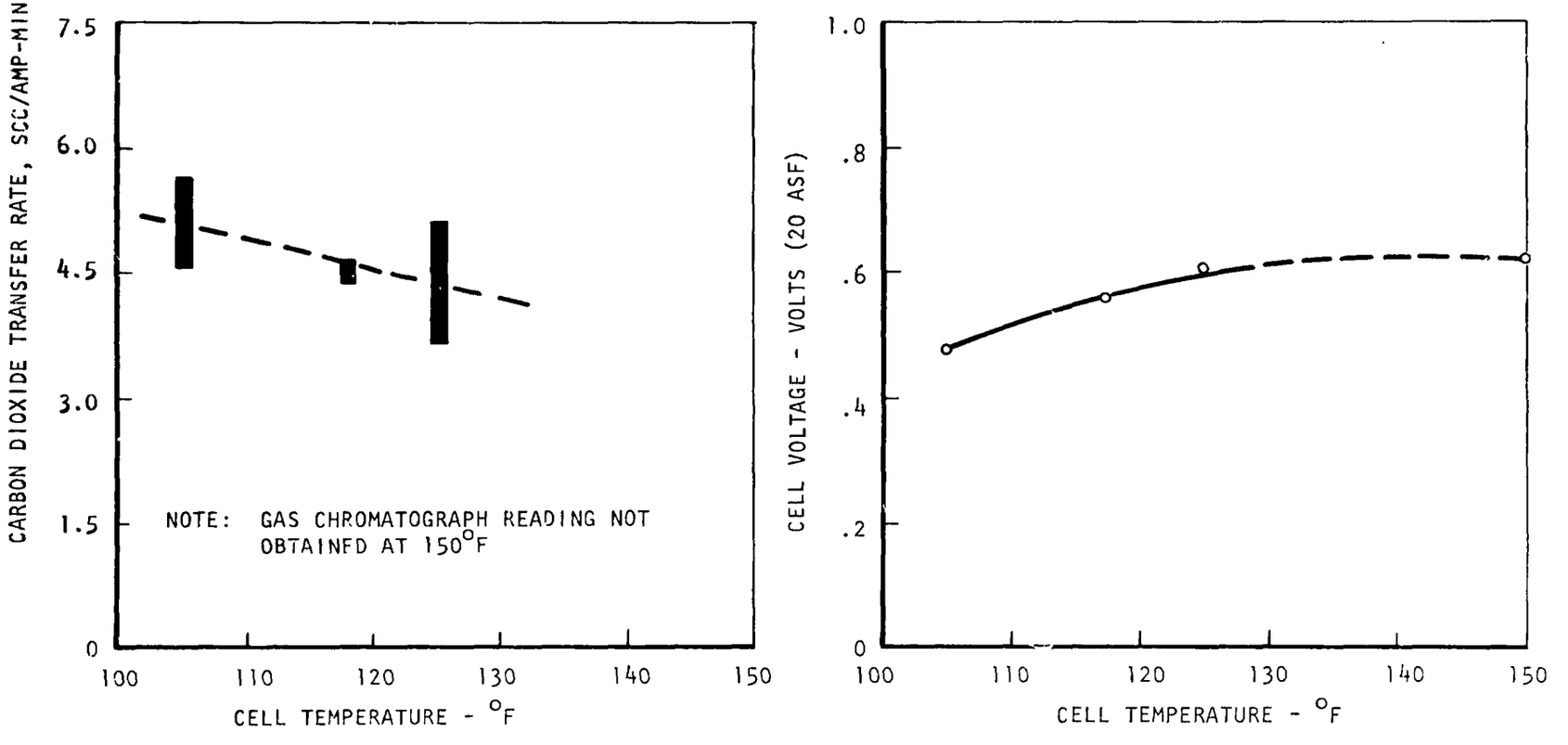

FIGURE 16 CO_2 CONCENTRATOR
SINGLE CELL PARAMETRIC TEST-VARIATION OF CELL TEMPERATURE

CONSTANT: 1 ATMOSPHERE
125°F

VARIABLE FLOW RATES

O_2: .87 TO .46 SL/AMP-MIN

H_2: 14.3 TO 10.3 Scc/AMP-MIN

CO_2: 7.2 TO 4.6 Scc/AMP-MIN

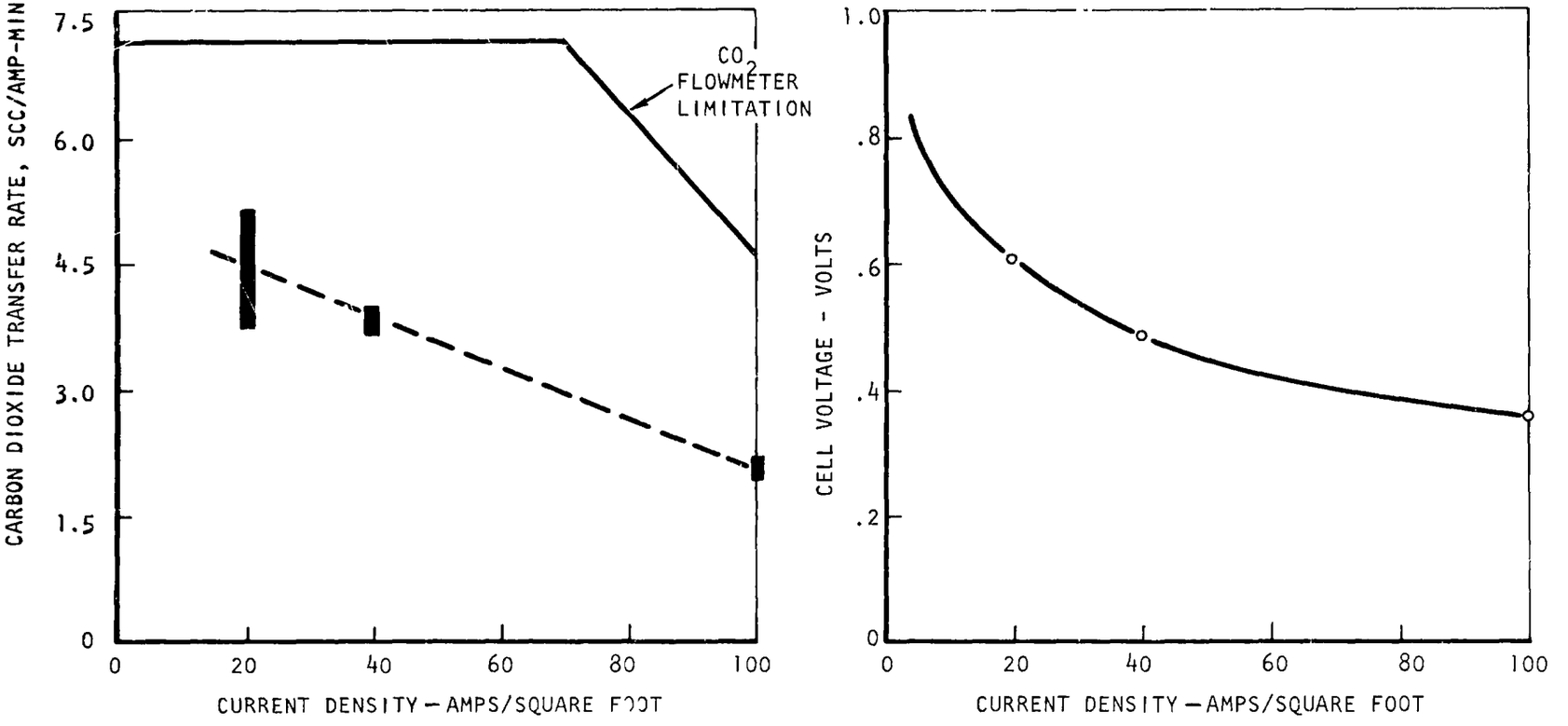

FIGURE 17 CO_2 CONCENTRATOR
SINGLE CELL PARAMETRIC TEST-VARIATION OF CURRENT DENSITY

CARBON DIOXIDE CONCENTRATOR MODULE - DESIGN I

Design Objectives

One of the objectives in the development of the on-baord aircrew oxygen generating system was to design, fabricate and test a full-scale laboratory model of a 0.12 lb/hr carbon dioxide concentrator module, ucilizing air-cooled fins for heat removal and the associated oxygen recycle loop with blower.

The design philosophy was to verify design concepts and module performance. Therefore, carbon dioxide transfer rate was not maximized nor were cell thickness and weight minimized.

Cell design was governed by the general design requirements as listed in Table II.

Moaule Design

A large portion of the module design had been accomplished prior to the initiation of the single cell parametric testing. The tests did, however, affect the module design in the following ways:

- The total active area was cut from 5 square feet to 2.5 square feet (or from 20 cells to 10 cells)
- The standard operating current density was increased from 20 ASF to 30.4 ASF

The first change is important for the module weight, volume, and costs are reduced while increasing the system reliability. The second change was reflected in the amount of silver used for heat transfer and in the design of the test rig electrical system.

Details of module construction can be explained by referring to Figure 18, a schematic of a single cell, ten of which make up a module, and Figure 19, a photograph of the cell components with the components called out. A module capable of transferring 0.1 lbs of carbon dioxide per hour is created by stacking ten cells in series. The module is completed by thermal (and electrical) insulation and end plates. Silver was finally selected for the gas cavity material and for the heat removal (current collector) plates

A computer program was written to aid in the design of the oxygen and hydrogen manifolds. This program computes the pressure drop through a tube of given length. A pressure drop 1/100 of the computed value is demanded for the manifold and then the hydraulic diameter of the manifold is computed. Such a pressure relationship insures that each cell will receive its share of the flow.

Pressure drop versus the number of inlets to each cell and the diameter of each inlet is presented in Figure 20 for the oxygen system and Figure 21 for the hydrogen system. Selection of seven inlet holes of 50-mil diameter for

TABLE II

CO_2 CONCENTRATOR MODULE DESIGN REQUIREMENTS

DESIGN REQUIREMENT	
CO_2 Transfer Rate	0.1 lb/hr (0.42 sl/min)
CO_2% at Pilot Return	0.5%

DESIGN OPERATING CONDITIONS	
CO_2 Transfer Rate	0.117 lb/hr (0.45 sl/min)
Current Density	30.4 ASF (7.6 amperes)
Hydrogen Feed Rate	1.7 sl/min
O_2 Circulation Rate	3.5 CFM @ 2 inches of water
Temperature	120°F

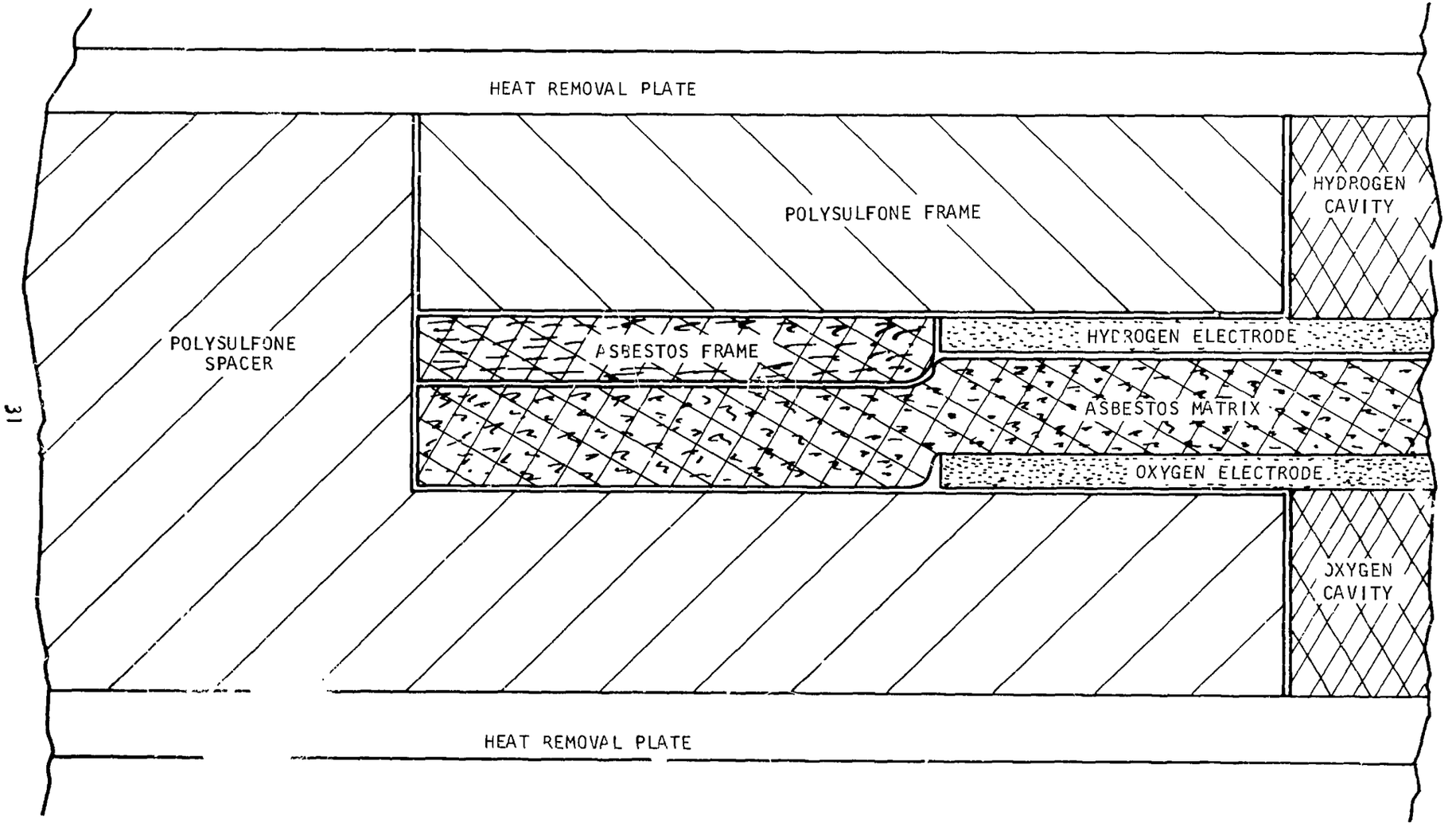

FIGURE 18 CO_2 CONCENTRATOR MODULE CELL CONSTRUCTION SCHEMATIC

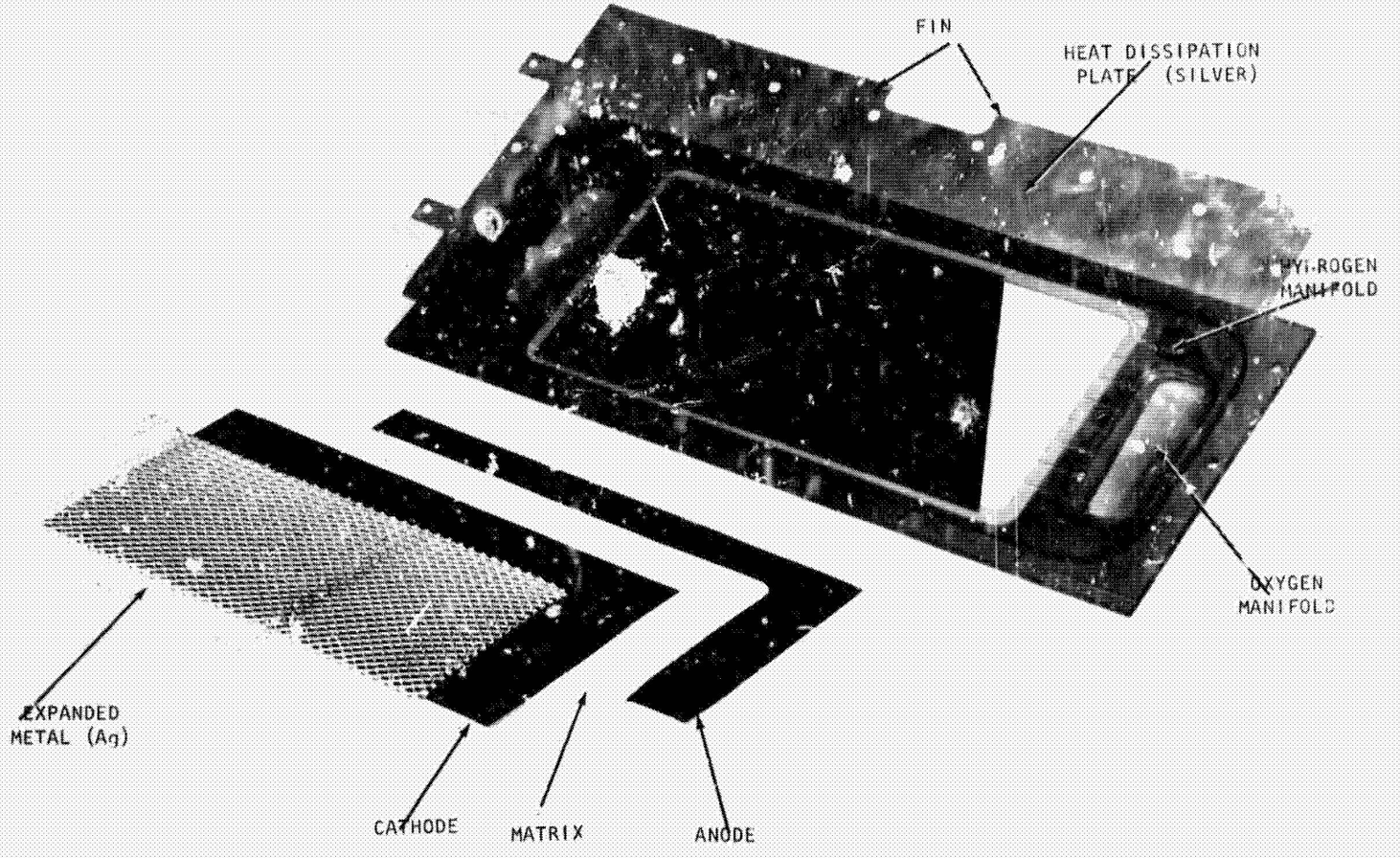

FIGURE 19 CO_2 CONCENTRATOR MODULE CELL COMPONENTS

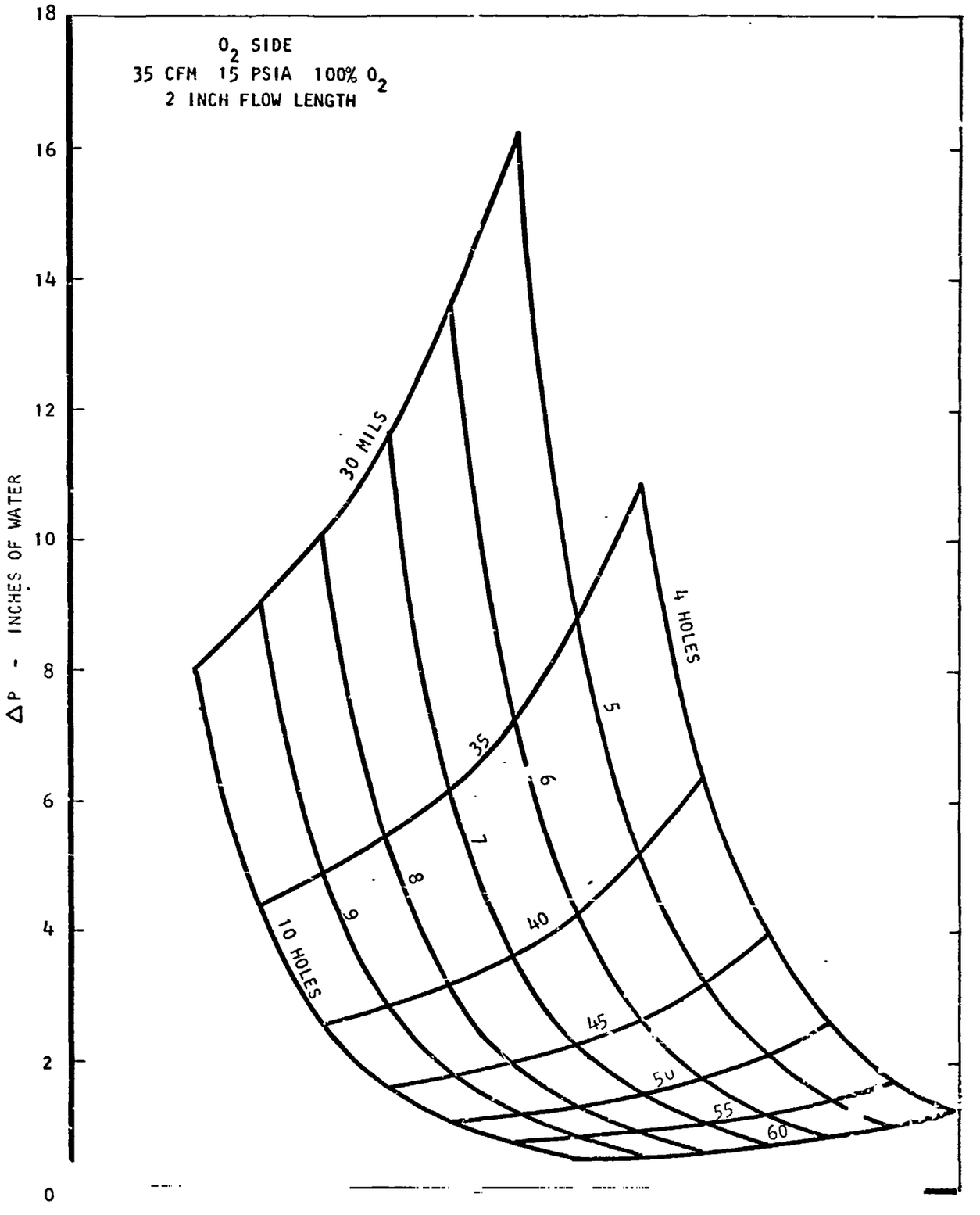

FIGURE 20 CO_2 CONCENTRATOR MODULE O_2 SIDE-PRESSURE DROP CHARACTERISTICS

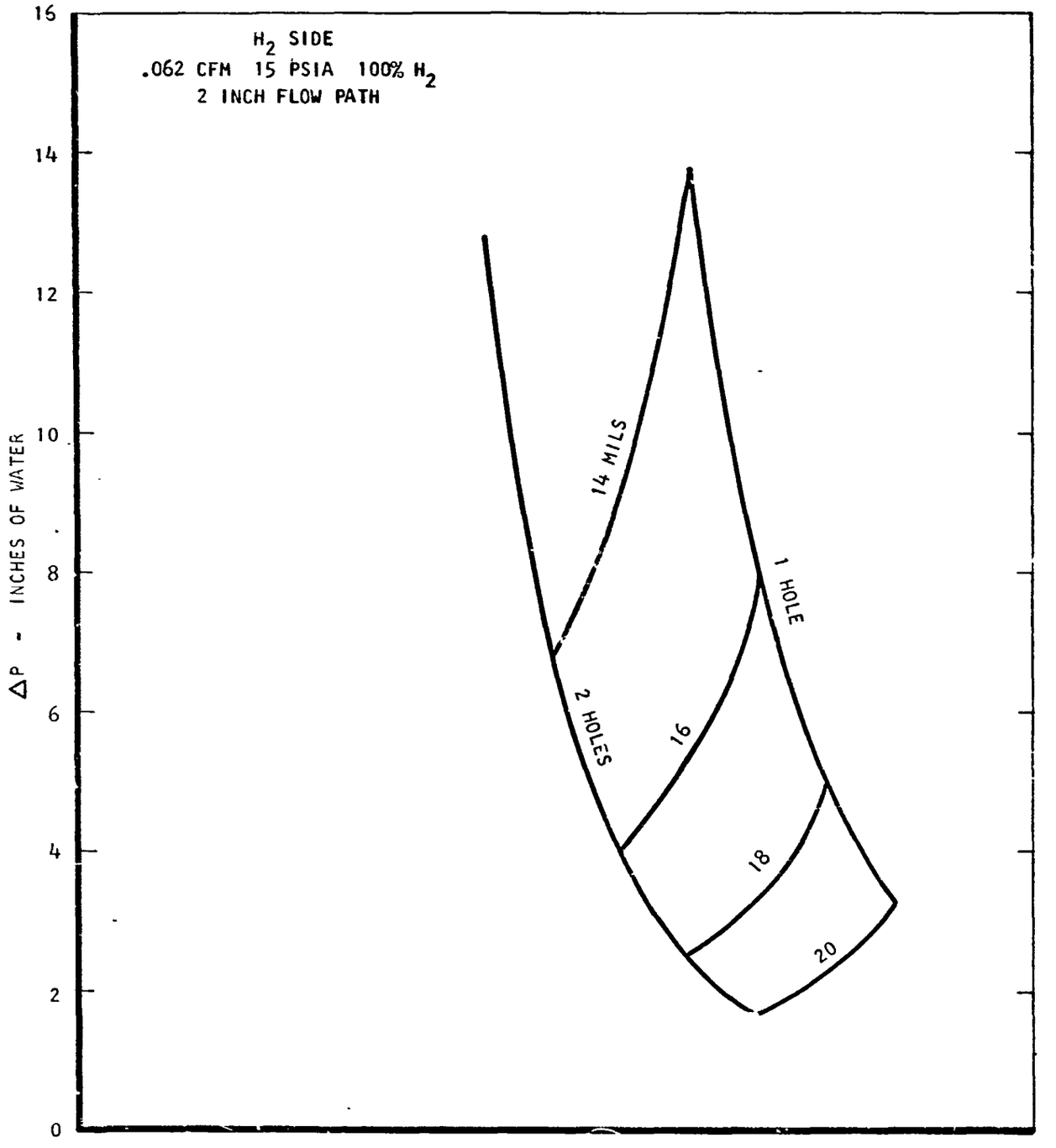

FIGURE 21 CO_2 CONCENTRATOR MODULE H_2 SIDE-PRESSURE DROP CHARACTERISTICS

the oxygen system requires a manifold hydraulic diameter of greater than 1.1 inches. Pressure drop should not exceed two inches of water. One inlet of 22-mil diameter was chosen for the hydrogen system. A hydrogen manifold diameter greater than 0.296 inches produces the proper pressure drop relationship. Total pressure drop should be less than 2.25 inches of water. A thermal analysis was performed to establish the heat removal requirements and provide a design baseline. Results are summarized in Table III. A stress analysis was performed to establish a design baseline. The results are summarized in Table IV.

A summary of the initial module design is given in Table V. Parts were fabricated to the drawings listed in Table VI. No special tools or techniques were required. Figure 22 shows the module as initially designed, fabricated and assembled.

Design Modifications

The carbon dioxide concentrator previously described and fabricated underwent 212 hours of parametric testing. During this test period it became apparent that a design modification was required to improve the flow distribution of the hydrogen gas. Figures 23 and 24 illustrate the original manifolding arrangement and the modified arrangement. In the original design, hydrogen entered a manifold and flowed in parallel through the cells. It was anticipated that an even distribution of flows would result by making the resistance to flow very large at the inlet to each cell and very small in the manifold area. Flow restrictors with hydraulic diameters of 22 mils and 11 mils were tried. In both cases hydrogen flow maldistribution was evident after short periods of operation.

In the modified design, hydrogen flows in a single series path through the ten cells. Each cell uses a portion of the hydrogen and adds a small amount of carbon dioxide before it enters the next cell. Thus, the first cell receives pure hydrogen and the last cell receives approximately 70% hydrogen and 30% carbon dioxide. Stable performance was obtained using this series flow pattern with the ten-cell modules tested.

This configuration was used in conducting the parametric tests as reported in this report. However, long-term moisture balance problems were encountered in long duration operation.

To increase the tolerance of the carbon dioxide concentrator to environmental changes, a hydrogen humidity exchanger was designed and assembled as an integral part of the concentrator stack. The configuration is shown schematically in Figure 25. Hydrogen enters the first cell after passing through two humidity exchange cells and then flows on in series to the other nine cells. The gas which leaves the tenth cell is recycled to the humidity exchanger. The humidity exchange cells are identical in construction to the concentrator cells. Polypropylene screen can be used in place of electrodes to provide support to the asbestos matrix. The asbestos is loaded with K_2CO_3 electrolyte at the same time as the concentrator cells and thus contains the same concentration at the beginning of the operation. The addition of the humidifier cells did not provide the desired moisture balance and control. These cells were eliminated and further tests were conducted with the configuration of Figure 24.

TABLE III

CO_2 CONCENTRATOR MODULE THERMAL CHARACTERISTICS

Cell Waste Heat at Design Point (30.4 ASF, 0.4 volts)	24.5 BTU/hr
Temperature Drop across Electrode Region	3.44°F
Temperature Drop to Midpoint	3.67°F
Heat Conductor Plate Thickness	0.02 inches pure Ag
Temperature Rise in Cooling Air	10°F
Required Air Flow Rate	22 CFM/20 cell stack
Temperature Difference between Fin and Inlet Air	18°F

TABLE IV

CO_2 CONCENTRATOR MODULE STRESS ANALYSIS SUMMARY

Assumed Maximum Pressure Difference - internal to external		15 psi
Bolt Spacing (maximum)		2 inches
Plastic Spacer		
	Stress	
Shear	25 psi	
Bearing	200 psi	
Bending	249 psi with 0.5 mil deflection	
Metal Plate		Margin of Safety
Shear	1300 psi	2.1
Bearing	3020 psi	2.3
Tear Out	338	78

TABLE V

CO_2 MODULE DESIGN SUMMARY

CO_2 Process Rate	0.12 lb CO_2/hr
Operating Current Density	30.4 amps/ft^2
Operating Temperature	110°F
Electrolyte	28 wt% K_2CO_3
Active Electrode Area/Cell	0.25 ft^2
Electrodes	AB-6
Asbestos	30 mil
Gas Cavity Material	60 mil expanded silver
Spacer Material	Polysulfone
Heat Removal Plates (Current Collectors)	20 mil Ag
Seals	Ethylene Propylene O-Rings
Approximate Module Size (without accessories)	7" x 13" x 3.1"
Approximate Module Weight	33 lbs

TABLE VI

NAOS CO_2 CONCENTRATOR MODULE PARTS LIST

Item No.	Quantity Required	Drawing No.	Description	Material
1	9	817369	Plate - Heat Removal	Silver
2	10	817351	Spacer	Polysulfone
3	20	817334	Electrode	AB-6
4	10	817335	Matrix	30 Mil Asbestos
5	10	817336	Frame - Electrode	30 Mil Asbestos
6	10	817333	Frame - H_2 Cavity	Polysulfone
7	20	817435	Current Collector	Silver
8	20	817395-8	O-Ring #5-464	E540-8
9	20	817395-9	O-Ring #5-805	E540-8
10	24	817395-10	O-Ring #5-616	E540-8
11	1	817436	Insulation - Top	Polypropylene
12	1	817382	Plate - Bottom	Silver
13	1	817437	Insulation - Bottom	Polypropylene
14	1	817394	Endplate - Bottom	Stainless Steel
15	1	817393	Endplate - Top	Stainless Steel
16	18	817395-16	Sleeve	Teflon
17	18	817438	Bolt	Steel
18	52	817395-18	Washer - Flat	Stainless Steel
19	18	MS21044C04	Nut, Self-Locking	
20	4	817439	Cover, Side	G-11 Phenolic Silicone Foam Rubber
21	16	817395-21	Screw, Machine - Round Head	#4-48 x 0.38" lg
22	16	817395-22	Washer, Lock	
23	1	817395-23	Thermoswitch	Fenwall #32411-0
24	2	817395-24	Screw, Machine-Round Head	#4-40 x 0.18" lg
25	1	817472	Plate - Top	Silver
26	4	817395-26	O-Ring #5-758	E540-8
27	36	817395-27	Washer, Fiber	
Assembly Drawing		817395		

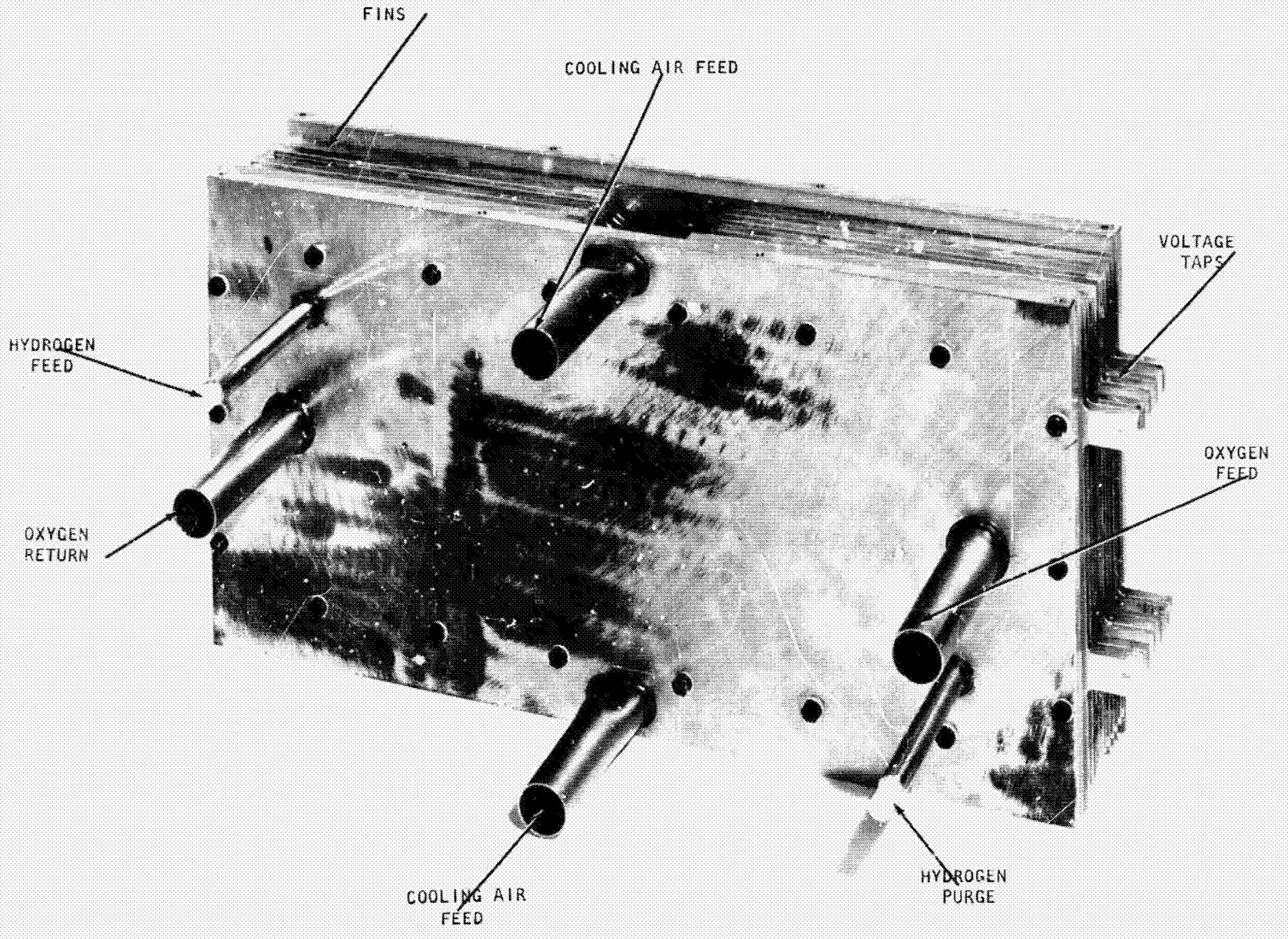

FIGURE 22 CO_2 CONCENTRATOR - 10 CELL MODULE

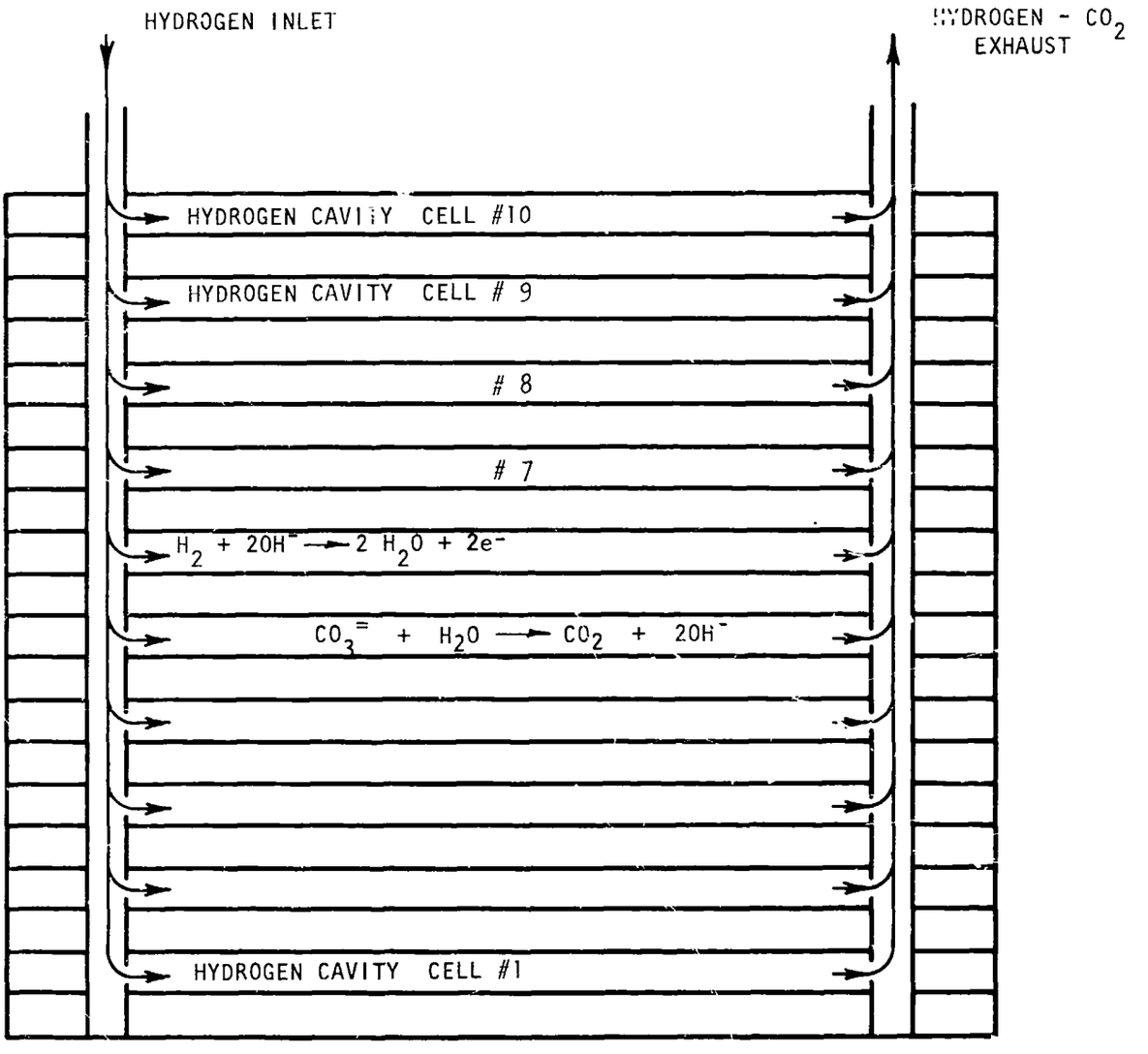

FIGURE 23 HYDROGEN MANIFOLD - ORIGINAL DESIGN

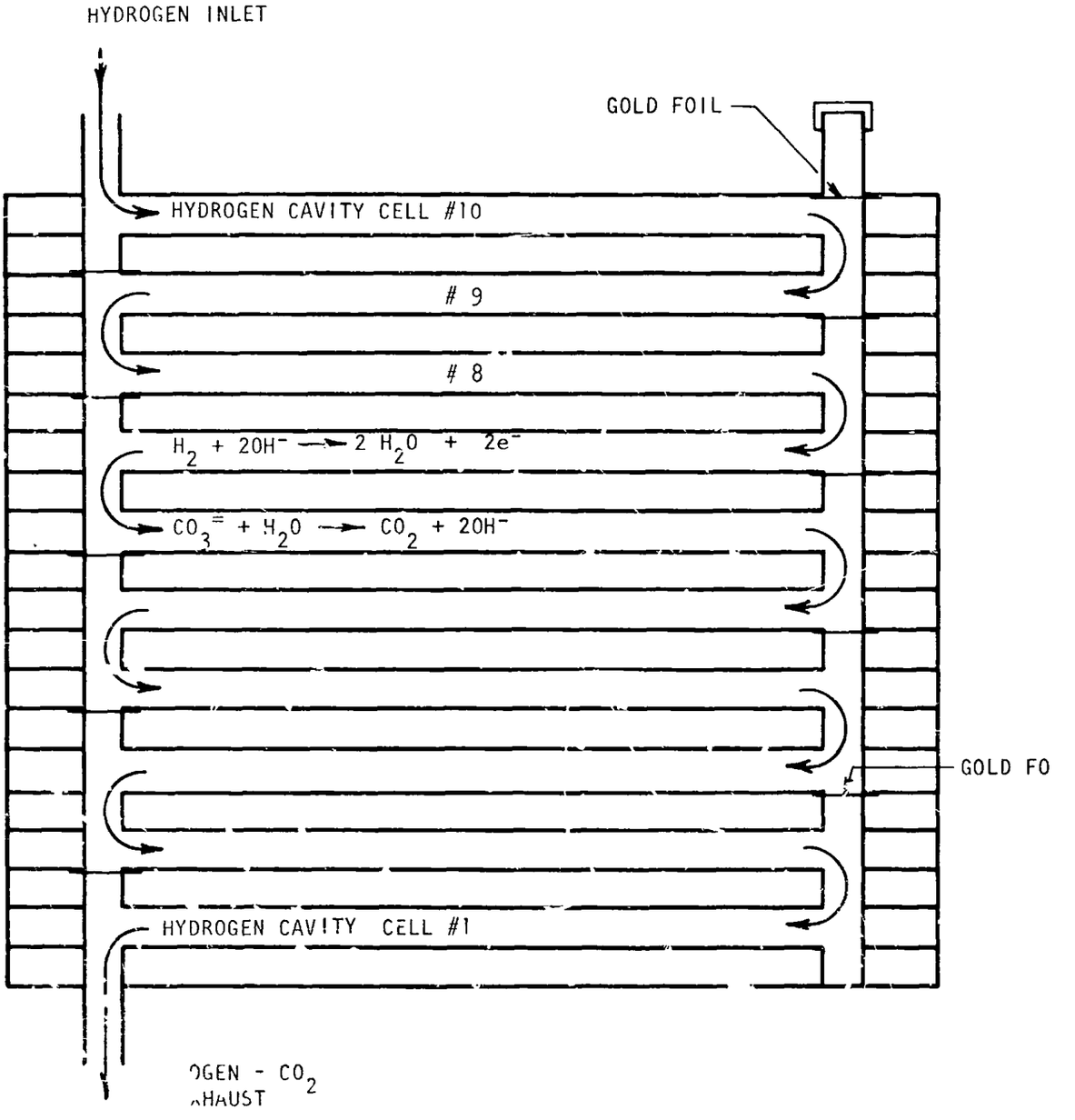

FIGURE 24 HYDROGEN MANIFOLD - SERIES HYDROGEN FLOW

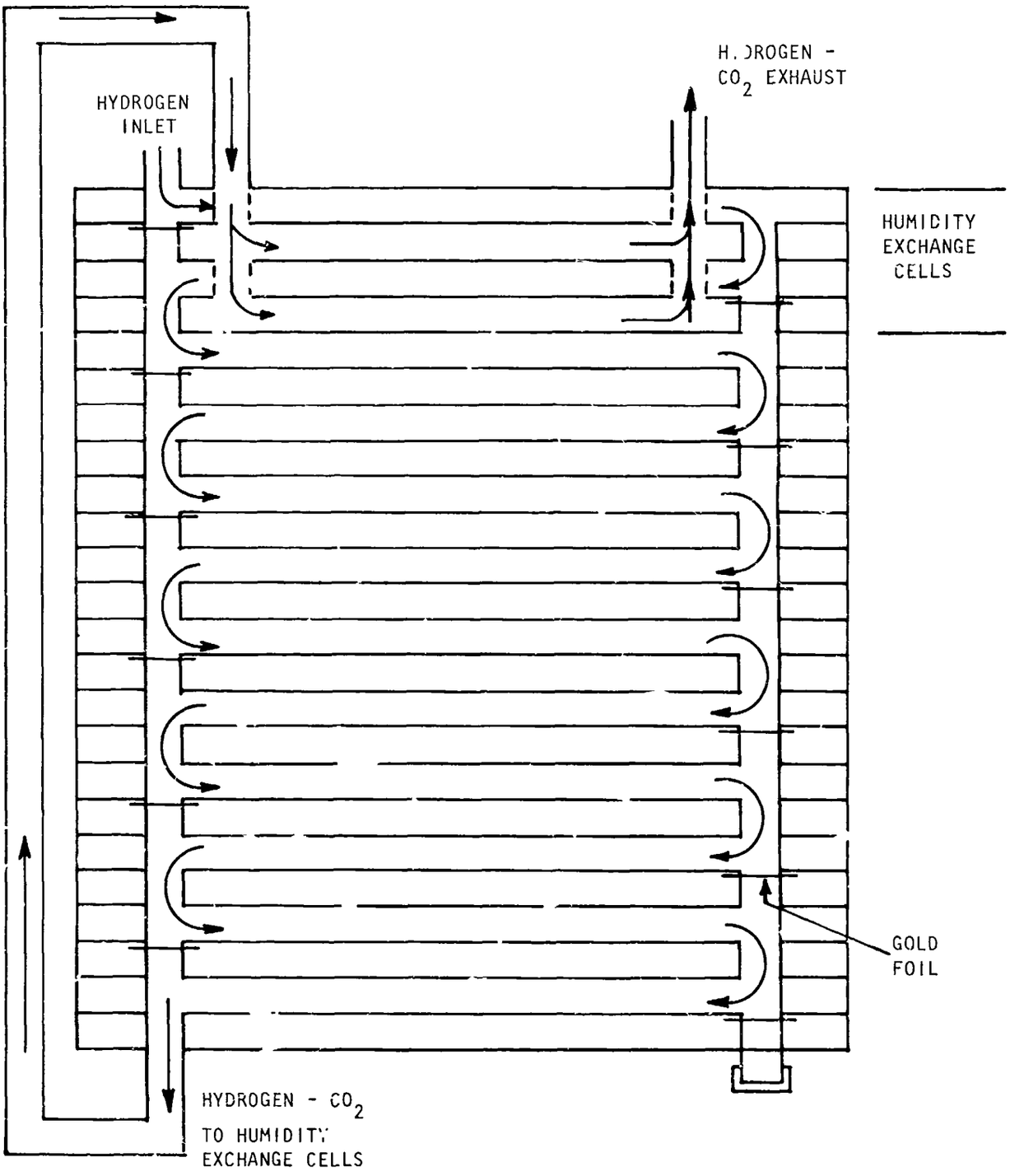

FIGURE 25 HYDROGEN MANIFOLD - SERIES FLOW WITH HUMIDITY EXCHANGE CELLS

Experience with the carbon dioxide concentrator has identified a problem associated with the water balance within the concentrator for long term continuous operation. The water that is formed as a result of the oxygen-hydrogen reaction is removed from the module, primarily, by the breathing gases and also by the hydrogen-carbon dioxide mixture leaving the concentrator.

In order to maintain equilibrium operating conditions, the net water loss must equal the water formation. Changes in breathing flowrates require changes in cell operating temperatures in order to maintain this balance. Studies were conducted, first, to measure and control the cell electrolyte concentration and, second, to determine methods to increase the cell tolerance to out-of-balance conditions. These studies are discussed in detail in the Design II module description.

CONCENTRATOR MODULE TEST RIG

Ten-Cell Module Configuration

The purpose of the carbon dioxide concentrator module test rig was to provide a system in which the NAOS carbon dioxide concentrator's performance could be mapped in various modes of operation.

Schematics are shown in Figures 26, 27 and 28 for the test rig configuration used in the 10-cell module testing.

Figure 26 is the schematic of the plumbing network necessary to support the ten-cell module operation. The module test system interface is shown by the breaks in the lines connected to the module. The recirculating oxygen loop consists of 3/4" O.D. tube simulating rebreather loop operation. The oxygen is circulated by a blower which is controlled from the console. This control allows the oxygen recirculation rate to be varied. In order to control electrolyte concentration in the cell, a heat exchanger was installed in the recirculating loop. Concentration control is accomplished by controlling the heat exchanger liquid coolant temperature at the desired oxygen dew point. As oxygen and carbon dioxide are consumed by the cell and vented through the bleed valve, the pressure level is maintained by the oxygen regulator. Carbon dioxide flow into the loop is controlled by a constant flow device in conjunction with a rotameter. Hydrogen flowrate is similarly controlled and monitored. Nitrogen is supplied to the loop and used to purge the module after operation. This is necessary to prevent possible corrosion while the system is not in operation.

Carbon dioxide analyzers are provided in both the hydrogen vent and the oxygen vent. An electrical schematic of these units is shown in Figure 28. These units provide a constant indication of the performance of the module by monitoring the carbon dioxide content of the exhaust gases. The oxygen stream analyzer reads 0-5% carbon dioxide and the hydrogen stream carbon dioxide analyzer reads 0-100% carbon dioxide. Due to the sensitivity of the analyzer thermistors to a reducing atmosphere, hydrogen flow is imposed on the hydrogen stream carbon dioxide analyzer only when a reading is required.

Oxygen and hydrogen pressure switches and a thermoswitch provide shutdown signals in case of a system malfunction. Figure 27 shows the malfunction system and the other control circuitry necessary to operate the test apparatus. The pressure switches operate the test apparatus. The pressure switches operate at 8 psig and the thermoswitch closes at 200°F. When an automatic shutdown occurs, a nitrogen purge is initiated. To prevent undue dehydration of the module the purge is limited to 180 seconds by a time delay relay unless all power is lost in which case the purge continues until manually terminated.

The temperature of the heat exchanger bath and the module is controlled by temperature controllers which, when a specific heat exchanger bath temperature is set, controls the module temperature to within a set differential. This arrangement prevents large differences in module and heat exchanger temperature which, if allowed to occur, would dry out the module. Module temperature is controlled by a 2000 watt air heater in combination with a circulating air loop.

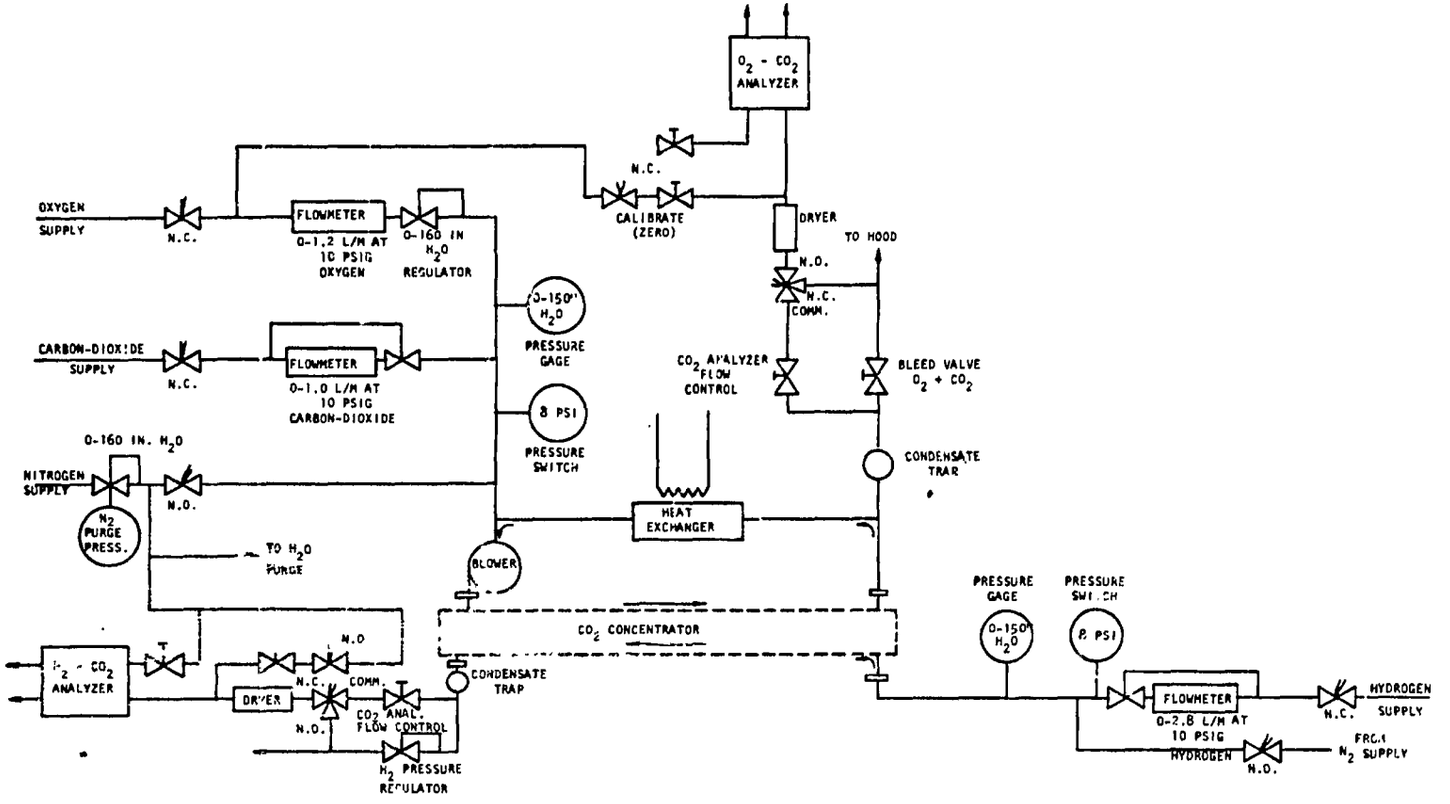

FIGURE 26 CO_2 CONCENTRATOR MODULE TEST SYSTEM SCHEMATIC

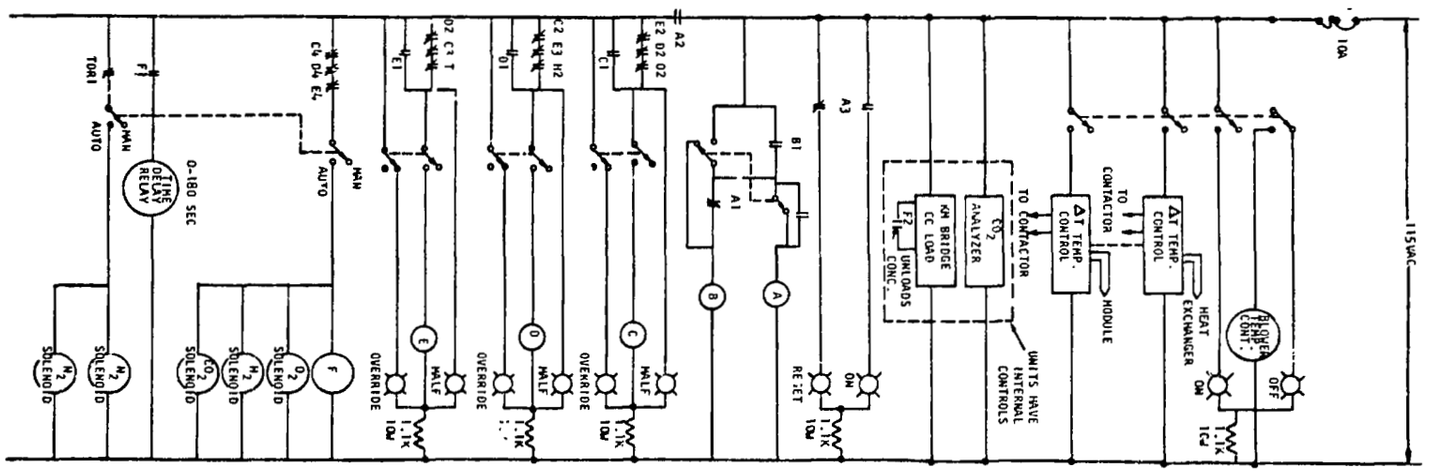

FIGURE 27 CO_2 CONCENTRATOR MODULE TEST SYSTEM CONTROL SCHEMATIC

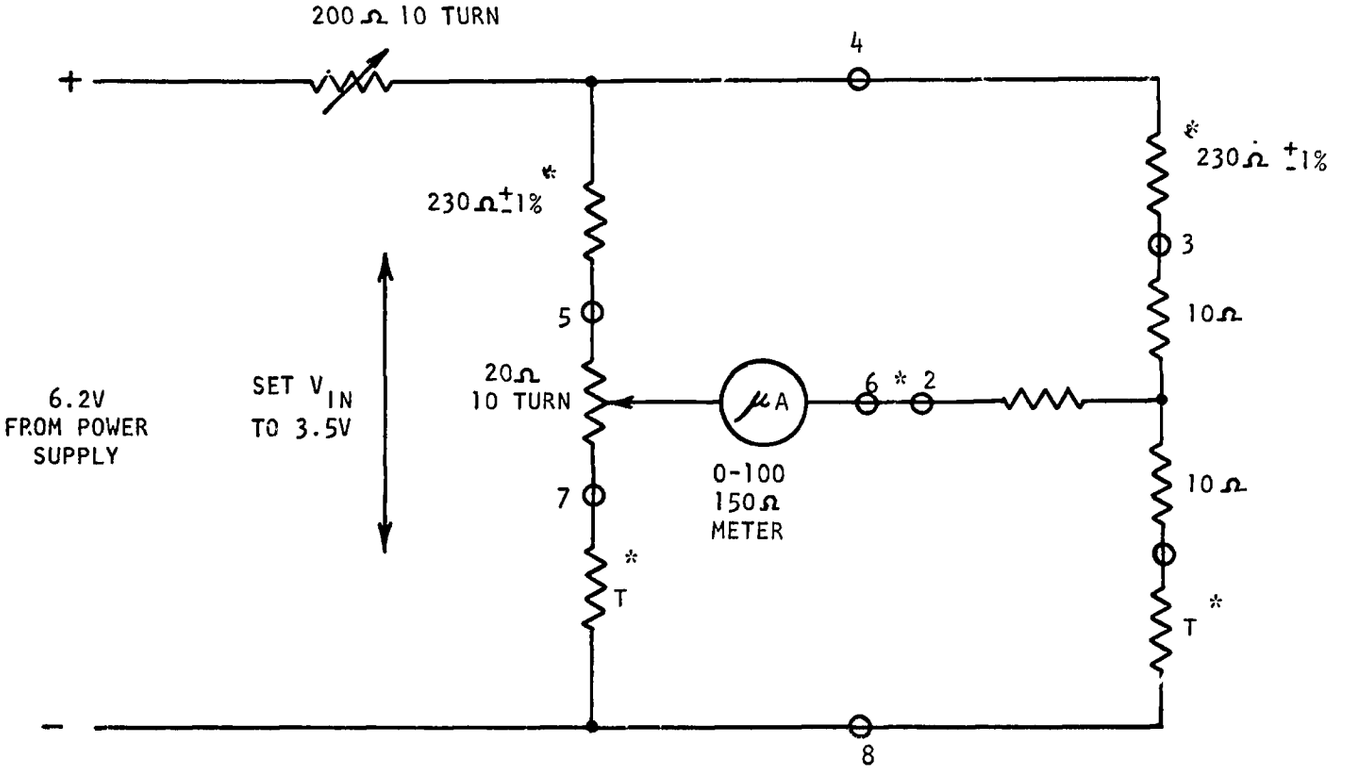

*PART OF VECO MODEL M'82 GAS ANALYSIS CELL

FIGURE 28 CO_2 CONCENTRATOR GAS ANALYSIS WIRING SCHEMATIC

Heat exchanger fluid temperature is maintained by a 1000 watt cylindrical heater. An interlock is provided to prevent operation of the heaters without the blower or circulating pump in operation.

In order to provide comprehensive data on the performance of the module, a variable frequency Kordesch-Marko Bridge was installed as a part of the constant current load system. This allows iR drop, iR-free and terminal voltage data to be taken at any time. Operation of the load system is accomplished from the control panel and modes can be changed at will without affecting module performance.

Figure 29 is a photograph of the test stand with the ten-cell module installed.

Fifteen-Cell Module Configuration

To accommodate the Design II fifteen-cell module and to improve its operating characteristics the test rig was modified prior to initiation of the fifteen-cell module test program. These changes and related tasks are summarized below.

1. Replace dehumidifier with humidifier/dehumidifier to facilitate an increase in the electrolyte inventory in the stack as well as a decrease.
2. Install new temperature controls for the stack and humidifier/dehumidifier.
3. Install flow meter in oxygen recycle loop.
4. Trace heat oxygen recycle loop.
5. Fabricate and install trace heated oxygen and hydrogen sample lines to dew point sensor and gas chromatograph.
6. Provide sample lines to the Beckman GC-2 gas chromatograph for CO_2, O_2 and H_2 determination.
7. Calibrate Beckman GC-2 Gas Chromatograph for above gases. Utilize pure gases introduced to the gas chromatograph at known atmospheric and subatmospheric pressures to provide a calibration over the complete area of gas concentration expected. Utilize certified gas mixtures to verify calibration determined in the prior method. Periodically recalibrate the Beckman to insure that calibration curve has not drifted. (Change in calibration for carbon dioxide in the 0-5% range not greater than 0.1% at 2½% carbon dioxide and 0.05% at 0.4% carbon dioxide over a one-month period.)
8. Increase voltage readout capability to 15 cells.
9. Increase temperature readout capability to 15 cells plus internal temperature measurement and trace heated line temperature measurement.
10. Remove automatic N_2 purge (no materials problems at open circuit voltages), but leave on manual N_2 supply to provide variable pO_2 level.

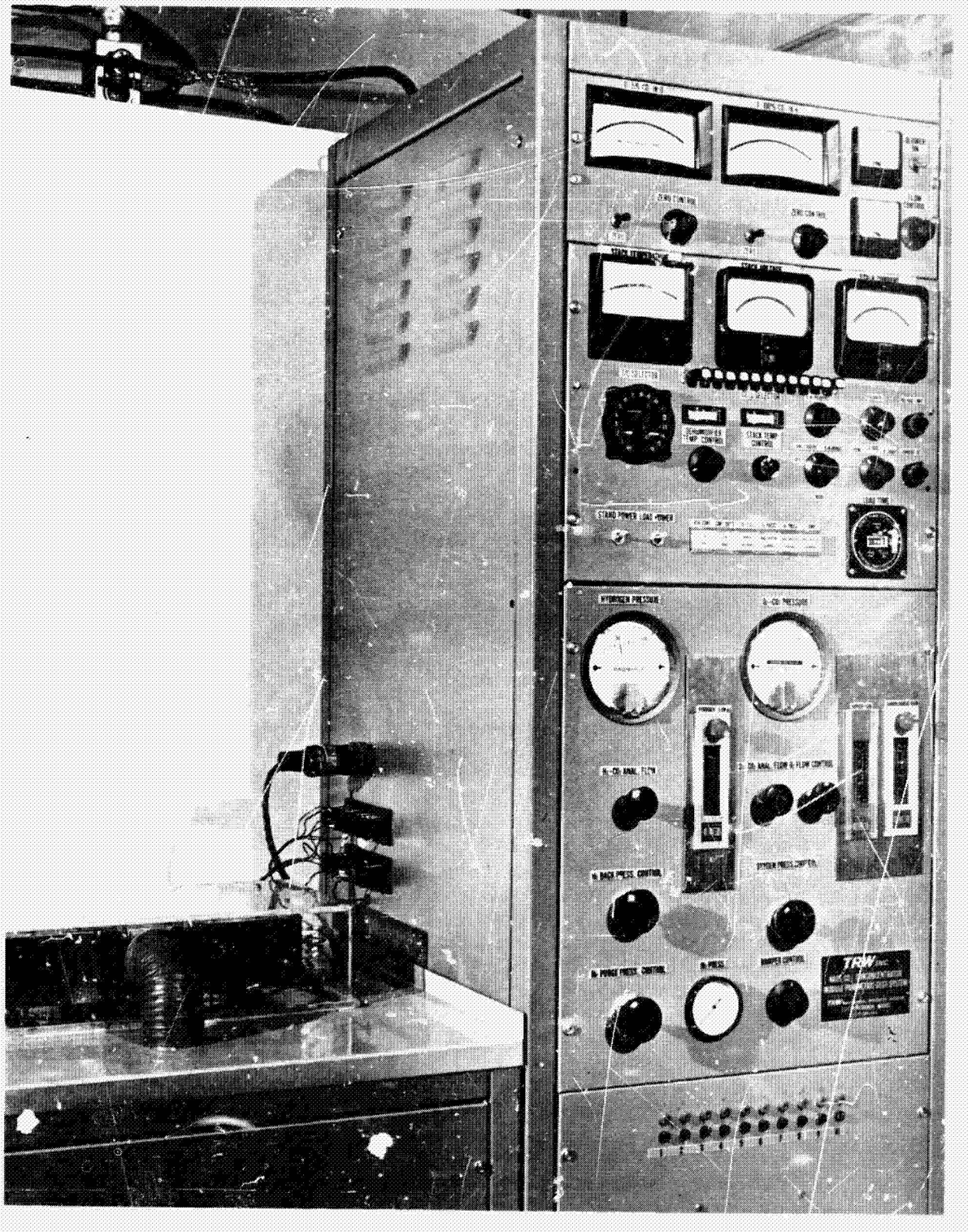

FIGURE 29 CO_2 CONCENTRATOR MODULE TEST SYSTEM

The current configuration of the test rig is represented by the plumbing and electrical schematics in Figures 30 and 31. Figure 32 is a photograph of the rig in its final configuration with the fifteen-cell module installed and operating.

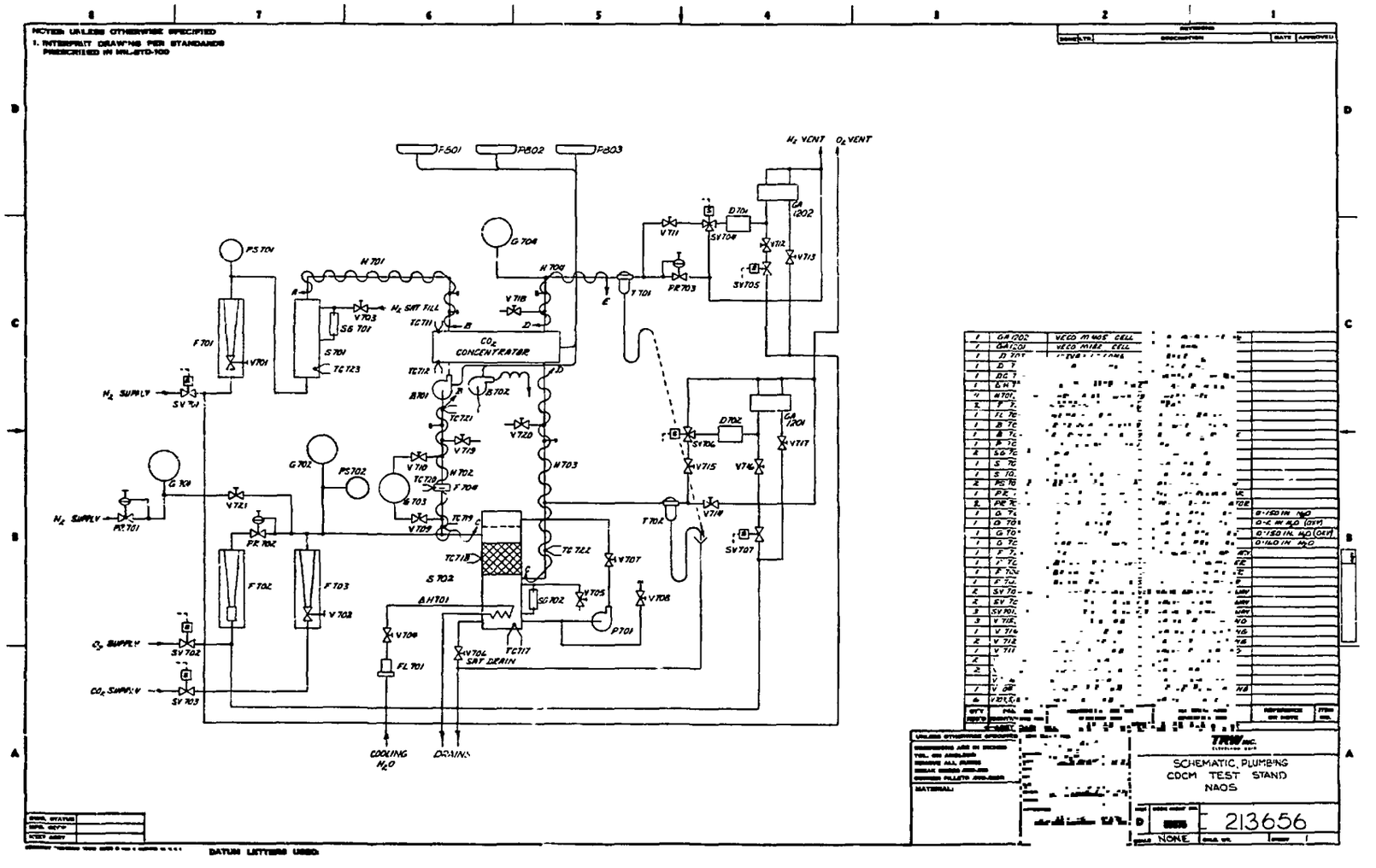

FIGURE 30 PLUMBING SCHEMATIC, CDCM TEST STAND

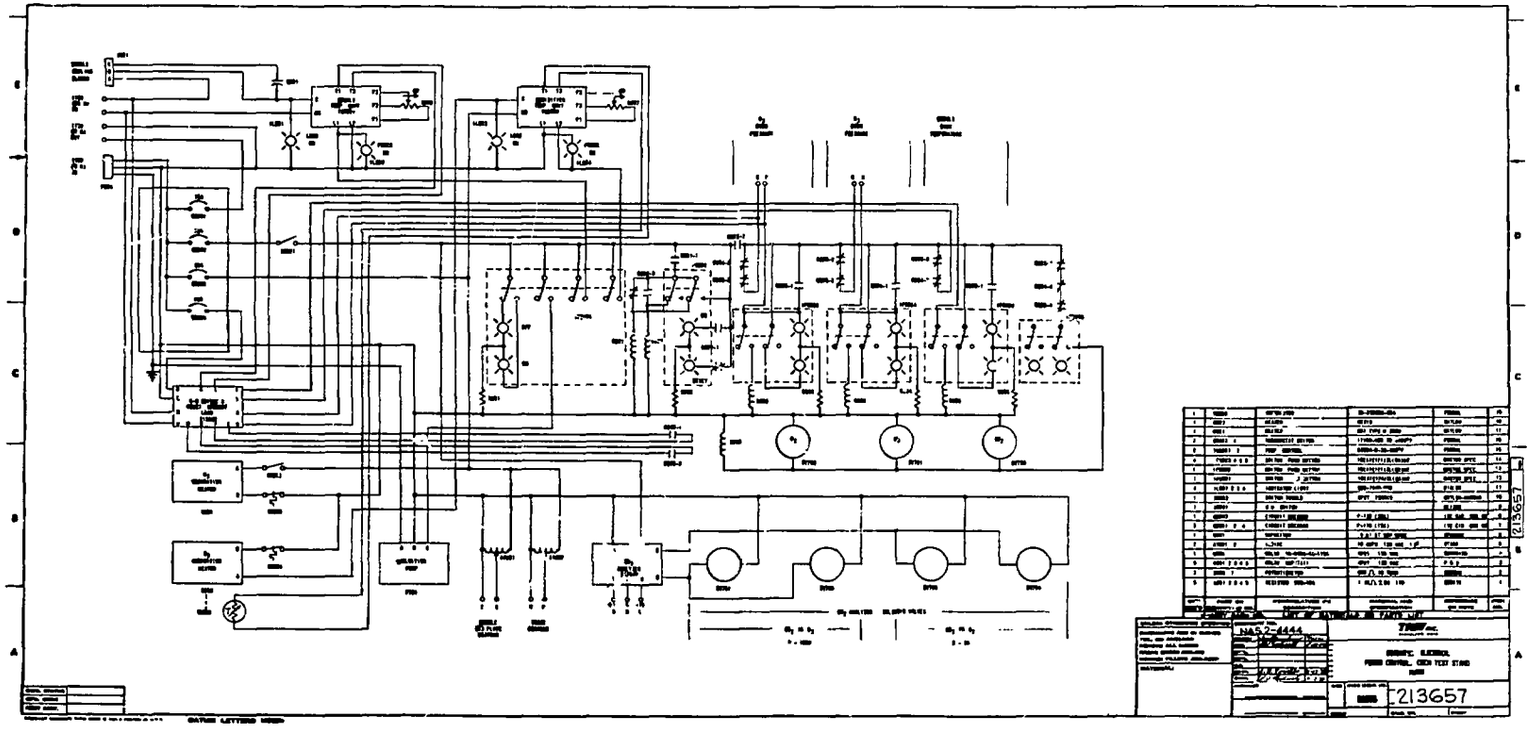

FIGURE 31 ELECTRICAL SCHEMATIC, CDCM TEST STAND

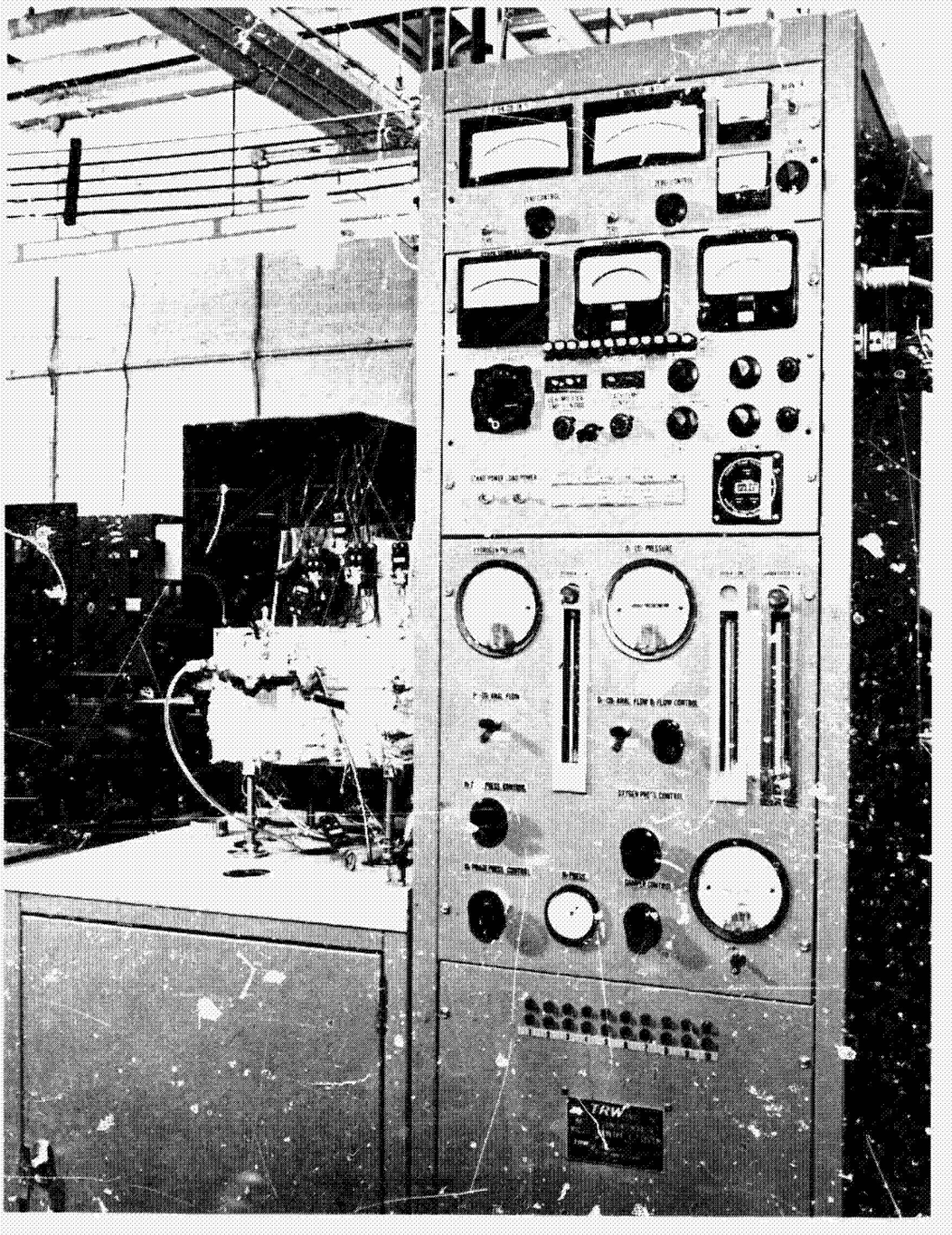

FIGURE 32 CO_2 CONCENTRATOR FIFTEEN-CELL MODULE TEST RIG

PARAMETRIC TEST - DESIGN I MODULE

After assembly and pressure check at 12 psig, the module assemblies were vacuum charged with 30 wt% K_2CO_3 solution. Prior to installation on the test stand, checks for cross-cell leakage were routinely made at a 5 psid pressure differential across the cell matrices.

The parametric test series was designed to provide operating data for the carbon dioxide concentrator as a function of the following: cell temperature, oxygen circulation rate, hydrogen flowrate, current density, and carbon dioxide transfer rate.

Parametric testing was initiated with the module having the parallel flow hydrogen configuration. Uneven flow distribution of the hydrogen yielded unstable cell performance. The module was modified as previously discussed and the complete test series was restarted. Results of the parametric tests are given below.

Design Condition Operation

The design requirements and design operating parameters of the carbon dioxide concentrator are summarized in Table II. Data obtained while operating the module near this design point are presented in Table VII and Figure 33. Interpretation of the data requires a brief explanation of the operation of the test rig. Carbon dioxide is introduced to the oxygen system at a fixed rate (in this case, 0.45 standard liters/minute). Mechanisms for the removal of the carbon dioxide are:

1. CO_2 transfer to the hydrogen stream.
2. Flow through the gas analyzer and small leaks.

The amount carried out by the second method can be estimated as follows:

Analyzer Flow: 0.1 sl/min x 1% CO_2 = 0.001 sl/min CO_2

Maximum Leakage: 0.2 sl/min x 3% CO_2 = 0.006 sl/min CO_2

This is a total of 7.0 scc/min removed by leakage and through the analyzer. Thus, during operation of the system, the percent of carbon dioxide in the oxygen stream will change until the amount entering is transferred. The system will then be in equilibrium. The maximum theoretical transfer rate of carbon dioxide by the electrochemical reactions occurring in the concentrator is 7.5 scc/amp-min/cell (assuming no transfer of carbon dioxide through the cell by bicarbonate ions). The minimum current at which the ten-cell module can operate while transferring 0.45 sl/min is:

$$(0.45 \text{ sl/min})/(0.0075 \text{ sl/amp-min/cell}) \times 10 \text{ cells}) = 6.0 \text{ amperes}$$

From the data of Figure 33 it is seen that in order to operate at this theoretical limit a high percentage of carbon dioxide must be tolerated. However, at a current slightly greater than 6.0 amperes, the percent of carbon dioxide at the oxygen exit (pilot return) drops rapidly. This indicates that a current

TABLE VII

CO_2 CONCENTRATOR MODULE OPERATION NEAR DESIGN POINT CONDITIONS

CO_2 Transfer Rate sl/min	Current Amps	CO_2 at O_2 Exit %	Voltage Output Volts	O_2 Circulation Rate CFM	Stack Temperature °F
0.45	10	0.27	4.5	2.7	125
0.45	7.5	0.3	4.3	2.7	120
0.45	7.5	0.35	4.3	2.7	120
0.45	6.0	2.0	5.0	2.7	115
0.45	6.0	1.7	4.95	2.7	117
0.45	10.0	0.28	4.28	2.7	121
0.45	8.0	0.37	4.61	2.7	120
0.46	7.0	0.72	5.0	2.7	120
0.45	6.5	1.43	5.35	2.7	120
0.45	10.0	0.35	4.25	2.7	123
0.45	7.0	0.44	4.90	2.7	130

H_2 FLOW	1.7 sl/MIN
O_2 CIRCULATION RATE	2.7 CFM
TEMPERATURE	117-130°F
TRANSFER RATE	.45 sl/MIN
ACTIVE ELECTRODE AREA	.25 SQ FT 10 CELLS

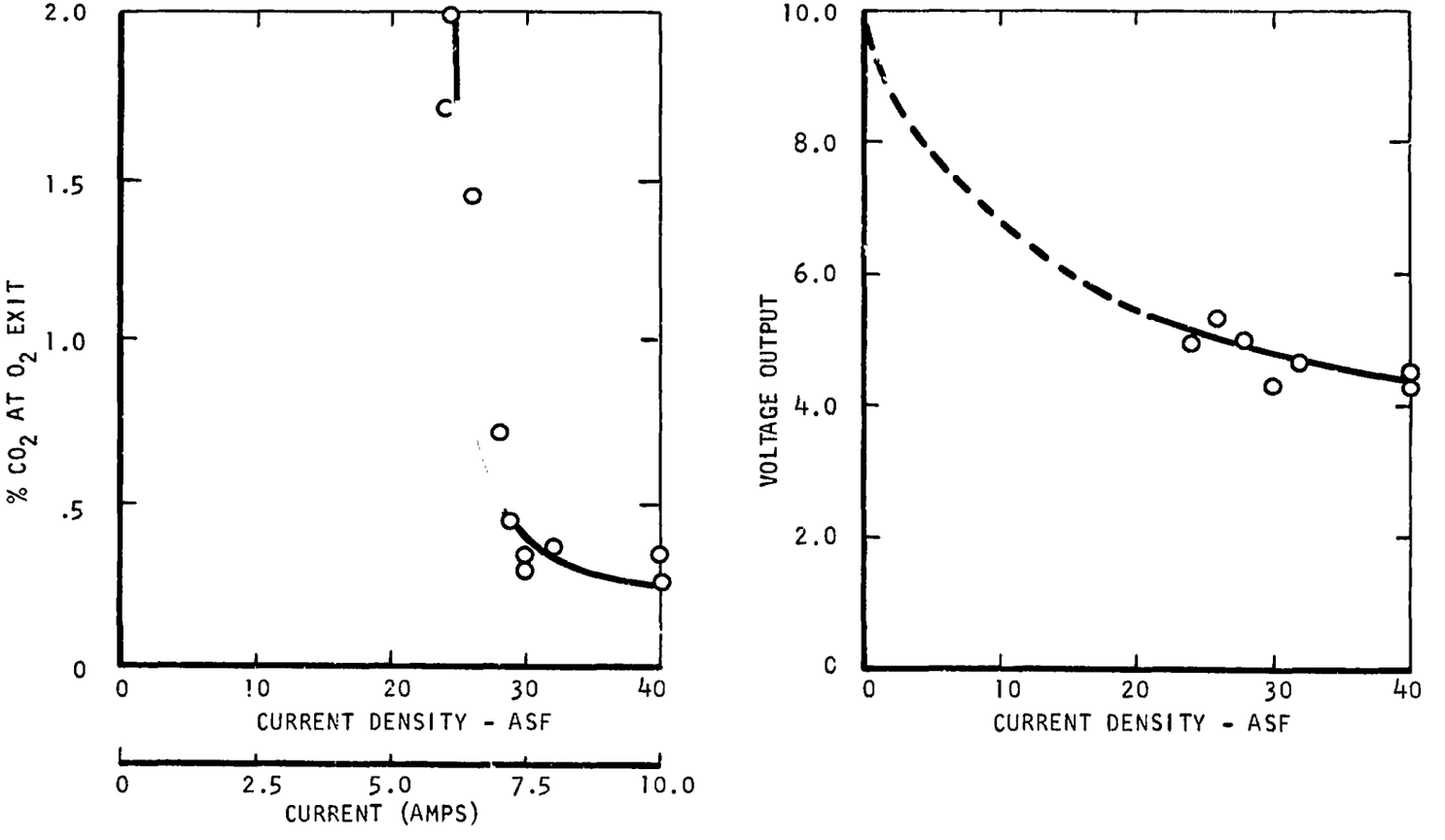

FIGURE 33 CO_2 CONCENTRATOR MODULE PARAMETRIC TEST - OPERATION NEAR DESIGN POINT

of 7.5 amperes will produce a carbon dioxide concentration at the oxygen exit of 0.5% or lower. Oxygen consumption by the concentrator at 7.5 amperes is 0.0493 lb/hr.

Temperature Variation

Table VIII and Figure 34 summarizes the equilibrium data obtained. The data indicate a trend with temperature similar to that noted in single cell testing, i.e., increase in cell voltage with cell temperature. Insufficient data was obtained to determine the effect of temperature on carbon dioxide transfer rate.

Oxygen Circulation Rate

Table IX and Figure 35 summarizes the variation of module performance as a function of oxygen circulation rate. Oxygen circulation serves two functions. Water produced in the reaction of hydrogen and oxygen is carried from the cell to a condenser where it is removed, and carbon dioxide is swept over the electrodes at a rate equal to or greater than the desired transfer rate. For example, to transfer 0.45 sl/min carbon dioxide with 1.0% carbon dioxide concentration at the system inlet, a flowrate of at least $0.45 \times \frac{100\%}{1\%} = 45$ sl/min is required.

The data presented in Figure 35 indicates that there is no significant trend in carbon dioxide transfer rate as a function of oxygen circulation rate over the range 2.0 CFM to 3.5 CFM (56 to 98 sl/min). One data point was run at 1.0 CFM (28 sl/min) which indicated that carbon dioxide transfer rate is adversely affected by low circulation rates. The inability of the test rig to maintain a proper water balance at low circulation rates limited the testing to one point. This trend was later verified in the Design II module tests.

Hydrogen Flowrate Variation

The effect of hydrogen flow on module performance is summarized in Table X and presented in Figure 36. The carbon dioxide transfer rate appears to be unaffected by the hydrogen flowrate. The percent carbon dioxide in the hydrogen stream is shown from experimental data and the calculated values. The correlation is excellent. As expected for an increasing hydrogen flowrate, the voltage output also increases.

Carbon Dioxide Transfer Rate Variation

The major causes of carbon dioxide transfer rate variation are the carbon dioxide partial pressure in the oxygen process stream and the current imposed on the module. The variation due to the current is primarily a change in operating capacity but the carbon dioxide partial pressure variation causes changes in electrolyte composition which actually changes the specific carbon dioxide transfer rate (volume of carbon dioxide transferred per ampere per minute). This relationship is shown in Figure 37. This curve was generated for a range of currents (6-10 amps) and a range of actual carbon dioxide transfer rates (0.45 to 0.65 sipm).

TABLE VIII

CO_2 CONCENTRATOR MODULE OPERATION
TEMPERATURE VARIATION DATA

CO_2 Transfer Rate sl/min	Current Amps	CO_2 at O_2 Exit %	Voltage Output Volts	O_2 Circulation Rate CFM	Stack Temperature ^oF
0.46	7.0	0.60	3.40	2.7	103
0.46	7.0	0.45	4.15	2.7	111
0.45	6.5	1.43	5.35	2.7	120
0.46	7.0	0.72	5.00	2.7	120
0.45	7.5	0.30	4.60	2.7	120
0.46	7.0	0.44	4.90	2.7	130
0.46	8.0	0.40	5.55	2.7	131

H_2 FLOW	1.7 SLPM
O_2 RECYCLE FLOW	2.7 SCFM
CO_2 TRANSFER RATE	.45 SLPM
NO. OF CELLS	10
ACTIVE AREA/CELL	.25 SQ. ST.
PRESSURE	30" H_2O GAGE

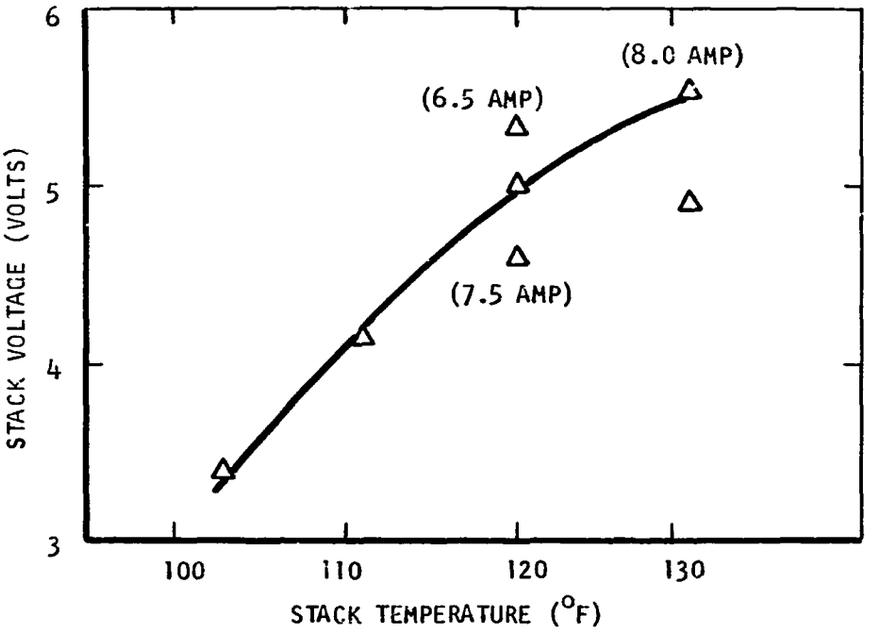

FIGURE 34 PERFORMANCE OF CDCM I - EFFECT OF STACK TEMPERATURE

TABLE IX

CO_2 CONCENTRATOR MODULE OPERATION
O_2 CIRCULATION RATE DATA

CO_2 Transfer Rate sl/min	Current Amps	CO_2 at O_2 Exit %	Voltage Output Volts	O_2 Circulation Rate CFM	Stack Temperature °F
0.46	7.0	2.1	0.580	1.0	118
0.45	7.0	0.7	0.525	2.0	120
0.46	7.0	0.72	0.500	2.7	120
0.43	7.0	0.72	0.545	3.6	120

H_2 FLOW	- 1.7 slpm
TEMPERATURE	- 120°F
CO_2 TRANSFER RATE	- 0.45 slpm
NO. OF CELLS	- 10
ACTIVE AREA/CELL	- 0.25 sq. ft.
PRESSURE	- 30" H_2O GAGE
CURRENT	- 7.0 AMPS.

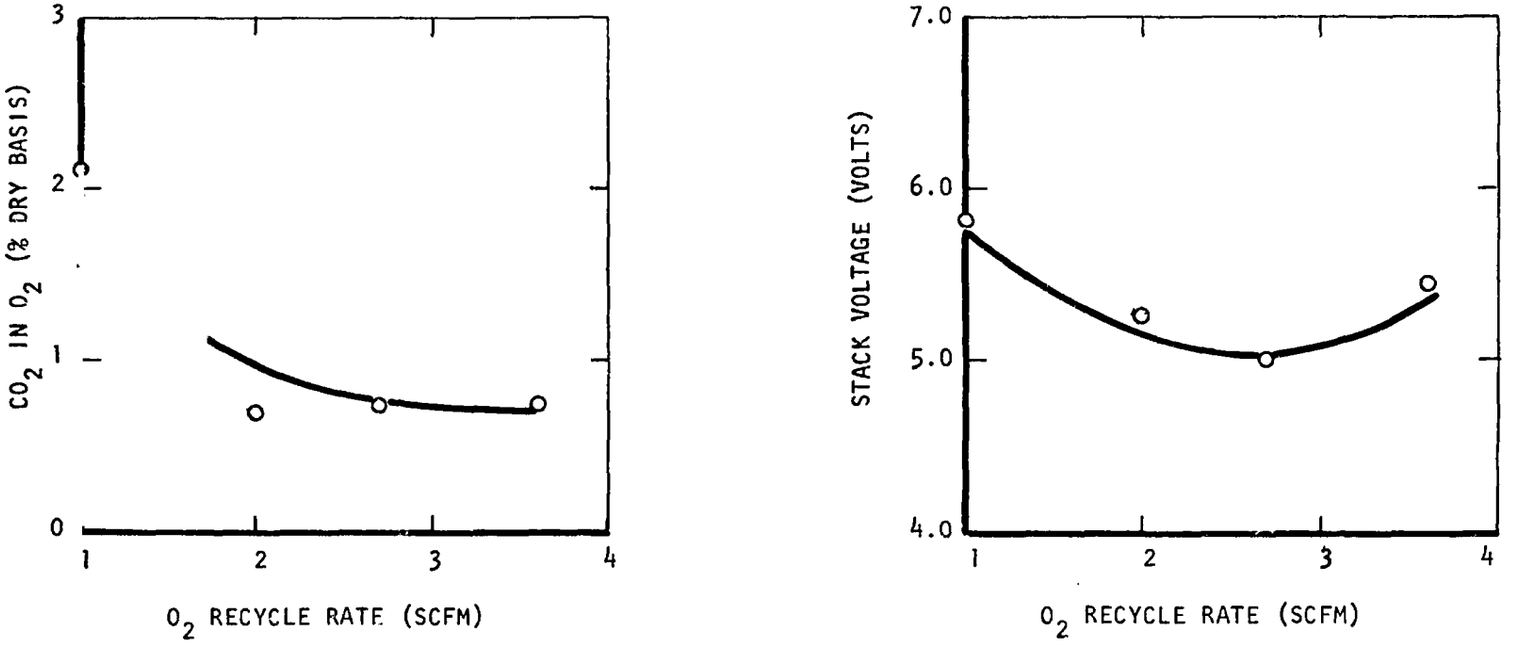

FIGURE 35 PERFORMANCE OF CDCM I - EFFECT OF OXYGEN RECYCLE RATE

TABLE X

EFFECT OF HYDROGEN FEED RATE

Hydrogen Feed Rate, SLPM	O_2 Recycle Rate, SCFM	CO_2 in O_2 Out, %	CO_2 in H_2 Out, %	Stack Voltage Volts	Current Amps	Temperature °F
1.10	2.7	0.34	60	4.25	10	120
1.20	2.7	0.38	50.5	5.05	10	120
1.38	2.7	0.35	32.8	5.20	10	120
1.67	2.7	0.31	19.2	5.25	10	120
1.67	2.7	0.33	20.1	4.75	10	120
1.78	2.7	0.46	18.9	4.60	10	120
2.20	2.7	0.34	19.2	5.18	10	120

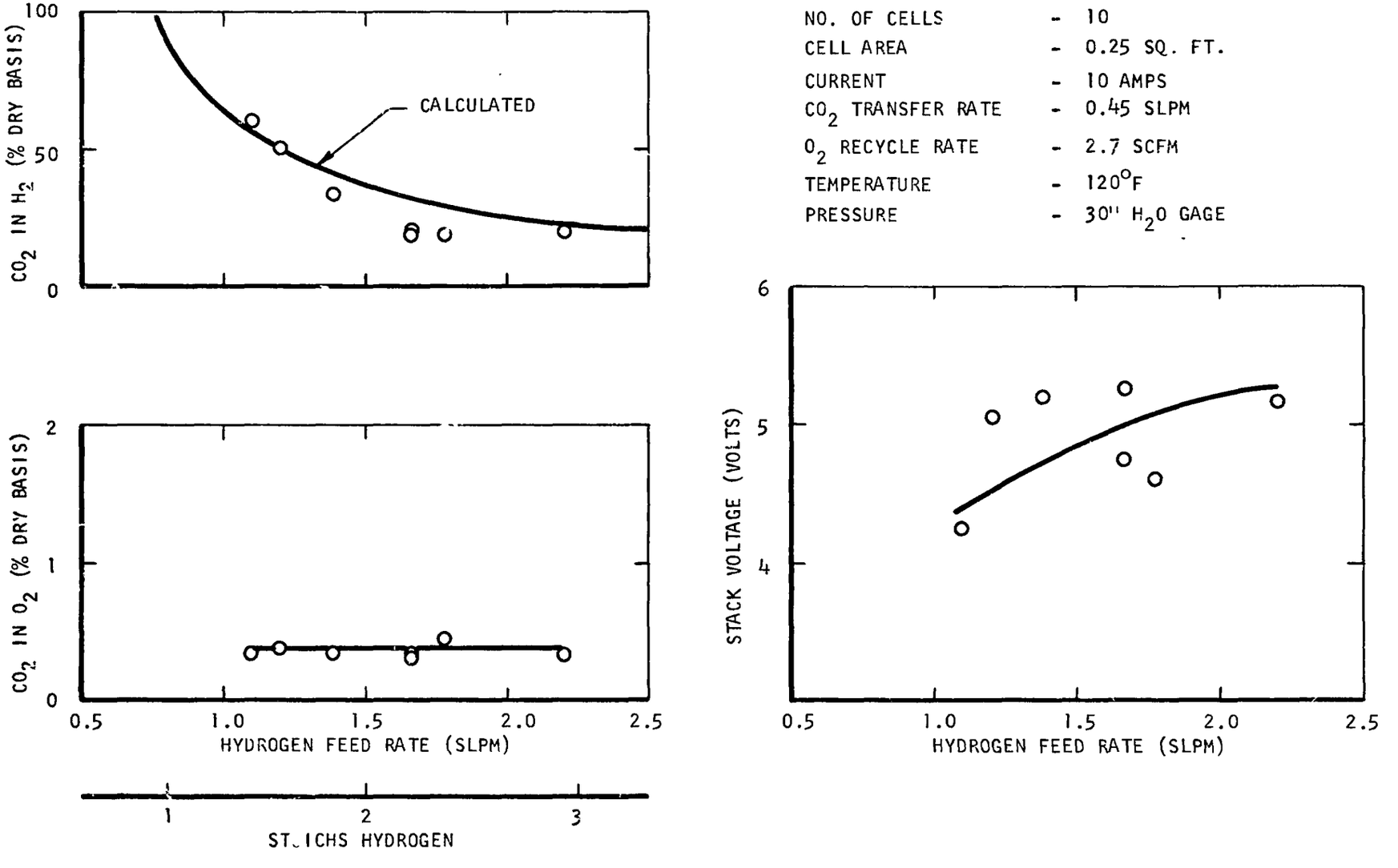

FIGURE 36 PERFORMANCE OF CDCM I - EFFECT OF HYDROGEN FEED RATE

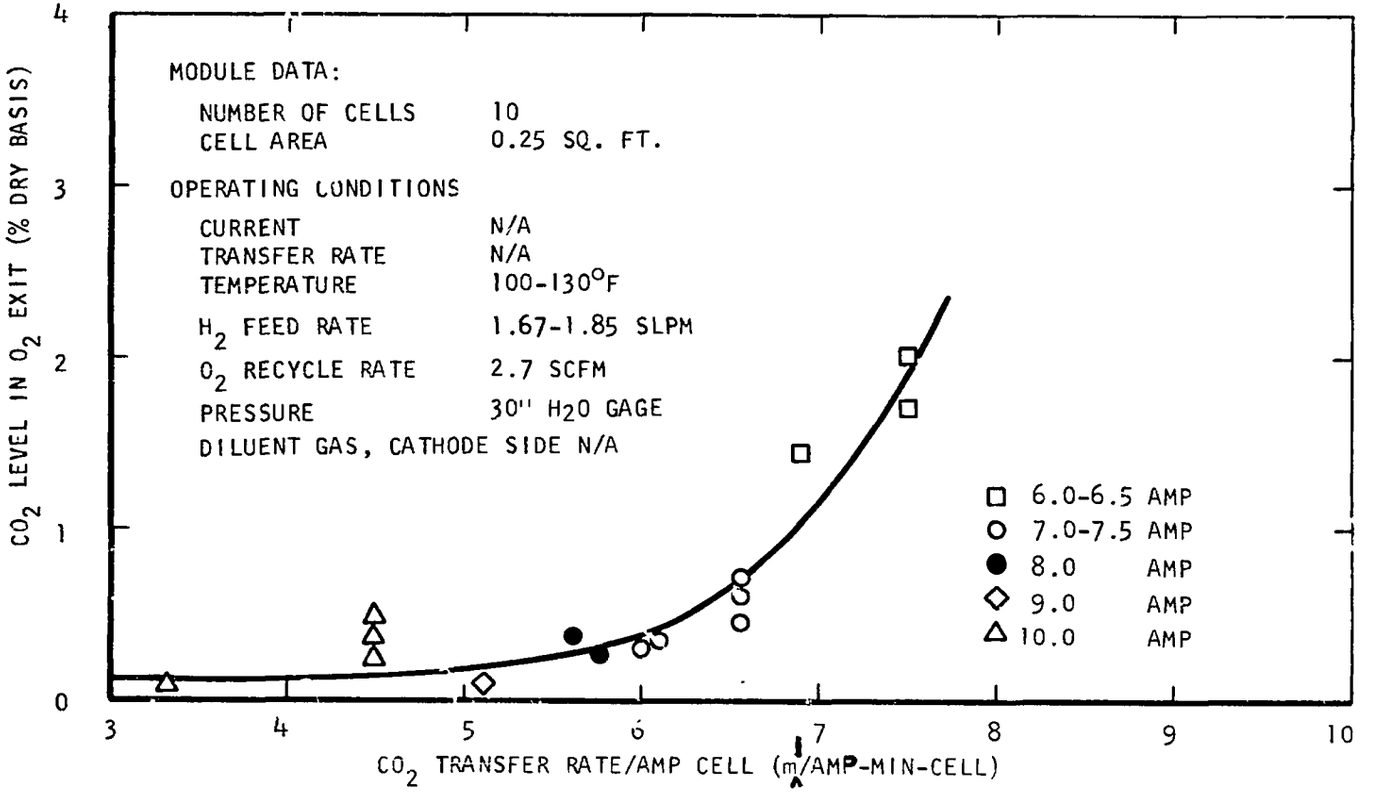

FIGURE 37 PERFORMANCE OF CDCM I, SPECIFIC TRANSFER RATE

Design Current Density Variation

In operation, the percentage of carbon dioxide in the oxygen cavity is equal to the inlet flowrate of carbon dioxide. At any current there is a maximum flowrate which can be transferred by the electrochemical mechanism which operates in the concentrator. Beyond this limit the pressure in the cavity will build as carbon dioxide continues to be added. This effect can be seen by referring to Figure 33. Variation of cell voltage as a function of current density is also shown; the dashed portion of the curve is an extrapolation of the data based on single cell performance.

After completion of the parametric tests, life tests were conducted with the Design I module. Mositure balance difficulties in long term operation led to the initiation of the Design II module development.

CARBON DIOXIDE CONCENTRATOR DESIGN II MODULE

Heat and Moisture Removal Evaluation

Consideration of a redesigned concentrator module was not limited to the original fin-cooled concept. Alternate heat and moisture removal methods considered were the static water feed cell for internal evaporative cooling and the circulating electrolyte cell for both heat and moisture removal.

Each concept was considered from the standpoint of thermal control, water balance control and water tolerance. A discussion of the demonstrated advantages and disadvantages of the concept as proposed for use in the redesign follow. In addition, known prerequisites for the successful application of each concept is noted.

Fin-Cooled Module. - This is considered to be a redesign of the original NAOS CDCM. Advantages are:

1. General design available.
2. Performance analysis made and related to experimental observations.
3. Failure modes analyzed and understood and areas for improvement recognized.

Disadvantages are:

1. Cannot be liquid-cooled as presently designed (without adding air-to-liquid heat exchanger and blower).

Required improvements based upon experience with first design.

1. Reduction of thermal gradients within module.
2. Greater water tolerance.
3. Humidity sensor for stack temperature control.
4. Improved materials of construction.
5. Greater matrix compression.
6. Improved sealing between cavities.
7. Decreased gas pressure drops.
8. Operation at 100% overcapacity.
9. Capability for direct liquid cooling.

Static Water Feed Module. - This is considered to be a design similar to that employed in the NAOS WEM. Advantages are:

1. General design available.
2. Operation demonstrated in WEM.
3. Gas humidity conditioning internal to module.
4. Performance analysis made and related to experimental observations on the WEM.
5. Evaporative cooling provided by internal humidification.

Disadvantages are:

1. Necessary to vent gas cavities periodically.
2. Incapable of meeting evaporative cooling load requirement simultaneously with humidity conditioning requirement.
3. Marginal capability to transport water at required rate to meet evaporative cooling requirement without developing excessive concentration gradients.
4. More complex cell design.
5. No demonstrated performance of concept in CDCM application.

Requirements that must be met for satisfactory operation are:

1. Operation in a mode that requires water consumption at all times in order to prevent electrolyte loss from humidifier cavities.

Circulating Electrolyte. - Advantages are:

1. Can effect heat removal with minimal temperature differences within the unit.
2. No chance of crossover from H_2 to O_2 as long as electrolyte flows.

Disadvantages are:

1. High internal resistance (2 matrices and free electrolyte space).
2. Cell-to-cell leakage currents.
3. Gas production in electrolyte requires liquid/gas separator.
4. Possibility of flooding gas cavities and system plumbing in the event of a malfunction.
5. Electrolyte pump required.

Requirements to be met for satisfactory operation are:

1. Must operate in a mode requiring water consumption, otherwise need an electrolyte still to remove product water.

Selected Approach. - Consideration of the advantages, disadvantages and requirements of the above concepts for the CDCM led to the conclusion that a redesigned, fin-cooled concentrator module possibly using an alternate electrolyte as indicated by preliminary studies would best meet all objectives. In the CDCM application, water balance control would be obtained by manipulating stack temperature in response to a humidity sensing element in the oxygen inlet stream.

Electrolyte Study

The first design used an aqueous solution of potassium carbonate (K_2CO_3) as electrolyte due primarily to its low cost and general availability.[2] Although this unit disclosed excellent performance in short term runs immediately after the unit was charged with electrolyte, long operational periods were usually terminated by gas mixing unless the oxygen humidity was raised to provide very dilute electrolyte within the concentrator. An extensive study was initiated

to identify the reasons requiring dilute operation from which it was disclosed that a significant conversion of carbonate to the bicarbonate occurred during operation. A study of the solubility of the latter component disclosed that it is less than one-half as soluble (in water) as the carbonate. Post-test examination of the first concentrator showed precipitation of bicarbonate on the anode and in the anode cavity of such magnitude that the electrode was masked from the gas phase and gas ports were severely blocked. By running the cell under dilute electrolyte conditions, the solubility of the bicarbonate is increased and the problem may be avoided. Operating with dilute electrolyte however, increases the probability of cell flooding or drying.

Criteria for Electrolyte Selection. -

Concentration/Vapor Pressure Depression: In cells with aqueous electrolytes, it is necessary to maintain the volume of the electrolyte to a value close to the charge volume. A volume increase will result in electrolyte run-off and liquid in the gas cavities of a cell and possible liquid carryout in the gas streams. A volume decrease greater than 57% (based upon initial volume, for a 30 mil matrix) will lead to gas crossover as determined by direct experimentation.

In capillary cells with wet-proofed, single porosity electrodes, solution volume is controlled indirectly by maintaining a constant temperature difference between the dew point of the gases in the cavities of the cell and the temperature of the electrolyte. A plot of the vapor pressure versus temperature relationship for K_2CO_3 at various concentrations is seen in Figure 38. For example, with 38 w/w% K_2CO_3 as electrolyte, the dew point of the gases flowing through the cell must be 104.8°F if the electrolyte is at 115°F. If dew point temperature decreases by 2°F (or electrolyte temperature increases by 2°F), the electrolyte concentration will increase to 42%. (Dew point rise as the result of water generation within a cell is not pertinent to the analysis at this time.)

Consulting with the specific volume curves of Figure 39, the solution volume will change from 1.85 to 1.60 cc/g K_2CO_3. This represents a decrease in liquid inventory in the cell by 13.5% based upon the initial conditions. This value is considerably less than the 57% limit noted above and therefore a decrease in dew point of 2°F is of little consequence. Note that the difference between dew point and solution temperature is 10.2°F.

If initial electrolyte concentration is 14%, the operating dew point is 113.2°F. This value is only 1.8°F below cell temperature. If it is again assumed that dew point temperature decreases by 2°F, the new concentration is 23% and the reduction in solution volume is found to be 42.5%. This value is much nearer the limiting value. These data are summarized in Table XI.

From this example, it is obvious that an electrolyte that provides maximum dew point depression is desirable in order to permit maximum latitude in automatic control of cell and gas dew point temperatures with minimal solution volume change.

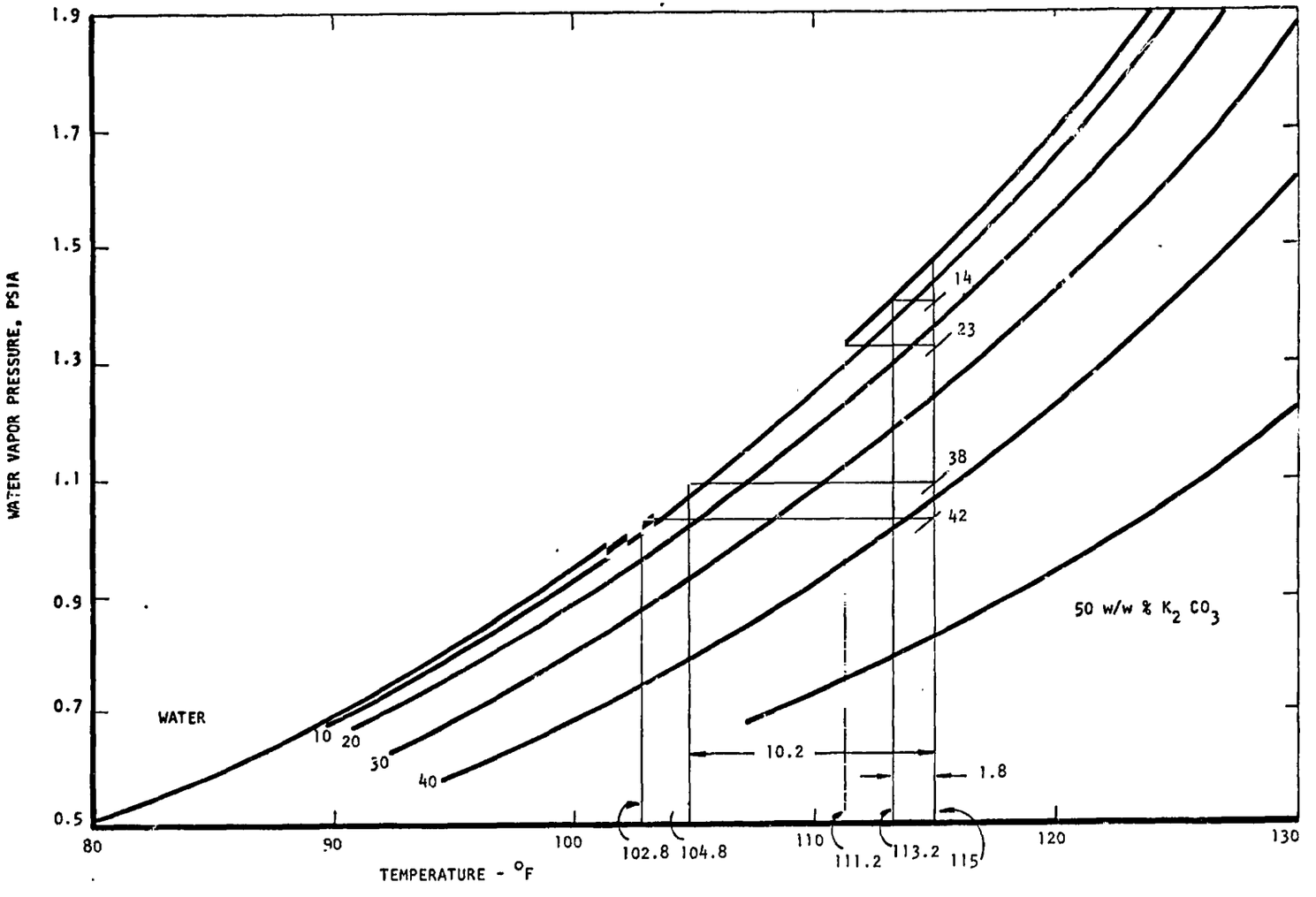

FIGURE 38 WATER VAPOR PRESSURE OF AQUEOUS SOLUTIONS OF $K_2 CO_3$ FROM INTERNATIONAL CRITICAL TABLES - VOLUME III, PAGE 299

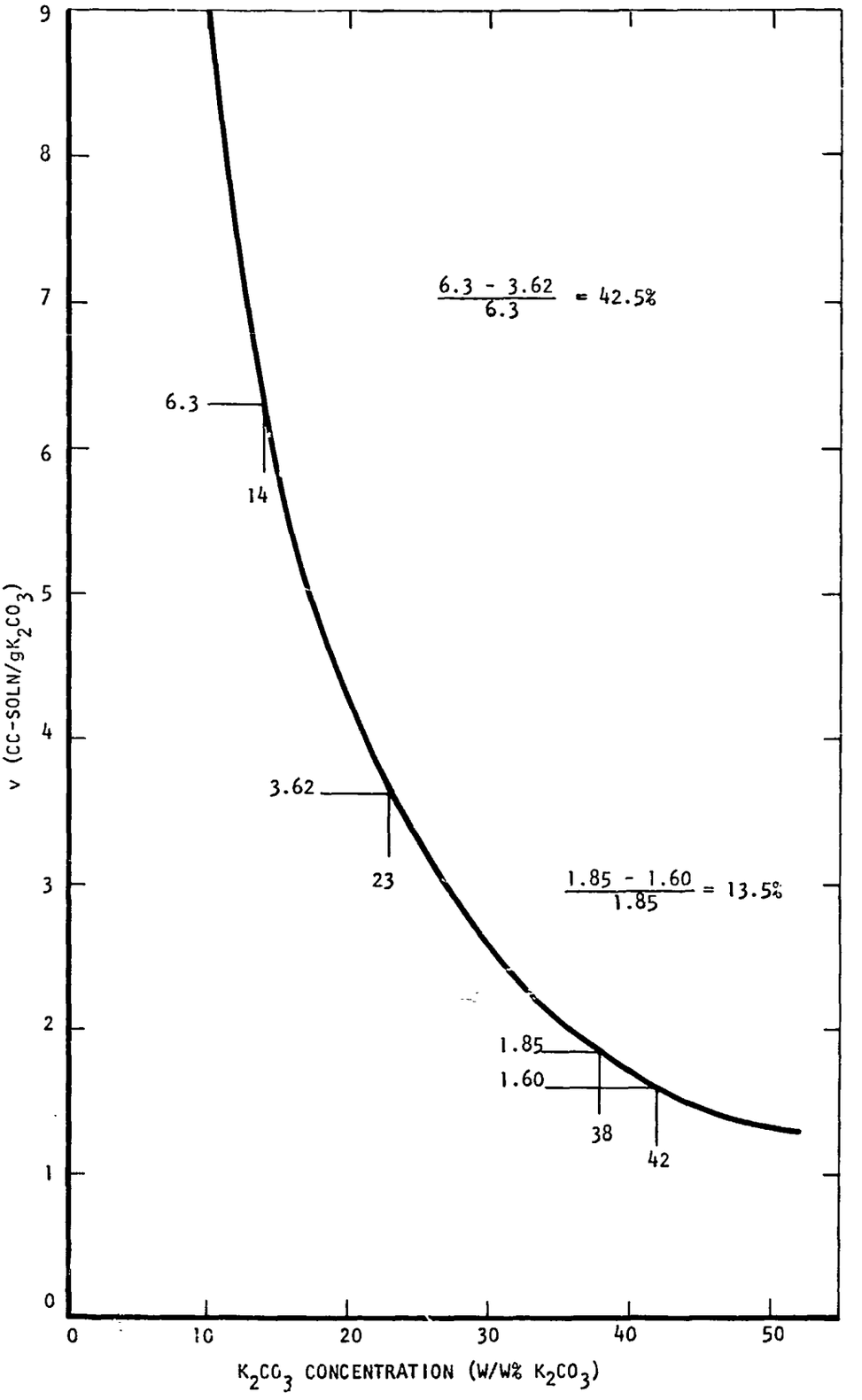

FIGURE 39 SPECIFIC VOLUME OF AQUEOUS SOLUTIONS OF K_2CO_3 FROM INTERNATIONAL CRITICAL TABLES, VOLUME III, PAGE 90

TABLE XI

SOLUTION VOLUME CHANGE, K_2CO_3

Cell Temperature - 115°F

Electrolyte - K_2CO_3

Dew Point Temperature - °F		Concentration w/w%		Solution Vol. Change	Dew Point Depression (Cell Temp. Minus Dew Point)
Initial	Final	Initial	Final	%	°F
104.8	102.8	38	42	-13.5	10.2
113.2	111.2	14	23	-42.5	1.8

Maximum permissible value - - - - - - - - - - - - -57.0

Bicarbonate Formation: In operation, a concentrator will have a significant partial pressure of carbon dioxide at the anode. In the solution reaction:

$$CO_2 + H_2O \rightleftharpoons H_2CO_3$$

carbon dioxide reacts with the water in the electrolyte to form carbonic acid. This in turn forms the bicarbonate of potassium from the carbonate as in the following reaction:

$$K_2CO_3 + H_2CO_3 \rightleftharpoons 2KHCO_3$$

Of interest here is the solubility of these two species.

Test data on small cells disclosed severe anode degredation when a precipitate was formed in the presence of high carbon dioxide levels. From the above discussion it may be assumed that the maximum carbonate concentration soluble at room temperature is charged into the cell. If the solubility of the bicarbonate formed at the anode is exceeded, precipitation will take place. It is therefore necessary to insure that both carbonate and bicarbonate are completely soluble at cell temperature and preferably also at room (or start-up) temperature.

Survey of Alkali Metal Carbonates. - Based upon the foregoing criteria, Table XII has been prepared. Tabulated are the room temperature (60°F) solubility of the carbonates and bicarbonates of cesium, lithium, potassium, rubidium and sodium. Note that cesium and rubidium are highly soluble both as the carbonate and the bicarbonate.

Of prime interest, as noted above, is the depression in dew point temperature obtained by using solutions saturated at room temperature. These data are tabulated for solutions at 100°C as obtained from the "Handbook of Chemistry & Physics." The depression for cesium carbonate was found experimentally.

The concentration of interest for any combination is the lower value since this is the compound most likely to precipitate. Thus, with potassium, the bicarbonate

TABLE XII

ROOM TEMPERATURE SOLUBILITY & SATURATION TEMPERATURE DEPRESSION
FOR FIVE ALKALI METAL CARBONATES

Alkali Carbonate-Bicarbonate	Mol. Wt.	Solubility (wt%)	Temp. (°C)	Concentration (w/w%)	Dew Point Temperature Depression at 100°C[1] (°F)
Cs_2CO_3	325.8	72.2	15	60	14.5 (150F)[2]
$CsHCO_3$	193.9	67.6	15		
Li_2CO_3	73.89	1.36	15		
$LiHCO_3$	67.96	5.21	13		
K_2CO_3	138.21	52.0	15	52	29.5
$KHCO_3$	100.12	23.5	15	23.5	5.5
Rb_2CO_3	230.95	69.0	15		
$RbHCO_3$	146.49	53.5	15		
Na_2CO_3	105.99	14.1	15	14.1	2.5
$NaHCO_3$	84.00	8.15	15	8.15	1.5

(1) Handbook of Chem. & Physics

(2) TRW data

concentration must not exceed 23.5 w/w% or precipitation at the anode may occur. With sodium, the bicarbonate concentration must not exceed 8.15 percent. Thus for these two materials, the usable dew point depression is only 5.5°F for potassium and 1.5°F for sodium assuming the complete conversion to bicarbonate and a solution temperature of 100°C. This indicates that volume control of the electrolyte solution is critical for these alkalies.

On the other hand, the cesium carbonate shows a bicarbonate solubility only 5% below that of the carbonate at room temperature. In addition, the saturation temperature depression is in the vicinity of 15°F at 150°F permitting rather coarse control of dew point temperature relative to electrolyte temperature.

In consequence of this finding, cesium carbonate is the recommended electrolyte. Rubidium carbonate is a possibility but has not been considered seriously due to its higher cost ($45/lb for Rb_2CO_3 versus $30/lb for Cs_2CO_3) and limited availability.

Test Data. - In the foregoing comparison of alkali metal carbonates, the solubility of the bicarbonate was referenced as if complete conversion to the bicarbonate occurs in a cell. In actuality only partial conversion occurs and consequently the degree of conversion is a factor of importance. In addition, the solubility of the carbonate in the bicarbonate and vice versa at a given solution temperature and water vapor dew point over the solution are critical factors in the performance of an electrolyte in a matrix cell.

Tests were run to determine the equilibrium carbonate/bicarbonate concentration as a function of anode gas carbon dioxide level for potassium and cesium carbonate. In addition, dew point depression data were established for a number of concentrations of cesium carbonate at two temperatures.

Potassium Carbonate Data: Carbon dioxide in contact with water will react to form carbonic acid, H_2CO_3, as below:

$$CO_2 + H_2O \rightleftharpoons H_2CO_3$$

The concentration of H_2CO_3 in moles per liter of solution is given by:

$$H_2CO_3 = CO_2 \text{ in solution} = 0.0338\ P_{CO_2}$$

where: P_{CO_2} = partial pressure of CO_2 in atm.

If the carbonic acid is formed in an alkali metal carbonate such as K_2CO_3

$$H_2CO_3 + K_3CO_3 \rightleftharpoons 2KHCO_3$$

The net reaction from the above is:

$$K_2CO_3 + H_2O + CO_2 \rightleftharpoons 2KHCO_3$$

The relationship between the partial pressure of carbon dioxide over the solution and the concentration of K_2CO_3 and $KHCO_3$ can be obtained from[1]:

$$P_{CO_2} = \frac{45f^2 N^{1.29}}{S(1-f)(302-t)}$$

Where:

N = potassium normality

f = fraction of total base present as bicarbonate

t = temperature, ^oF

PCO_2 = equilibrium partial pressure of CO_2, mm Hg

S = solubility of pure CO_2 in water under a pressure of 1 atm., g moles CO_2/liter

Within a cell, the electrolyte mixture must be in water vapor equilibrium with the inlet gas. Usually the cell temperature and supply gas dew point are chosen to match the known vapor pressure characteristics of the charging solution; namely K_2CO_3. If K_2CO_3 is converted to $KHCO_3$ having a differing vapor pressure concentration relationship, the volume of solution in the cell may change to such a degree that the cell either floods or dries excessively. The change in solution volume, if it occurs, changes the potassium normality in the above expression and therefore this relationship can not be used directly.

Therefore, instead of continuing test runs in a matrix cell, the experimental situation was simplified to a test tube partially filled with electrolyte through which the carbon dioxide containing gas was bubbled. A gas sparger was used to insure intimate contact between gas and liquid. The electrolyte solution was maintained at 125^oF by placing the tube in a heated cabinet. The gas was a mixture of carbon dioxide with hydrogen with the 25/75 proportion typical of the highest carbon dioxide concentration in the anode cavity of the CDCM.

The gas mix was pre-saturated to 117^oF dew point prior to introduction to the cell to provide an electrolyte concentration of 32.6 percent. The mix was bubbled through the electrolyte for 48 hours. At the end of that time it was noted that a solid had appeared on the walls of the test tube. Upon cooling the liquid to room temperature, a large amount of precipitate appeared. Both the liquid and the precipitate were analyzed. The solid was identified as all $KHCO_3$ and the liquid was a mixture of 11% K_2CO_3 by weight.

A second test was conducted at the same condition but with 20% KOH in the bubbler. The reaction proceeded from the hydroxide to the carbonate and bicarbonate with the formation of copious amounts of precipitate. Analysis of the mixture 137 hours after start of the test disclosed the solid to be 80 w/w% $KHCO_3$ and the liquid 12.2% K_2CO_3 and 23.2% $KHCO_3$. These values are nearly identical to the

[1] Sherwood, T. K., Pigford, R. L., Absorption and Extraction, pg 358, 1952.

above. Seidell[1] presents data on the mutual solubility of $KHCO_3$ and K_2CO_3 at a number of temperatures. These data are plotted in Figure 40. The maximum concentration of $KHCO_3$ in the liquid for any given concentration of K_2CO_3 is plotted at the corresponding temperature on the curve. $KHCO_3$ levels in excess of the value plotted will lead to precipitation.

Note that the equilibrated concentrations given above, 11, 24.5 and 12.2, 23.2 K_2CO_3 and $KHCO_3$, respectively, lie exactly on the curve at 122°F (~ 125°F).

These numbers correspond to a K_2CO_3 concentration (before $KHCO_3$ conversion) of 28.6% which is the maximum K_2CO_3 concentration the cell (stack) should be charged at in order to prevent $KHCO_3$ precipitation at 125°F with an anode gas composition of 25/75, CO_2/H_2 at 117°F dew point.

Solution volume measurements were made during these tests. It was observed that a slight increase in solution volume occurred during the run and therefore there is no reason to anticipate cell crossover as the result of this process.

Cesium Carbonate Data: No saturation temperature depression data for aqueous solutions of Cs_2CO_3 could be found in the literature. Consequently, these data were experimentally determined. The apparatus for this determination is shown in Figure 41. Note that a gas recycle loop was used to provide flow over the dew point sensor. The gas was impinged against the surface of the sample to prevent splashing and possible introduction to the sensor. The sample was maintained at temperature by a water bath. All lines in the loop were trace-heated well above the bath temperature. Determinations were made at a nominal temperature of 150°F and 125°F on 60, 40 and 20% Cs_2CO_3 solutions. Each determination was preceded by, and followed by, a test on water as the sample in order to check the performance of the system. Although some problems were experienced with the dew point instrument, the data is felt to be accurate within ±0.5°F. Specific gravity determinations were made to predict the solution volume curve.

The tabular data using the Cambridge Hygrometer are seen in Table XIII. The vapor pressure depression data are plotted in Figure 42 along with the solubility data for Cs_2CO_3. These data are replotted in Figure 43 with vapor pressure as ordinate, temperature as abcissa and carbonate concentration as parameter. Density data are given in Table XIV and a solution volume plot is shown in Figure 44.

A literature search for data on cesium carbonate provided the phase diagram shown in Figure 45.[2] Note that the freezing point of the 60% solution is -14°F. Further carbonate to bicarbonate conversion runs were made with Cs_2CO_3 as electrolyte. These tests were run with 60 w/w% Cs_2CO_3 at 125°F with 111°F dew point. The first series were run with a 25/75, CO_2/H_2 mix and the second with 50/50, CO_2/H_2 mix to typify conditions in the Stage I Carbonation Cell application.

---

[1] "Solubilities of Inorganic & Metal Organic Compounds," Atherton, Seidell, Vol. I, 1953, Van Nostrand.

[2] "Comptes Rendus," Carbonnel, L., Rollet, A. P., Vol. 256, pp. 2178-2181, (1963).

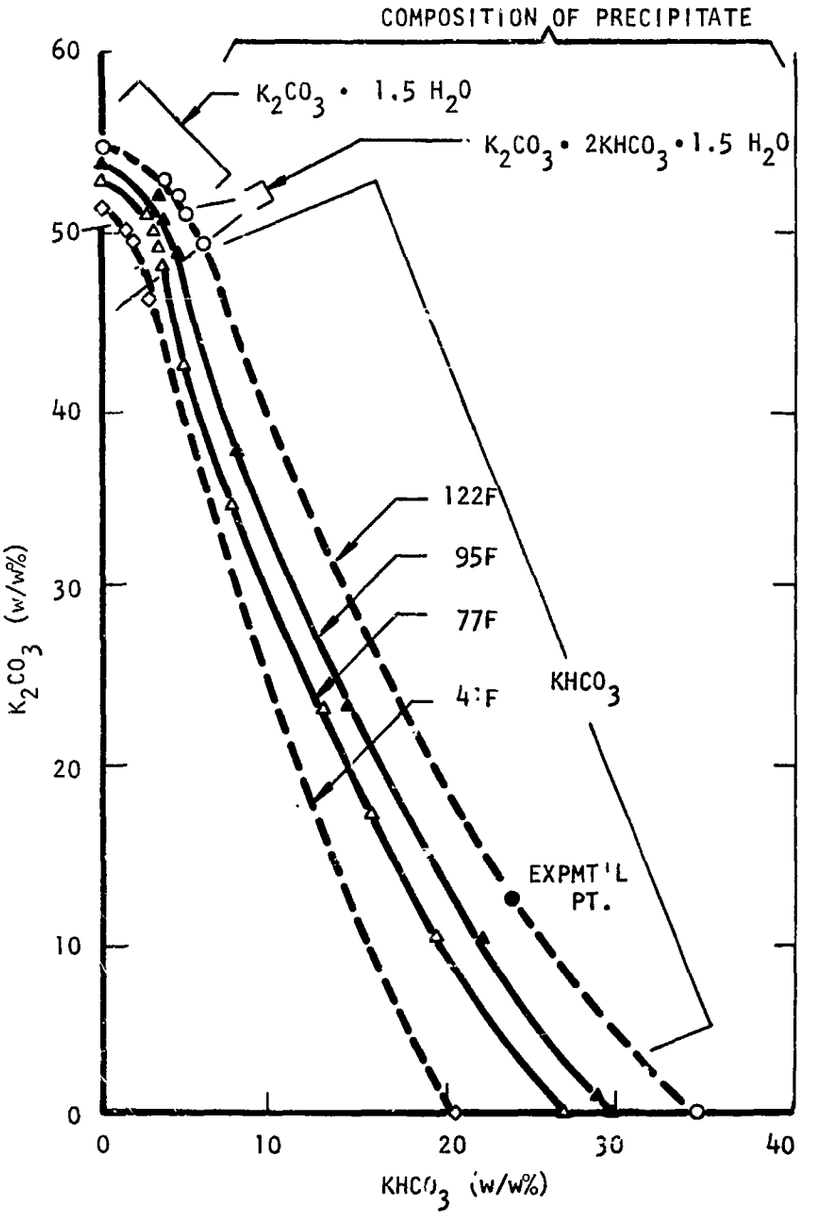

FIGURE 40 SOLUBILITY OF K_2CO_3 IN AQUEOUS SOLUTIONS OF $KHCO_3$ AND VICE VERSA AT SEVERAL TEMPERATURES

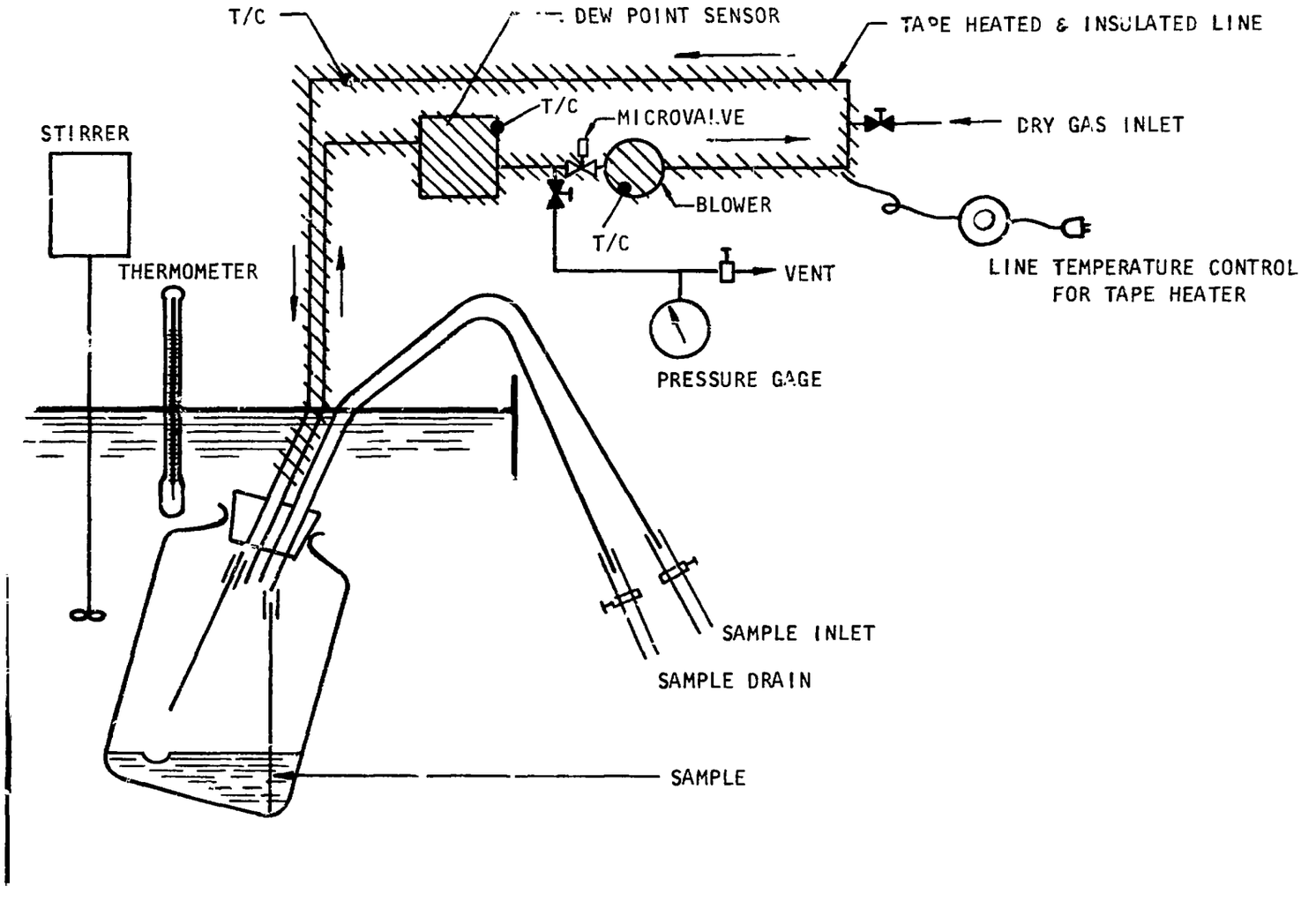

FIGURE 41 APPARATUS USED TO DETERMINE DEW POINT OF AQUEOUS ELECTROLYTE SOLUTIONS

TABLE XIII

DEW POINT DEPRESSION OF AQUEOUS Cs_2CO_3 SOLUTIONS

	Nominal 150°F					Nominal 125°F		
Date of Determination	4/7	4/8	4/8	4/8	4/8	4/8	4/9	4/9
Solution Temp. (°F)	148.0	147.8	147.8	147.5	147.5	124.5	124.5	124.5
Concentration (w/w%)	60	40	60	40	20	60	40	20
Measured Dew Point (°F) (1)	133.0	141.0	132.0	141.5	144.5	111.0	120.0	124.2
Correction to Dew (2) Point Temp. based on test with H_2O	+1.0	+1.0	+1.0	+1.5	+1.5	+0.8	+0.5	+0.5
Corrected Dew Point (°F)	134.0	142.0	133.0	143.0	146.0	111.8	120.5	124.7
Dew Point Depression	14.0	5.8	14.8	4.5	1.5	12.7	3.0	-0.2

(1) With Cambridge Vapor Mate II Model 137C1. Dew Point accuracy = ±1.4°F.

(2) Each data point with electrolyte preceded by a data point for water from which the correction was derived.

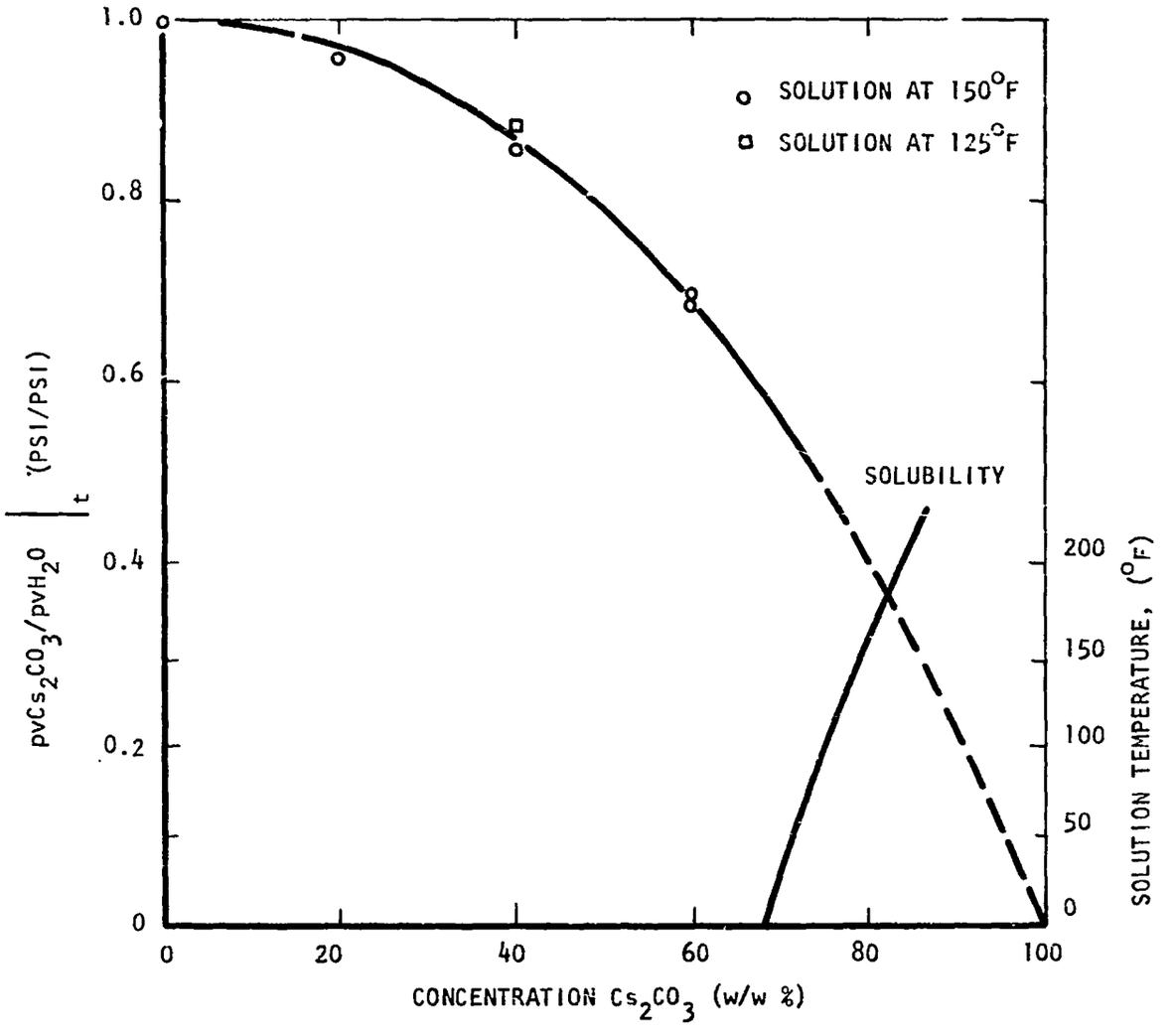

FIGURE 42 VAPOR PRESSURE DEPRESSION FOR AQUEOUS SOLUTIONS OF Cs_2CO_3 AT TWO TEMPERATURES

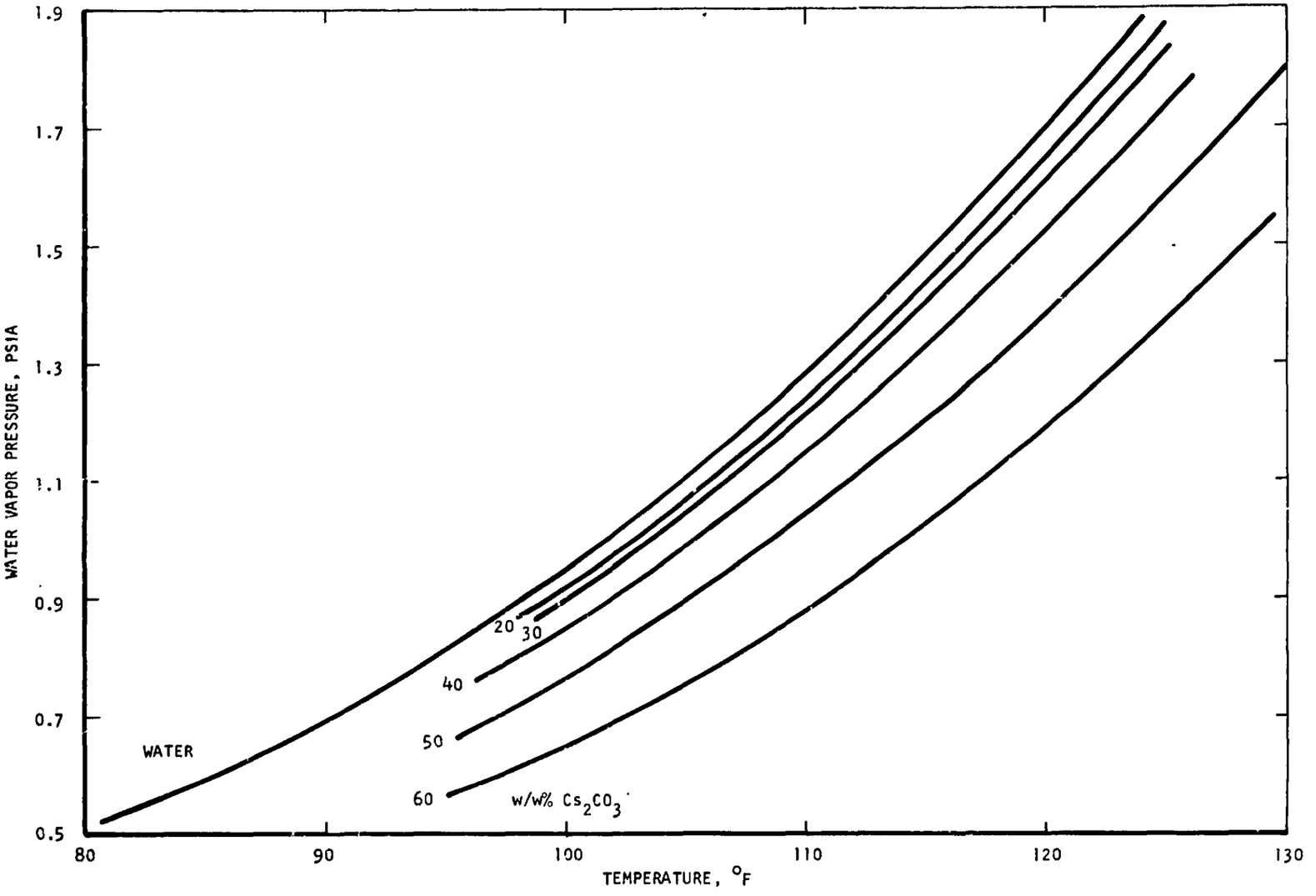

FIGURE 43 WATER VAPOR PRESSURE OF AQUEOUS SOLUTIONS OF Cs_2CO_3

TABLE XIV

DENSITY OF AQUEOUS Cs_2CO_3 SOLUTIONS AT ROOM TEMPERATURE

	Concentration (w/w%)		
	60	40	20
ρ(gm/cc)	1.93[1]	1.51	1.40
v(cc soln/g Cs_2CO_3)[2]	0.862	1.66	3.57

[1] Two preparations

[2] $v = \frac{1}{c\rho}$ c = concentration in %/100

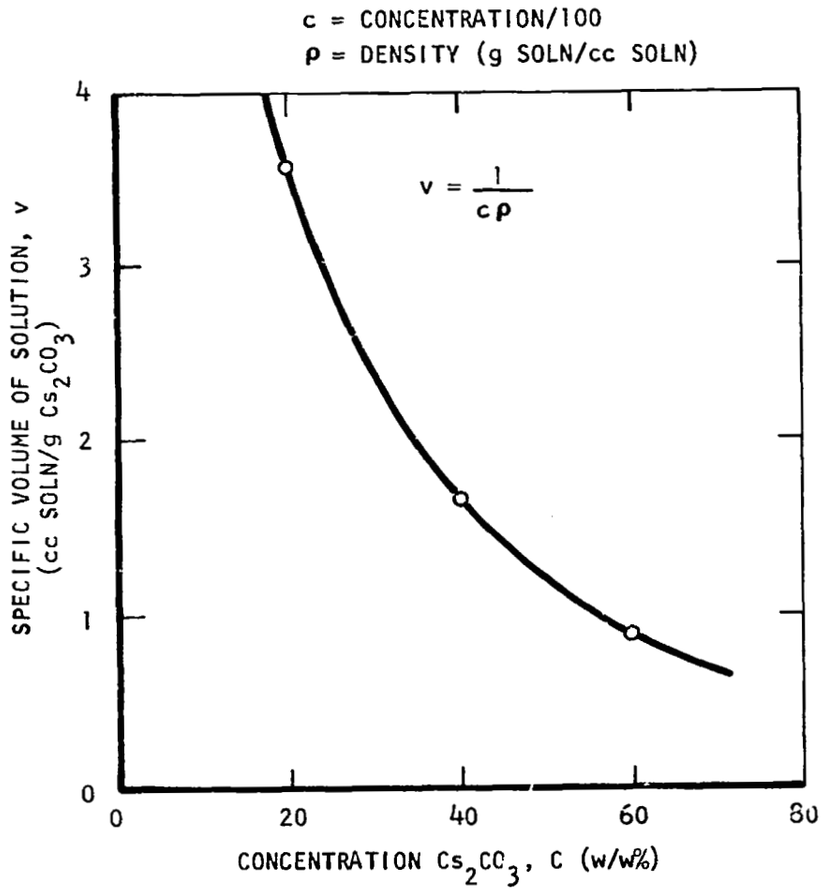

FIGURE 44 SPECIFIC VOLUME OF AQUEOUS Cs_2CO_3 SOLUTIONS

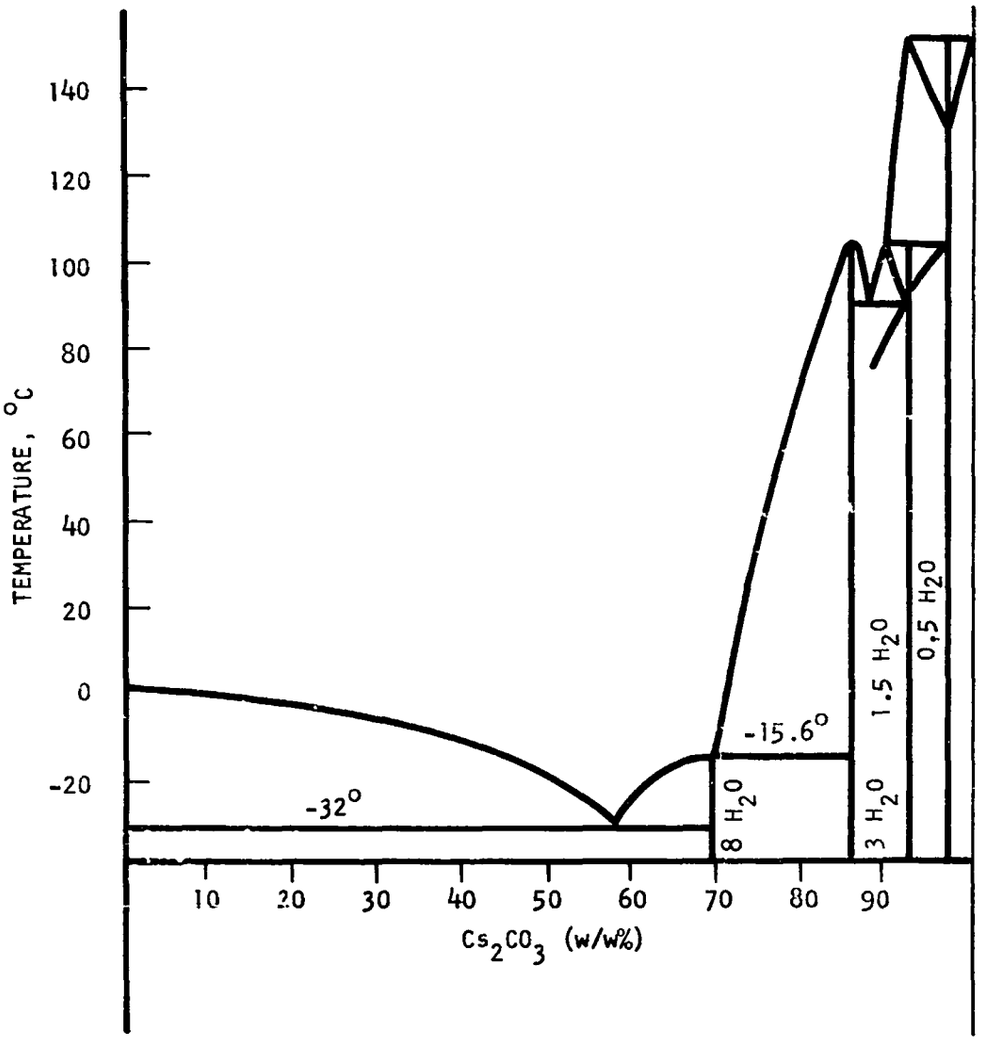

FIGURE 45 PHASE DIAGRAM Cs_2CO_3 - H_2O

in both cases, it was necessary to filter the solution before test due to the presence of alumina (identified by the vendor as a drying agent used in the production of Cs_2CO_3). This procedure should be followed in the preparation of all Cs_2CO_3 electrolytes.

The liquid from the test tube was decanted at temperature and used to prepare one pair of samples. The analysis of this pair was 10.4/43.95 and 10.1/45.20 w/w% $Cs_2CO_3/CsHCO_3$, respectively. The liquid was cooled and seeded with Cs_2CO_3 to see if a precipitate was formed. No precipitate was noted. The cold solution was filtered and analyzed in pairs as 10.7/43.95 and 9.55/30.20 w/w% $Cs_2CO_3/CsHCO_3$, respectively. Obviously this concentration of Cs_2CO_3 does not lead to precipitation at the aforementioned conditions. An electrolyte volume increase of approximately 6% was noted at the end of this run.

The second series run with the 50/50 CO_2/H_2 gas mixture showed an analysis of 4.52/57.30 and 4.05/58.20 w/w% Cs_2CO_3, respectively, for the decanted, hot solution and 4.18/57.5 and 4.19/57.5 w/w% Cs_2CO_3, respectively, for the cold, seeded and filtered solution. Again, no precipitate was noted either by observation in the test tube or as indicated by the analysis.

In the latter case, the volume of the electrolyte increased by approximately 10% after conversion. The above noted volume increases were small and could readily be offset by a small decrease in dew point of the entering gas if necessary.

Although the ionic conductance of Cs_2CO_3 solutions was not measured directly, the iR drop of small cells charged with this electrolyte has been determined. The iR drop of one cell charged and operated with 60 w/w% Cs_2CO_3 varied between 36 and 39 mv at a current density of 40 ASF. This number is for a 30 mil matrix and a cell temperature of 125°F. The iR drop of a cell charged and operated with 32.6 w/w% K_2CO_3 was 35 mv at the same conditions. Obviously there is relatively little difference in conductance between the two electrolytes.

It might be noted that visual inspection of the silver electroplate on the endplates of the cell charged with Cs_2CO_3 disclosed the plate to be bright and unmarked by evidence of corrosion upon cell tear-down. This unit was at temperature for approximately 700 hours and under load for at least three-fourths of this time.

Water Tolerance of Cesium Carbonation Solutions. - Using the data generated in the test program, it is possible to determine the decrease in electrolyte volume for a 2°F decrease in entering gas dew point temperature as presented above for potassium carbonate. Again, assume the concentrator to be operating at 115°F. The above data disclosed that a 60 w/w% Cs_2CO_3 solution may be utilized without incurring $CsHCO_3$ precipitation at anode gas compositions as high as 50% carbon dioxide at 1 atmosphere; consequently, assume a charge concentration of 55%. The data summarized in Table XV were obtained by use of Figures 43 and 44.

The tabular data shows that a 2°F decrease in gas dew point temperature (or electrolyte temperature increase of 2°F) will reduce solution volume by 10%. The data also shows that the dew point depression is 10°F and the final concentration does not exceed 60%. Comparison of these data with the tabular data for K_2CO_3 discloses that the dew point depression of 55% Cs_2CO_3 is

TABLE XV

SOLUTION VOLUME CHANGE, Cs_2CO_3

Cell Temperature - 115°F

Electrolyte - Cs_2CO_3

Dew Point Temperature - °F		Concentration w/w%		Solution Vol. Change	Dew Point Depression (Cell Temp. Minus Dew Point)
Initial	Final	Initial	Final	%	°F
105	103	55	59	-10	10

Maximum permissible value - - - - - - - - - - - - - -57.0

approximately the same as 38% K_2CO_3 and that the solution volume change for a 2°F decrease in dew point temperature is 10% for Cs_2CO_3 and 13.5% for K_2CO_3. Obviously, from the standpoint of dew point depression[3] (controlability)[2], minimum solution volume change (water tolerance) and freedom from bicarbonate precipitation, cesium carbonate is the preferred electrolyte.

Module Design

Performance Analysis, CDCM I. - During the parametric tests on CDCM I, a continuing problem of low or reverse cell voltage and gas crossover was experienced. The reason for these phenomena were sought by conducting long-term moisture balance tests on the concentrator. However, a definitive explanation for the performance malfunctions could not be arrived at. Calculations were then made for the purpose of examining temperature gradients within the unit. The results of these calculations were used to determine the increase in electrolyte concentration at the maximum loading point and to determine whether or not the average electrolyte concentration could increase to the point that the solution volume would be reduced to the point of gas crossover. The analytical data could also be inspected for conditions that would lead to bicarbonate precipitation in the anode gas cavity.

Heat Rejection: The heat rejected by a single cell of the CDCM is based upon a current of 10 amperes which is consistent with the maximum current required at the peak carbon dioxide rejection rate for the new design. Cell area is 0.241 ft^2 for a current density of 41.6 ASF. The heat rejection rate per cell is 38.5 BTU/hr at a cell voltage of 0.1 volt.

Inspection of the data obtained for a freshly charged stack of the first design, at a current density of 40 ASF, disclosed that the nominal cell voltage was 0.4 volt.

In operation over long time intervals, cell voltage in some instances would decrease and then reverse. These conditions were usually associated with dry cells and subsequent bicarbonate precipitation at the anode and resultant anode failure.

Temperature Variations within Working Area of Cell: The individual cell is cooled by means of heat conduction via a 0.020 in. thick, silver bipolar plate with fin extensions. The working area of the cell is 4.06 by 8.56 with the fin extending along the longer side. The root of the fin is 0.88 in. out from the edge of the active area of the cell. In this region, the structural framework, drawbolts and seal area are located.

Confining attention to the analysis of the temperature gradient existing between a longitudinal center line and the edge of a cell, this region may be treated as a fin with constant heat input. It is found that the temperature profile in this area is parabolic in shape. There is no heat flow across the longitudinal center line and the maximum temperature gradient occurs at the edge of the area.

The maximum temperature difference exists between a point on the longitudinal center line and the edge of the active area. This difference ranges from $5.7^{o}F$ at a cell voltage of 0.1 volt to $2.7^{o}F$ at a voltage of 0.7 volt. The temperature difference between the area average value and the temperature at the edge of the cell ranges from $3.8^{o}F$ at a voltage of 0.1 to $1.78^{o}F$ at 0.7 volt.

Temperature Difference between Active Area and Fin Root: A temperature gradient occurs between the edge of the active area of the cell and the fin root. The temperature difference across this region is almost $5^{o}F$ at 0.1 volt and approximately $2.3^{o}F$ at a cell voltage of 0.7 volt.

Temperature Difference between Fin Root and Ambient Air: The original design provided a fin, heat transfer area of 0.167 ft^2, and an air side coefficient of 11 BTU/hr-ft^{2}-^{o}F. Assuming an air flowrate of 40 cu. ft. per minute and an appropriate fin effectiveness, the difference between inlet air temperature and fin root temperature was calculated to be $12.5^{o}F$ for a cell running at a voltage of 0.7 and $26^{o}F$ for a cell running at a voltage of 0.1.

Electrolyte Control: Figure 46 shows the temperature profile across a transverse section of a cell for four different cell voltages. The plotted temperatures are the excesses over the temperature of the ambient cooling air. Of concern is the temperature distribution within the active area of a cell at differing cell voltages. Note that the area average cell temperature for a cell polarized to a terminal voltage of 0.1 volt is $18^{o}F$ above the average cell temperature for a cell running at a voltage of 0.7. In both instances, it is assumed that all cells are supplied with air at the same temperature and that there is no mechanism by which heat from the hotter running cell can flow to adjacent cells. Typically, in a stack construction, heat may be transferred from a hot cell to adjacent cooler cells through the matrix and bipolar plate. A computation of the temperature difference between a cell polarized to a terminal voltage of 0.3 volt, adjacent to cells running at a voltage level of 0.5, disclosed a temperature difference of $1.7^{o}F$ instead of the $4^{o}F$ value noted in Figure 46.

Consequently, any tendency toward the development of temperature differences between cells due to differences in the degree of polarization is reduced by internal thermal shunting. This shunting effect will be reduced if thermal

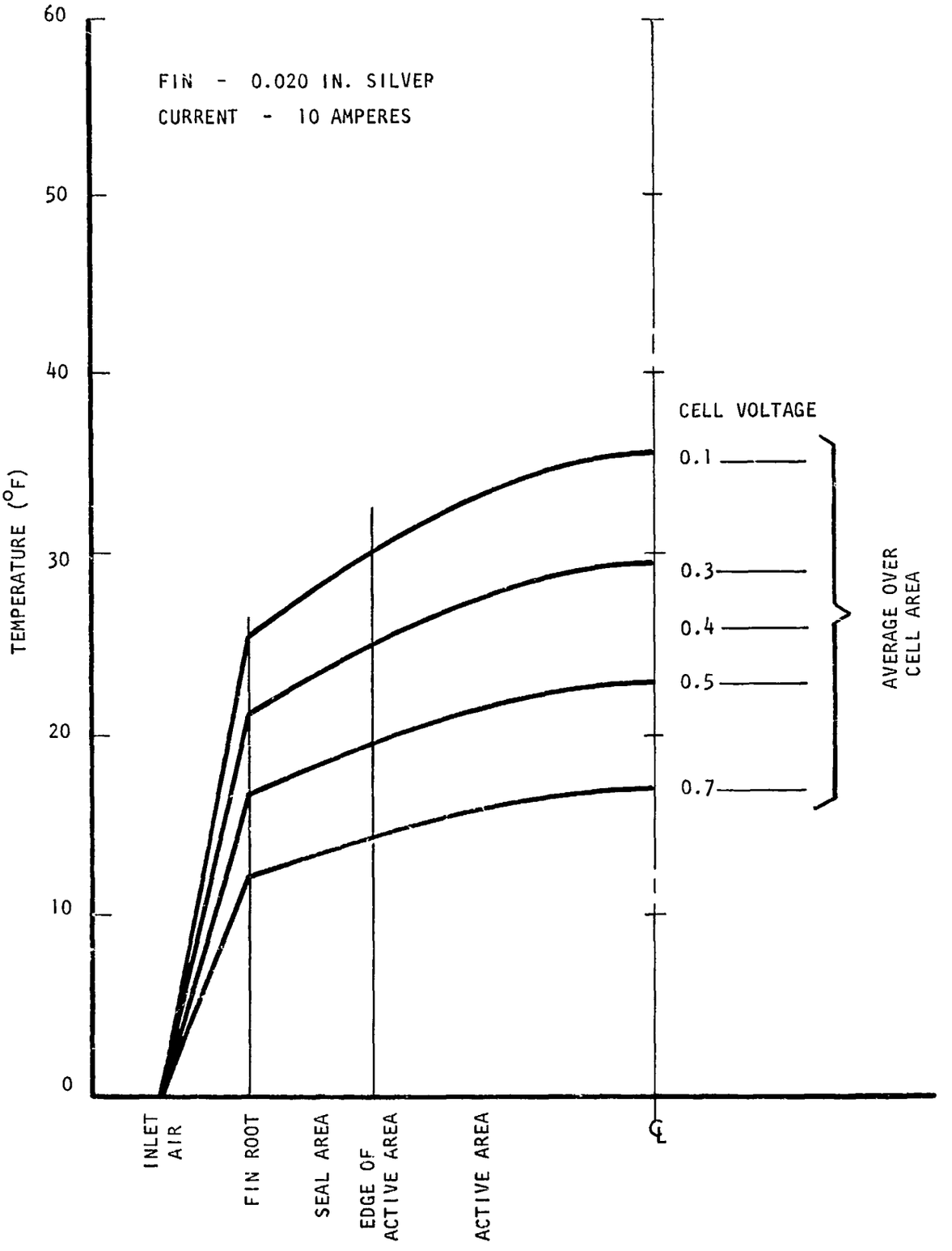

FIGURE 46 TEMPERATURE PROFILE - TRANSVERSE SECTION

contact between the gas cavity filler and the bipolar plate and cell electrode is not maintained. The thermal conductance from the electrode of a cell via the gas cavity filler material to the bipolar plate was computed to be 1000 BTU/hr ft^2-^oF. Neglecting contact resistance between the filler material and the opposing surfaces, the maximum temperature difference that could be developed between the electrode and the bipolar plate is 0.04^oF with the cell polarized to a terminal voltage of 0.1 volt. Consequently, in the absence of contact resistances, the temperature difference between the electrolyte in the cell and the bipolar plate is negligible.

In summary, it can be said that relatively large temperature differences may exist between cells running at high voltage versus cells running at low voltage in the same stack. Thermal mapping computations disclosed that a temperature difference of 1.7^oF will occur between a cell running at 0.3 volts adjacent to cells running at 0.5 volts whereas the plotted data indicate that this difference may be as much as 4^oF depending upon the degree of contact between the electrodes and the bipolar plate.

Since the contact resistance between cell components emerged as a significant factor determining the internal temperature distribution of the cell, all components of the first designed unit were carefully checked for dimensional stackup. It was found that due to a buildup in dimensional tolerances there was essentially no compression on the cell components. Consequently, cell hot spots could be expected due to the development of excessive thermal resistance between the gas cavity filler and the adjacent components. Tests with the components of this unit in a hydraulic press disclosed that the cell frames should be 0.020 in. thinner in order to provide a clamping load of approximately 50 psi over the area of the cell.

The analysis also disclosed that during off cycles of the cooling blower, excessive temperature differences may be developed between cells operating at different voltages. Consequently, it is desirable to throttle blower flow in order to insure continuous operation at the maximum loading condition. Alternatively, a thermal shunt between the cells in the fin region could be provided depending upon the design of the stack. This latter alternative was not explored further.

Since the degree of thermal contact within the unit is not well defined for the first design, no further analysis was made. However, design objectives for the second unit were clearly defined as a result of this work.

Design, CDCM II. - Fifteen cells form the redesigned module capable of transferring approximately 0.10 lb CO_2/hr continuously and 0.2 lb CO_2/hr peak. The thermal analysis was conducted at a design baseline condition and at 100 percent overcapacity. The results of all analyses are summarized in Table XVI.

Referring to the table, a fifteen-cell stack was chosen in order not to exceed a current density of 40 ASF at the 100 percent overcapacity condition. Stack thickness reflects this increase in the number of cells over the first design. Stack voltage is 6 volts at a nominal voltage of 0.4 per cell. In order to remove product water without developing excessive concentration gradients within the cell (and excessive changes in solution volume) the oxygen rate must be 3.6 SCFM at the 40 ASF condition.

TABLE XVI

CDCM DESIGN SUMMARY

	Base Line	100% Overcapacity
Geometrical Characteristics		
No. of cells	15	
Active area (sq. ft.)	0.236	
Stack size (in.)	14 long x 7 wide x 4.2 thick	
Electrical Characteristics		
Current density (ASF)	21	42
Current (AMPS)	5	10
Anode	Pt on Pt experimental	
Cathode	AB-6	
Stack voltage at 0.4v/cell (volt)	6	
Flow Characteristics		
CO_2 transfer rate (#/hr)	0.11	0.22
O_2/CO_2 recycle rate (SCFM)	3.6	3.6
H_2 rate (SLPM)	1.7	1.7
O_2/CO_2 pressure drop, parallel cells ($"H_2O$)	2.0	2.0
H_2 side pressure drop, series cells ($"H_2O$)	6.0	6.0
Thermal Characteristics		
Operating temperature (min, °F)	100	110
Heat rejection rate/cell at 0.4 volt (BTU/hr)	28.3	56.6
Maximum temperature variation within active area at 0.1 volt (°F) (1)	1.5	3
Temperature rise above air temperature at 0.4 volt avg. over cell area (°F) (2)		26
Nominal Gas Composition		
($\%CO_2$ on dry basis)		
Cathode in	[illegible]	1.42
Cathode out	[illegible]	0.5
Anode in	[illegible]	0.0
Anode out	29.0	58.0

(1) With 0.040 inch thick copper bipolar plate.

(2) With 40 CFM cooling air, fin area of 0.167 sq. ft. and air side film coefficient of 11 BTU/hr - sq. ft. °F.

Operation at the baseline c[illegible]tion can be achieved at a stack temperature of 100°F; however, at the max[illegible]ondition, operation at 110°F is required in order to remove product w[illegible]thout setting up e[illegible]essive concentration gradients. This requirement can be seen by reference to Figure 47. The temperature scale on the chart refers to the mean electrolyte temperature as measured by a sensor in the effluent oxygen stream within the oxygen manifold.

In the figure, the inlet and outlet dew point conditions are plotted versus the maximum and minimum cell temperatures (edge and center line, respectively) at a voltage 0.1 above and below a nominal 0.4 value. This plot provides data on the point-to-point electrolyte concentration in the cell. Preliminary plots of this type, for a 20 mil fin disclosed that at the maximum voltage (minimum polarization) condition, the electrolyte concentration at the edge of the cell was zero. Consequently, a smaller temperature gradient across the working area of the cell must be achieved by means of a thicker fin. The concentration excursions shown in Figure 47 are typical of a 40 mil copper fin at a stack current of 10 amps.

Figure 48 shows the cell temperature profile and regions of maximum and minimum electrolyte concentration in a cell. It is assumed that operation is at a nominal temperature of 110°F at a voltage of 0.4 volts in this figure. The inlet and outlet temperature and electrolyte concentration locus for these conditions can be readily related to the psychrometric plot of Figure 47. With reference to Figure 47, note that for a 10 amp stack current and cell voltage of 0.5, the discharge concentration is excessively low (10%). This is the direct result of lower heat dissipation and lower cell temperature for this (cooler running) cell. In pra[illegible], this extreme is not likely to be found since cell-to-cell heat conduction is not considered in these calculations. The average concentration and solution volume change from the charge concentration of 55% at two currents, two voltages and two stack temperatures are given in Table XVII.

Referring back to Table XVI, the carbon dioxide concentration at the anode gas outlet of the stack is 29% at the baseline condition and 58% at the maximum condition. Electrolyte tests disclosed that no bicarbonate precipitation was found at an anode gas carbon dioxide concentration of 50% at an electrolyte temperature of 125°F and; consequently, the probability of precipitation in the concentrator is minimal.

Module Fabrication

To a significant degree, the method of sealing a cell determines the method of fabrication and the cost of cell components.

O-ring seals permit the use of a flat-faced cell housing with the O-ring grooves machined into each face by end milling. However, a study of the performance of O-rings in CDCM I and the WEM disclosed that electrolyte and/or gas leakage has been a continuing problem. Ring dimensions, gland dimensions and surface finish as well as ring compounds have been studied with the aid of one of the larger O-ring fabricators without any conclusive results. Consequently, further consideration of O-ring seals for the redesigned CDCM was abandoned.

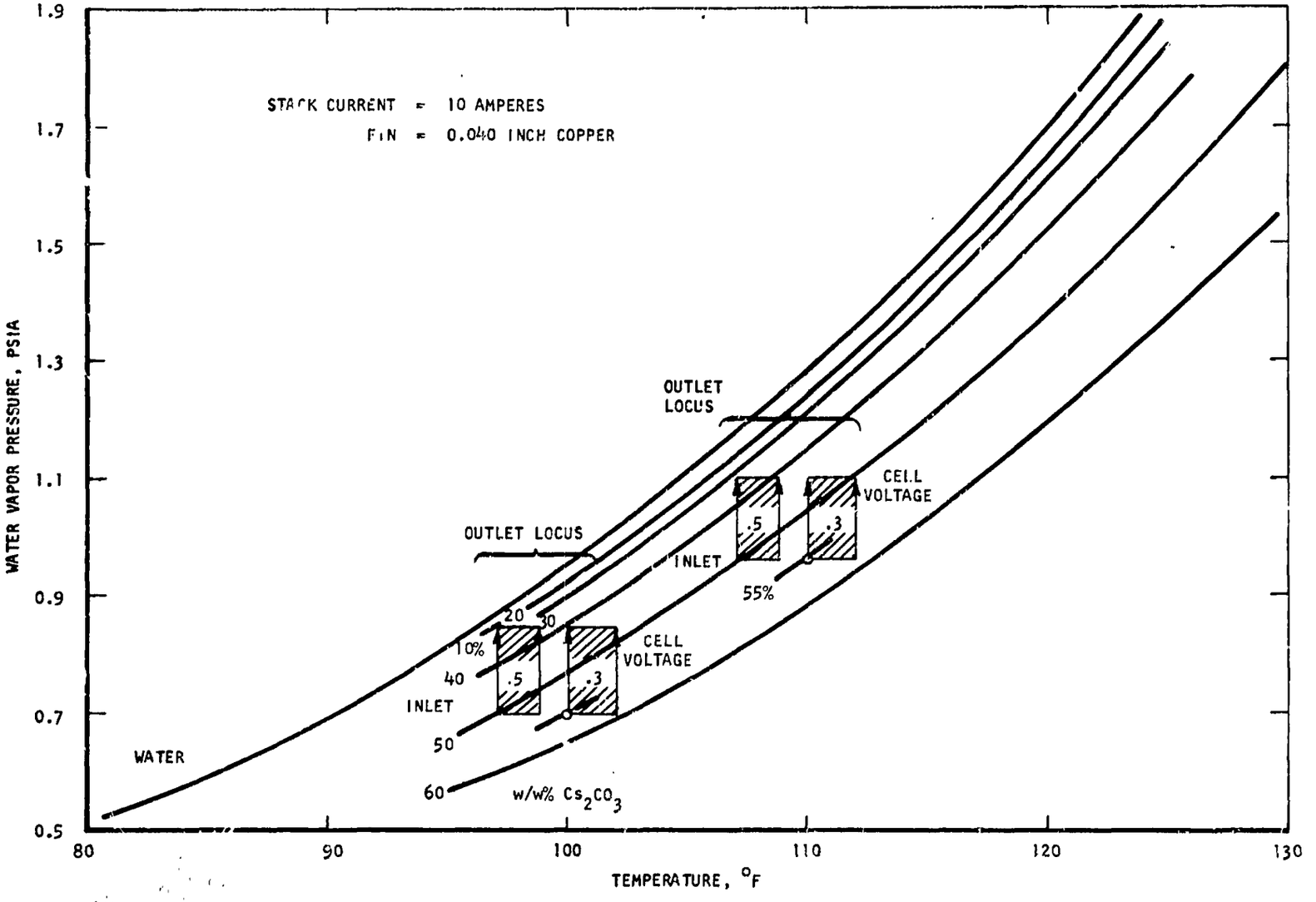

FIGURE 47 WATER VAPOR PRESSURE OF AQUEOUS SOLUTIONS OF Cs_2CO_3 - MODULE OPERATING CONDITIONS SUPERIMPOSED

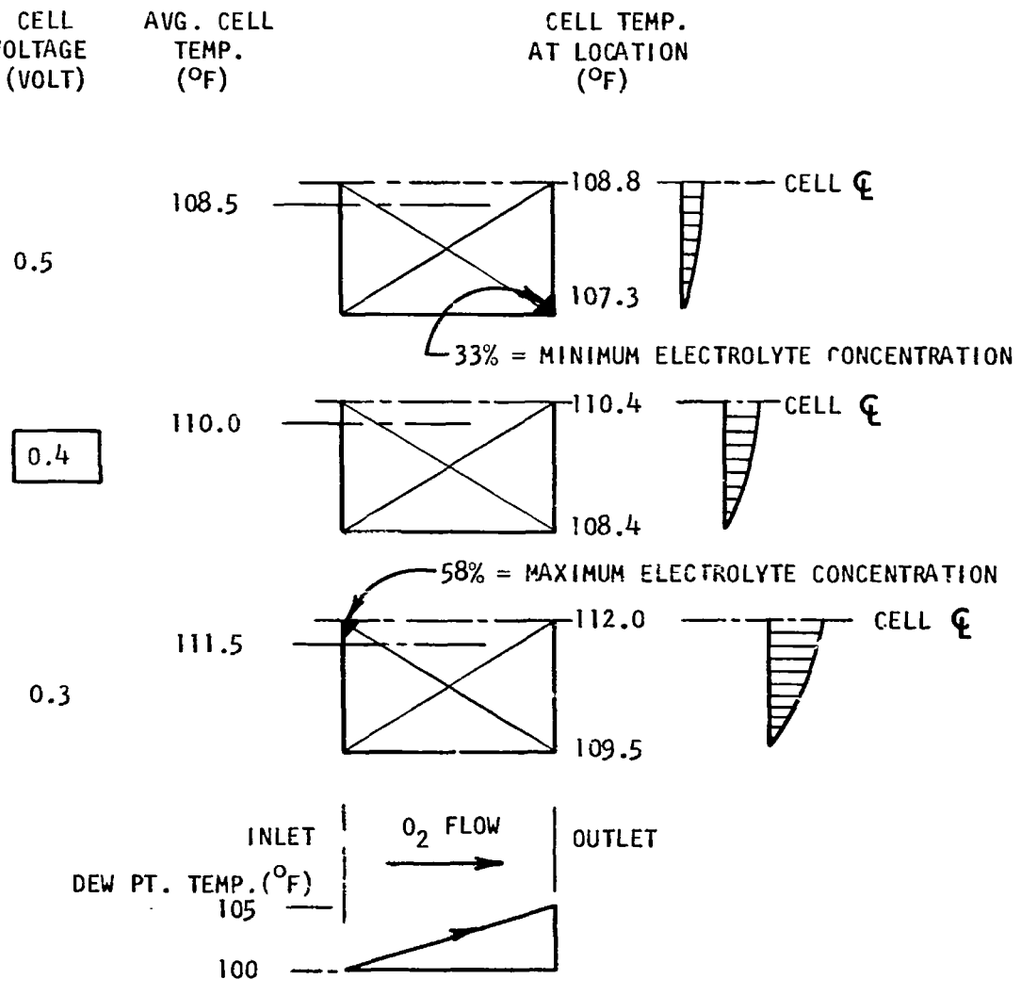

CONDITIONS:

1. NO. CELLS	=	15	5. LOAD CURRENT	=	10 AMPS
2. CELL AREA	=	0.25 SQ. FT.	6. COOLING AIR RATE	=	40 SCFM
3. FIN	=	0.040 IN. THK., CU	7. COEFFICIENT	=	11 BTU/HR-SQ.FT.-°F
4. FIN AREA	=	0.167 SQ. FT.	8. O_2 RECYCLE RATE	=	3.6 SCFM

FIGURE 48 TEMPERATURE PROFILE FROM CELL TO CELL AND CELL EDGE TO CELL CENTER (OVER WORKING AREA). MAXIMUM AND MINIMUM ELECTROLYTE CONCENTRATIONS

TABLE XVII

CONCENTRATION EXCURSIONS & VOLUME CHANGES IN CDCM

Stack Temperature, °F	100			
Inlet Dew Point, °F	90			
Stack Current, Amp	5 (design)		10 (max)	
Cell Voltage	0.5	0.3	0.5	0.3
Average Concentration, w/w%	50	55	45	53
Average Solution Vol. Change, %	+20	0	+45	+10
Stack Temperature, °F	110			
Inlet Dew Point, °F	100.5			
Stack Current, Amp	5 (design)		10 (max)	
Cell Voltage	0.5	0.3	0.5	0.3
Average Concentration, w/w%	51	56	47	53
Average Solution Vol. Change, %	+15	0	+30	+10

For 40 mil copper fin, charge conc. = 55%

Incorporation of Parker, Gask-O-Seals into the faces of the machined plastic cell housing was explored. In this process the seal configuration is molded into the plastic part after machining grooves in the desired regions. The method was not deemed feasible because of cost and lead time as well as concern relative to damage of the cell housing during the molding operation.

Due to the satisfactory performance of a molded flat gasket in a similar application, this approach was considered in conjunction with the machined cell housing. In order to effect a seal, the flat gasket would be provided with a raised region of limited area in order to provide the large compressive load necessary to ensure sealing. This approach requires that the cell housing be relieved on both sides in order to accommodate the thickness of the gasket. This additional machining operation adds materially to the cost of the part. In addition, a thin molded gasket with a thicker region is quite expensive due to mold costs.

It became apparent at this point that consideration of a molded plastic cell housing would remove most of the cell design limitations inherent in the machined part. With the molded part, the compression region of the gasket is provided by a raised region on the face of the cell housing rather than by utilization of a gasket with a mold[illegible]ib. Consequently, a flat, die-cut gasket may be utilized with a lar[illegible] in cost. It was also planned that the hydrogen compression mani[illegible]ded since this component in its optimum form would be costly to manuf[illegible] machining.

With the design approach es[illegible]shed, detail and assembly drawings of each component were prepared. The assembly drawing of CDCM II is shown in Figure 49. A cross-section through the oxygen manifold is shown in Figure 50 with all items identified. A tabulation of materials of construction for the items of Figure 50 is given in Table XVIII.

Figure 51 shows a photograph of the stack components exclusive of the endplates, for both the original and redesigned units. Note that the redesigned unit uses flat gaskets in lieu of the O-rings used in the original design.

Also note that the fin plate assembly comprises a copper core with titanium clads on both sides instead of the solid silver fin plate used in the original design. The clads shown in the photograph have not yet been bonded or welded. The current carrying tabs seen on the gas cavity filler will be welded to the titanium clad and will be in pressure contact with the electrodes.

The plastic cell housing and compression manifold are shown in Figure 52. Prior to the decision to mold these components, work was initiated to determine the molding characteristics of polysulfone sheet stock. Blanks approximately the length and width of the cell housing were preheated in an oven at 250°F. The blanks, after heating, were transferred to a heated platen press operating at a temperature of 425°F. It was found that loads in the order of thirty tons would readily form the blank into a typical, simplified cell structure.

On the basis of these tests, the total design was co[illegible]leted and a vendor located to fabricate the plastic parts by compression moldi[illegible]. After the mold was

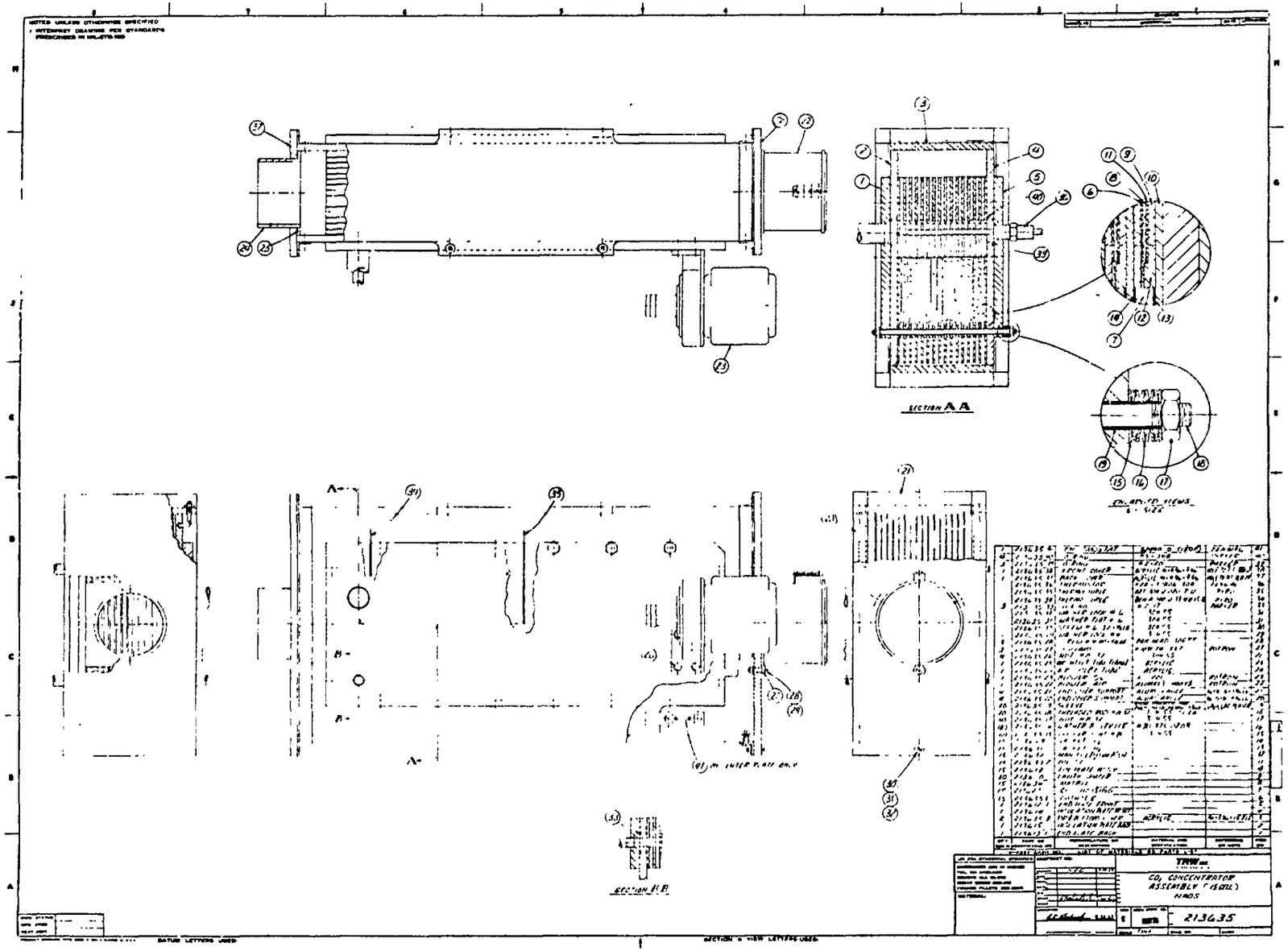

FIGURE 49 CO_2 CONCENTRATOR ASSEMBLY (15 CELL) NAOS

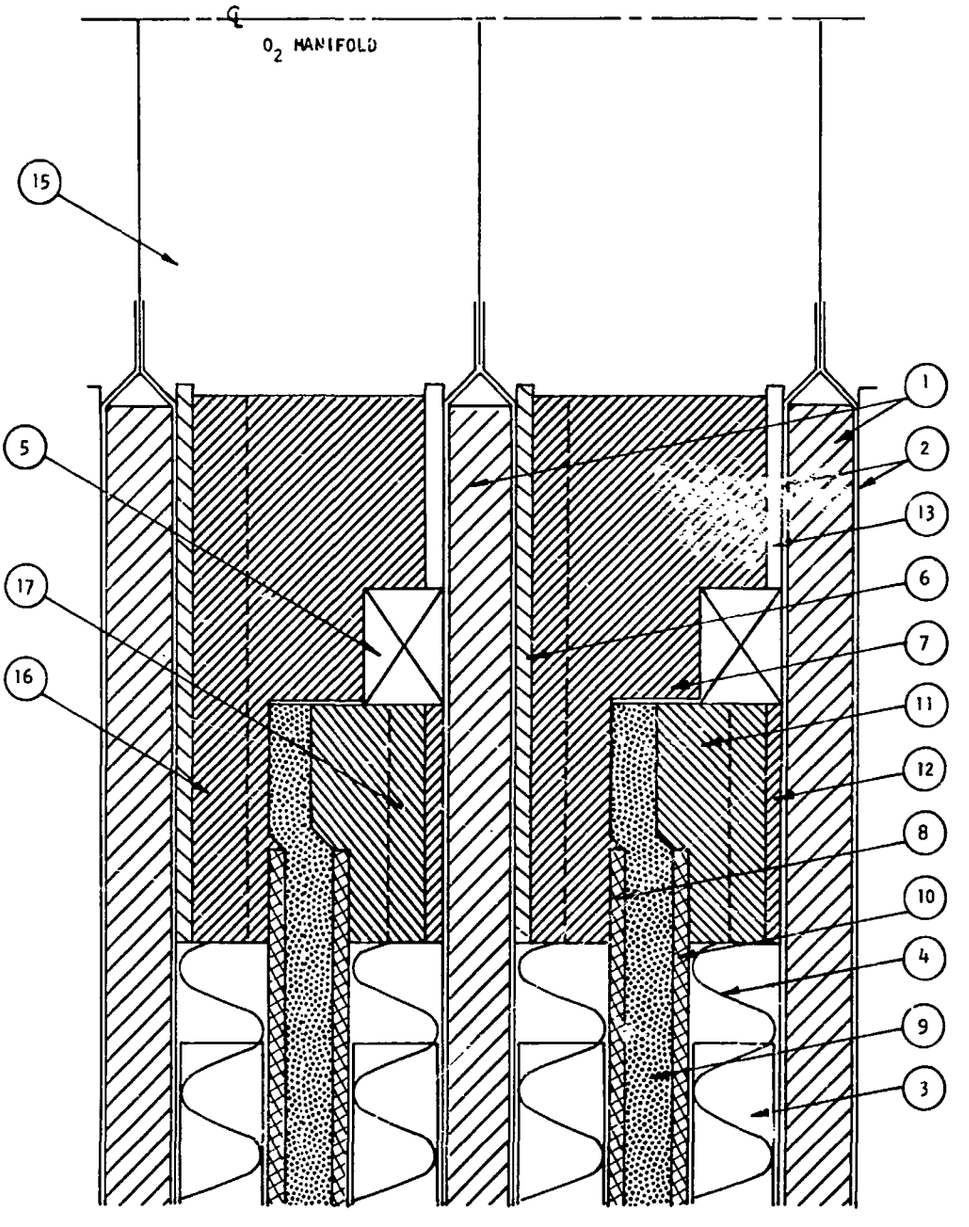

LEGEND:

1	- BI-POLAR PLATE	9	- MATRIX
2	- CLAD	10	- ANODE
3	- CURRENT TAB	11	- FRAME, H_2
4	- CAVITY SPACER	12	- PORT COVER, H_2
5	- DISTRIBUTION MANIFOLD, H_2	13	- GASKET, H_2 SIDE
6	- PORT COVER, O_2	14	- GASKET, O_2 SIDE (NOT SHOWN)
7	- CELL HOUSING	15	- MANIFOLD, O_2
8	- CATHODE	16	- PORT, O_2
		17	- PORT, H_2

FIGURE 50 CO_2 CONCENTRATOR MODULE SECTION THROUGH O_2 MANIFOLD

TABLE XVIII

MATERIALS SELECTIONS, CDCM II

Cathode	American Cyanamid Standard AB-6
Anode	American Cyanamid Pt on Pt (10 mg/cm^2)
Matrix	Fuel Cell Board, 0.030 inch thick
Gas Cavity Filler	Expanded Titanium, Exmet Distex 10Ti 35-1/0
Cell Housing	Polysulfone, P-1700
Gasket	Ethylene Propylene Rubber, EPR, 50 Duro
Bipolar Fin Plate	ETP Copper, 0.040 inch thick
Clad	Ti, A-40, annealed, 0.005 inch thick
Current Tabs	Platinum, 0.001 inch
Endplate Insulator	Polysulfone
Endplate	316 Stainless Steel
Drawbolts	316 Stainless Steel

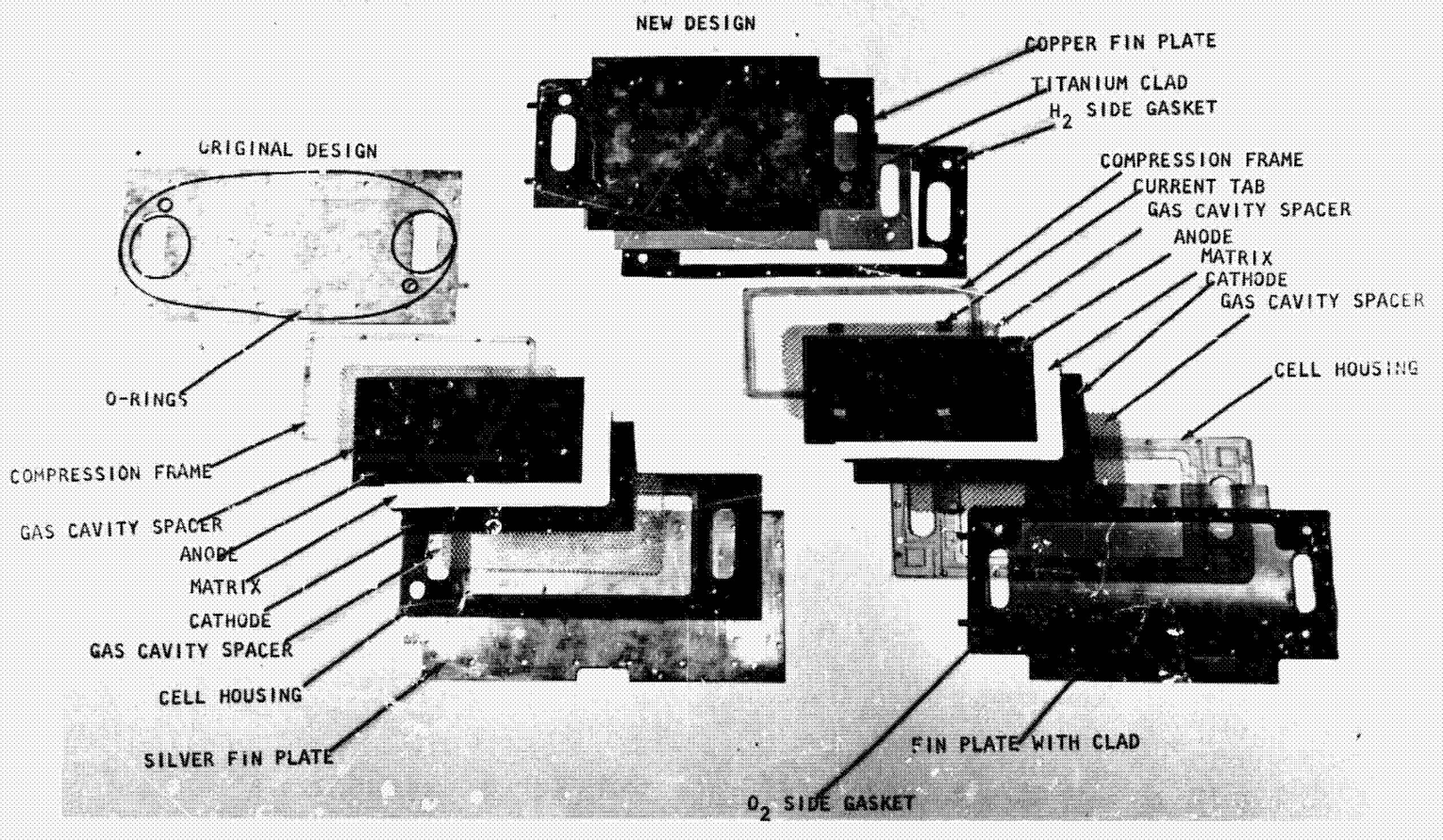

FIGURE 51 CARBON DIOXIDE CONCENTRATOR MODULE COMPONENTS

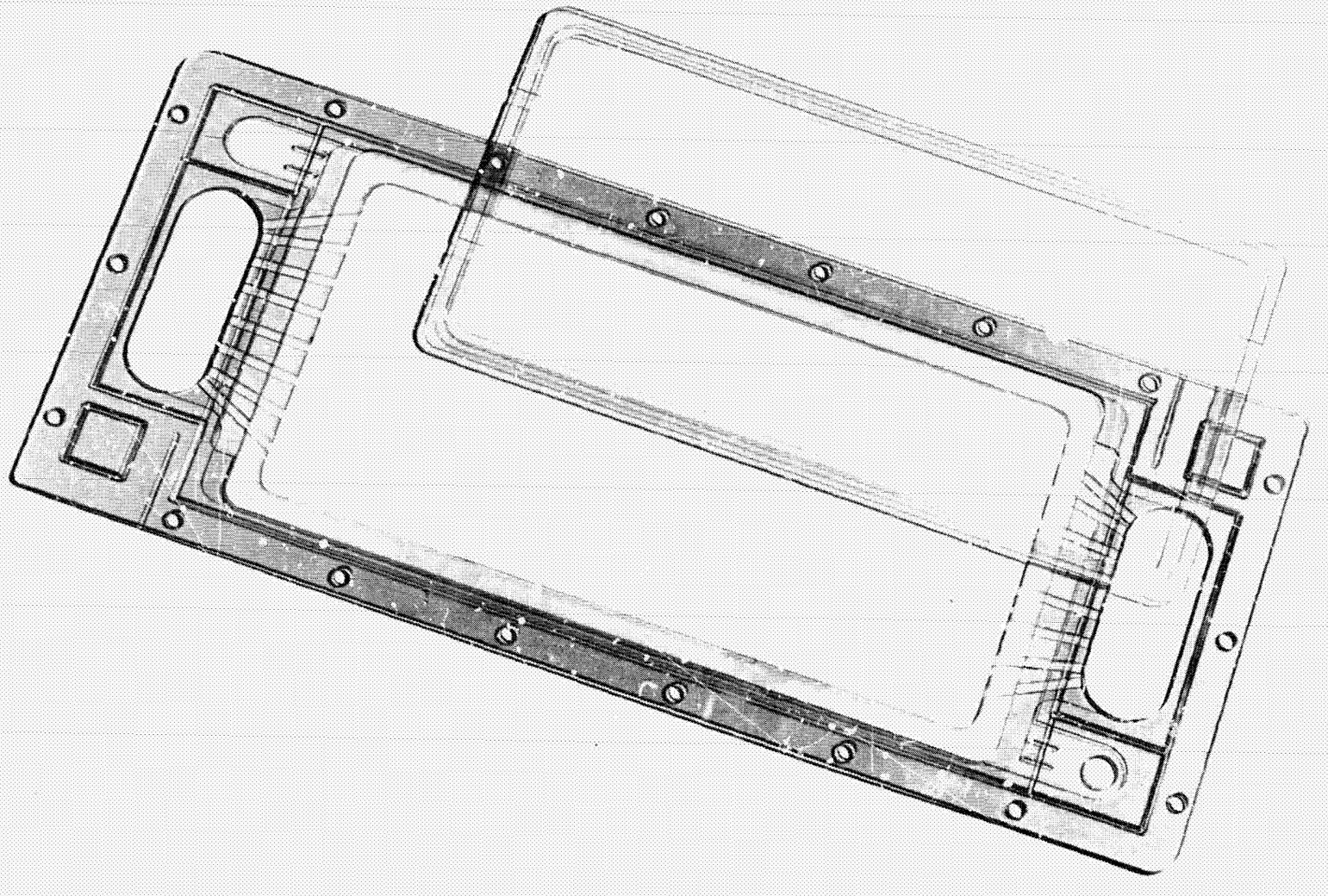

FIGURE 52 PLASTIC CELL HOUSING COMPONENTS FOR REDESIGNED CO_2 CONCENTRATOR

completed for the compression manifold, a part was fabricated and found to contain a large number of both surface and internal bubbles. A study at TRW disclosed that the internal bubbles resulted from water vapor trapped within the material and the surface bubbles were the result of air entrapment in the mold. It was found that the internal bubbling could be minimized by maintaining the molding temperature as low as possible consistent with forming requirements. The surface bubbles could be eliminated by sealing and evacuating the mold cavity prior to forming the blank into the mold.

Due to the fact that the mold for the cell housing is a great deal more complex than the relatively simple compression manifold, it was decided that this mold should be filled by the injection process. The first runs made on an injection molding machine disclosed that excellent parts could be fabricated; however, a number of minor problems were identified. All of these were readily solved. The raised region of the flat face of the cell housing referred to above as the bulb or seal area was completely free of any defect.

The fin plate assembly is shown in Figure 53. The 0.040" thick copper plates were fabricated by die cutting rather than stack milling as in the past. The die cut parts were found to be free of edge rollover and burrs. The drawbolt holes were drilled into these components by means of a drill fixture in a later operation.

The 0.005" thick titanium cladding sheets were fabricated with a steel rule die. A negligible amount of edge deformation was seen in the fabricated parts. Based upon the above observations, die cutting appears to be a satisfactory method of fabricating these components.

A quotation was solicited on the ultrasonic weld of the two titanium cladding sheets to each other at the perimeter of the hydrogen and oxygen ports. The tooling cost for this process was found to be excessively high and consequently this approach was abandoned. A TIG weld, using a small hand-held electrode, was employed to weld two pieces of the cladding sheet to each other. A rudimentary tool was used to clamp the sheets tightly together during the welding process. The hand weld appeared to be excellent. Each welded assembly was placed in a leak test fixture and the majority found to be free of defects. A few skips and cracks were found in some that were readily repaired.

Verification Testing

The design of the carbon dioxide concentrator was verified by assembly and operation of two single cells in the single cell life test stand and assembly of a four-cell submodule and subsequent operation in the parametric test rig.

Single Cells. - Two single cells of the same design as the redesigned module were assembled. Copper tubes were soldered to the fin region of the fin plates in order to allow use of the test stand coolant and temperature control facility for the maintenance of cell temperature. Endplates were 1/4 in. thick acrylic plastic with stiffeners in the region of the oxygen manifold seal area.

These cells were leak-tested and charged with 52% Cs_2CO_3. After checking for the absence of crossleaks these units were installed in the life test stand.

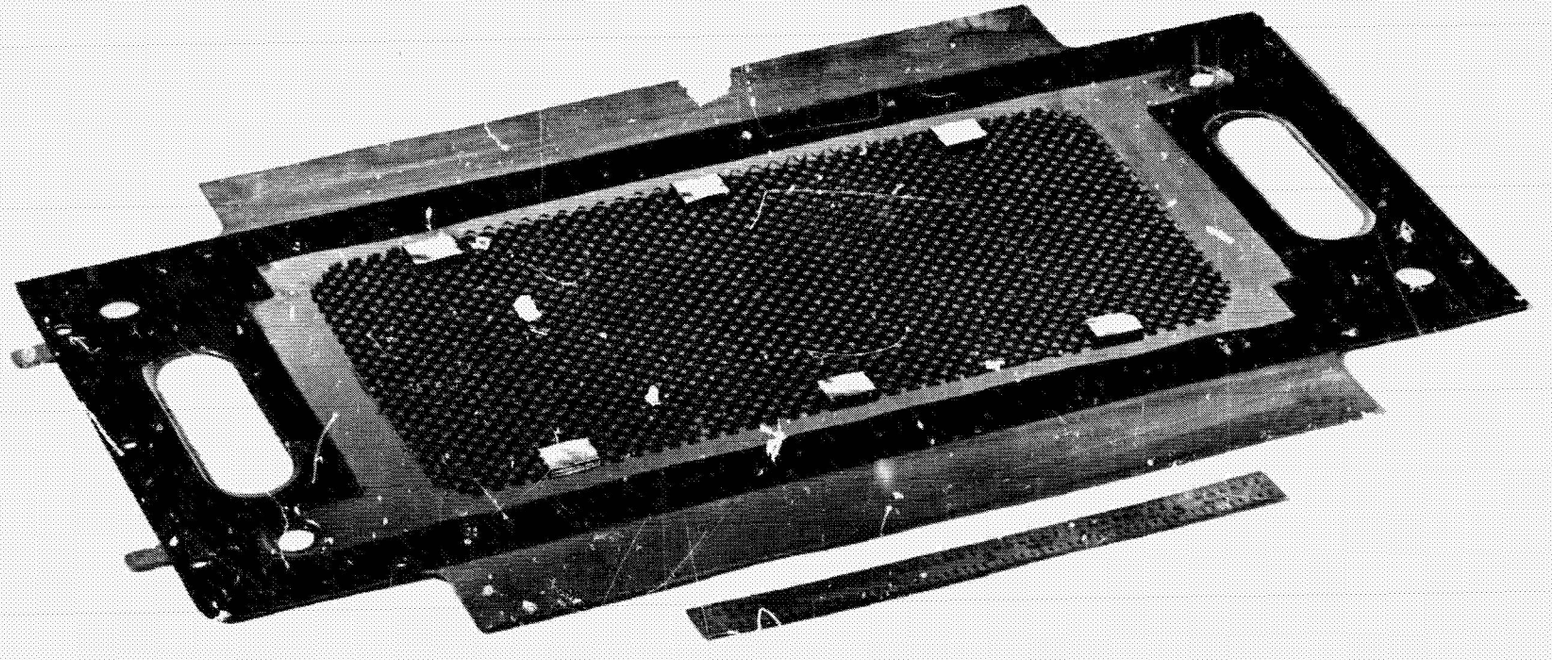

FIGURE 53 FIN PLATE ASSEMBLY FOR REDESIGNED CO_2 CONCENTRATOR

Verification of basic module redesign was established by stable operation of the first cell up to 10 amps (40 ASF) and subsequent long-term stable operation at 4 amps (16 ASF).

Four-Cell Module Assembly. - The four-cell module is seen in Figure 54 without air shrouds or thermal insulation. The stack temperature control thermistor can be seen installed in the oxygen discharge manifold. During assembly, it was found that the oxygen side gasket required a greater window opening than provided by the vendor in order to prevent the gasket from overlapping certain regions of the cell housing. Therefore, these gaskets were razor cut as required. The drawing for this component has been modified to reflect the change. Since the relative position of the gasket and cell housing is critical, these components were secured to each other during assembly with a thin layer of silicone grease.

The stack was assembled with a drawbolt torque of 30 inch-pounds as found necessary to insure the absence of leakage. This torque is excessively large and it was found on tear-down that in spite of the mounting procedure noted above, some lapping did, in fact, occur. In any event, the unit was leak-free at 10 psig. It was subsequently charged with 55% Cs_2CO_3 and when wetted showed no external-to-internal leakage at 28" Hg internal vacuum pressure and no cross-leakage at 10" Hg pressure difference.

To further explore internal-to-external leakage, a single cell unit, carefully prepared to avoid any possibility of gasket lapping, was assembled between the plastic and stainless steel endplates. This cell was pressurized with air and immersed in water. No leakage was found at 40 psig air pressure. The charged and drained unit was installed in the parametric rig and tested at the conditions shown in Table XIX. The gas rates and load current given correspond to a 0.4 man unit of the original NAOS design. The blower and heating/cooling facility in the test stand was used to thermally control the module.

The performance of the module on the design verification test is seen in Figure 55. Note that the carbon dioxide concentration in the effluent oxygen was less than 0.5% during most of the test. Cell voltage averaged 0.5V. The carbon dioxide transfer rate per amp-minute-cell is in the region of 6 to 6.7, determined from carbon dioxide input to the oxygen side. The specific transfer rate of carbon dioxide can also be deduced from carbon dioxide analysis of the anode gas, measurement of the hydrogen feed rate and measurement of cell current. The specific transfer rate deduced by the above calculation at each test condition is also plotted in Figure 55 and shows good agreement with the directly measured value.

During the period of 76 to 138 hours of load time, the hydrogen source was valved off. Anode potential increased from the region of hydrogen consumption to oxygen (and carbon dioxide) evolution. Power was required by the unit in this mode of operation and consequently a DC supply was added to the electrical current loop. The data gathered in this period is shown in Figure 56. Note that the carbon dioxide level on the feed side of the module is in the region 0.4 to 1.0%. Cell voltage averaged at approximately 1.22 volts. The specific transfer rate is essentially as noted before.

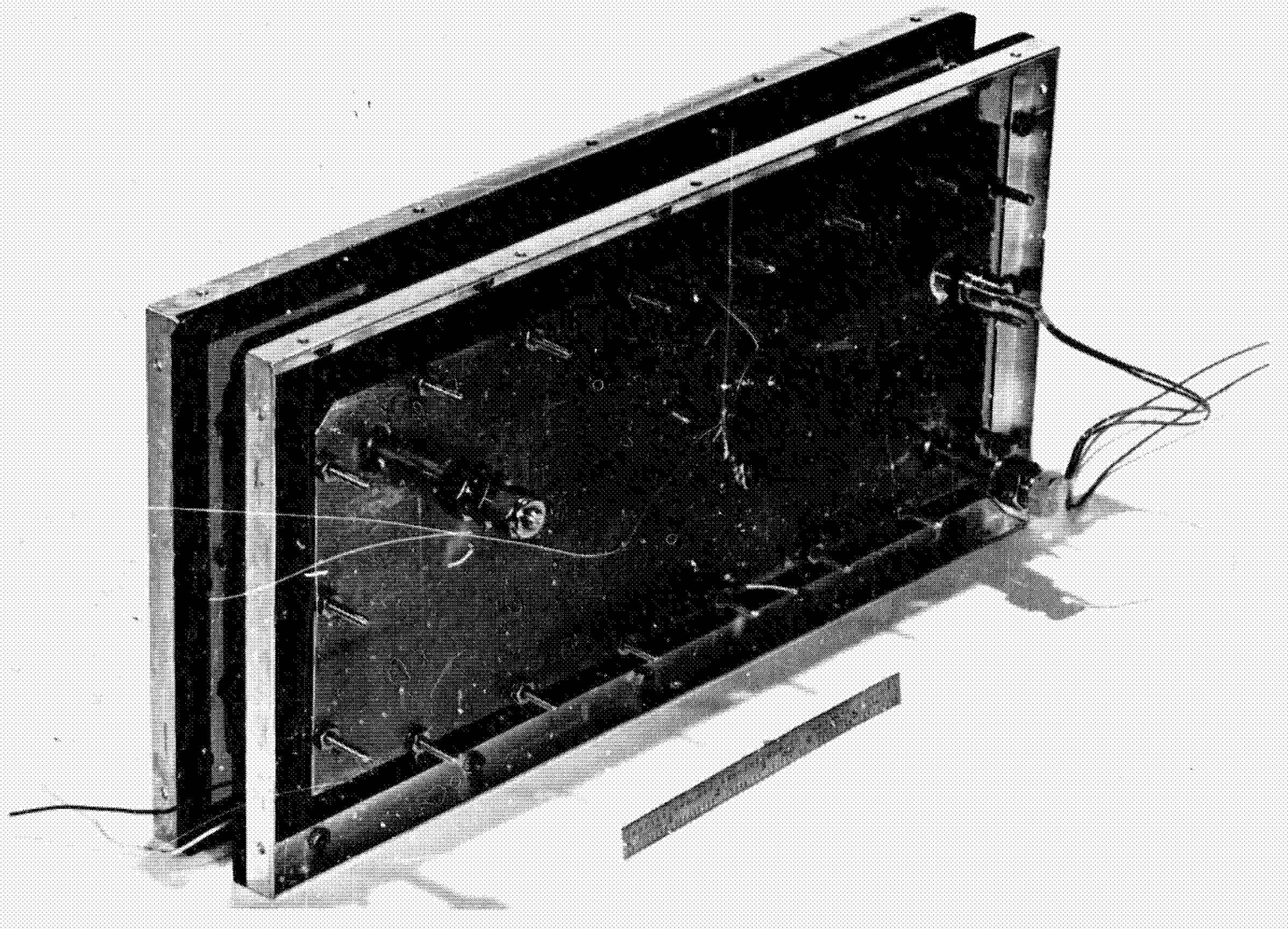

FIGURE 54 FOUR-CELL REDESIGNED CO_2 CONCENTRATOR MODULE

TABLE XIX

OPERATING CONDITIONS FOR
DESIGN VERIFICATION TEST RUN

Stack Current, amp	7.5
Cell Temperature, ^{o}F	110 nominal
Oxygen Saturator, ^{o}F	100 average
Hydrogen Saturator, ^{o}F	100 average
Electrolyte	Cs_2CO_3
Electrolyte Concentration w/w%	55
Gas Pressures, in. H_2O gage	20
CO_2 Flowrate, SLPM	0.18
H_2 Flowrate, SLPM	0.64
Oxygen Recycle Rate, SCFM	1.4

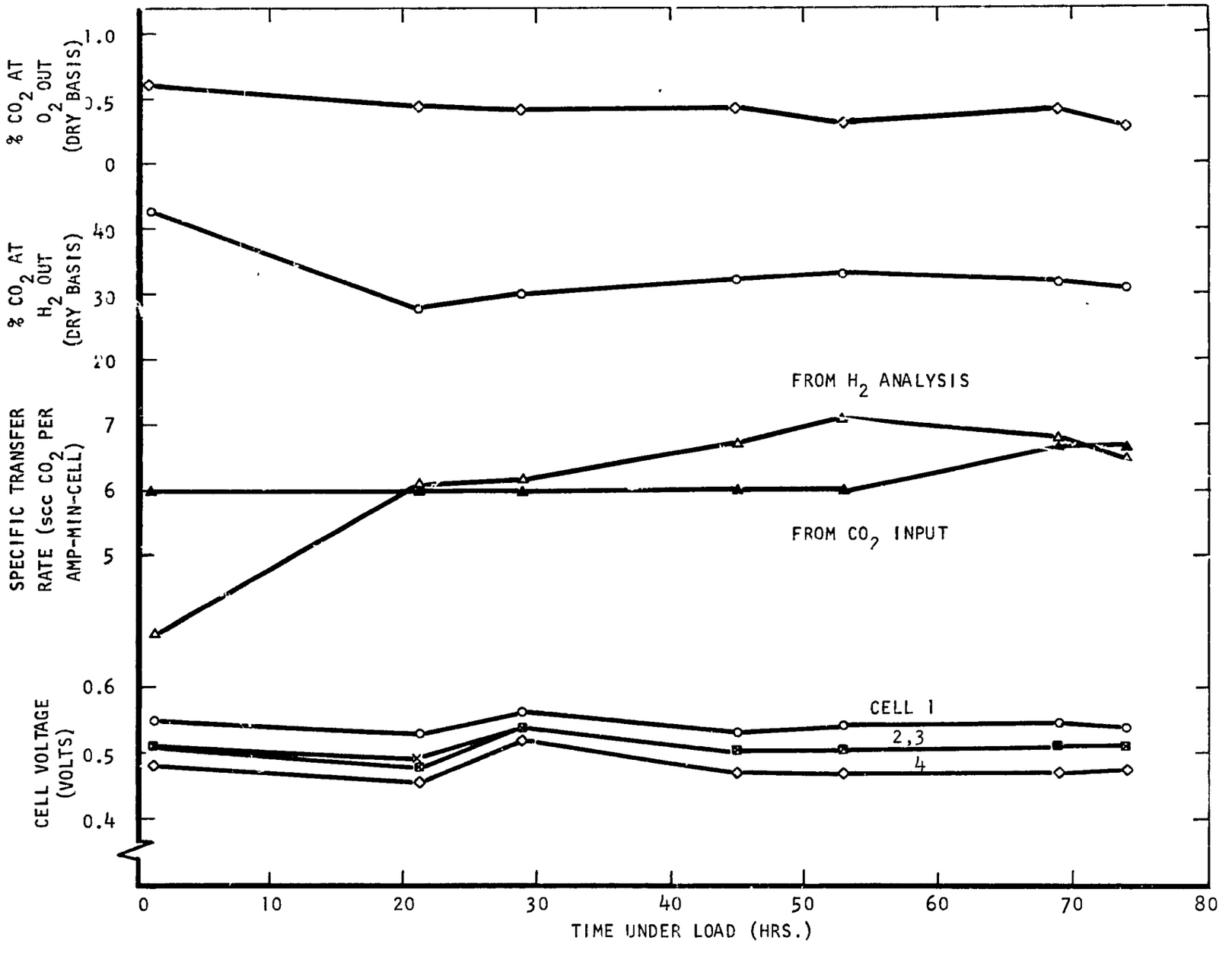

FIGURE 55 DESIGN VERIFICATION RUN - 4-CELL CONCENTRATOR MODULE

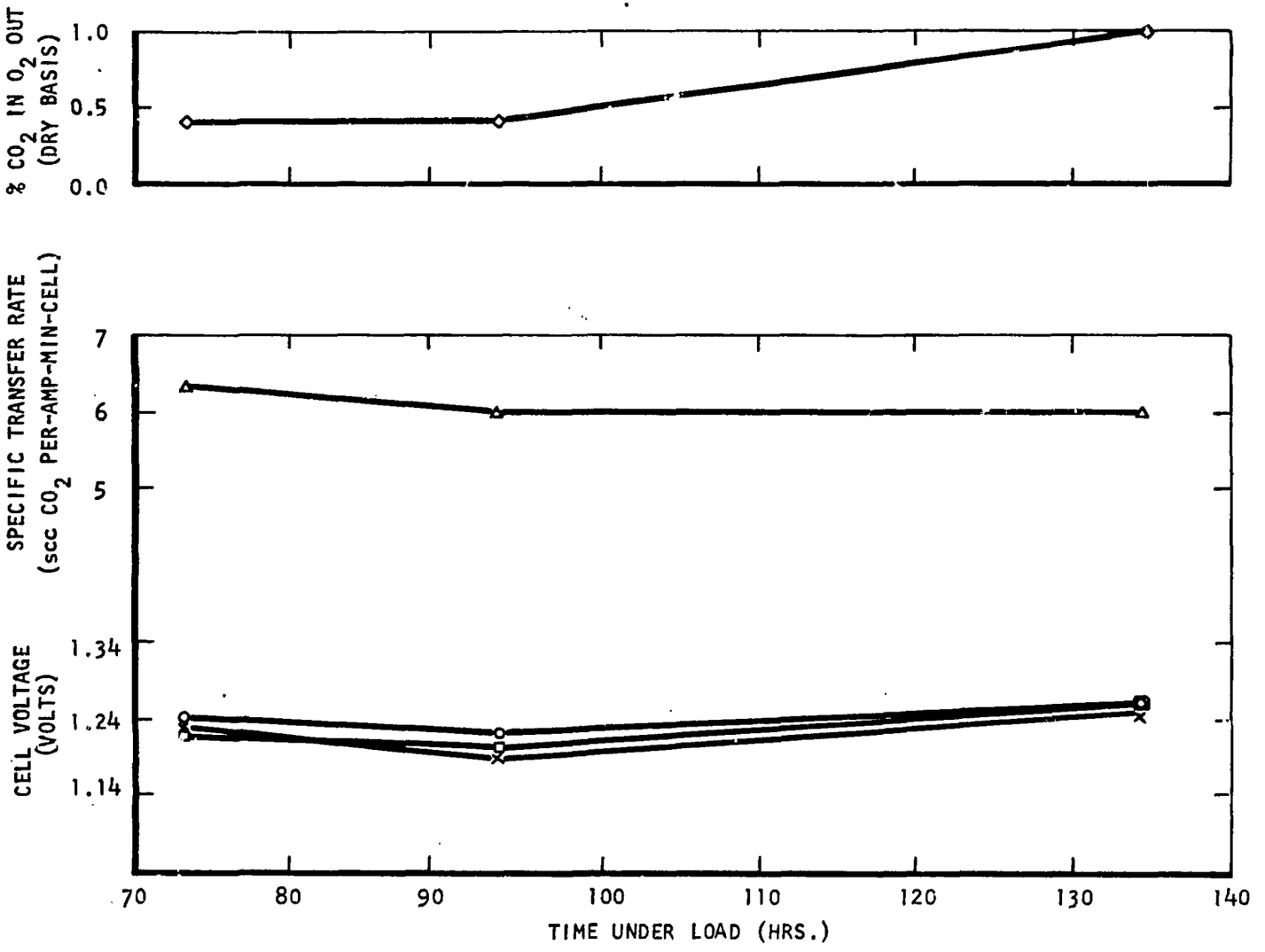

FIGURE 56 DESIGN VERIFICATION RUN - 4-CELL CARBONATION MODULE

The voltage of a one-man carbonation stack of ten cells will be 12.3 volts on the above basis, at 7.5 amperes. The corresponding power input for a one-man unit is 92.3 watts required when a hydrogen source is unavailable.

Upon completion of the tests, the unit was dismantled for a post-test examination. The following observations were made:

1. Drawbolt torque was 10-15 inch-pounds (from 30 inch-pounds) disclosing some relaxation of the internal structure.

2. Noted slight O-ring flattening. (O-rings between plastic and metal endplates).

3. Titanium foil colored violet, blue and yellow. These are oxides of titanium as follows:

Violet,	Ti_2O_3,	Titanium sesquioxide
Blue,	Ti_3O_5,	Blue oxide
Blue,	TiO_2,	Titanium dioxide
Yellow,	TiO_3,	Hydrated peroxide

   The presence of these oxides is anticipated since titanium becomes passive in the electrochemical environment (i.e., pH and voltage region) by virtue of the formation of the oxide layer formed during operation.

4. Excellent edge compression of the matrix was noted.

5. The matrix peeled readily from the AB-6 electrode but had to be soaked loose from the Pt on Pt electrode.

6. Both gaskets showed excellent bulb (raised region on cell housing) imprint.

7. All parts in excellent condition and can be reused as desired (except for matrix). Gaskets will not be reused since these are considered expendable.

PARAMETRIC TESTS - DESIGN II MODULE

Fifteen-Cell Module Assembly

To accurately position both gaskets, they were secured to the fin plate assembly by a very thin layer of adhesive applied in the drawbolt area. With gaskets having a larger "window" area (approximately 1/32 in.) no lapping is possible and this step is unnecessary (except for convenience in assembly).

After assembly, the unit was pulled down with extra long drawbolts to take up assembly slack. The final drawbolts were then installed with the Belleville washers and the unit pulled up uniformly to a torque of 10 inch-pounds. Water immersion tests showed leakage at several randomly located points.

To determine the load necessary to reduce the thickness of a cell to 0.250 inch (2 fin plates, no gaskets, cell housing, asbestos, 2 electrodes, compression manifold and 2 gas cavity fillers) an assembly of these parts was made and placed in a hydraulic press. The thickness of the assembly was reduced and the corresponding load was found to be 4000 pounds or twice the assumed load. The reason for the greater load than anticipated may be found in the fact that earlier tests were conducted with relatively soft silver Exmet whereas the final configuration uses relatively stiff titanium Exmet. In addition, a wider clamp region at the edge of the matrix is used. Since the endplate deflection was based upon assumptions leading to a compressive load of 6000 pounds, no concern was felt about this disparity.

The completed fifteen-cell module assembly is shown in Figure 57. The parametric test sequence was conducted on the test rig as modified for operation with the fifteen-cell module. In Figure 58, the module is shown installed in the test rig for the parametric test series. The test system is capable of testing the concentrator over the following ranges of listed parameters:

Module Temperature:	Ambient to 150°F
Inlet Gas Dew Point Temperatures:	10°F below module temperature
Carbon Dioxide Flowrate:	0-1.3 slpm
Oxygen Flowrate:	0-1.1 slpm
Oxygen Recycle Rate:	0-6/6.5 scfm (depends upon operating condition)
Hydrogen Flowrate:	0-3.7 slpm
Total Pressure Level, both gases:	Ambient to 150" H_2O (with appropriate modifications to condenser traps)
Stack Current:	0-20 amps
Individual Cell Voltages	0-1.5 volts
Stack Voltage:	0-15 volts
IR Drops:	0-0.15 volts/cell 0-1.5 volts/module

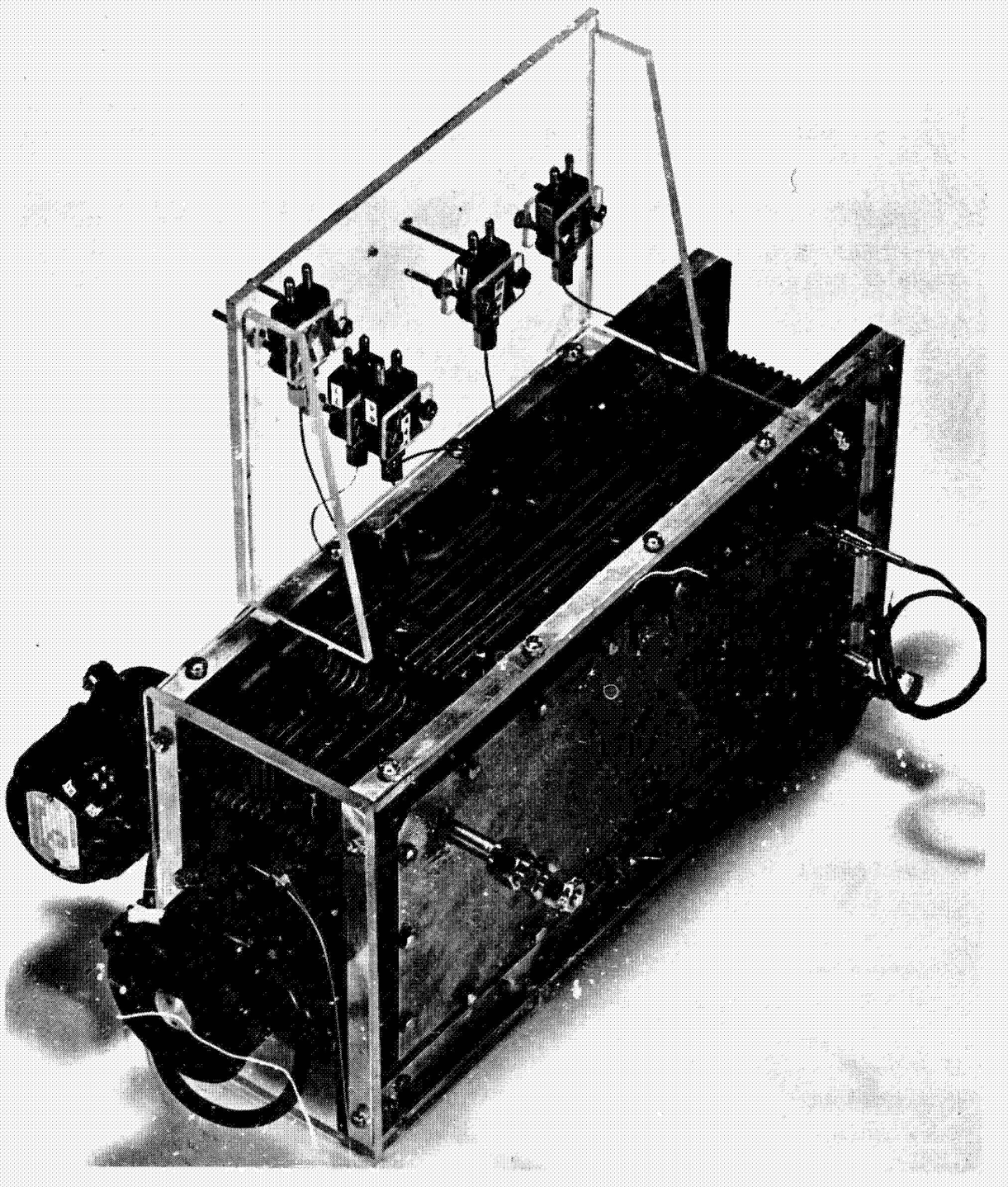

FIGURE 57 15-CELL MODULE WITH SHROUD AND BLOWERS

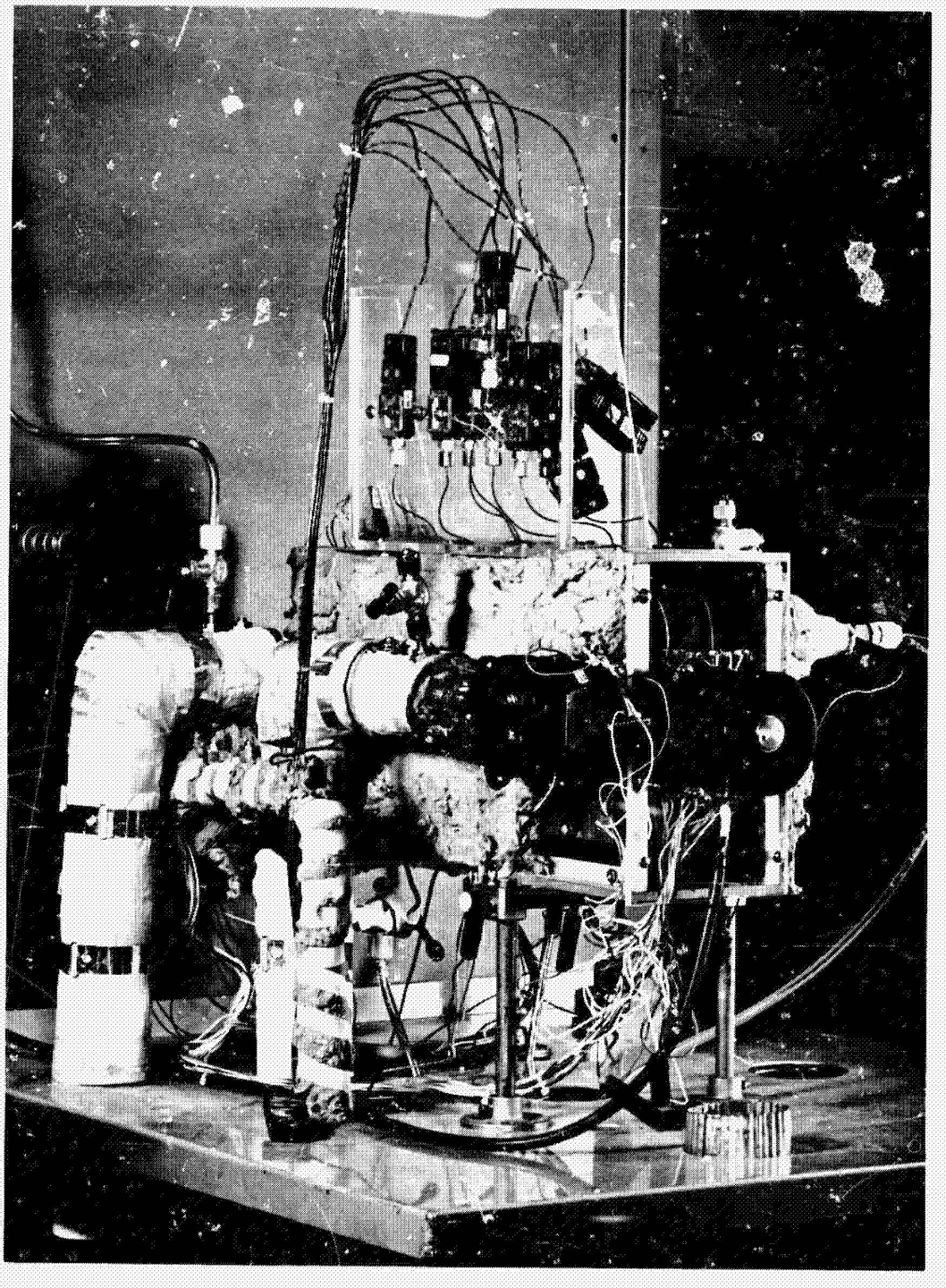

FIGURE 58 MODULE INSTALLED IN TEST SYSTEM

The parametric test sequence comprised five test series as indicated in Table XX. As a reference, the following conditions are considered to be standard for the CDCM tests:

1. Carbon dioxide transfer rate = 0.45 SLPM (0.11 lb/hr)
2. Hydrogen supply rate = 1.7 SLPM
3. Oxygen recycle rate = 3.6 SCFM (102 SLPM)
4. Stack current = 5.0 ampere
5. Stack temperature = 110°F
6. Dehumidifier temperature = 100°F
7. Pressure of hydrogen and oxygen = 20" water gage

These conditions were set up over weekends and between test series in order that the unit be maintained under load continuously.

With reference to Table XX, the values listed show the systematic variation of each parameter introduced to complete the test sequence. The following describe the test data generated during each sequence.

Performance as a Function of Ratio: CO_2 Transfer Rate to Current

The objective of this test series was to generate a series of curves relating the carbon dioxide concentration in the influent and effluent oxygen from the stack to the transfer rate and current (density).

It is known from prior work and by reference to theory that the concentration of carbon dioxide on the cathode side of a cell determines the relative proportion of bicarbonate to carbonate in the electrolyte. The conversion from bicarbonate to carbonate and vice versa is slow and consequently long equilibrium times are required to generate steady-state data. By maintaining a constant ratio between the carbon dioxide transfer rate and stack current it is possible to maintain the carbon dioxide level at the cathode approximately constant. In this test series, four levels of the ratio of carbon dioxide transfer to current and four currents were run. In order to insure that equilibrium was obtained at each condition, the carbon dioxide level leaving the stack, the carbon dioxide level in the hydrogen and the stack voltage were observed with time. When the values were constant, the data was recorded. The test values that were set up are indicated on Table XX and the test data generated during this series is given in Table XXI.

The relatively large number of tests made at the 5 ampere condition, the design carbon dioxide transfer rate, were obtained during weekend runs. The carbon dioxide levels tabulated were obtained by means of a Beckman GC-2 gas chromatograph calibrated for carbon dioxide, oxygen, hydrogen and nitrogen. The total pressure at the time of calibration was 14.5 psia and thus all concentration data given in percent can be converted to partial pressure in millimeters of mercury by multiplying by 7.5 $\left(\frac{14.5}{14.7} \cdot 760 \cdot \frac{1}{100}\right)$.

TABLE XX

CDCM TEST SEQUENCE

Test Series		Cell Temp. °F	Dehumidifier Temp. °F	Pressure H_2 & O_2 psig	Supply Rates CO_2 SLPM	Supply Rates H_2 SLPM	O_2 Recycle Rate SCFM (SLPM)	Stack Current amp	pO_2 psia
I	0.5X Des. CO_2 Transfer	110	100	20	0.113	1.7	3.6 (102)	2.5	~15
					0.225			5.0	
					0.338			7.5	
					0.450			10.0	
	1.0X Des. CO_2 Transfer				0.225			2.5	
					0.450			5.0	
					0.675			7.5	
Performance as a function of ratio: CO_2 transfer rate to current					0.90			10.0	
	1.25X Des. CO_2 Transfer				0.281			2.5	
					0.562			5.0	
					0.844			7.5	
					1.125			10.0	
	1.50X Des. CO_2 Transfer				0.338			2.5	
					0.675			5.0	
					1.01			7.5	
					1.35			10.0	
II		100	90	20	0.45	1.7	3.6 (102)	5.0	~15
Effect of stack temperature		110	100						
		120	110						
		130	120						
III		110	100	20	0.45	1.7	3.6 (102)	5.0	0.3
									1.1
Effect of pO_2 at cathode (N_2 diluent)									2.4
									4.0
									8.2
									15.3
IV		110	100	20	0.45	0.6	3.6 (102)	5.0	~15
Effect of hydrogen feed rate						0.9			
						1.3			
						1.7			
						2.0			
V		110	100	20	0.45	1.7	2.9	5.0	~15
Effect of oxygen recycle rate							3.7		
							4.2		
							4.8		

TABLE XXI

PERFORMANCE AS A FUNCTION OF THE RATIO, CO_2 TRANSFER TO CURRENT

Stack Current amp	CO_2 Transfer Rate, slpm	CO_2 in O_2 % in	CO_2 in O_2 % out	CO_2 in H_2 % out	Stack Voltage volts	Cell Voltage millivolts max.	Cell Voltage millivolts min.	Stack No.	Test Span hrs.
0.50X Design CO_2 Transfer									
5.0	0.24	0.27	0.029	17.5	8.30	600(2)	522(15)	2	233-300
7.5	0.33	0.39	0.27	30	6.70	510(2)	418(15)	2	228-233
10.0	0.45	0.48	0.05	48	5.90	457(2)	349(15)	2	207-228
[illegible] Design CO_2 Transfer									
2.5	0.24	0.95	0.80	13	12.4	841(3)	786(15)	1	52-70
[illegible]	0.45	0.55	0.15	29	8.8	640(3)	578(15)	1	0-25
[illegible]	0.45	0.80	0.33	26	9.94	690(3)	615(15)	1	70-90
[illegible]	0.45	0.85	0.41	27	9.5	695(2)	613(15)	2	163-180
[illegible]	0.45	0.85	0.45	27	9.9	708(2)	635(15)	2	0-5
[illegible]	0.45	0.85	0.47	27	9.8	708(2)	625(15)	2	55-73
[illegible]	0.70	0.70	0.10	45	7.18	508(3)	425(15)	1	31-52
10.[illegible]	0.89	1.00	0.20	61	6.00	440(2)	335(15)	1	25-31
10.0	0.85	0.90	0.10	58	5.42	404(2)	288(15)	1	117-138
1.25X Design CO_2 Transfer									
2.5	0.29	1.90	1.65	17	12.14	840(1)	788(15)	1	161-191
5.0	0.55	1.55	1.05	28	10.5	730(2)	642(15)	1	90-117
7.5	0.84	1.70	0.90	53	7.20	550(2)	424(15)	1	138-145
10.0	1.13	2.1	0.85	63	5.20	430(2)	240(15)	1	145-161
1.50X Design CO_2 Transfer									
2.5	0.40	3.83	3.65	18	12.4	885(2)	815(15)	1	27-32
5.0	0.70	3.6	3.1	38	10.56	750(1)	659(15)	1	191-196
5.0	0.70	4.3	3.75	35	10.9	789(2)	690(15)	2	5-27
7.5	1.00	4.4	3.5	56	8.42	610(1)	510(15)	1	196-215
7.5	1.03	5.0	3.70	52	8.4	622(4)	509(15)	2	32-49
10.0	1.38	6.0	5.4	56	6.00	516(2)	168(15)	1	50-55

The table shows the maximum and minimum cell voltages along with the particular cell showing this voltage. For reference purposes the cell adjacent to the endplate to which the recycle blower is mounted is Cell #1. This cell receives hydrogen directly from the hydrogen saturator. In nearly every case the highest performing cell is at the hydrogen inlet end of the stack and the lowest performing cell is at the outlet end of the stack.

Note that two stacks were used during the test sequence. The first stack constructed crossed over during an overnight test and the resultant high temperatures partially melted the cell housings at the oxygen inlet end. At this point in the test program, the loggers were shut down during the overnight runs due to the excessive use of chart paper. In addition, no low voltage shutdown instrumentation was available at this time.

The most probable reason for stack crossover was identification of low leakage resistance between the stack temperature control thermistor and ground. Apparently water entered the leads of the thermistor at some point in time and caused this problem since high leakage resistance was restored by oven drying the unit. It was determined that the effect of low leakage resistance was comparable to resetting stack temperature to a higher value which would result in stack dry-out and gas crossover.

In order to prevent a reoccurrence of this problem, a low voltage shutdown circuit was incorporated in the test system along with a new thermistor in the stack and a timer on the loggers such that a 40 second cycle of operation was initiated every 15 minutes of clock time.

No subsequent occurrences of this type were seen during the rest of the test effort. The performance of the second stack was identical to that of the first determined by running comparison tests.

Referring to Table XXI, note that each test extended over significant time intervals as required to obtain reliable steady-state information. As can be seen, a run at one-half design carbon dioxide transfer at 2.5 amperes stack current was not taken. This is due to the fact that the carbon dioxide level in the effluent oxygen from the stack was so low in the preceding 5-ampere run.

The data represented in Table XXI have been plotted in Figures 59 and 60. Note that the objective of maintaining a constant, average carbon dioxide level at the cathode side of the stack was met. It can be seen that the stack voltage is a strong function of current but does not seem to be a systematic function of the transfer rate.

All of the data shown in Figures 59 and 60 can be replotted in the form of specific transfer rate as a function of the average carbon dioxide level at the oxygen side of the stack. The specific carbon dioxide transfer rate is computed by dividing the transfer rate set up during the test by the product of stack current and the number of cells. The average carbon dioxide level is merely the average of the inlet and outlet carbon dioxide concentrations observed during each test. These data are plotted in Figure 61 in which it is seen that the specific transfer rate varies from three to approximately eleven milliliters per ampere-minute-cell. The transfer rate of six is obtained

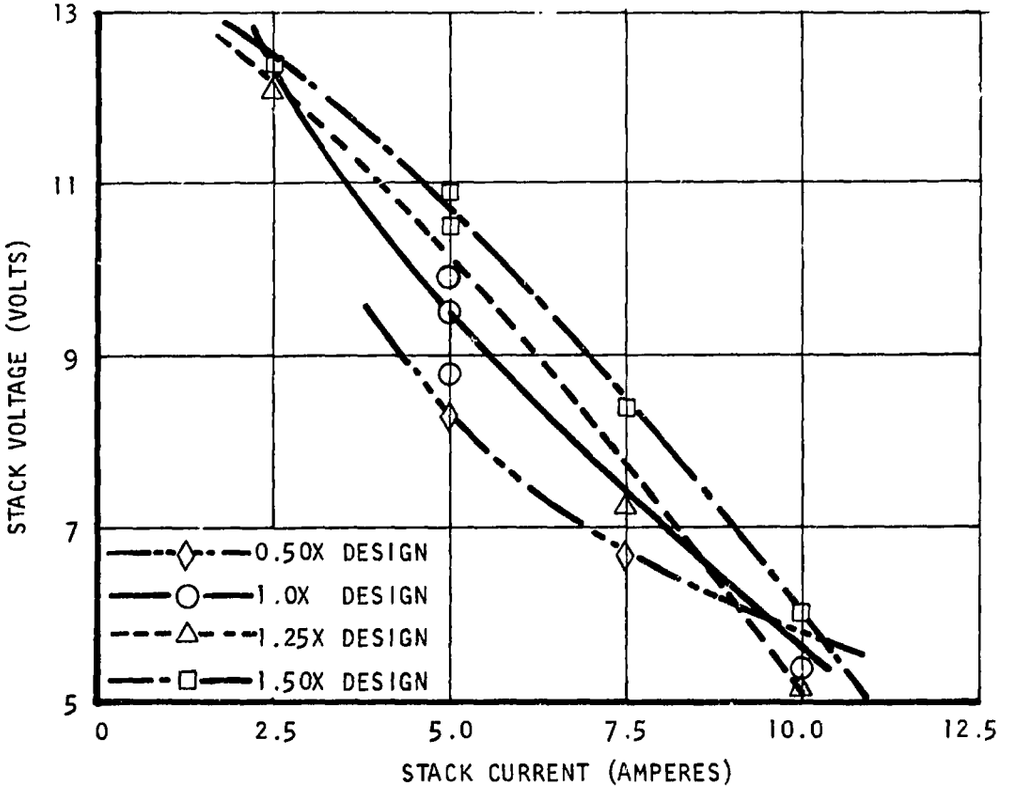

FIGURE 59 PERFORMANCE AS A FUNCTION OF THE RATIO, CO_2 TRANSFER TO CURRENT

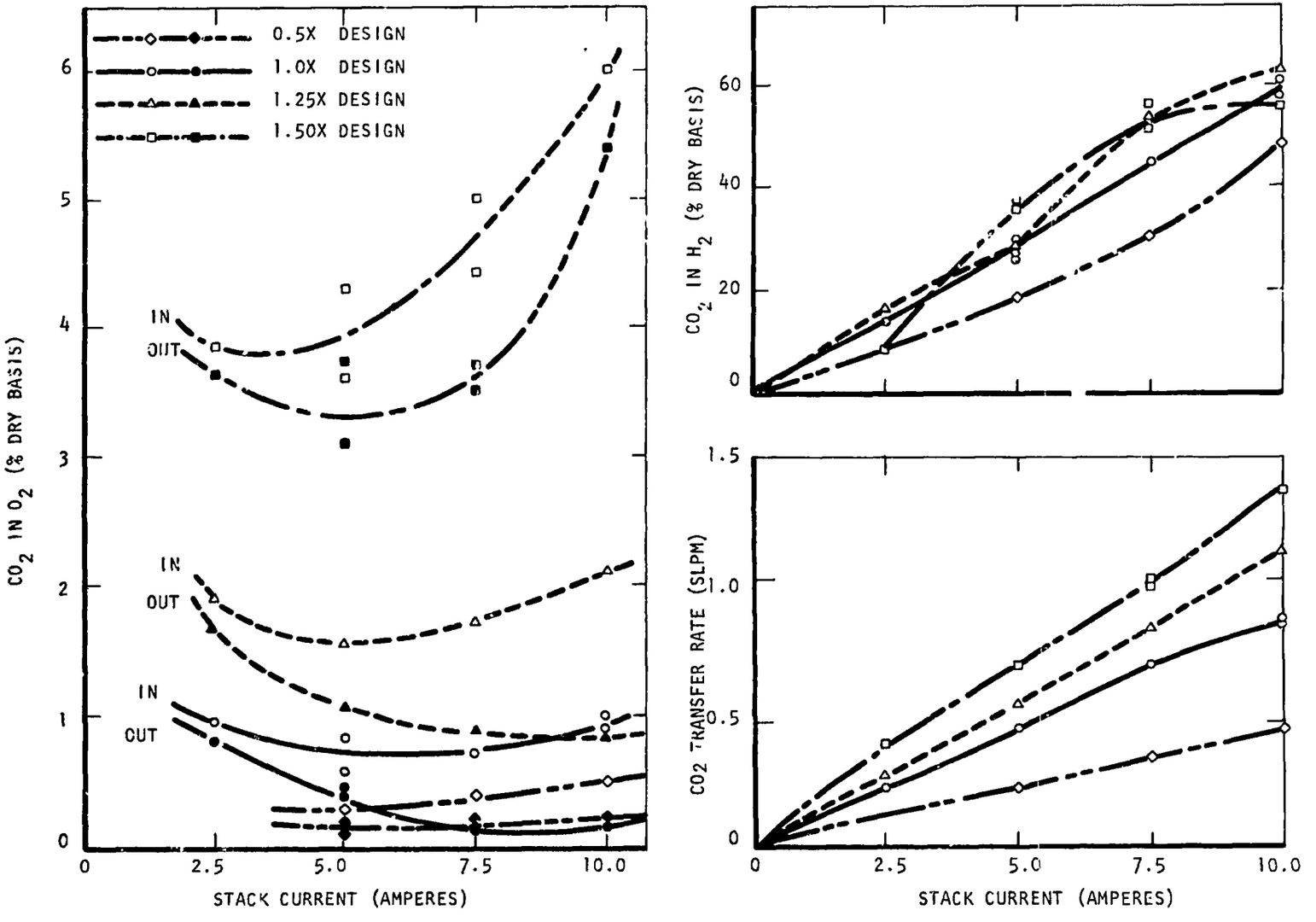

FIGURE 60 PERFORMANCE AS A FUNCTION OF THE RATIO, CO_2 TRANSFER TO CURRENT

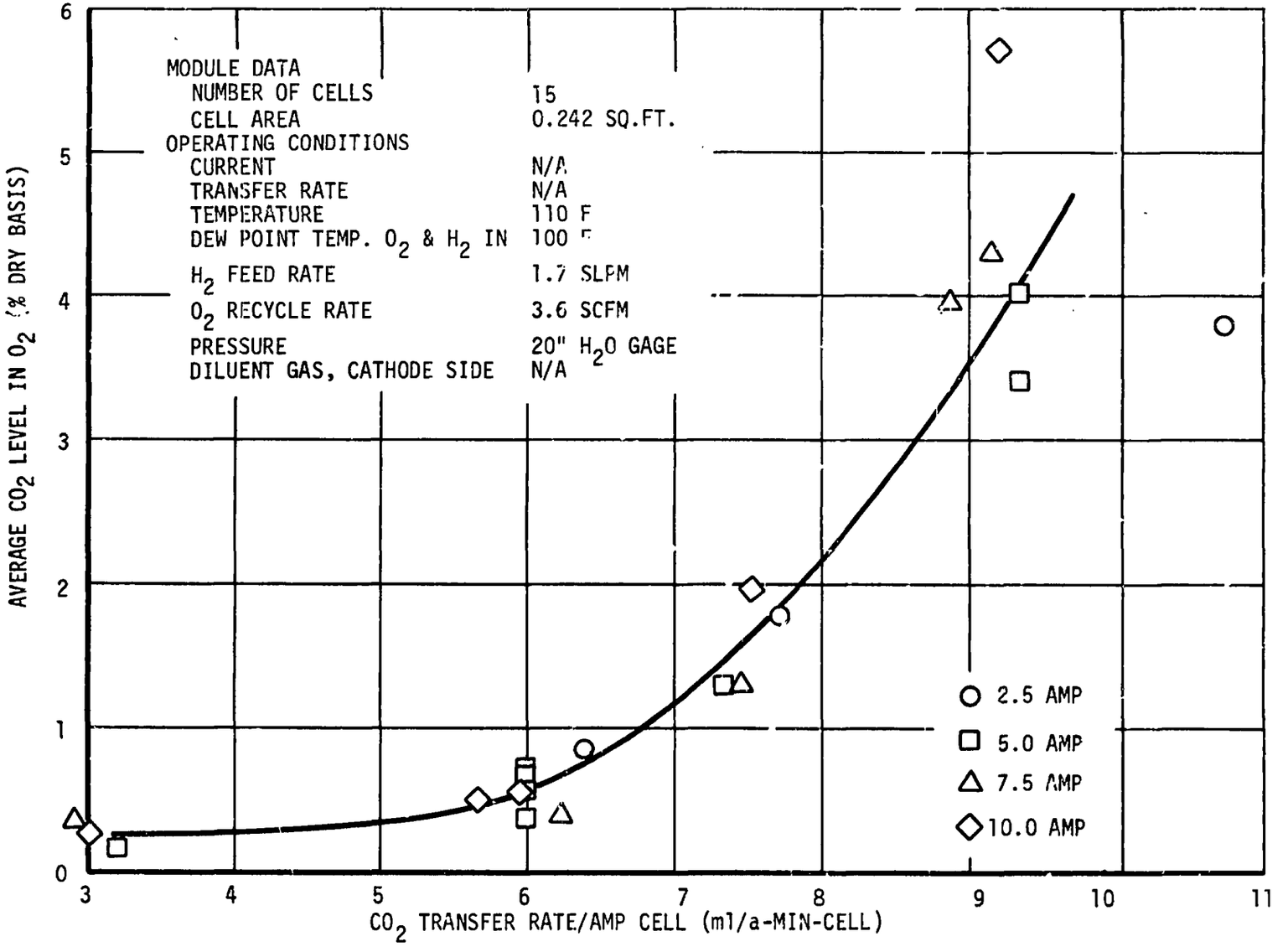

FIGURE 61 PERFORMANCE OF CDCM II, SPECIFIC TRANSFER RATE

at carbon dioxide levels in the order of 0.6 percent. At carbon dioxide levels in the range of 1/2 to 1 percent (3.8 to 7.6mm CO_2) the transfer rate is in the region of five to seven.

Theoretically, the carbon dioxide transfer rate via the hydroxyl ion alone is zero, by carbonate ion alone is 6.95 ml/ampere-minute-cell and is 13.9 ml/ampere-minute-cell when transfer is effected solely by the bicarbonate ion. Figure 61 discloses that both ions are effecting carbon dioxide transfer as expected by the theoretical analysis of the process.

These data were used to generate the performance map of the CDCM shown in Figure 62. This map shows, for example, that at a stack current of 5 amperes and a carbon dioxide transfer rate of 0.45 slpm, the carbon dioxide level in the oxygen leaving the unit will be in the order of 0.3 percent. This value shows that the design objective value of 0.5 percent maximum has been achieved. The current density at which the unit is operating is approximately 22 amperes per sq. ft. and the stack voltage is approximately 9.5 volts. Experimental points for current and transfer rates associated with the computed curves are plotted and shown to lie closely to the curve value.

The rate of oxygen consumption by a cell is 3.75 ml/ampere-hour or 0.05 lb/hr for the module at a stack current of 5.0 amperes. This rate is directly proportional to stack current.

Effect of Stack Temperature

Performance as a function of stack temperature is given in Table XXII and plotted in Figure 63. Stack temperature was varied from 100-130°F with the dehumidifier temperature maintained 10° below these values.

For the purpose of this test series, the hydrogen was humidified with water vapor at a temperature 10° below stack temperature. In application in the NAOS system it is desirable to avoid the necessity for hydrogen humidification prior to entry into the concentrator stack. Consequently, it is desirable to operate the concentrator at the minimum temperature in order to prevent drying of the cell at the inlet end of the stack. Operation of the WES at 80 psia and at a temperature of 165°F will provide hydrogen to the concentrator at 100°F dew point temperature if condensation in the connecting lines is avoided, thus the concentrator may be operated at the design condition of 110°F.

Note that at the lower temperatures the stack voltage decreases by approximately 2 volts below that at the normal design temperature of 110°F. By reference to the tabular data, the spread in individual cell voltage is less than 0.1 volt and consequently operation at the lower temperatures does not unduly affect the voltage differences within the stack. Consequently, sustained operation at the lower temperature is permissible. Note also that the carbon dioxide level leaving the stack is reduced as stack temperature is lowered.

Design calculations indicate that sustained operation at the 10 ampere level at the lower stack temperature limit of 100°F is likely to cause excessive changes in electrolyte concentration within the cells because of the reduced

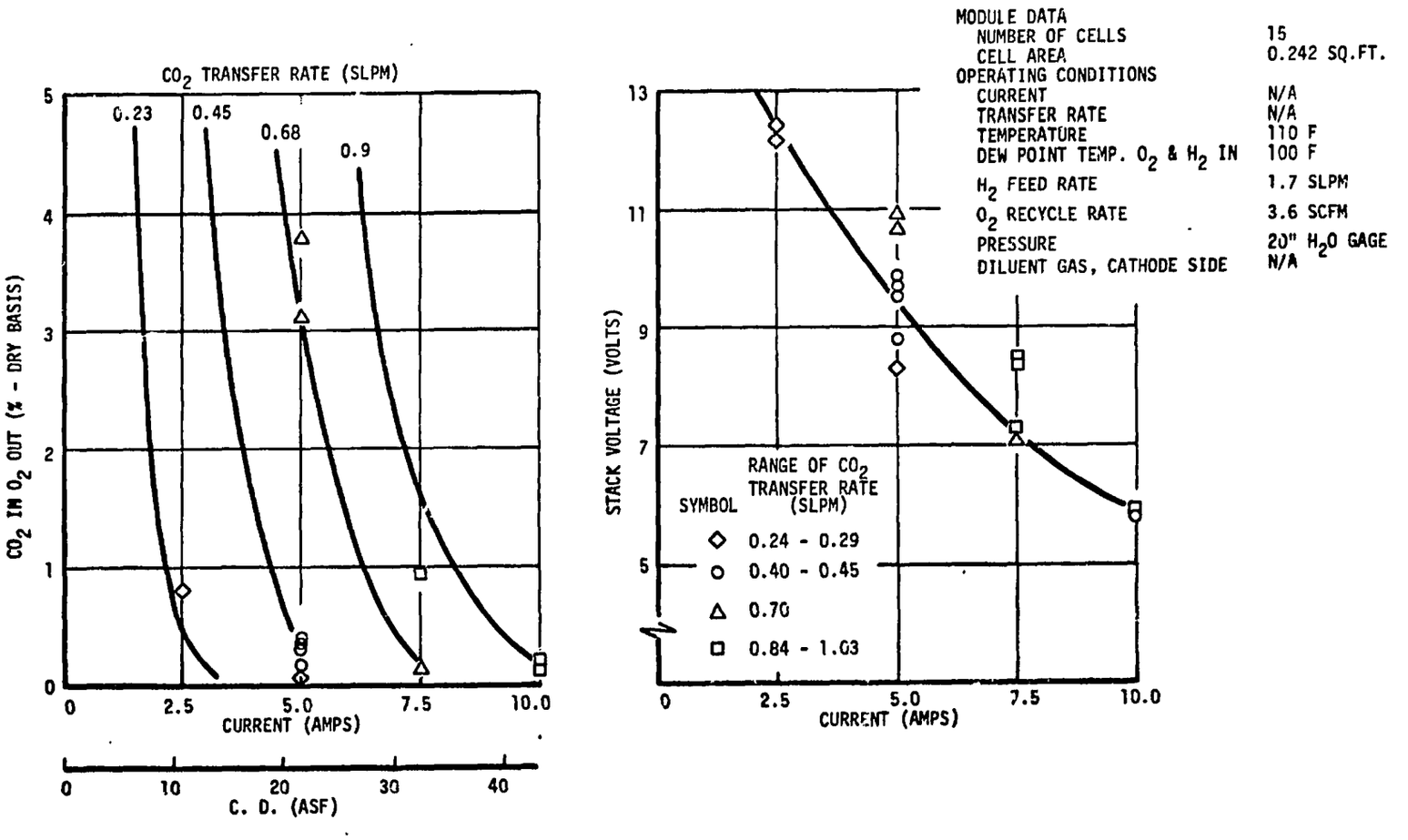

FIGURE 62 PERFORMANCE OF CDCM II, CO_2 TRANSFER RATE, pCO_2 AT CATHODE, STACK CURRENT AND VOLTAGE

TABLE XXII

EFFECT OF STACK TEMPERATURE

Stack Temp. °F	CO_2 in O_2 % in	CO_2 in O_2 % out	CO_2 in H_2 % out	Stack Voltage volts	Cell Voltage millivolts max.	Cell Voltage millivolts min.	Test Span hrs.
100	0.60	0.19	28.00	8.3	603(2)	529(15)	631-654
110	0.74	0.31	29.3	9.6	700(3)	619(15)	594-631
120	0.84	0.37	28.6	10.7	760(2)	700(15)	565-586
130	0.84	0.34	28.0	11.0	788(2)	733(15)	586-594

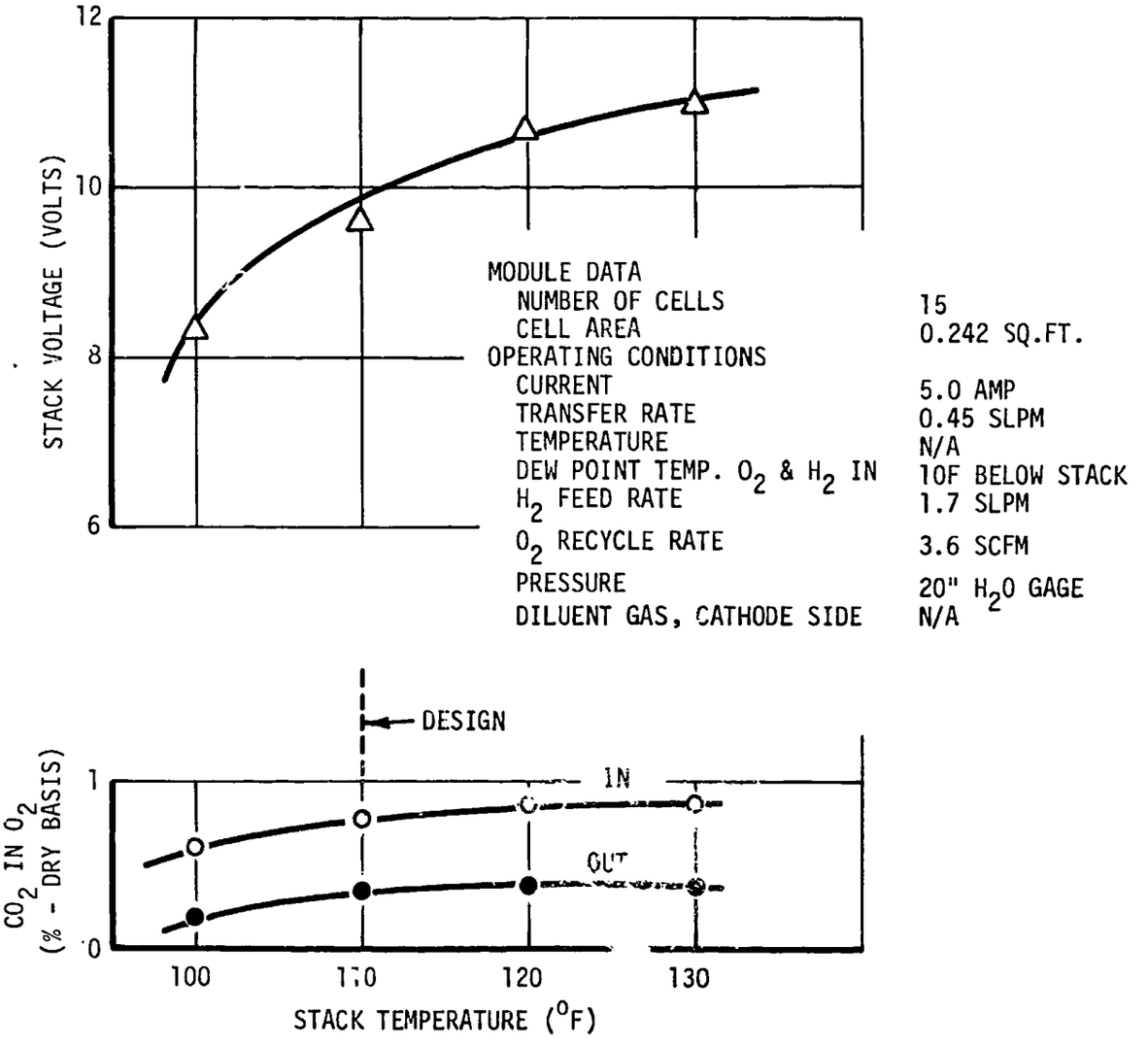

FIGURE 63 PERFORMANCE OF CDCM II - EFFECT OF STACK TEMPERATURE

capability of removing product water at this condition. Sustained operation at currents up to 10 amperes is permissible at the higher temperature.

Effect of pO_2 at Cathode (N_2 diluent)

The effect of reduced pressure operation, as found during altitude operation of the unit, was studied by diluting the oxygen in the recycle loop with nitrogen. It has been shown in other studies that insofar as electrochemical performance is concerned, data determined with this type of test will be nearly identical with data obtained with reduced total pressure without a diluent. It should be pointed out however, that gas velocity and pressure drops will differ but these effects on electrode performance are usually small. Prior to these test runs a sampling system was prepared and connected to the stack in such a way that a sample could be extracted for chromatographic and dew point analysis and reinserted in the loop in order that there be no loss of diluent.

To set up for a test, nitrogen was inserted into the recycle loop and a bleed elsewhere in the loop was opened. A Beckman E-2 oxygen analyzer was installed in the sampling system in order to determine the oxygen concentration. No significant performance change was found until the oxygen concentration was decreased below 20 percent. At the level of 2 percent or 0.3 psia dry oxygen, the stack voltage was unstable. However, at the level of 7.3 percent corresponding to 1.1 psia, voltage performance was stable with time and the data point was taken. Additional data points were obtained as tabulated in Table XXIII and plotted in Figure 64. Note that there is a slight reduction in carbon dioxide level in the recycle loop as the partial pressure of oxygen is reduced, however, no significance is attached to this decrease. This test indicates that there is very little reduction in stack voltage at oxygen partial pressures down to 3 psia.

Effect of Hydrogen Feed Rate

Data showing the effect of hydrogen feed rate is given in Table XXIV and plotted in Figure 65. The tabulated data shows, as expected, that at the lower hydrogen feed rate the performance of the last cell in the stack decreases. The plotted data shows that the maximum carbon dioxide level in the effluent hydrogen is 90 percent. A further reduction in flowrate was not possible due to the fact that the voltage of Cell #15 dropped precipitously with very small changes in hydrogen flowrate. The carbon dioxide level in the effluent hydrogen can be calculated assuming the hydrogen consumption rate is 0.450 standard liters per amp-hour-cell. The calculated curve shows excellent agreement with the experimental data. Note that the hydrogen feed rate was decreased to a level only very slightly above one stoichiometric.

The decrease in stack voltage performance observed in this series is primarily due to a reduction in the performance of the latter cells of the stack. Note that the voltage of the second cell in the series hydrogen configuration for the entire series of tests is in the region of 682 to 708 millivolts, whereas the voltage of the last cell in the stack decreases from 625 millivolts to 510 millivolts, reflecting the large increase in carbon dioxide concentration in the latter cells of the stack when the hydrogen flowrate is dropped. Note

TABLE XXIII

EFFECT OF OXYGEN PARTIAL PRESSURE

O_2 Partial Pressure Inlet %	psia	CO_2 in O_2 % in	out	CO_2 in H_2 % out	Stack Voltage volts	Cell Voltage millivolts max.	min.	Test Span hrs
2	0.3				Unstable			
7.3	1.1	0.70	0.28	28	8.70	635(4)	563(15)	560.4-562.9
15.6	2.40	0.79	0.42	27	8.60	630(2)	542(1)	559.0-560.4
25.9	3.99	0.74	0.31	29	9.45	690(2)	608(1)	562.9-565.2
53.2	8.20	0.79	0.42	26	9.57	672(4)	578(1)	541.6-559.0
99.3	15.3	0.91	0.50	29	9.50	689(2)	592(15)	353.4-394.1

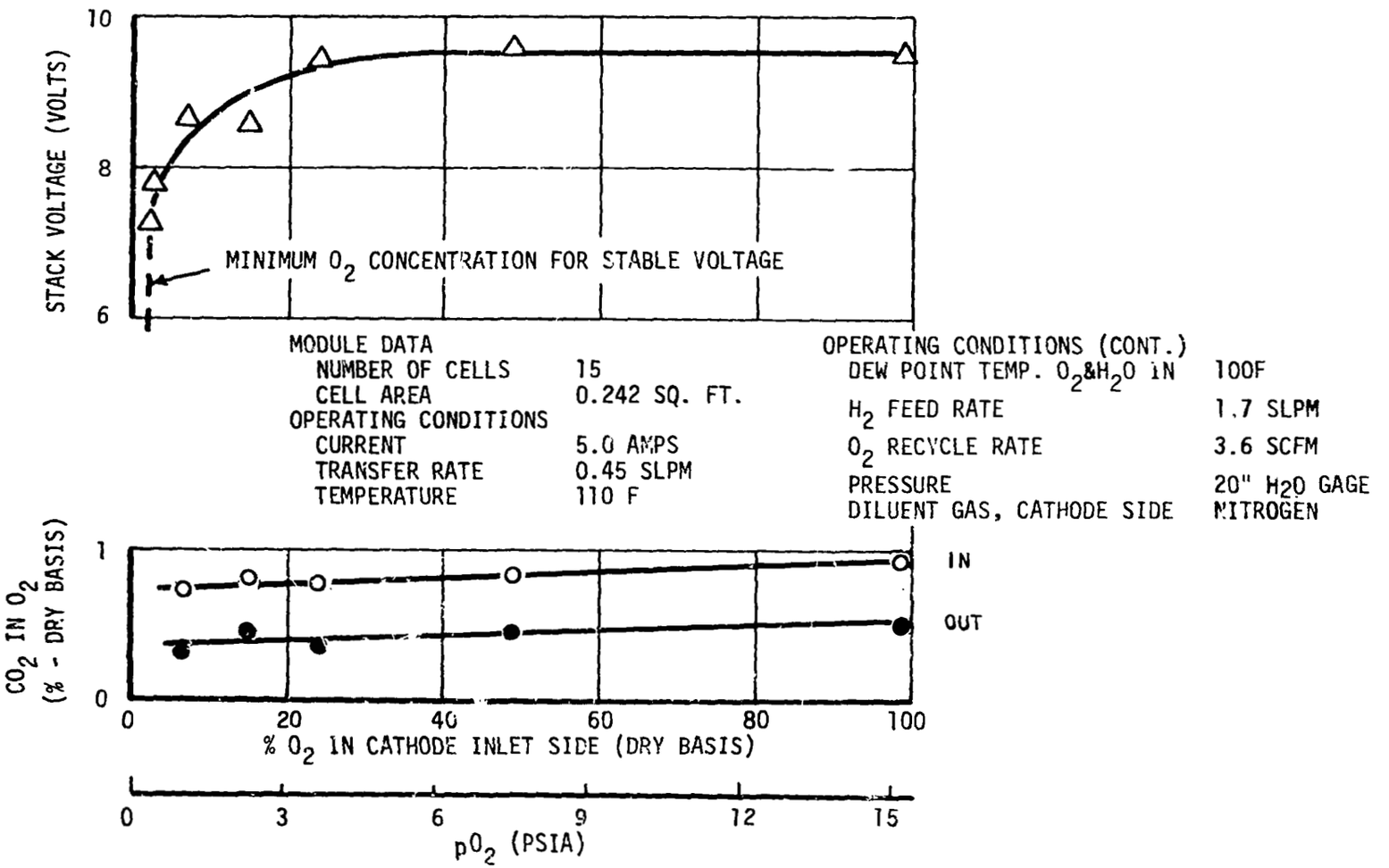

FIGURE 64 PERFORMANCE OF CDCM II - EFFECT OF pO_2 AT CATHODE

TABLE XXIV

EFFECT OF HYDROGEN FEED RATE

Hydrogen Feed Rate, slpm	Stoichs Hydrogen	CO_2 in O_2 %		CO_2 in H_2 %	Stack Voltage volts	Cell Voltage millivolts		Test Span hrs
		in	out	out		max.	min.	
0.6	1.07	1.2	0.7	92	8.8	682(2)	510(15)	146-150
0.88	1.57	1.05	0.6	56	9.4	698(2)	614(14)	150-152
0.90	1.60	0.92	0.56	48	9.4	690(2)	586(15)	76-80
1.3	2.31	0.90	0.56	37	9.6	700(2)	609(15)	73-76
1.7	3.02	0.85	0.47	27	9.8	708(2)	625(15)	55-73
2.01	3.58	0.80	0.40	22	9.6	695(2)	609(15)	102-146

FIGURE 65

PERFORMANCE OF CDCM II - EFFECT OF HYDROGEN FEED RATE

MODULE DATA	
NUMBER OF CELLS	15
CELL AREA	0.242 SQ.FT.
OPERATING CONDITIONS	
CURRENT	5.0 AMPS
TRANSFER RATE	0.45 SLPM
TEMPERATURE	110 F
DEW POINT TEMP. O_2 & H_2 IN	100 F
H_2 FEED RATE	N/A
O_2 RECYCLE RATE	3.6 SCFM
PRESSURE	20" H_2O GAGE
DILUENT GAS, CATHODE SIDE	N/A

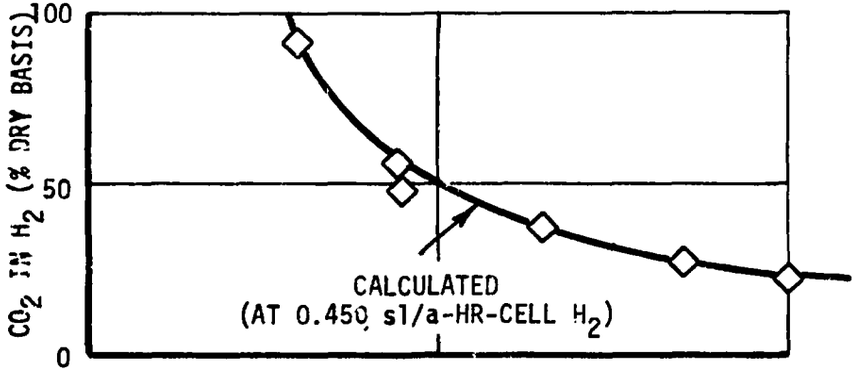

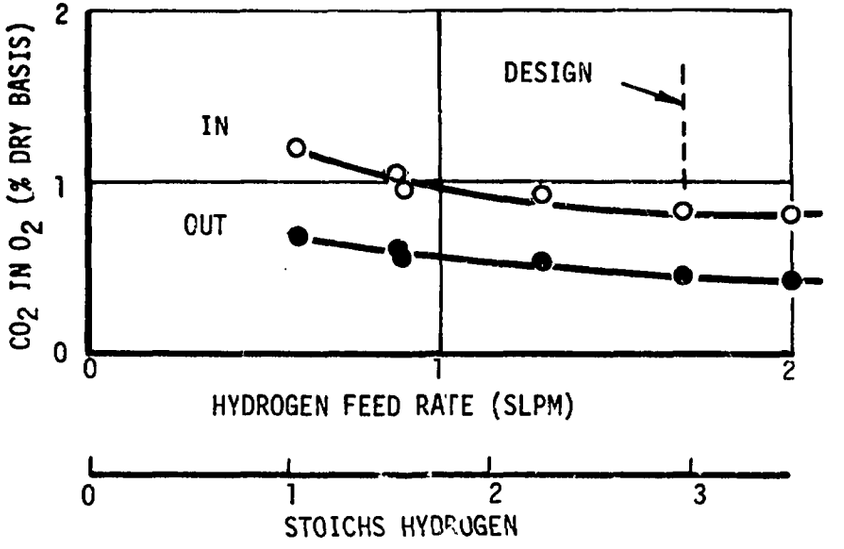

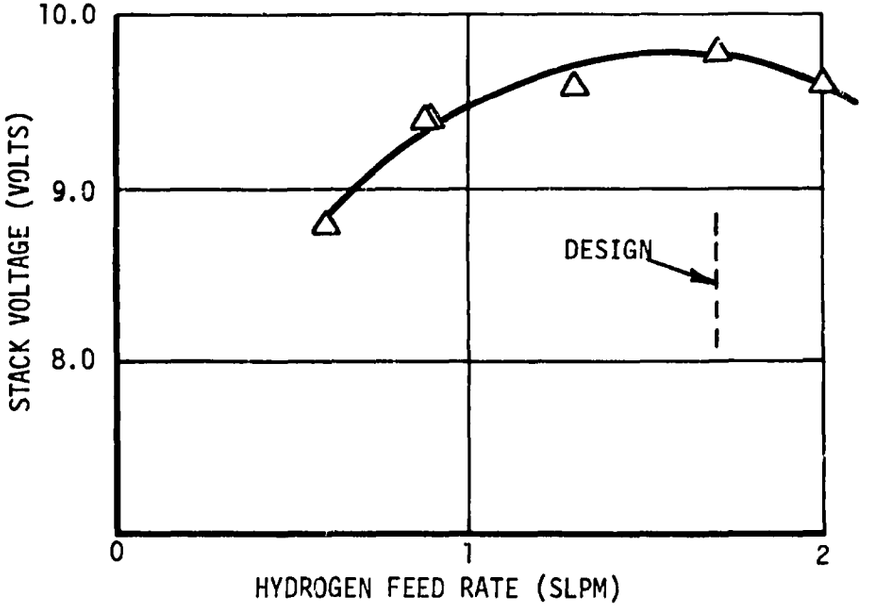

also that there is some effect upon the carbon dioxide level in the oxygen, particularly that there is a small rise in average carbon dioxide level at the reduced hydrogen flowrate.

Effect of Oxygen Recycle Rate

The effect of oxygen recycle rate on the performance of the stack is given in Table XXV and plotted in Figure 66. The reduction in stack voltage observed with an increase in oxygen recycle rate was unexpected and possibly suggests a change in water balance on the unit. Note that at the lower recycle rates, the difference in carbon dioxide level between the inlet and outlet of the stack on the oxygen side increases. This is to be expected since the carbon dioxide transfer rate remained constant during the series. Some increase in carbon dioxide level in the recycle loop is found at the lower recycle rates and is probably due to less efficient scrubbing of carbon dioxide out of the oxygen as the result of decreased mixing in the oxygen cavity of the cells.

Pressure Drop Data

The pressure drop through the unit is plotted in Figure 67. The upper curve shows the static pressure loss in the series, cell flow configuration for the hydrogen side of the fifteen-cell unit. The hydrogen flow is given as liters per minute saturated with water at room temperature. Pressure drop data gathered on the four-cell unit and multiplied by 15/4 agrees will with the fifteen-cell data.

The lower curve shows the static pressure loss in the parallel, cell flow configuration for the four-cell unit both for flow rate per cell and flow for the fifteen-cell stack. The flow rate is given for water saturated oxygen at room temperature in cubic feed per minute.

Performance Summary Comparison

Table XXVI lists the design objective values of concentrator performance for the redesigned unit and the values achieved during the test effort. All objectives were achieved except for the temperature variation within the stack. The variation given in the table is cell-to-cell temperature difference as observed by internal thermocouples whereas the design objective value is cell centerline-to-edge of active area temperature difference, assuming no cell-to-cell difference. The cell-to-cell difference is the more significant value and is caused primarily by lack of thermal shunting between cells as discussed in a prior section. Temperature difference within any cell was within the design value.

TABLE XXV

EFFECT OF OXYGEN RECYCLE RATE

Oxygen Recycle Rate, SCFM	CO_2 in O_2 %		CO_2 in H_2 %	Stack Voltage	Cell Voltage millivolts		Test Span
	in	out	out	volts	max.	min.	hrs
2.9	0.93	0.40	28	9.5	698(2)	608(15)	180-185
3.7	0.85	0.41	27	9.5	695(2)	613(15)	163-180
4.2	0.60	0.22	28	9.0	652(2)	578(15)	160-163
4.8	0.55	0.20	29	8.7	635(2)	550(15)	157-159

MODULE DATA	
NUMBER OF CELLS	15
CELL AREA	0.242 SQ. FT.
OPERATING CONDITIONS	
CURRENT	5.0 AMPS
TRANSFER RATE	0.45 SLPM
TEMPERATURE	110 F
DEW POINT TEMP. O_2 & H_2 IN	100 F
H_2 FEED RATE	1.7 SLPM
O_2 RECYCLE RATE	N/A
PRESSURE	20" H_2O GAGE
DILUENT GAS, CATHODE SIDE	N/A

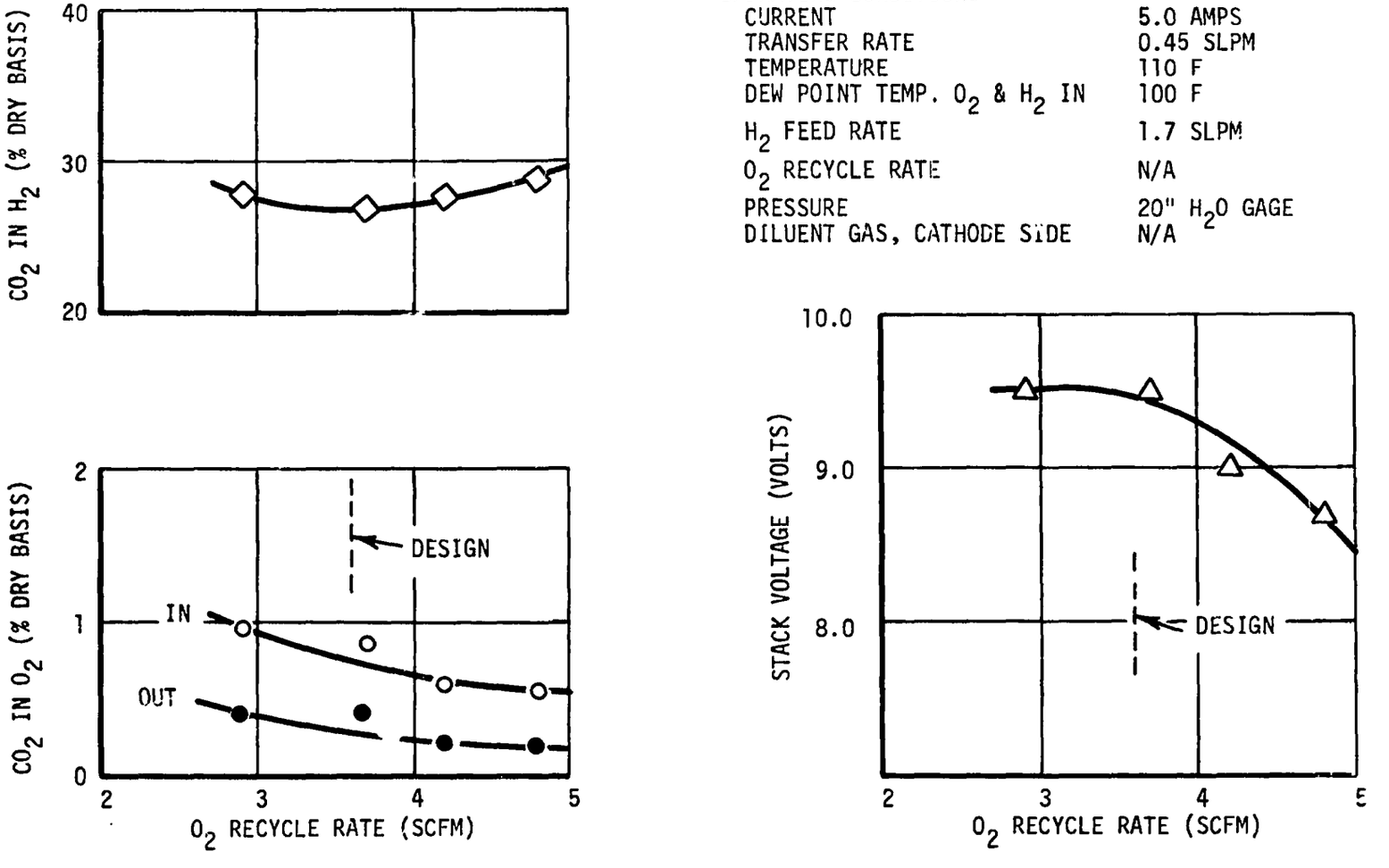

FIGURE 66 PERFORMANCE OF CDCM II - EFFECT OF OXYGEN RECYCLE RATE

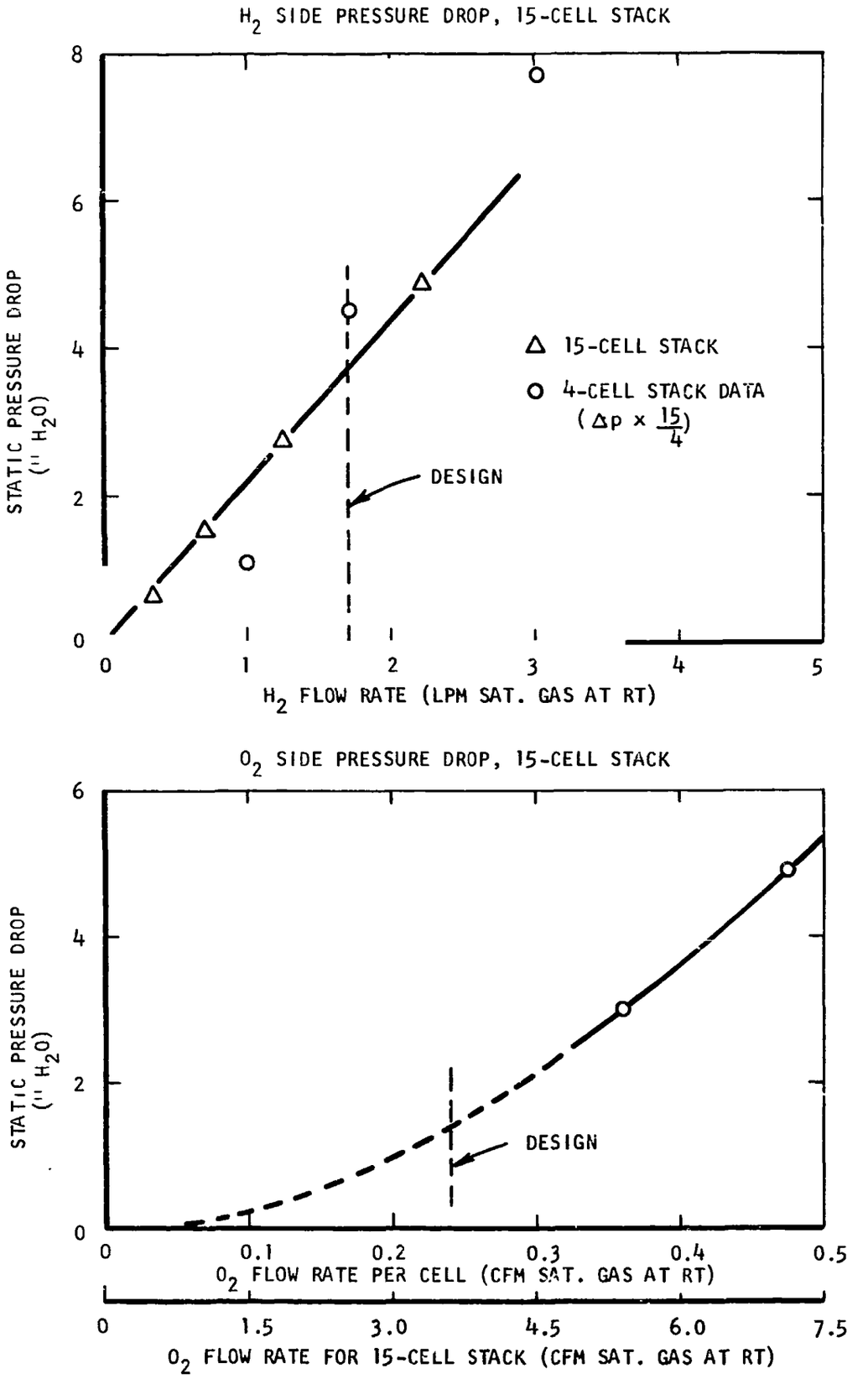

FIGURE 67 H_2 & O_2 SIDE PRESSURE DROP, 15-CELL STACK

TABLE XXVI

PERFORMANCE SUMMARY COMPARISON TO DESIGN OBJECTIVES

	Design Objective Value	Measured Value
Electrical Characteristics		
Current, Amp	5.0	5.0
Stack Voltage	6.0 (10 amp)	6.0 (10 amp)
Flow Characteristics		
CO_2 Transfer Rate (#/hr)	0.11 (0.45 slpm)	0.11
O_2/CO_2 Recycle Rate (SCFM)	3.6	3.6
H_2 Rate (SLPM)	1.7	1.7
O_2/CO_2 Pressure Drop ("H_2O, max)	2.0	1.4
H_2 Side Pressure Drop ("H_2O, max)	6.0	3.7
Thermal Characteristics		
Operating Temperature, ^oF	110	110
Maximum Temperature Variation at 0.65 volt, (^oF)	1.5	2
Nominal Gas Composition (% CO_2 on dry basis)		
Cathode In	0.95	0.75
Cathode Out	0.5	0.3
Anode Out	29.0	28.0

LIFE TESTING

The life test program included evaluation of the Design I and II modules and single cells of four distinct configurations. The Design I module life test program included three separate test phases which were identified as cyclic, endurance and long term life tests. For the Design II module only, long-term tests were conducted after the parametric test program. The objectives of the long-term test phase were the evaluation of the following: cell and module performance, accessory component performance, construction materials during and after long-term exposure to cell electrolyte, cell potential, and product gas flow.

Design I Module

Cyclic Testing. - Module No. SN01 was used for parametric and then cyclic testing. In this test phase, the module assembly was subjected to a series of twenty cycles simulating aircraft mission operating cycles. It was initially intended that each cycle should consist of a module start-up, ten hours of continuous operation at module design conditions, and a module shutdown sequence. After the completion of each operating period the module was allowed to return to room temperature and pressure conditions before initiating the next operating cycle. The start-up and shutdown sequence for each of the cycles is presented in Table XXVII. A summary of the module operating parameters during the twenty operating cycles is given in Table XXVIII. This test phase successfully demonstrated module capability during intermittent duty cycle operations.

Endurance Testing. - During this test phase, module assembly No. SN02 was subjected to continuous operation at design point carbon dioxide removal rate conditions for a period of 528 hours (22 days). This phase of the testing was conducted in the laboratory breadboard system test rig facility. Consequently, the detailed results of this test phase will be found in the Laboratory Breadboard System Final Report, NASA CR-73396.

Long-Term Operation. - Long-term operation of the Design I module was hampered by the inability to maintain moisture balance over long-term periods of operation. The module did, however, demonstrate long life capability by satisfactory operation after thousands of hours exposure to operating and chemical environments. The total time on load for the two builds of module SN01 was 1,100 hours. The performance of the module is summarized in Figure 68.

Module Moisture Balance Tests. - During initial life test runs it became evident that gas crossover was occurring in some of the cells in the ten-cell module. Consequently, a test aimed at obtaining moisture balance data was initiated.

Dew point sampling stations were inserted in the oxygen and hydrogen inlet and outlet lines in order to monitor these data as the stack warmed up without load and under a subsequent five ampere load period.

The data gathered in the no load portion of this run indicated that the dew point of the effluent oxygen was only $2^{\circ}F$ to $4^{\circ}F$ below the effluent oxygen temperature whereas this difference would be expected to be in the order of $10^{\circ}F$ at the charge concentration used. Under load this difference increased

TABLE XXVII

CO_2 CONCENTRATOR CYCLIC TESTING
START-UP/SHUT-DOWN PROCEDURE

START-UP:

Test rig condition from previous run:

A. Dehumidifier bath at temperature

B. Stack at room temperature

C. Blowers off but with desired operating conditions set

D. Reactant solenoids closed but pressure controls set and flowrate controls set

E. Current off but with desired current set

1. Push heater control button "ON"

2. Throw blower power control "ON"

3. Push control circuits button "ON" - wait 20 seconds

4. Throw current control switch "ON"

Total time from 1 to 4 is roughly 30 seconds, stack comes to normal operating temperature in 20 minutes.

SHUT-DOWN:

Reverse steps 1 to 4. No time delay is required between 4 and 3. Stack temperature cools to room temperature in several hours.

TABLE XXVIII

NAOS CO_2 CONCENTRATOR CYCLIC TEST SEQUENCE

CYCLE NO.	1	2	3	4	5	6	7	8	9	10	11	12	13	14	15	16	17	18	19	20
DATE	9/10	9/11	9/12	9/13	9/16	9/17	9/18	9/19	9/20	9/23	9/24	9/25	9/26	9/27	9/30	10/1	10/2	10/3	10/4	10/7
HOURS ON LOAD	7.3	10	6.8	10	10	10	10	8.4	10	10	10	10	10	9.7	9	10	9.8	10	10.2	9.8
CO_2 TRANSFER RATE SL/MIN	0.46	0.45	0.45	0.45	0.45	0.45	0.45	0.46	0.46	0.46	0.46	0.46	0.46	0.37	0.46	0.47	0.47	0.47	0.45	0.43
EQUILIBRIUM $\%CO_2$ AT O_2 EXIT	0.35	0.31	0.41	0.35	0.40	0.37	0.35	0.31	0.33	0.31	0.30	0.34	0.31	0.2	0.40	0.38	0.35	0.32	0.3	0.31
CURRENT, AMPS	8 & 10	8	8	8	8	8	8	8	8	8	8	8	8	8	8	8	8	8	8	8
VOLTAGE, VOLTS																				
MAXIMUM	6.1	5.0	5.4	5.7	5.7	5.3	5.22	5.15	4.95	4.78	4.60	4.59	4.40	4.08	4.99	4.70	4.57	4.58	4.4	4.42
MINIMUM	4.8	3.75	3.9	5.0	4.9	4.9	4.8	4.19	4.5	3.58	4.09	3.95	3.80	3.4	4.50	4.22	3.95	4.00	4.0	4.15
AVERAGE TEMP., °F	125	120	120	120	120	120	120	120	120	115	115	115	112	112	115	115	114	113	113	113

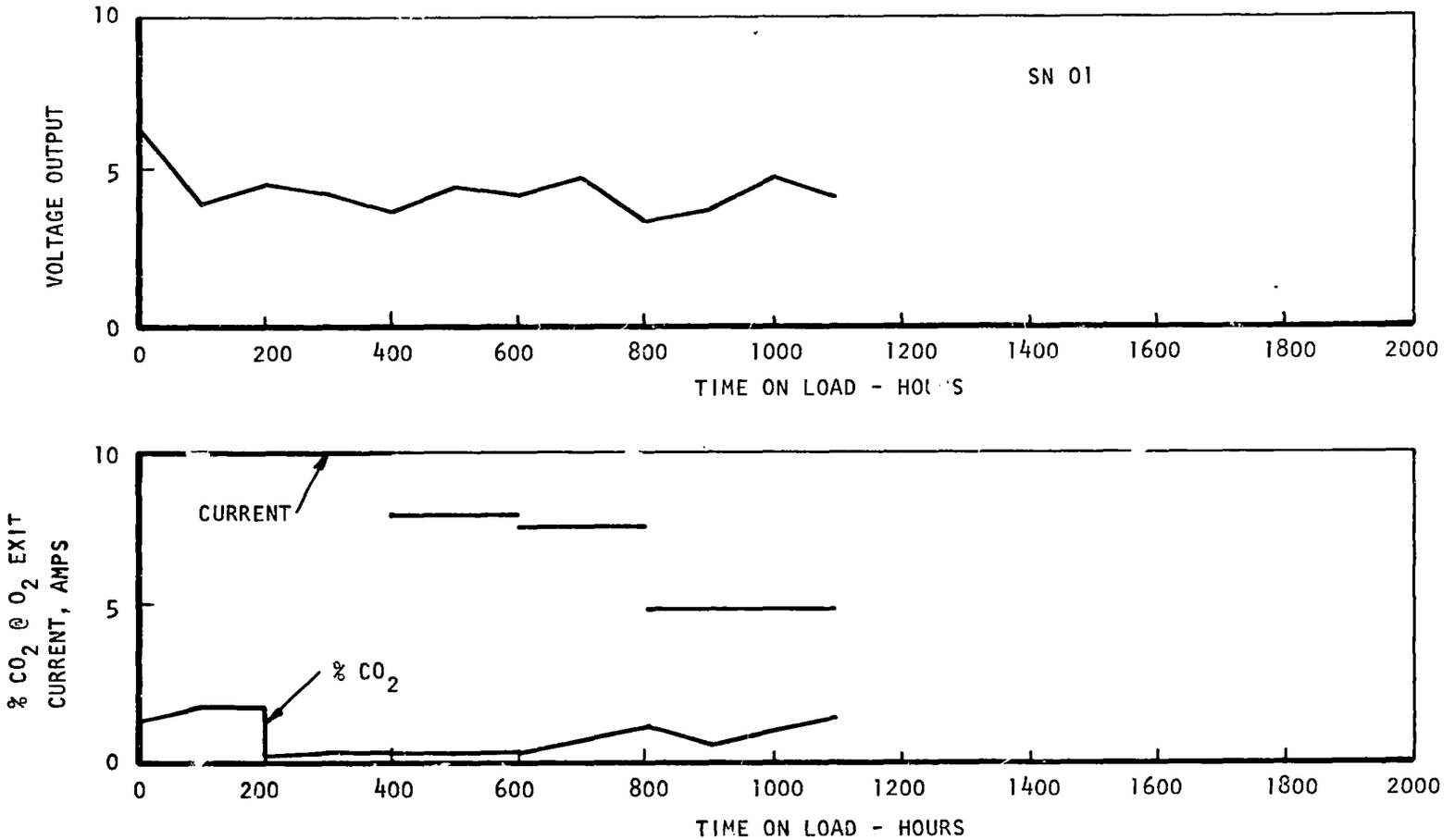

FIGURE 68 CO_2 CONCENTRATOR MODULE NO. SN-01 - TEST SUMMARY

to $8^{o}F$-$10^{o}F$ contrary to expectation. The temperature differential should run smaller for the load condition than the no load condition due to water generation. This test was terminated after an overnight run due to a gas crossover.

In-depth study of the data gathered during a number of runs lead to the following, most probable, interpretation of the module's characteristics:

1. The mean electrode temperature was not equal to the effluent oxygen temperature as determined by a thermocouple in the oxygen stream outside of the cell.

2. Localized "hot spot" temperatures existed within the cells due to low thermal conductance between the electrodes and the silver cooling plate via the Exmet gas cavity filler. Poor thermal contact was likely to be randomized within the module (depending upon the prior history of deformation of the Exmet screens).

   The crossed-over cells were similarly randomized in location within the module, thereby tending to validate the belief that "hot spots," in fact, did exist. The presence of hot spots increased the vapor pressure of the water in the electrolyte and leads to excessive water evaporation, matrix drying and gas crossover.

A list of other possible reasons for crossover observed in the aforementioned tests are noted below. Most of these phenomena were studied by an in-house effort on small cells tested under precisely controlled conditions.

1. Crossover as the result of excessive pressure difference across cells due to the high pressure drop through the hydrogen side of the stack in the series flow configuration.

   The small cell tests indicated the same water tolerance for a small pressure differential as to a large differential, thereby demonstrating that crossover is independent of pressure differential.

2. Inaccurate data on the water vapor pressure depression of aqueous K_2CO_3 solution. Small cell data support the accuracy of available data[3] (International Critical Tables).

3. Improper influent hydrogen dew point This could explain crossovers in cells near the effluent end of the module.

4. Carbonate to bicarbonate conversion and bicarbonate precipitation on the anode side of a cell. This has been seen in small cell tests but has not led to gas crossover. This may lead to crossover in the module, however, for if a hydrogen port is plugged, the anode gas cavities receive full line hydrogen pressure (10 psig) upstream of the plug. Conversion to bicarbonate and bicarbonate precipitation does change the electrolyte vapor pressure which leads to moisture balance problems.

Means by which the water tolerance of the module may be increased in order to make it relatively insensitive to changes in environmental temperature were

studied. It was necessary to improve the heat transfer characteristics of the stack in order to avoid localized regions of high temperature; to find an electrolyte having greater solubility of the bicarbonate to avoid precipitation; and to reduce the pressure drop through the hydrogen side of the module. This was done in the Design II development.

Design II Module

At the end of the parametric test series, the module had accumulated 678 hours under continuous load. At this time the unit was placed on life test at the standard conditions of test noted in Figure 69. The performance of the unit is also demonstrated in Figure 69. Note that stack voltage is stable around an average value of 9.6. Carbon dioxide level in the effluent oxygen is approximately 0.4 percent for the first 600 hours of test and 0.3 percent to 1,200 hours at which time a slow rise to 0.55 percent is noted.

Random variations in the performance of the module are due to rig servicing techniques such as condensate drain off, sample bleed for the gas chromatograph, etc. At 846 hours under load, Cell #6 performed as if partially shorted. An unsuccessful attempt was made to rectify this situation. Subsequent to this time the apparent short condition spontaneously cleared itself without explanation.

At 1519 hours, the rig shut down due to bearing failure in the oxygen recycle blower. The shutdown was initiated by reduction of stack voltage to 8.5 from a running value of 9.6 volts. The blower rotor was replaced and the stand started up one-half hour later. Performance prior to the hut down was completely restored. The run continued until the stand was shut down at the conclusion of the revised test program. A total of 1845 continuous load hours were logged on the second module (509 hours parametric test time). A total of 169 hours were logged on the first module (all parametric test time). No electrolyte recharges were necessary to sustain the operation of either unit during the test series.

Test operations were terminated upon completion of contract requirements with the module capable of full operation. A disassembly inspection was not performed.

Single Cells

The primary objective of the single cell life tests was to obtain data on compatibility of cell materials when exposed to normal carbon dioxide concentrator cell operating environment. Difficulties in maintaining the stable cell operation were attributable to: 1) test rig design characteristics and 2) use of the potassium carbonate electrolyte which led to moisture balance problems.

Nickel Endplates. - Cells 1Ni and 2Ni used initially in the parametric test phase were maintained in operation for the life test phase. Operation was maintained using the potassium carbonate electrolyte until it was determined that cesium carbonate electrolyte perovided more stable operation. Figures 70 and 71 give the performance summary for cells 1Ni and 2Ni while operating with potassium carbonate for 8732 and 8266 hours, respectively. At this time both cells were rebuilt and charged with cesium carbonate (52% w/w).

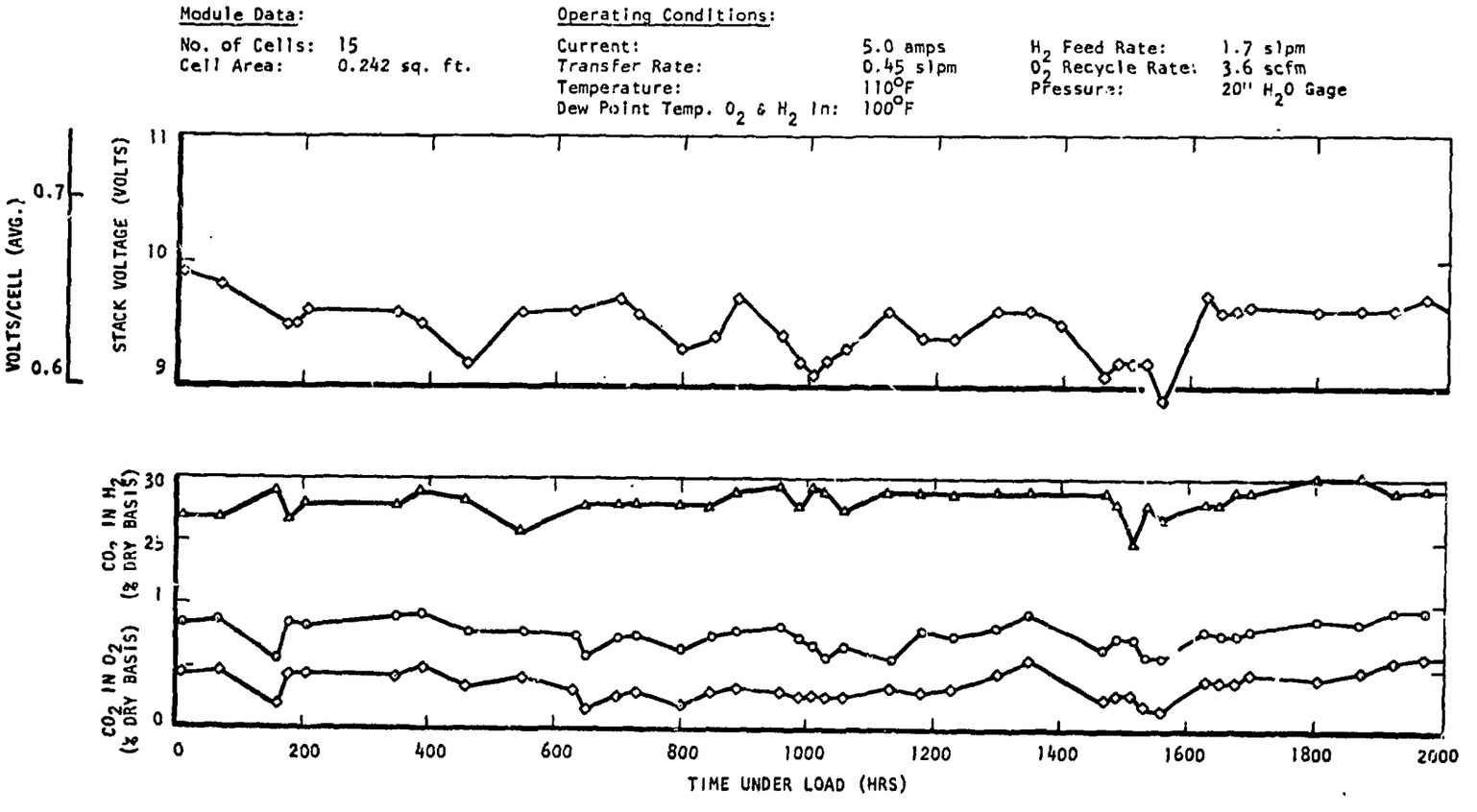

FIGURE 69 PERFORMANCE OF CDCM II ON LIFE TEST

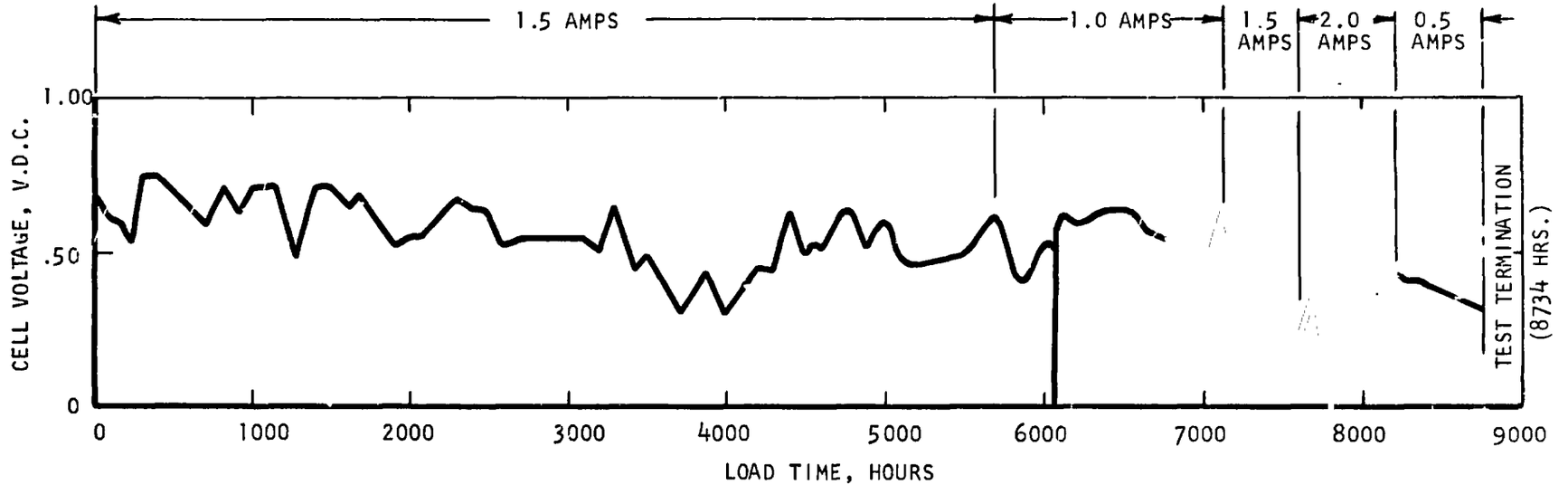

FIGURE 70 CO_2 CONCENTRATOR SINGLE CELL (1 Ni) LIFE TEST WITH K_2CO_3 ELECTROLYTE

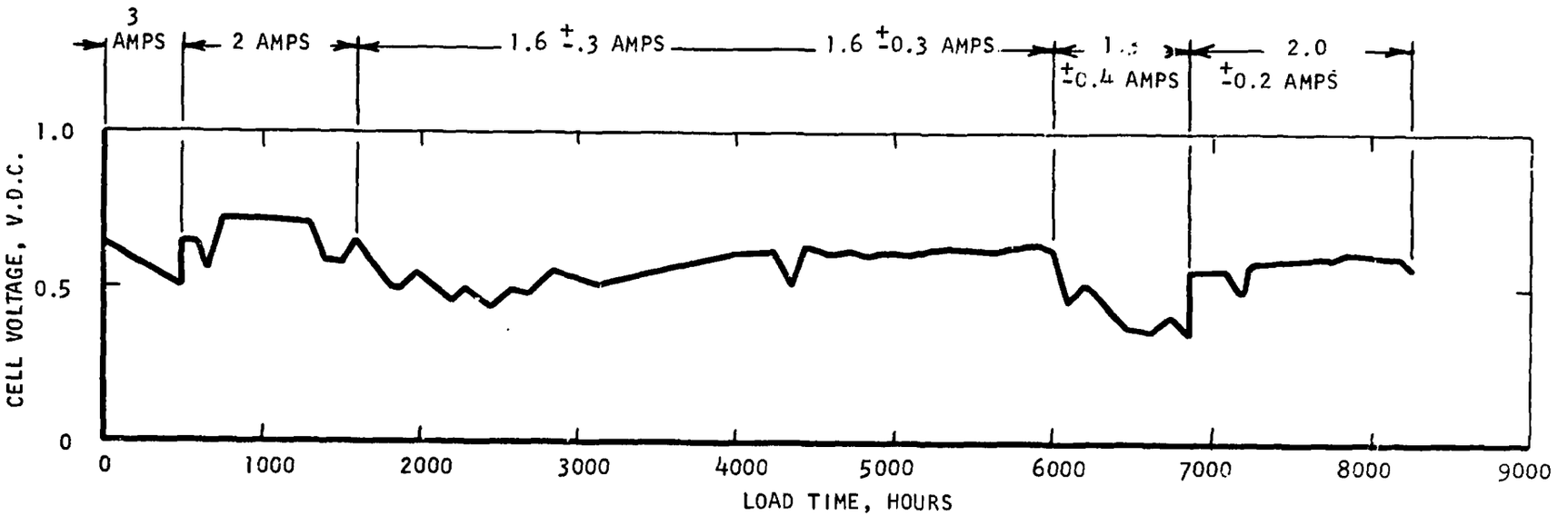

FIGURE 71 CO_2 CONCENTRATOR SINGLE CELL 2Ni, LIFE TEST PERFORMANCE

Performance for cells 1Ni and 2Ni are summarized in Figures 72 and 73. Moisture balance problems due to rig design were still evident during this test period but were much less severe compared to the operation with potassium carbonate.

Tests were terminated after 2,952 and 4,805 hours operation with the cesium carbonate electrolyte for a total 11,684 and 13,071 hours test time on cells 1Ni and 2Ni, respectively. Observations made during the cell disassembly and post-test teardown and inspection procedures are contained in Appendix B of this report.

Summaries of shutdowns occurring during the life testing are given in Tables XXIX and XXX for cells 1Ni and 2Ni.

Polysulfone Endplates. - Generally poor performance was obtained with the polysulfone endplate cells due to poor thermal conductivity of the polysulfone and the cracking of the material around the inlet-outlet fittings. Cell 1P operated for only 256 hours due to the cracking problem while cell 2P operated for a total of 3,577 hours, which includes 3,252 hours of operation after the cell had been stored for five months after the initial 325 hours of cell operation. Figure 74 shows cell performance while Table XXXI presents a summary of the cell and test rig shutdowns.

Titanium Endplates. - After determining that cell 1P was inoperable, it was decided to test a carbon dioxide concentrator cell similar in construction to those used in the ten-cell modules. This cell was constructed with titanium endplates. The cell was placed on test in the life test stand with an independent temperature controller. After an adjustment period to stabilize the water balance, the voltage leveled out. Single cell 1Ti was rebuilt at elapsed time of 1,420 hours following a gas crossover (anode/cathode). The expanded metal spacers were spotwelded to the electrodes and a 45 mil asbestos electrolyte matrix was installed. After approximately 1,705 hours elapsed time, the performance was low and it was concluded that the cell had "dried out." An attempt was made to seal the cell through humidification by dropping the cell temperature below the humidifier temperature. This was unsuccessful and the test on this cell was not resumed. The data obtained is presented in Figure 75 and Table XXXII.

Design II Cells. - Two cells of the Design II module configuration were designated 1M and 2M, charged with 52% w/w Cs_2CO_3 and life tests initiated. Load current on each of the cells was maintained at 4.0 amps. Average cell voltage versus time curves for cells 1M and 2M are shown in Figures 76 and 77. No shutdowns occurred during the 1,560 and 1,465 hours operating time accumulated on each cell. Observations made during cell disassembly post-test teardown and inspection procedures are contained in Appendix B of this report.

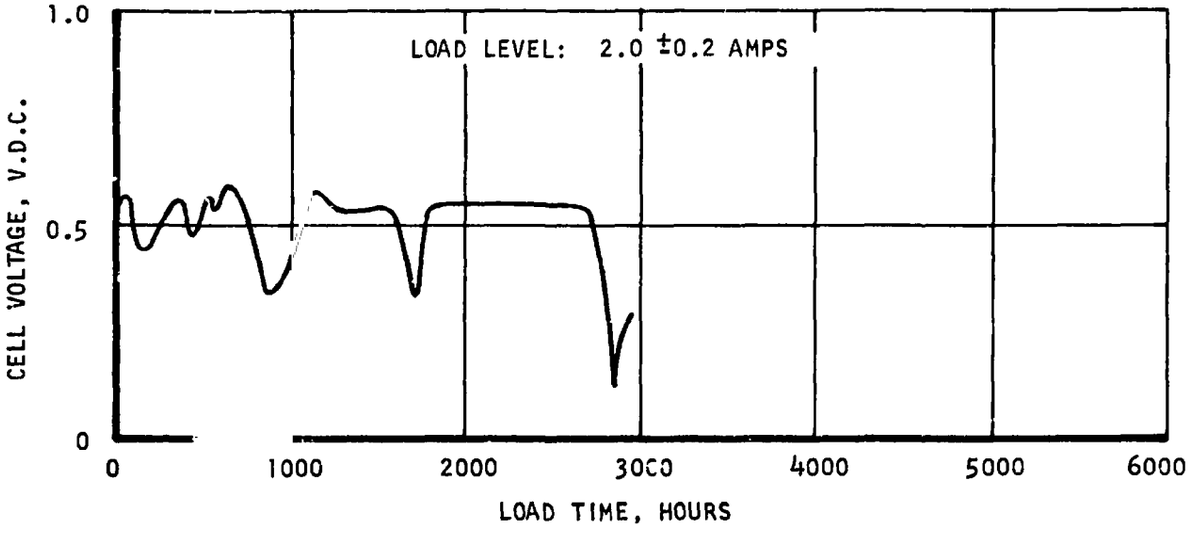

FIGURE 72 CO_2 CONCENTRATOR SINGLE CELL (1 NI) LIFE TEST WITH $Cs_2 CO_3$ ELECTROLYTE

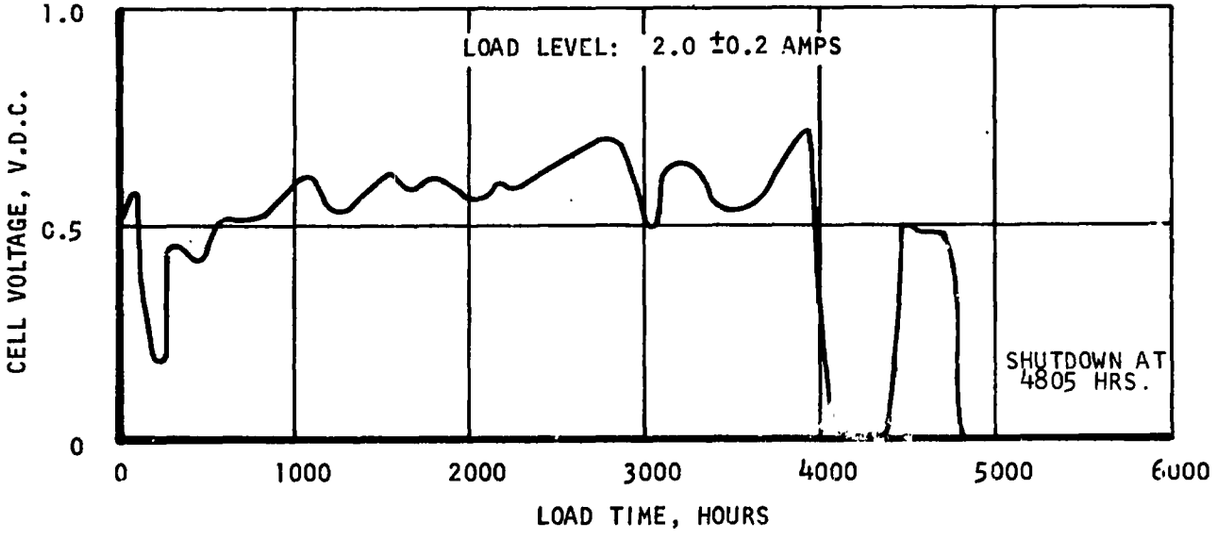

FIGURE 73 CO_2 CONCENTRATOR SINGLE CELL (2 Ni) LIFE TEST WITH $Cs_2 CO_3$ ELECTROLYTE

TABLE XXIX

CO_2 CONCENTRATOR SINGLE CELL (INi) LIFE TEST
SHUTDOWN SUMMARY

Elapsed Time (in life test) Hours	Cause of Shutdown	Corrective Action
	Cell INi-1	
59.8	Load too low	Recharge
232.8	Cross leakage	Recharge
544.9	Cross leakage	Recharge
690.5	Load too low	Recharge
2067.0	Stand and building modification	Restart
6057.7	Cross leak	Rebuild Cell
	Cell INi-2	
7617.9	Poor performance	Recharge
7917.3	Poor performance	Recharge
8641	Building power failure	Restart
8734	Termination of test with K_2CO_3	Rebuild cell, charged with Cs_2CO_3 electrolyte
	Cell INi-3	
82*	Plant power off	Restart
112	Plant power off	Restart
1290	Plant power off	Install constant current control equipment and restart
2952	Test termination	

*reset timer to 0 hours

TABLE XXX

CO_2 CONCENTRATOR SINGLE CELL (2Ni) LIFE TEST
SHUTDOWN SUMMARY

Elapsed Time (In life test) Hours	Cause of Shutdown	Corrective Action
	Cell 2Ni-1	
459.9	Moved to life test stand	Restart
707.4	Cross leakage	Recharge
1219.7	Electrical modification	Restart
1370.5	Humidifier overfilled	Excess drained
2721.4	Test stand and building repair	Restart
5759.6	Load too low	Recharge
6877	Faulty line heater	Repair line heater
8266	Coolant line rupture	Rebuild cell
	Cell 2Ni-2	
267	Poor performance	Recharge cell, with Cs_2CO_3 electrolyte
807	Building power failure	Restart
1665	Plant power off	Restart
1696	Plant power off	Restart
2510	Rig modification	Install constant current control equipment
2862	Plant power off	Restart
4468	Poor performance	Recharge
4805	Test termination	

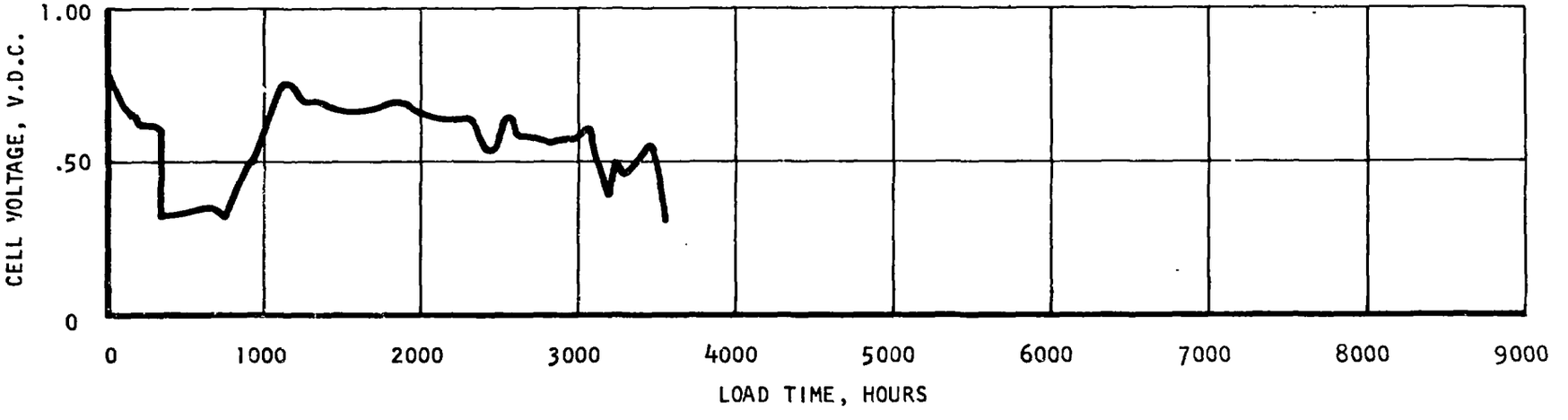

FIGURE 74 CO_2 CONCENTRATOR SINGLE CELL (2P) LIFE TEST
WITH K_2CO_3 ELECTROLYTE

TABLE XXXI

CO_2 CONCENTRATOR SINGLE CELL (2P) LIFE TEST
SHUTDOWN SUMMARY

Elapsed Time (in life test) Hours	Cause of Shutdown	Corrective Action
69.7	Cross leak	Raised humidifier temperature
160	No voltage display	Recharge
278	Cross leak	Humidified in place
905	Building power failure	Restart
2493	Cross leak	Recharged
3577	Low performance	Test stopped, cell to be replaced

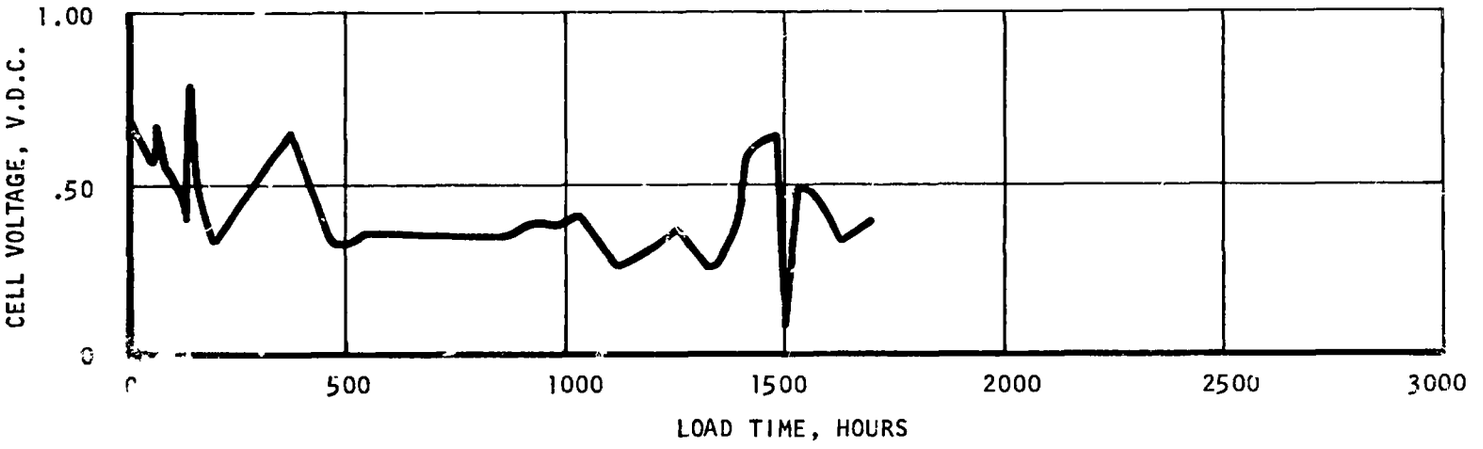

FIGURE 75 CO_2 CONCENTRATOR SINGLE CELL (ITi) LIFE TEST
WITH K_2CO_3 ELECTROLYTE

TABLE XXXII

CO_2 CONCENTRATOR SINGLE CELL (ITi) LIFE TEST
SHUTDOWN SUMMARY

Elapsed Time (in life test) Hours	Cause of Shutdown	Corrective Action
132.2	Load too low	Recharge
436.2	Load too low	Recharge
1407.2	Load too low	Recharge
1420	Crossover	Rebuild
1513.0	Dryout	Restart
1705.1	Cell dryout	Test stopped cell to be replaced

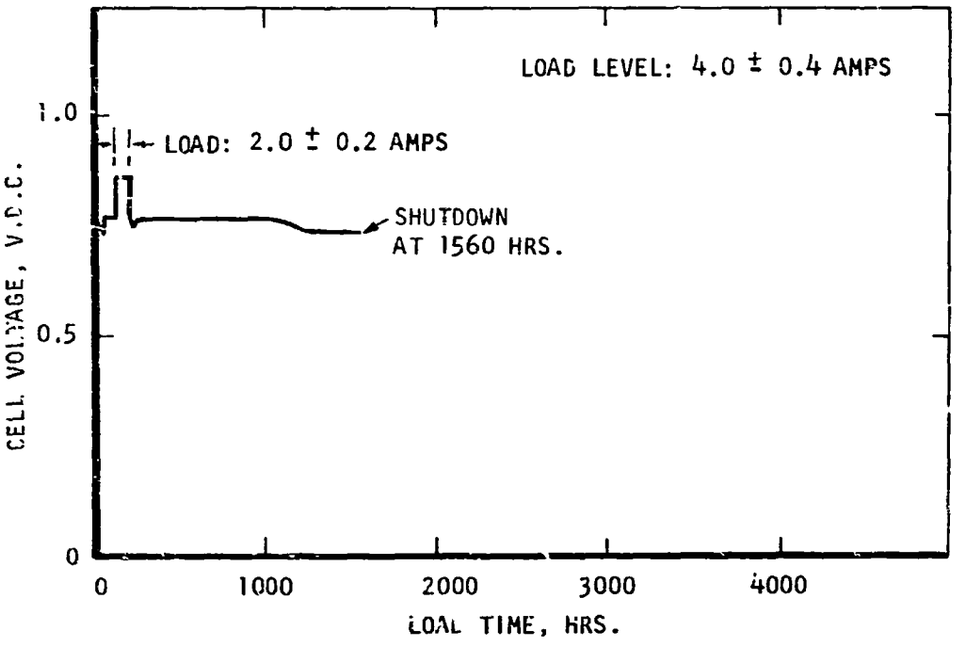

FIGURE 76 CO_2 CONCENTRATOR SINGLE CELL (1M) LIFE TEST WITH $Cs_2 CO_3$ ELECTROLYTE

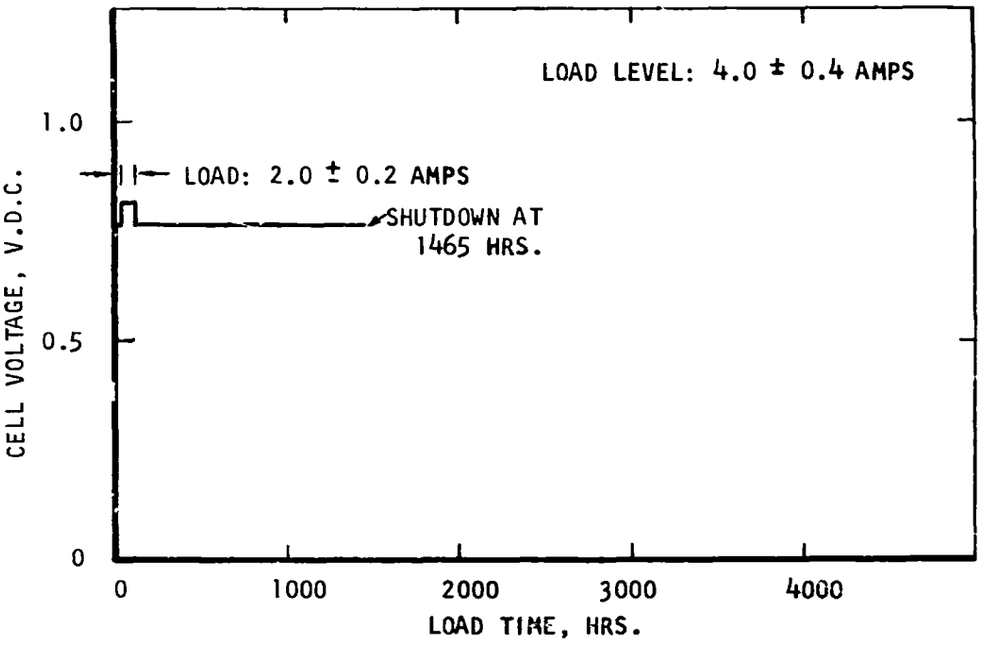

FIGURE 77 CO_2 CONCENTRATOR SINGLE CELL (2M) LIFE TEST WITH Cs_2 CO_3 ELECTROLYTE

CONCLUSIONS

The following conclusions relative to the carbon dioxide concentrator module assembly were reached on the basis of information derived from the NAOS development program.

1. Silver is not a suitable material for long-term module operation over the complete range of operation from full load to open circuit conditions.

2. Potassium carbonate solution is not a suitable electrolyte for normal stable operation.

3. Long-term operation of carbon dioxide concentrator cells and modules is feasible using cesium carbonate electrolyte.

4. The titanium clad copper assembly is suitable for use as a bipolar plate in the carbon dioxide concentrator.

5. The carbon dioxide concentrator module meets the system design requirements for carbon dioxide removal, using the series hydrogen flow pattern.

6. The carbon dioxide concentrator module is capable of maintaining carbon dioxide partial pressures below 1mm Hg in the closed loop system.

7. The ability of the concentrator module to maintain design performance capability for extended periods of continuous operation was successfully demonstrated.

8. Operation of the module in an ON-OFF cycle characteristic of short-term aircraft operation is entirely satisfactory.

9. Full operation after long storage periods is possible.

RECOMMENDATIONS

Based on NAOS program experience, the following recommendations are made:

1. Perform investigation necessary to provide additional data on methods which can be used to increase the specific transfer rate of carbon dioxide at low carbon dioxide partial pressures.

2. Module development should be continued with the objective of developing an efficient carbon dioxide concentrator for use in either aircraft or spacecraft life support systems.

APPENDIX A

CARBON DIOXIDE CONCENTRATOR - THERMAL ANALYSIS

APPENDIX A

CARBON DIOXIDE CONCENTRATOR - THERMAL ANALYSIS

An analysis was made on the carbon dioxide concentrator Design I to study the various heat removal methods applicable to aircraft such as the F-111 and to establish the interface requirements with respect to the Carbon Dioxide Concentrating Subsystem (CDCS). Wherever possible, estimates of general module configuration, including weight and volume, were made and subsystem support component requirements for the various cooling methods defined.

The heat removal methods applicable to aircraft use and selected for consideration are: 1) forced convective cooling (air or liquid over external fins or liquid through internal passages), 2) evaporative cooling, and 3) electrolyte circulation.

In the reaction of hydrogen and oxygen to form water in the concentrator, an energy release occurs. This change is slightly dependent on cell operating temperature. At the expected cell operating temperature ($120^{o}F$) the energy change is 5,850 BTU/lb of water formed. A portion of the total energy change is removed in the form of useful electrical energy and is not considered in this analysis. The magnitude of the electrical energey is represented by the cell voltage. The remaining portion is removed in the form of waste heat. Figure 1 indicates the required heat removal rate as a function of cell voltage.

The cell operating temperature is assumed to be approximately $120^{o}F$ for most of the cooling methods considered. The minimum temperature which may be required is $100^{o}F$. Temperature gradients through the stack, or across an electrode should not exceed $5^{o}F$.

F-111 Environmental System

The F-111 weapons system uses both air and a liquid coolant in its environmental control system. The liquid coolant, however, is used in an evaporative cooling mode and will, therefore, reach temperatures in excess of those required for the CDCS module.

The aircraft air conditioning system basically uses air at $-65^{o}F$ and mixes it with $390^{o}F$ air to obtain desired temperature levels for cabin cooling, pressure suit cooling, and electronic equipment cooling. Various types of modulating valves and temperature sensors are used to perform these functions. A similar system could be used to supply cooling air at a desired temperature level to NAOS system components or their secondary cooling loops.

Heat Removal Methods

Forced Convection - Air. - The CDCS modules now being used for laboratory and flight breadboard testing are cooled by forced air convection. The waste heat, generated at the electrodes, is carried to external fins. In this design, the temperature gradient from the center line of the electrode to the fin will not exceed $4^{o}F$ and the maximum temperature difference in the modules does not exceed $8.0^{o}F$.

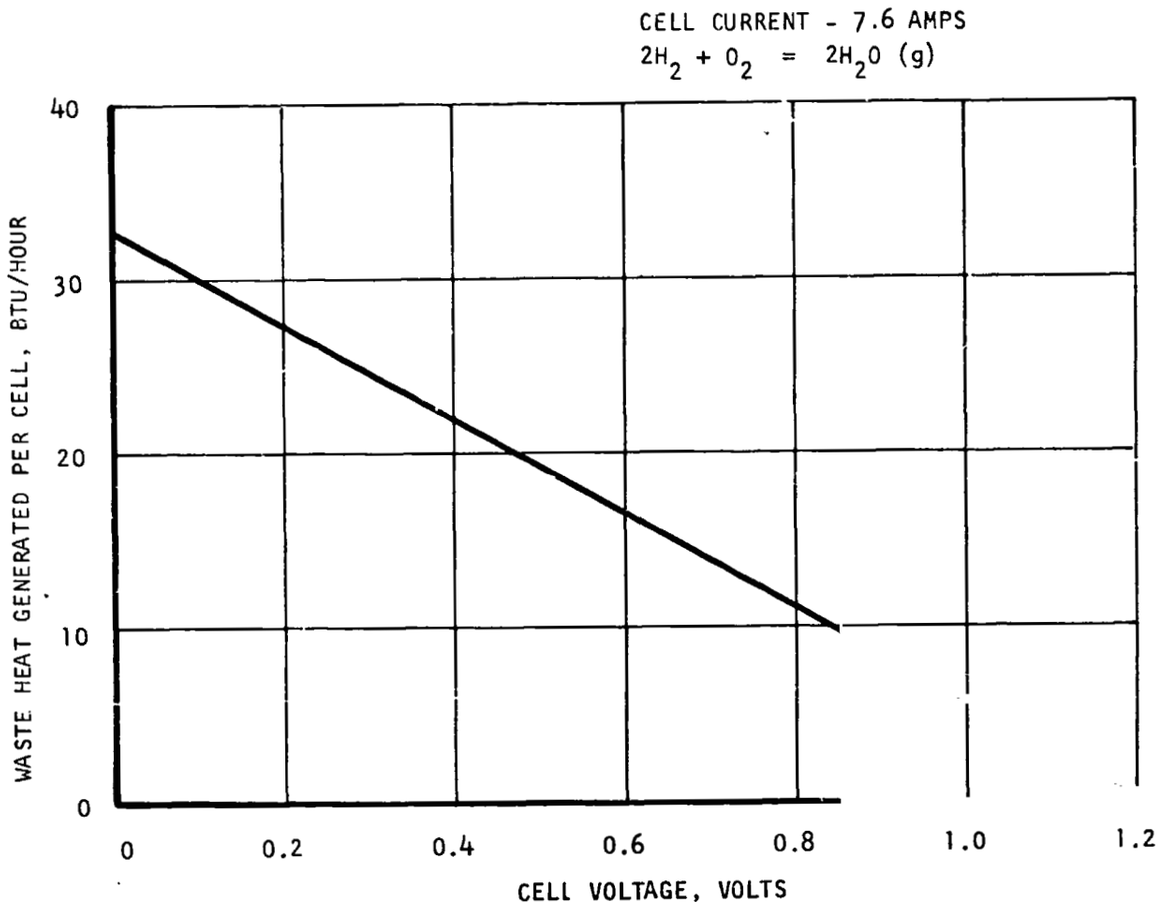

FIGURE A-1 HEAT GENERATION RATE FOR OXYGEN-HYDROGEN REACTION - CO_2 CONCENTRATOR CELL

Several design parameters affect the choice of the fin dimensions. These include:

		PRESENT	FUTURE
1.	Cell Thickness	0.172 inches	0.120 inches
2.	Cell Length	13 inches	11.5 inches
3.	Fin Width	1/2 inch	as required
4.	Air Temperature Pickup	very small	$10^{o}F$
5.	Flowrate and Allowable Pressure Drop	~100 CFM 9" H_2O	23 CFM (determined by 4) not available

Assuming a flow passage configuration similar to that now used and a $10^{o}F$ air temperature pick-up, the following results were obtained:

Air Temperature Inlet to Maintain $100^{o}F$ Stack	$64^{o}F$
Air Exit Temperature	$74^{o}F$
Fin Temperature	$92^{o}F$
Air Flowrate	23 CFM
Approximate Pressure Drop	0.25" H_2O

Changes in the fin geometry would not significantly affect the results presented above. The cooling air could be supplied from the F-111 air conditioning system by mixing $-65^{o}F$ air with $390^{o}F$ air. A temperature sensor and modulating valve similar to those used elsewhere in the aircraft would be used.

Forced Convection - Liquid. - The present module design can be slightly modified to allow for direct liquid cooling. This is accomplished by adding coolant flow passages around the cell edges. This is equivalent to using liquid in place of air to cool the fins. The silver plate is used to conduct the heat from the electrodes to the coolant.

An analysis was made to determine the approximate interface requirements : inlet coolant temperature, flowrate, and pressure drop . The coolant was assumed to be water. The flowrate required to limit the temperature gradient through the stack was determined to be 49 lb/hr. A flowrate of 60 lb/hr was assumed for the calculations. The results indicate that the coolant should be available at $90^{o}F$. The pressure drop through the CDCS would not exceed 6.2 psi.

The CDCS design can also be modified in such a way that a large portion of the silver metal is eliminated and the cooling channels placed in contact with the expanded metal. The coolant plate is formed by bonding together two polysulfone plates, each of which contains coolant grooves. The resulting plate is electroplated with silver and a protective coat of platinum. The metal provides electrical contact from cell to cell.

Depth of the cooling channels is determined by the pressure drop which is allowed at the operating temperature and flowrate. This also depends upon the manifolding provided. A series flow path through the ten-cell stack would require a thicker plate than parallel flow but more reliable cooling of the cells would be obtained.

Evaporative Cooling. - Waste heat can be removed from the CDCS by allowing excess water to evaporate from the cell cavities. The heat removal burden is transferred from the CDCS module to the rebreather loop dehumidifier.

Figure A-2 shows the equilibrium cell temperature as a function of cell voltage for various total pressures which vary with cabin altitude. Evaporative cooling has the significant advantage that it eliminates water balance problems if a static water feed is incorporated as is done with the electrolysis subsystem. This allows the CDCS to operate independent of outside influences and requires no temperature control of any kind, nor blowers, pumps or aircraft service. The heat load on the dehumidifier is raised, however, to include the CDCS but no added services or components are required.

Electrolyte Circulation. - Electrolyte can be circulated through the CDCS cells and an external heat exchanger to remove the heat with a liquid or air coolant. The cell design would be such as to place an open passage within the cell matrices to allow a liquid flow passage. This method requires a pump for circulation, a heat exchanger, a circulating loop pressure control referenced to the cell gas-side pressure, and control for the heat exchanger.

The circulating electrolyte method could also include the advantages of evaporative cooling if the cell were purposely operated at higher temperature so that some of the heat load would be latent, thus the product water would be removed from the electrolyte. A water feed into the electrolyte loop to maintain constant loop volume would maintain the electrolyte concentration relatively constant. This would be the main advantage of this method. However, the complexity and additional components required would tend to off-set these advantages for aircraft use.

In summary, it appears that several cooling methods are feasible. Liquid cooling systems require smaller plumbing and control valving hardware than air systems. Using liquid cooling for the entire oxygen system, including the water electrolysis module, electronics package, rebreather dehumidifier and the CDCS would result in a compact system. This, however, would require a detailed analysis including the aircraft services and the thermal considerations of several components using a common cooling loop. The results of the present study indicates that sufficient advantages occur with the evaporative cooling method to justify further consideration of this method for the CDCS.

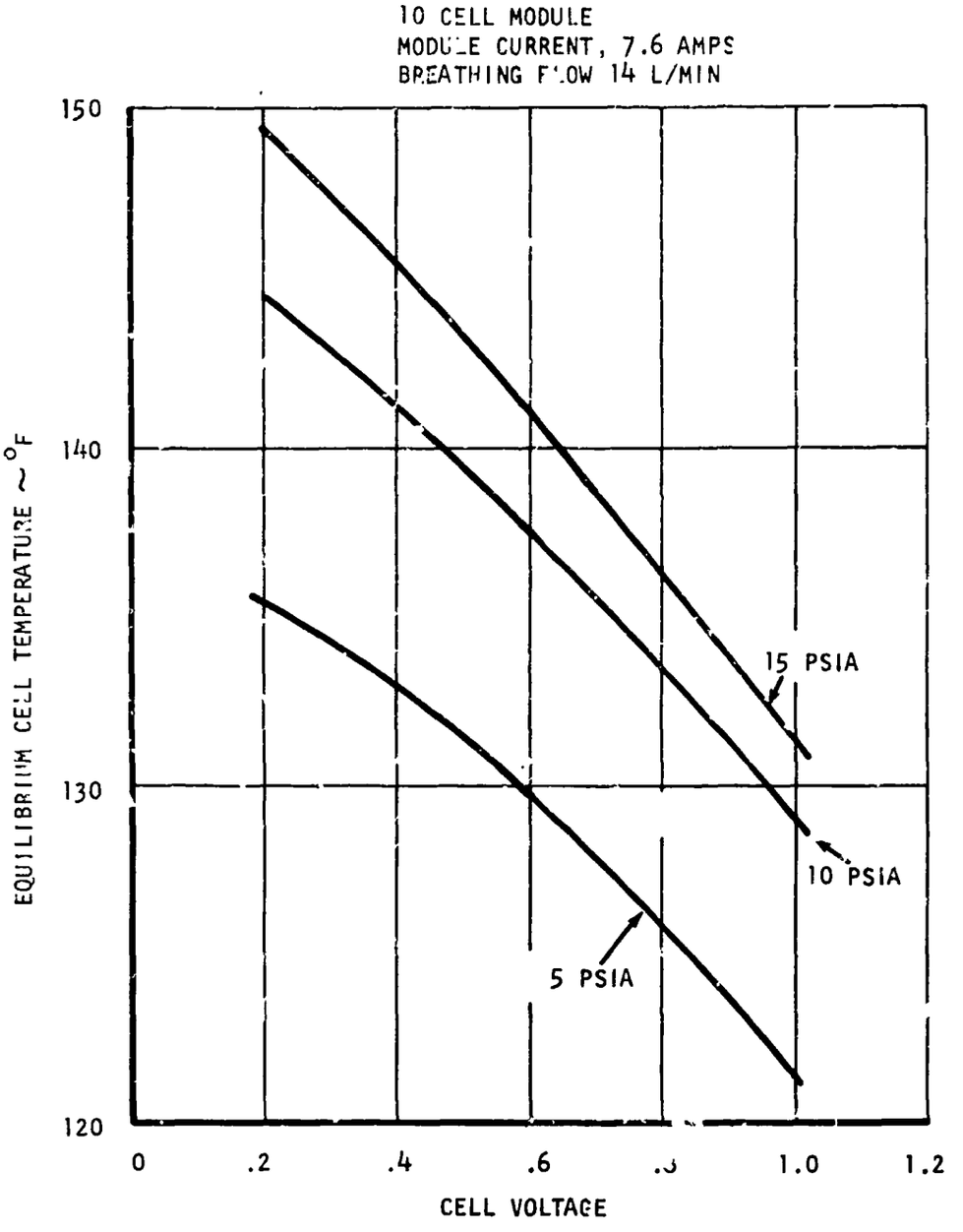

FIGURE A-2 CO_2 CONCENTRATOR MODULE EQUILIBRIUM CELL TEMPERATURE FOR EVAPORATIVE COOLING

APPENDIX B

POST-TEST INSPECTION OF CARBON DIOXIDE CONCENTRATOR SINGLE CELLS

APPENDIX B

POST-TEST INSPECTION OF CARBON DIOXIDE CONCENTRATOR SINGLE CELLS

CELL 2Ni:

1. Assembly - small amounts of external leakage indicated by a blue discoloration of the copper heat sink plate.

2. Cathode endplate - no deposits in evidence and no evidence of corrosion on the pin tips as observed under 25X magnification. A thin blue, purple and yellow discoloration of the nickel at the back of this cavity was noted. The electrical continuity between the endplate and the pin tip as determined by an ohmmeter and probe showed no evidence of a resistive layer on the pin tip surface.

3. Cathode - showed no evidence of corrosion but there was some platinum loss in the region around the gold foil gas deflector at the oxygen inlet. The platinum lost from the electrode was found to be adhered to the matrix. Microscopic examination of the electrode showed no areas of corrosion. The exposed wire area was gold in color and showed no evidence of gold electroplate loss.

4. Matrix very dry. Generally white in appearance except for a few areas in which the matrix had apparently picked up platinum by adhesion. Matrix was slightly green to gold in color near the bottom cavity of the cell. Peeling the dried matrix disclosed that the darker discoloration found in areas on the cathode side extended within the thickness of the matrix. The anode was firmly adhered to the matrix.

5. Anode - appeared to be no loss of platinum black other than what adhered to the matrix when the unit was disassembled. The exposed wires of the electrode appeared to be gold-plated and there was no apparent loss of this electroplate on either side of the anode.

6. Anode endplate - no deposits were found. Some surface discoloration in the form of a blue-black to black coating was seen within the gas cavity. Most of the pin tips were bright in color. An electrical resistance check between the endplate and pin tip showed no evidence of a resistive layer. Under microscopic examination the pin tips appeared to have an etched appearance which looked somewhat like mud cracks.

In summing the above, there appears to be markedly little corrosion within this unit. Components are shown in Figure B -1.

CELL 1Ni:

1. Assembly - this unit showed obvious signs of external leakage.

2. Cathode endplate - showed no evidence of deposits whatsoever. The pin tips showed good electrical continuity with the bulk of the plate. The

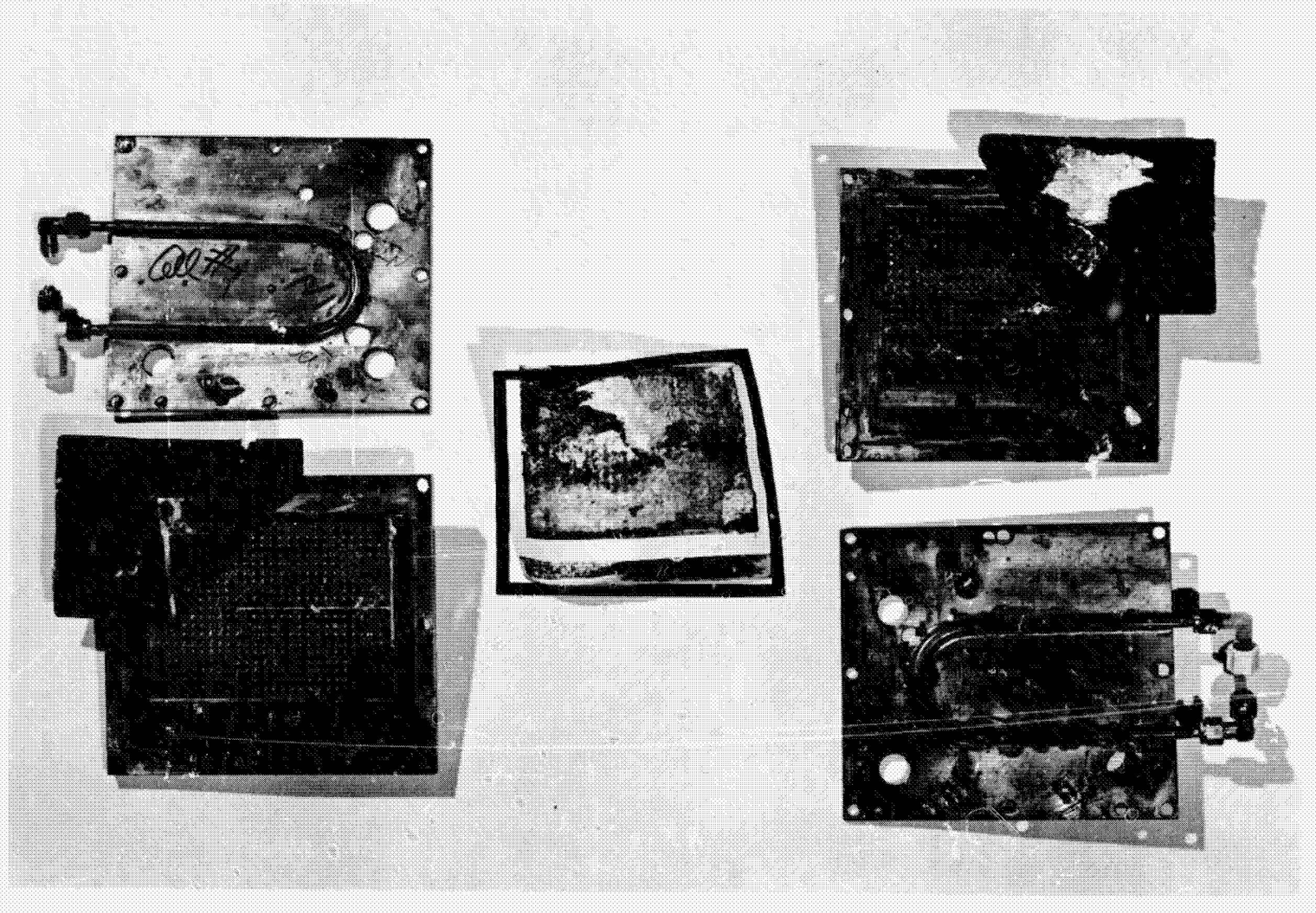

FIGURE B-1 CELL (IN1) COMPONENTS - POST-LIFE TEST CONDITION

back of the gas cavity showed a slight coating of dried carbonate. Under magnification there appeared to be a slight etching of the pin tips.

3. Cathode - appeared to be in "new" condition.

4. Matrix - appeared to be moist in this disassembly as opposed to the dry condition of the matrix in Cell 2Ni. The cathode side of the matrix had very few discolored areas but the anode side was very dark. The green discoloration on the anode side was very intense compared to that on the cathode side.

5. Anode - appeared to be in excellent condition and showed no evidence of deposits or loss of platinum other than what occurred when it was stripped from the matrix. The anode showed no evidence of gold loss from the plated nickel wire.

6. Anode endplate - was dark and didn't appear as if the darkness is solely platinum black. It appeared as if this discoloration was a corrosion product. Some slight amount of etching appeared to be noticeable on the pin tips on the anode side. No evidence of an electrically resistive layer could be found. Components are shown in Figure B-2.

CELL 1M:

1. Assembly - gaskets very tightly adhered the polysulfone cell housing to the titanium clad fin plate.

2. Cathode fin plate - titanium clad on this side of the cell showed a few areas of blue and violet discoloration but for the most part the titanium had a very slight yellowish cast. Some areas of the gas cavity filler showed a black discoloration that appeared to be platinum black.

3. Cathode - in "as new" condition.

4. Gasket - oxygen side gaskets showed an excellent seal markoff.

5. Matrix - moist and white on the oxygen side and darkened on the hydrogen side. Opposite the hydrogen inlet there were two regions wherein the catalyst on the hydrogen electrode obviously became quite hot and the adjacent matrix became very dry. The catalyst was transferred from the hydrogen electrode to the matrix in this region. There appeared to be a very slight greenish discoloration on the cathode side of the matrix.

6. Anode - appeared normal in all respects except for the burned regions mentioned above.

7. Anode fin plate - scattered regions of intense blue color; however, the major portion was yellowish as indicated above for the oxygen endplate. Quite a bit of solidified carbonate in the hydrogen ports. Some evidence of leakage as indicated by copper discoloration along the long dimensions of the cell. The hydrogen gasket shows evidence of lapping over the compression frame in this region. Obviously implied that the gasket was

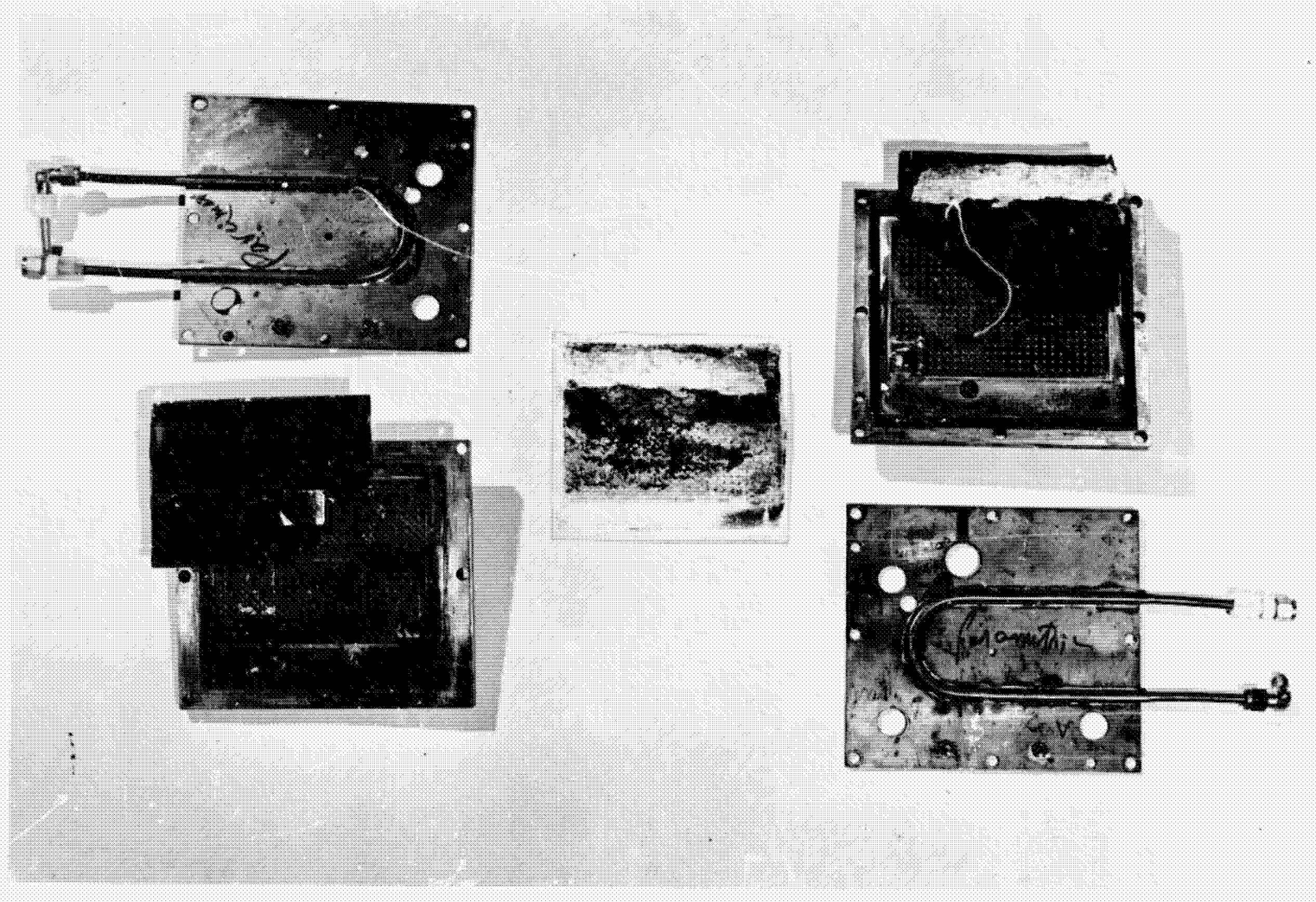

FIGURE B-2 CELL (2Ni) COMPONENTS - POST-LIFE TEST CONDITION

not sealing as it should have. No electrically resistant layer was found in the structure. This was verified by laying a platinum electrode against the gas cavity filler and connecting one probe of an ohmmeter to the electrode and the other to the copper fin plate.

8. Gasket - showed evidence of lapping as mentioned above. Showed continuous markoff in compression region.

9. Figure B-3 shows 1M cell components and Figure B-4, Cell 2M components. There were no essential differences noted between Cell 1M and 2M except for the 2M matrix discoloration.

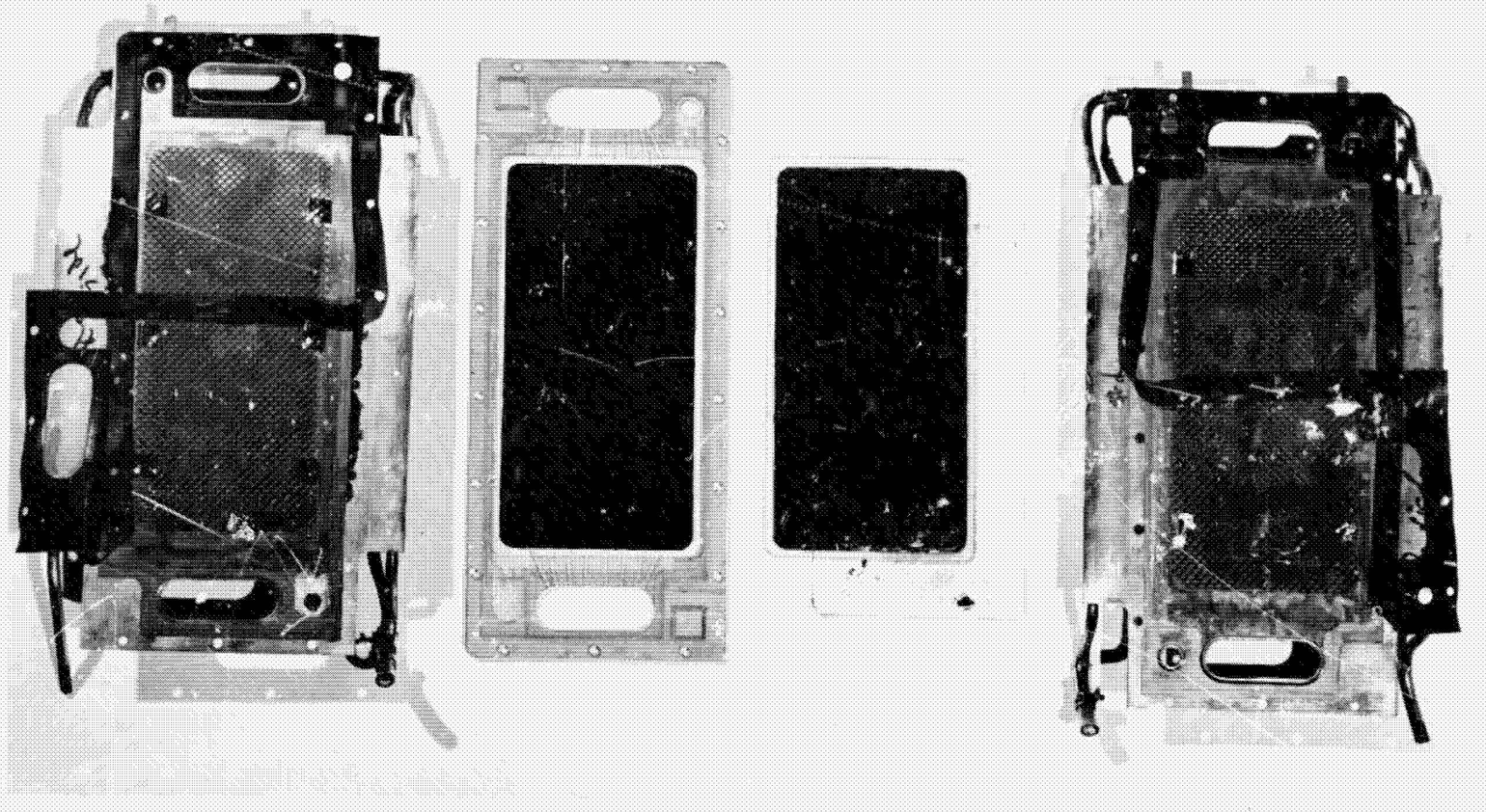

FIGURE B-3 CELL (1M) COMPONENTS - POST-LIFE TEST CONDITION

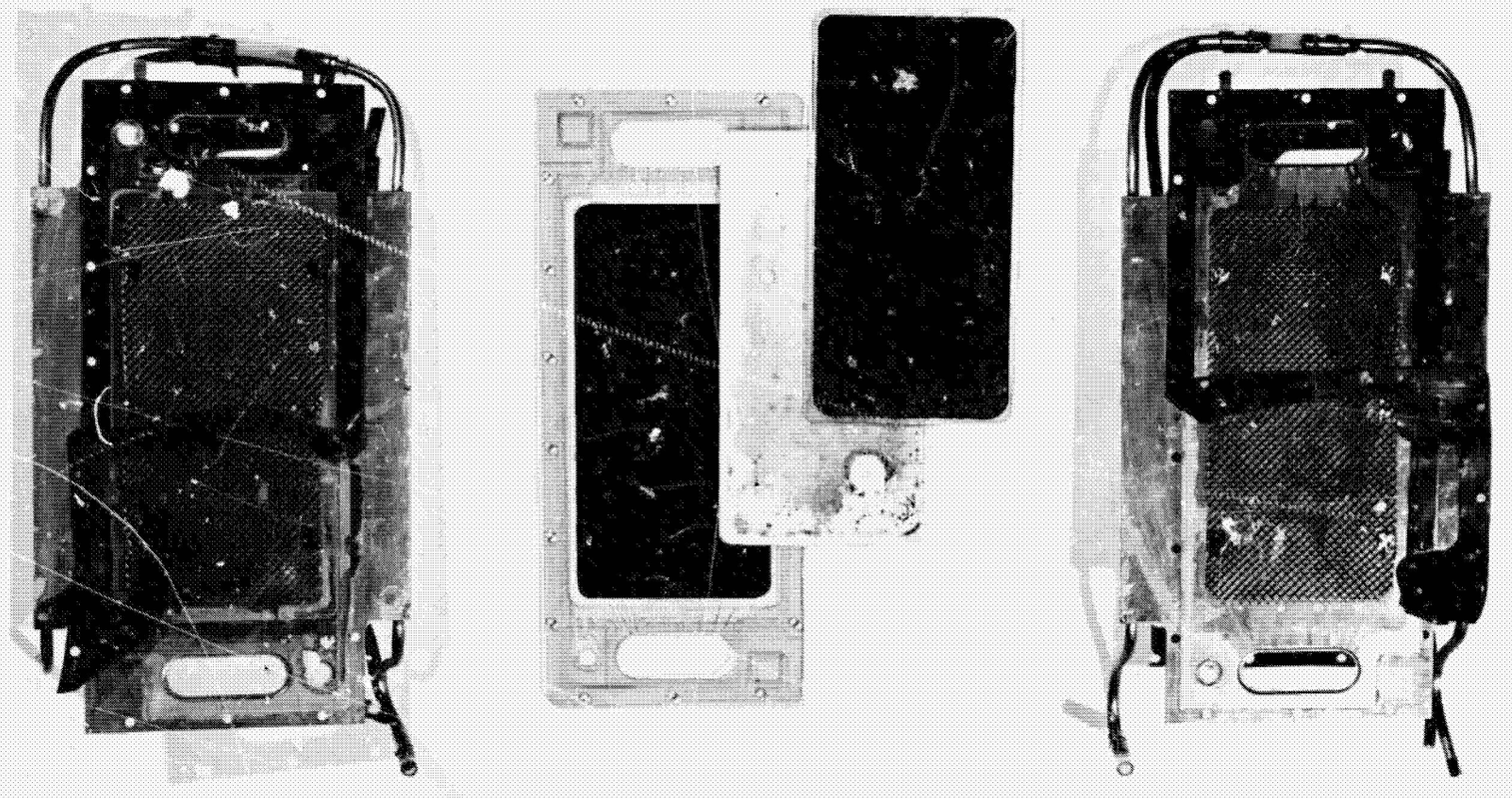

FIGURE B-4 CELL (2M) COMPONENTS - POST-LIFE TEST CONDITION